ASSESSMENT OF TWIN TUNNEL INDUCED GROUND DEFORMATION BY EMPIRICAL AND NUMERICAL ANALYSES (EURASIA TUNNEL: NATM PART, ISTANBUL, TURKEY)

A THESIS SUBMITTED TO
THE GRADUATE SCHOOL OF NATURAL AND APPLIED SCIENCES
OF
MIDDLE EAST TECHNICAL UNIVERSITY

BY

EBRU AĞBAY

IN PARTIAL FULFILLMENT OF THE REQUIREMENTS
FOR
THE DEGREE OF DOCTOR OF PHILOSOPHY
IN
GEOLOGICAL ENGINEERING

JANUARY 2019

Approval of the thesis:

ASSESSMENT OF TWIN TUNNEL INDUCED GROUND DEFORMATION BY EMPIRICAL AND NUMERICAL ANALYSES (EURASIA TUNNEL: NATM PART, ISTANBUL, TURKEY)

submitted by **EBRU AĞBAY** in partial fulfillment of the requirements for the degree of **Doctor of Philosophy in Geological Engineering Department, Middle East Technical University** by,

Prof. Dr. Halil Kalıpçılar
Dean, Graduate School of **Natural and Applied Sciences** _____

Prof. Dr. Erdin Bozkurt
Head of Department, **Geological Engineering** _____

Prof. Dr. Tamer Topal
Supervisor, **Geological Engineering Dept., METU** _____

Examining Committee Members:

Prof. Dr. Nurkan Karahanoğlu
Geological Engineering Dept., METU _____

Prof. Dr. Tamer Topal
Geological Engineering Dept., METU _____

Prof. Dr. Erdal Çokça
Civil Engineering Dept., METU _____

Prof. Dr. Bahtiyar Ünver
Mining Engineering Dept., Hacettepe University _____

Assoc. Prof. Dr. Mutluhan Akın
Geological Eng. Dept., Nevşehir Hacı Bektaş Veli Uni. _____

Date: 31.01.2019

I hereby declare that all information in this document has been obtained and presented in accordance with academic rules and ethical conduct. I also declare that, as required by these rules and conduct, I have fully cited and referenced all material and results that are not original to this work.

Name, Last Name: Ebru Ağbay

Signature:

ABSTRACT

ASSESSMENT OF TWIN TUNNEL INDUCED GROUND DEFORMATION BY EMPIRICAL AND NUMERICAL ANALYSES (EURASIA TUNNEL: NATM PART, ISTANBUL, TURKEY)

Ağbay, Ebru

Ph.D., Department of Geological Engineering

Supervisor: Prof. Dr. Tamer Topal

January 2019, 309 pages

Pre-support systems become very important for inner-city shallow tunnels especially while applying New Austrian Tunneling Method (NATM) which requires some deformation to relieve the stress. Previous studies about assessing the magnitude of surface displacements caused by twin tunneling do not include the effects of pre-support system and stress release by deformation. Moreover, most of the established empirical equations were obtained by using data from tunnel passing through clayey soil.

Objective of this thesis is to introduce a detailed procedure for obtaining modification factor including the effects of pre-support system and of rock mass quality and which can be used as a reduction ratio in prediction methods used for twin tunnel induced surface settlement.

Twin tunnel induced surface settlement data comes from Asian side of the Eurasia Tunnel excavated by using NATM method and supported by forepoling and umbrella arch method.

The steps that need to be completed in order to achieve the determined objective are; i) performing numerical analysis on the selected 12 cross section lines along tunnel route to update the geological profile at which there is no borehole drilled and to

approximate the results of numerical models to actual field measurement in terms of maximum surface settlement, ii) conducting parameter study in which the distance between pipes in the pre-support systems was used as a variable, iii) obtaining a statistical formula that presents the decreasing effect of pre-support system on maximum surface settlement.

It was concluded that twin tunnel-induced surface settlement mainly depends on deformation modulus of the geo-materials around tunnel. Deformation modulus was obtained by evaluating rock mass quality which is controlled by fracturing and surface weathering. A new formula predicting twin tunnel induced ground deformation is proposed as a modification factor of Herzog's equation.

Keywords: Eurasia tunnel, İstanbul, Finite element, Modification factor, NATM, Pre-support system, Surface settlement, Twin Tunnel

ÖZ

SAYISAL VE AMPİRİK ANALİZLER YARDIMIYLA İKİZ TÜNEL KAYNAKLI ZEMİN DEFORMASYONLARININ DEĞERLENDİRİLMESİ (AVRASYA TÜNELİ, NATM KISMI, İSTANBUL, TÜRKİYE)

Ağbay, Ebru

Doktora, Jeoloji Mühendisliği Bölümü

Tez Yöneticisi: Prof. Dr. Tamer Topal

Ocak 2019, 309 sayfa

Ön destek sistemi, zemin gerilmesinin azalması için bir miktar deformasyona ihtiyaç duyan NATM (yeni Avusturya tünel açma yöntemi) tekniği ile şehir içinde açılan sığ tüneller için çok önemli olmaktadır. İkiz tünel kazısı sebebiyle oluşan yüzeydeki oturma miktarının tahminini yapan önceki çalışmalar, ön destek sisteminin ve deformasyonla zemin gerilme salınım etkisini göz önünde bulundurmamıştır. Bununla birlikte, var olan ampirik denklemlerin çoğu killi zeminden geçen tünellerden gelen verilerle elde edilmiştir.

Bu tezin amacı, ön destek sisteminin ve kaya kütlesi kalitesinin etkilerini içeren ve ikiz tünel kaynaklı yüzey oturması için kullanılan tahmin yöntemlerinde azaltma oranı olarak kullanılabilecek modifikasyon faktörünü elde etmek için ayrıntılı bir prosedür sunmaktır.

İkiz tünel kaynaklı yüzey oturma verileri, NATM yöntemi kullanılarak kazılan ve boru süren ile desteklenen Avrasya Tüneli'nin Asya yakasından gelir.

Belirlenen amaca ulaşmak için tamamlanması gereken aşamalar şunlardır: i) sondaj bulunmayan alanlarda jeolojik profili güncellemek ve sayısal modellerin sonuçlarını maksimum yüzey oturması açısından gerçek arazi ölçümüne yaklaştırmak için tünel güzergâhı boyunca seçilen 12 kesit çizgisinde sayısal analizin yapılması, ii) ön

destek sistemindeki borular arasındaki mesafenin değişken olarak kullanıldığı parametre çalışmasının yapılması, iii) ön destek sisteminin maksimum yüzey oturması üzerindeki etkisini azaltan istatistiksel bir formül elde etmek.

İkiz tünel kaynaklı yüzey oturmasının esas olarak tünel çevresindeki malzemelerin deformasyon modülüne bağlı olduğu sonucuna varılmıştır. Deformasyon modülü kırılma ve yüzey bozuşması ile kontrol edilen kaya kütlesi kalitesi değerlendirilerek elde edilmiştir. İkiz tünel kaynaklı yüzey oturmasını tahmin eden Herzog denklemine modifikasyon faktörü olarak yeni bir formül önerilmiştir.

Anahtar Kelimeler: Avrasya tüneli, İstanbul, Sonlu eleman, Modifikasyon faktörü, NATM, Ön destek sistemi, Yüzey tasmanı, İkiz tünel

To My Dear Son, Başar who makes my life more valuable

ACKNOWLEDGEMENTS

I am heartily thankful to my advisor, Prof. Dr. Tamer Topal, who have created the irreplaceable space for me to do this thesis and improve myself as a researcher in the best possible way. I greatly perceive the freedom you have given me to find my own way and the advisement and endorsement you offered when needed.

Besides my advisor, I would like to thank the rest of my thesis monitoring committee: Prof. Dr. Nurkan Karahanoğlu and Prof. Dr. Erdal Çokça, for their wise comments and emboldening, but also for the contentful question which incented me to widen my research. Additionally, I am grateful to my thesis examining committee members: Prof. Dr. Bahtiyar Ünver and Doç. Dr. Mutluhan Akın for their constructive criticism.

Special thanks to my life, my other half, Can Barış Ağbay, whose support, encouragement, quiet patience and unwavering love were undeniably the bedrock upon which the past nine years of my life have been built.

I am greatly indebted to Oğuz Ayırga for his crucial initiative at the beginning of my doctorate study, and support to get permission of tunnel data from Yapı Merkezi Holding. Hereby, I am truly thankful to Yapı Merkezi Holding for providing tunnel data.

I would like to thank Korhan Demir for answering my questions about tunnel data in the progress of this thesis and Karim Yousefibavil for helping to understand the packaged software stages.

I appreciate the financial support of The Scientific and Technological Research Council of Turkey – TÜBİTAK during my doctorate study with the National Scholarship Program for the Graduate Students.

TABLE OF CONTENTS

APPENDICES

LIST OF TABLES

TABLES

LIST OF FIGURES

FIGURES

CHAPTER 1

INTRODUCTION

Nowadays, inner city traffic load has augmented because of densely populated area and transportation troubles. This causes to use of subway transportation systems such as metro tunnels. Even though they have many advantages, tunnel construction may bring about undesired effects on civil structures, particularly through weak materials or many existing structures. Some of these disadvantages of tunneling may cause major ground deformation and groundwater level variation. Therefore, safe tunnel design and construction requires the following items:

1-Stability: Ground characteristics should be considered while opening the tunnel.

2-Surface deformation: Surface structures above tunnel may be affected by excavation induced deformation, this effect should be considered during design stage.

3-Effectivity of supports: Temporary or permanent tunnel support should have sufficient capacity against the existing load. Hence, it is vital to understand the current loads before the support is applied (Mair and Taylor, 1996).

Underground tunnel going through congestion of inner city, in sites which has not sufficient spaces for geotechnical investigations, and also in sites with unconsolidated sediments can induce a number of difficulties for engineers. Therefore, much more time and cost should be spent for these issues during excavation works. Mitigation of ground deformation is one of the main issues for inner city tunnel construction (Fowell, 2003).

1.1. Research Statement

Istanbul's transportation infrastructure needs significant investment and improvement. Together with rapid population growth and economic development lasting for many years; considerable pressure has been added on the existing transport system. The transportation between the two continents has become a major issue with the three existing bridges presently operated over their capacities as evidenced by severe daily delays in crossings over the Bosphorus. The Eurasia Tunnel Project is planned to alleviate this pressure by providing a fourth road crossing of the Bosphorus and bringing essential benefits to passengers in Istanbul.

Researchers and designers generally use pre-support techniques for underground excavation and these are divided into two fundamental techniques: (i) support employed in surrounding area of the crown above the face and (ii) face support (Kumar and Prasad, 2016). The pre-support techniques become very important for inner-city shallow tunnels especially while applying New Austrian Tunneling Method (NATM) which requires some deformation to relieve the stress. Previous studies about assessing the magnitude of maximum surface displacements caused by NATM-twin tunneling do not include the decreasing effect of the pre-supporting. Moreover, established empirical equations were mostly obtained by using data from tunnel passing through clayey soil. In comparison, Herzog's equation gives higher maximum ground settlements than those measured in the field.

The purpose of this study is to introduce a detailed procedure for obtaining modification factor based on pre-supporting techniques and rock mass quality, which can be used as a reduction ratio in an existing equation for calculating maximum surface settlement above openings of twin tunnel structures based on the real surface settlement data obtained from the Eurasia Tunnel NATM Part.

To complete the course of action, a number of specific tasks were completed; i) performing numerical analysis on the selected 12 cross section lines along tunnel alignment to update the ground profile in which there is no borehole drilled and to approximate the results of numerical models to actual field measurements in terms of

maximum surface settlement, and ii) conducting parameter study in which the distance between pipes in the pre-support systems was used as a variable, iii) obtaining a statistical formula that presents the decreasing effect of pre-support system on maximum surface settlement.

1.2. Location of the Study Area

The Eurasia Tunnel Project is located between Kazlıçeşme and Göztepe along a 14.6 km route including a total 5.4 km twin-tunnel that crosses the Bosphorus under the seabed, with an aim to alleviate Istanbul's transcontinental traffic load. Additionally a road tunnel to cross the Bosphorus, The Eurasia Tunnel Project also includes the enhancement and broadening of current roads that lead to the tunnel on both sides of the Bosphorus for 9.2 km in total. In this study, data are coming from the part of Asia NATM tunnels that join the Asia Transition Box (ATB) at km: 9+520. The twin tunnels are about 900 m and 1000 m long at Westbound and Eastbound directions, respectively and they end at two portals at the Asian side. Approximately 11 m diameter tunnels are roughly elevated by 30-40 m towards the Asian direction. Depth from the ground surface to the tunnel axis varies from average 31 m (ATB) to 16 m at the Asian side. The two tunnels follow parallel routes 25 m apart till km: 9+990 and then separated (Figure 1.1).

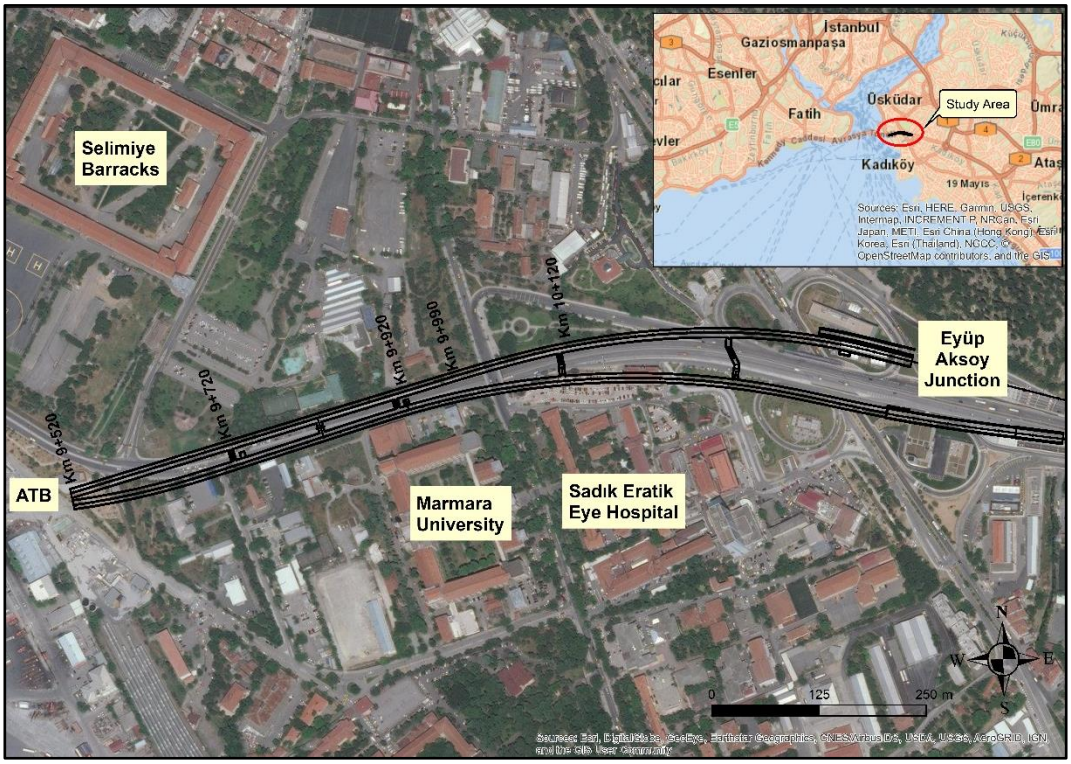

Figure 1.1. Site plan of NATM part of the Eurasia Tunnel

1.3. General Geology of the Study Area

Carboniferous aged Trakya formation and Cretaceous aged volcanics are observed in the investigation site. Geological properties of the geological units are explained at the following section.

1.3.1. Trakya Formation

The Trakya formation comprises of intercalated sequences of sandstone, shale, mudstone and siltstone. They are characteristically dark grey-green or greyish-brown owing to weathering. Sandstone is the most abundant rock type in this formation, and limestone and conglomerate interbeds, and lenses are found between the layers. The thickness of the Trakya formation varies between 600 and 1700 meters (Eroskay, 1985). They are believed to have been deposited by submarine turbidity currents and generally from marine origin (Pettijohn, 1972).The Trakya formation is usually

exposed in the west of Istanbul, particularly in Ikitelli, Cebeciköy, Şişli, Beşiktaş, Levent and Gaziosmanpaşa. Greenish brown andesite and diabase dykes, up to 10 m thick, are widespread in the study area, and generally follow a NW-SE direction. Dips are between 65^{o} and 85^{o} and in NE-SW direction. When they are fresh, they can be easily identified in the field. However, in the highly weathered conditions, yellowish brown dykes can only be distinguished with difficulty from the greywackes (Eroskay, 1985). The Trakya formation ranges in age from late Tournaisian to late middle Visean (Carboniferous). The Trakya formation is highly fractured, faulted, folded, and is also weathered especially along the discontinuities. The major structural characteristic of the area are NW-SE and NE-SW trending faults. Dense crack surface developments are examined and rock masses are entirely fractured in same places. Usually, three or four clearly defined major sets of joints are determined. Minor sets or random joints also occur in study area. The strike directions of the joints are almost NW-SE and NE-SW.

1.3.2. Volcanic Dykes

It is known that numerous andesitic and diabasic dykes and sills are observed in the Palaeozoic rocks in the İstanbul region. The dykes in this region are yellow to beige and green, highly fractured and massive. Locally cataclastics were observed along the contacts of the dykes with the surrounding sedimentary rocks. Dyke thickness has a range of 10-20 cm to 10-11, but due to the deformation and the exposure condition of the dykes, they cannot be followed for long distances along the strike.

1.3.3. Artificial Fill

Artificial fill is encountered with thickness of 7.00 m – 8.00 m in the area that is found on D-100 highway. Thickness of the artificial fill is 4.00 m in the west area. In other areas, thickness of the artificial fill reaches 2 m. It is identified that these were of sandstone and mudstone origin. The artificial fill is encountered as embankment on the slopes.

1.4. Research Methodology

This study focuses on introducing a detailed procedure for obtaining modification factor including the effects of pre-support system and of rock mass quality and which can be used as a reduction ratio in prediction methods used for twin tunnel induced surface settlement.

Therefore, firstly, geotechnical parameters, normally obtained from laboratory and field tests, were determined properly. However, in the scope of this project, laboratory and field tests were not sufficient, various codes, standards and state-of-the-art reports were considered. Since granular soils are not suitable for sampling in routine site investigation work, field tests were used to determine their engineering properties like strength and compressibility. In this study, standard penetration test (SPT) is the main source for correlations. Few pressuremeter tests (PMT) are available. Laboratory tests were performed on some of the samples. Borehole logs and descriptions, core photographs, laboratory and field tests have been studied to determine the rock profiles and the rock mass characteristics. Most profiles are composed of sandstone, sandstone/mudstone and mudstone layers. Occasionally there are diabase layers. The Geological Strength Index (GSI) system approach has been found appropriate to use in the interpretation of the geotechnical properties of the rock masses relevant to design of temporary support system for tunnel excavation and reinforced concrete lining in the long run. GSI was introduced to estimate the reduction in rock mass strength for different geological conditions. It gives a GSI value estimated from rock mass structure (blocky, block size description etc.) and rock discontinuity surface condition. The direct application of GSI value is to estimate the parameters in the Hoek-Brown strength criterion for rock masses. Sandstone and mudstone have been separated into sub-units in terms of RMR and GSI values, namely; sandstone units S0, S1, S2, S3 and mudstone units M0, M1, M2, and M3. Moreover, rock mass quality was found for the mudstones and sandstones as poor to fair categories. Geotechnical parameters of these sub-units were determined by considering both RocLab results and literature correlations, and wise engineering judgment of them.

Secondly, finite element program Phase[2] (Rocscience, 2012), with Mohr-Coulomb elasto-plastic material model was used to model the rock mass behavior. Axisymmetric finite element analysis was performed in this thesis. Axisymmetric models were executed in the plane-strain analyses to determine the factor of relaxation. Since the tunnel length in third dimension is extremely large according to the tunnel cross section, the two dimensional plane-strain model was utilized to simulate the tunneling. In the numerical model, the material softening method was utilized to specify the amount of distortion before installation of rock support (Swoboda, 1979; Swoboda et al., 1994, Vlachopoulos and Diederichs, 2009). Tunnelling was modelled by removing the elements inside a tunnel boundary. The top heading, bench and invert excavation orders were applied in the plane-strain analysis. Twelve cross section lines were selected along the tunnel alignment to perform numerical analysis according to sufficient number of field measurement points (at least 5 points) representing each of the twin tunnels and at the location where distance between tunnels are within the range of active tunnel interaction and avoiding pocket tunnel (Figure 1.2).

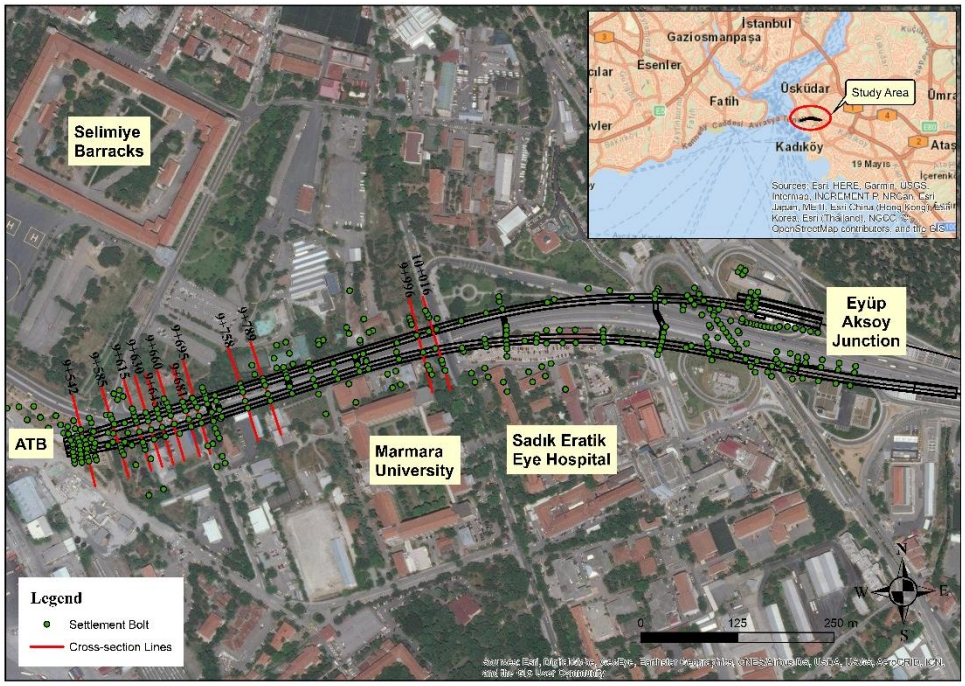

Figure 1.2. Site plan of NATM part of the Eurasia Tunnel with twelve cross-section lines

The third step was to conduct parameter study in which the distance between pipes in the pre-support systems was used as a variable. It was performed to get the relation between percent decrease in maximum surface settlement and distance between the pipes in forepole and umbrella arch systems. This correlation was then tested whether it was statistically significant or not. Then this obtained relation was accepted as modification factor (i.e. reduction ratio) in terms of pre-support effects for an existing prediction equation of twin tunnel induced surface settlements.

Flowchart of research methodology adopted in this thesis is presented in Figure 1.3.

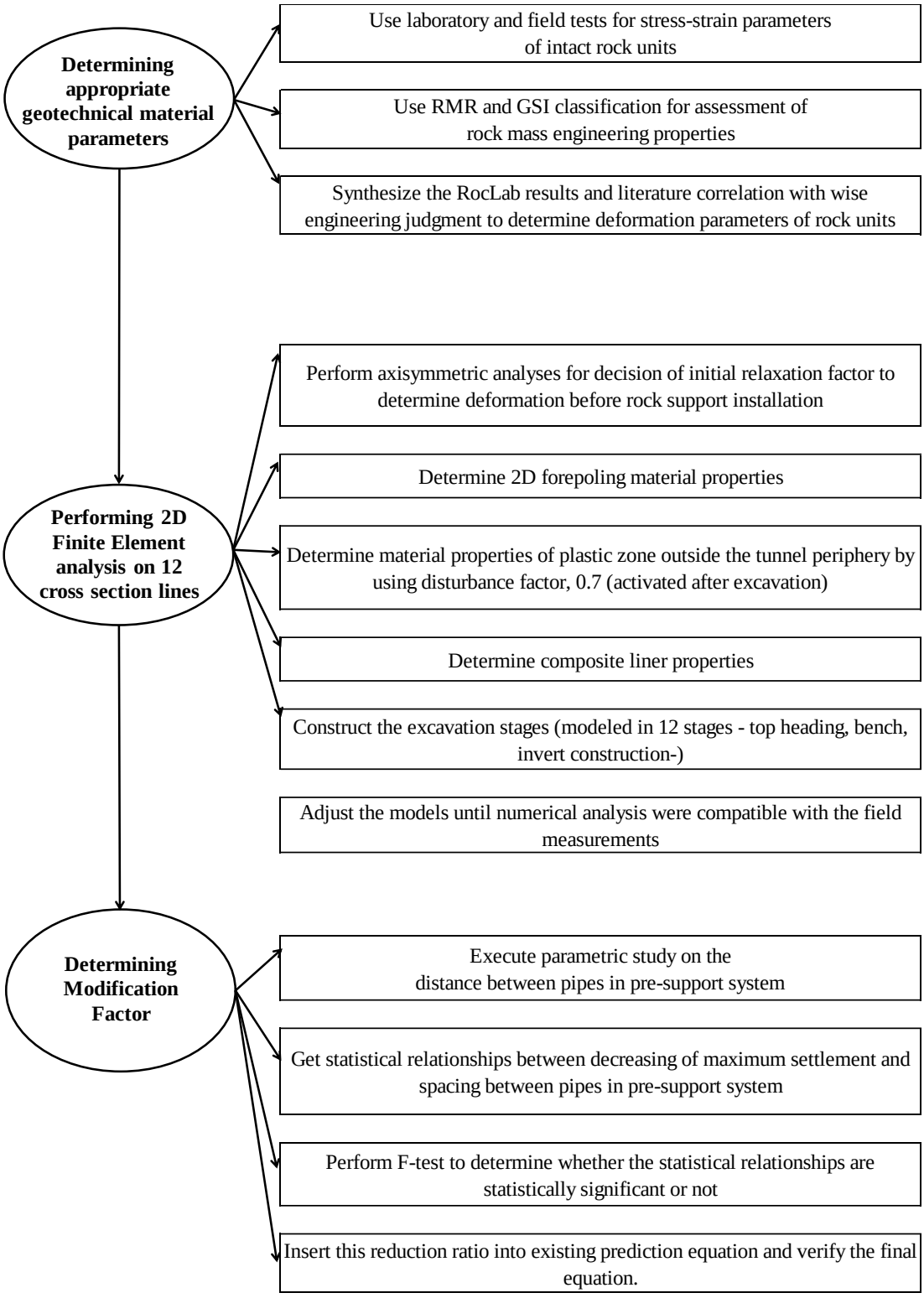

Figure 1.3. Flowchart of research methodology

1.5. Thesis Outline

A review of previous researches about tunnel induced settlement prediction methods, numerical analysis of tunnel construction and pre-support issues were presented in Chapter 2.

In Chapter 3, geotechnical investigations were discussed. Field and laboratory testing were presented in terms of theory and application. Rock mass classification and rock mass strength determination are also discussed to determine geotechnical design parameters for rock.

Chapter 4 supplied information about Finite Element Analysis and related program Phase^2 2D. It is comprised of the primary topics of the research which involve finite element analysis (2D), evaluation of the geotechnical parameters utilized in computations and application of the 'step-by-step' excavation. Moreover, the axisymmetric analysis performed in Phase^2 was scrutinized and the output of analyses were interpreted.

Results and discussions were presented in Chapter 5; it includes the outcome of maximum settlement calculated by previous formulas. Then parameter study was performed using 12 cross sections to determine modification factor.

Chapter 6 concluded the thesis and some recommendations were given in this chapter.

CHAPTER 2

LITERATURE REVIEW

Assessment of ground settlements and their effects on above structures are essential stage in the design of tunnel structure. The surface settlement trough is the manifestation of the movements from around the tunnel cavity. Several methods and approaches are now obtainable for evaluating the direction and relative magnitude of surface displacements caused by tunneling.

2.1. Prediction Methods for Single Tunnel Induced Surface Settlement

2.1.1. Empirical Methods

Empirical method supplies the easiest computation and hence widely utilized in functional practices.

The form of the surface trough above an underground tunnel construction was firstly analized by Martos (1958) who offered that ground settlement could be corresponded by a Gaussian or normal distribution curve.

Peck (1969) proposed a resemble shape of transverse trough that appears above single tunnels for ground movements and confirmed by many site investigations and centrifuge tests (Figure 2.1). The semi-empirical approach has been adopted for computing ground deformation based on Equation (2.1);

$$S_V = S_{max} exp\left(-\frac{x^2}{2i^2}\right) \quad (2.1)$$

where;

Sv is the value of settlement,

Smax is the theoretical maximum settlement at the tunnel center-line,

x is the lateral distance from the tunnel center-line, and

i is the lateral distance from the tunnel center-line to the point of inflection in the Gaussian distribution curve.

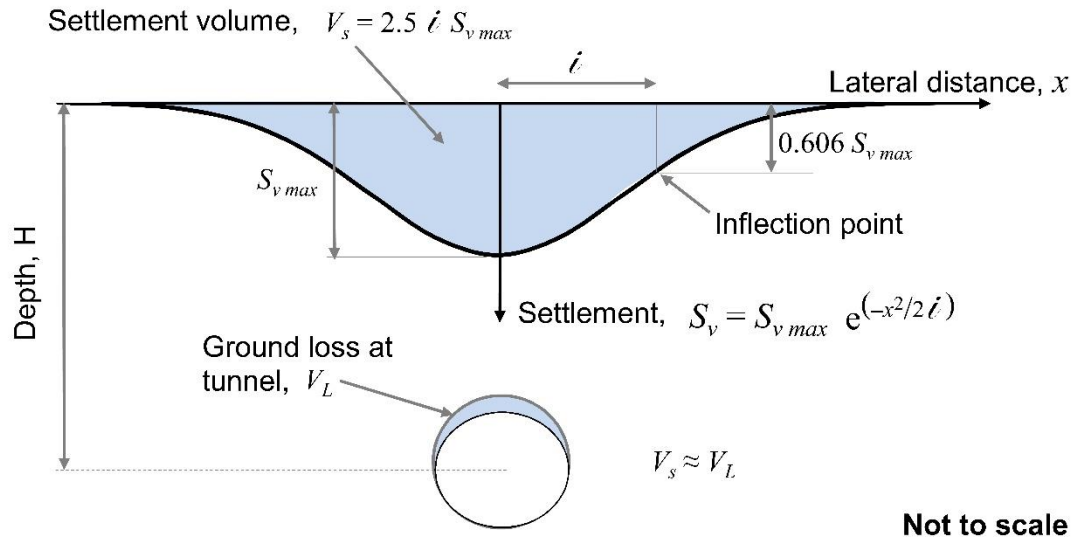

Figure 2.1. Properties of Gaussian functions used in prediction of surface settlement (Peck, 1969)

Due to the nature of the cutting process the bored shape of a tunnel will always be larger than the final shape creating a set of displacements towards the cavity. This phenomenon has been described by the term “ground loss” or, the more often used, ‘volume loss’ (Peck, 1969).

Peck (1969) defined that the ground settlements were radial displacements in the direction of the cross section and longitudinal deformations on the tunnel axis (Figure 2.2). These two movements have proven difficult to separate, and therefore, assessments of volume loss have been determined by considering a plane-strain scenario.

In other words, tunneling is a three-dimensional problem. For analysis purposes, some studies have separated this into two, two-dimensional problems (Figure 2.2).

These are the transverse settlement trough (x-z plane, referred to as the plane-strain scenario) and the longitudinal settlement trough (y-z plane).

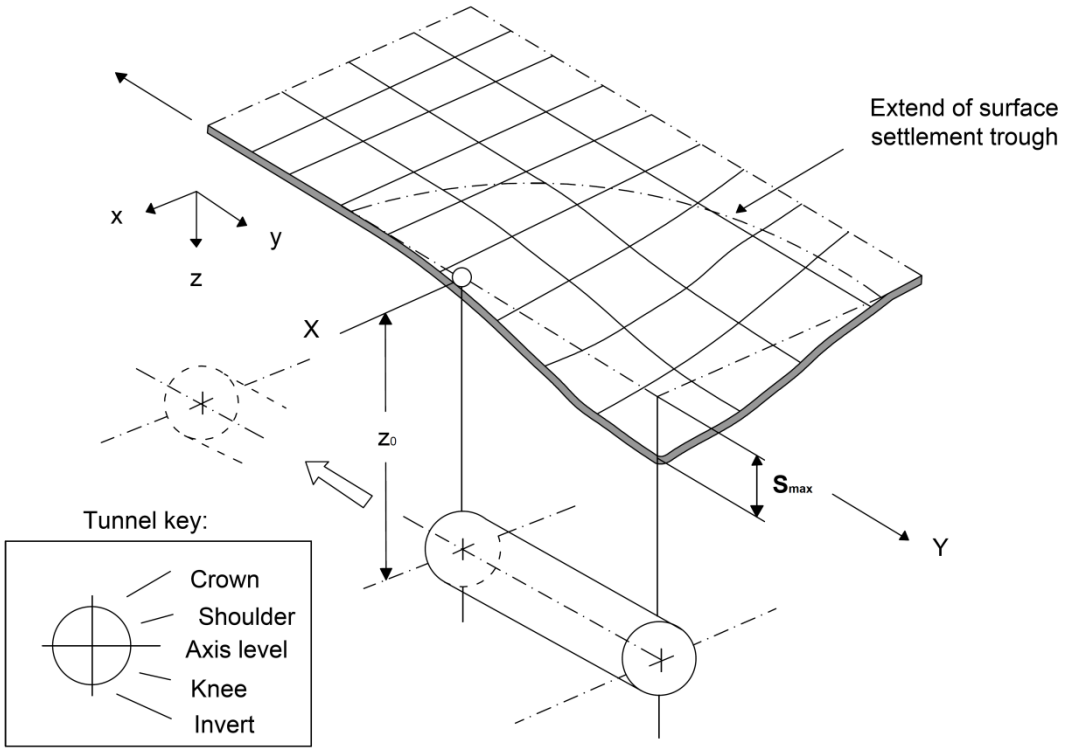

Figure 2.2. Settlement above a progressing tunnel heading (Attewell and Yeates, 1984)

Methods of tunnel construction fall into one of two categories. Mair & Taylor (1997) defined them as an open face (i.e. New Austrian Tunneling Method, NATM) and a closed face (i.e. tunnel boring machine, TBM) tunneling, where open faced tunneling has easy entree to the tunnel face and closed face tunneling utilizes a face support technique.

For open face tunnels (Figure 2.3) the main reasons of settlements can be specified as:

A. The ground movement towards the non-supported tunnel face.

B. Radial ground movement towards the primary liner.

C. Long term radial ground movement towards the liner.

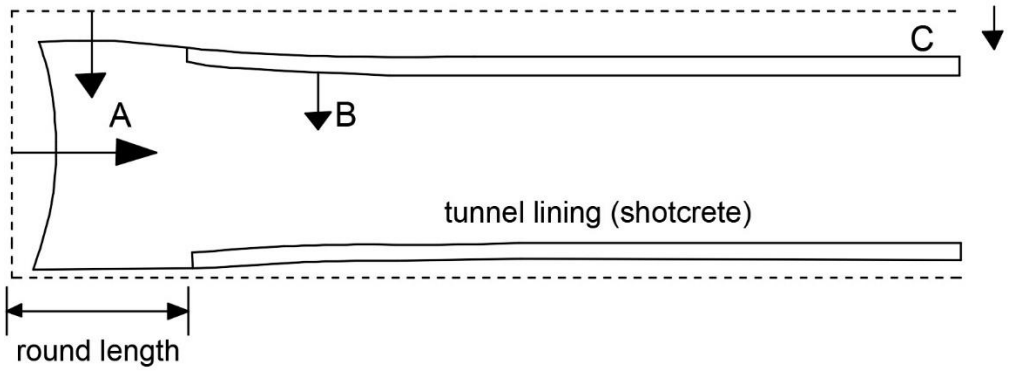

Figure 2.3. Principal components of ground deformation: top view of open face tunneling (modified from Elmanan and Elarabi, 2015)

In general, the long-term settlements occur because tunnels act like drains (it is considered here that tunnel lining is impermeable relative to surrounding ground). In the short-term, the volume loss around a tunnel opening should be similar to the volume of the surface settlement profile. This is mainly due to difficulties in gathering field measures around the tunnel opening whereas measurement of surface displacements is relatively straight forward. It is usual to denote these two volumes as:

V_T is volume of 'ground lost' around the bored tunnel and

V_S is the volume of surface settlement trough.

Therefore, in the undrained case $V_T = V_S$, and V_L is volume loss usually expressed as a percentage of the tunnel cross-sectional area. The volume of the ground settlement profile can be obtained by;

$$V_S = \frac{V_L}{100}\left(\frac{\pi D^2}{4}\right) \tag{2.2}$$

where D is the bored tunnel diameter.

Integrating Equation (2.1) twice shows the relationship below;

$$V_S = \sqrt{2\pi} \cdot i \cdot S_{max} \tag{2.3}$$

where V_S is volume of surface settlement.

In order to determine the magnitude of settlements, Equation (2.2) and Equation (2.3) can be combined to produce Equation (2.4);

$$S_{max} = 0.313 \frac{V_L D^2}{i} \tag{2.4}$$

where V_L is volume loss in percentage, and D is the bored tunnel diameter.

S_{max} controls the magnitude of the settlement trough and i (or trough width) determines the extent.

V_L is ground loss and calculated from equation $V_L = \pi * u * D$ where u is given in Equation (2.5).

$$u = \frac{D}{2} \cdot \left(\frac{1+\vartheta}{E_y}\right) \cdot (P_ş + \gamma \cdot Z_0) \tag{2.5}$$

Where D is tunnel diameter, ν is poisson's ratio, E_y is deformation modulus around tunnel periphery, γ is unit weight of material around tunnel, Z_0 is tunnel depth.

The other parameter which has an effect on the maximum settlement is settlement trough width, i which is closely related to the deformation modulus of tunneling medium and deformation modulus is dependent on the lithology, weathering, joint condition of rock medium. Therefore, in the literature, i value is generally related to tunnel depth and tunnel diameter and widely used formulas for i are given in Table 2.1.

Table 2.1. Equations for *i*-value proposed by several authors

Autor	***i - value***	**Remark**
Peck (1969)	$\frac{i}{R} = \left(\frac{z_0}{2R}\right)^n$ n = 0.1 to 0.8	Based on field observations
Atkinson and Potts (1977)	i = 0.25 (z_0 + R) In case of loose sand i = 0.25 (1.5z_0 + 0.5R) In case of dense sand and over consolidated clay	Based on field observations
O'Reilly and New (1982)	i = 0.43z_0 + 1.1 In case of cohesive soil i = 0.28z_0 - 0.1 In case of granular soil	Based on field observations of UK tunnels
Mair (1993)	i = 0.5z_0	Based on field observations worldwide
Clough (1981)	$\frac{i}{R} = \alpha\left(\frac{z_0}{2R}\right)^n$ a= 1 and n= 0.8	Based on field observations of USA tunnels
Arıoğlu et al. (2002)	i = 0.38 Z_0 in case of limestone-marn, consolidated clay	Based on field observations of İstanbul-Mevhibe İnönü tunnel
Arıoğlu et al. (2002)	i = 0.40 Z_0+ 1.92	Based on field observations of İstanbul-Mevhibe İnönü tunnel
Arıoğlu et al. (2002)	(2i/D) = 1.181 $(Z_0/D)^{0.78}$	Based on field observations of İstanbul-Mevhibe İnönü tunnel
Chakeri (2012)	i = 0.6054 (0.87Z_0 + 0.13D) - 2.8562	Based on results of numerical analysis
Note: z_0 , is the tunnel depth below surface and R is the radius of the tunnel		

Short term settlement (undrained case) was more drastic than long term consolidation settlement (Sugiyama et al., 1999). It is observed that quantification of the long term settlements above tunnel is influenced by creep behavior of the clay, and the main

support used in the tunnel excavation phase could be roughly modeled by the tunnel periphery with permeable flow. Moreover, the behavior of long-term surface deformation includes a combination of consolidation, ground stress relief and creep (Wang et al., 2012).

The prediction of sub-surface displacements and their effect on underground services is commonly based on extrapolations from surface measurements (Figure 2.4).

Wu and Lee (2003) have performed a number of centrifuge model tests of unlined single and parallel tunnels with plane strain condition to investigate the surface settlement, especially subsurface settlement trough. A shallower tunnel produces a narrower surface settlement trough at a depth of z_0 and it could be regarded as the surface settlement trough induced by a tunnel embedded at the shallower depth of (z-z_0). Therefore, Equation (2.7) is applicable for determining subsurface settlement trough and i_0 is width parameter and $S_{max,z0}$ is maximum subsurface settlement of the subsurface settlement trough.

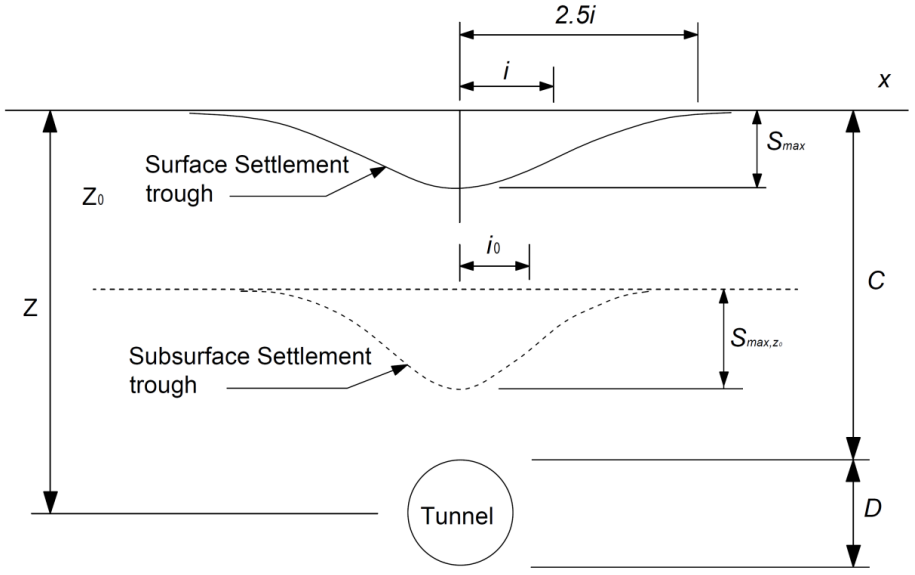

Figure 2.4. Surface and subsurface settlement troughs (Mair et al., 1993)

$$\frac{i_0}{z} = 0.29 \times \left(1 - \frac{z_0}{z}\right) + \frac{D}{2z} \tag{2.6}$$

and

$$\frac{S_{max,z_0}}{D} = 0.00327 \times \left(\frac{z-z_0}{D}\right)^{-0.43} V_L \quad (2.7)$$

Subsurface movements are prone to be of higher order of magnitude than ground settlements, particularly in deeper tunnels with dense soils. On the contrary, deformation in unconsolidated or compressible materials may be greater at the ground level than at the tunnel level. A transparent soil model which is developed to examine both the tunnel induced surface deformation profile and also settlement distribution of soil around the tunnel (Ahmed and Iskander, 2011).

Hajihassani et al. (2013) concluded that the geotechnical properties of soil play a crucial role in planning, designing and constructing a tunnel. The surface and subsurface deformation can be influenced by the types of soil, for example, clayey soils create higher settlements than other types of soil. For instance, in greenfield condition, the relative density of sand and cover to diameter ratio affect the surface settlement (Marto et al., 2015). Lee and Rowe (1989) observed that the ratio of independent shear modulus to vertical modulus controlled the settlement trough form. Moreover, they noted that the surface deformation was not much affected by soil stiffness anisotropy in terms of the stiffness ratio and Poisson's ratio because of tunneling in soft clay in which soil plasticity controlled surface settlement.

Fattah et al. (2012) stated that there are major inequalities between empirical solutions to determine surface settlement trough because of different comments and database collection by different researchers. Moreover, a major trouble is the incompatibility of soil condition and applicability of the empirical formulas to different types of soils.

The empirical techniques to estimate surface settlement propose the ground surface settlement trough similar to normal distribution. In addition, this method cannot deal with complicated ground conditions and other factors causing settlement because of containing limited parameters. There are some crucial limitations of this technique such as excavation methods, unsuitability to a variety of ground conditions,

subsurface settlements and horizontal movements. Moreover, they cannot produce solution of tunnel with liner (Yahya and Abdullah, 2014).

2.1.2. Analytical Methods

Verruijt and Booker (1996) derive a implicit formula by utilizing homogeneous, isotropic and elastic half space equations. These equations comprise some effects of the tunnel deformation and compressibility of the soil (first suggested by Sagaseta, 1987). The tunnel deformation described consists of radial contraction and shape ovalisation (Figure 2.5).

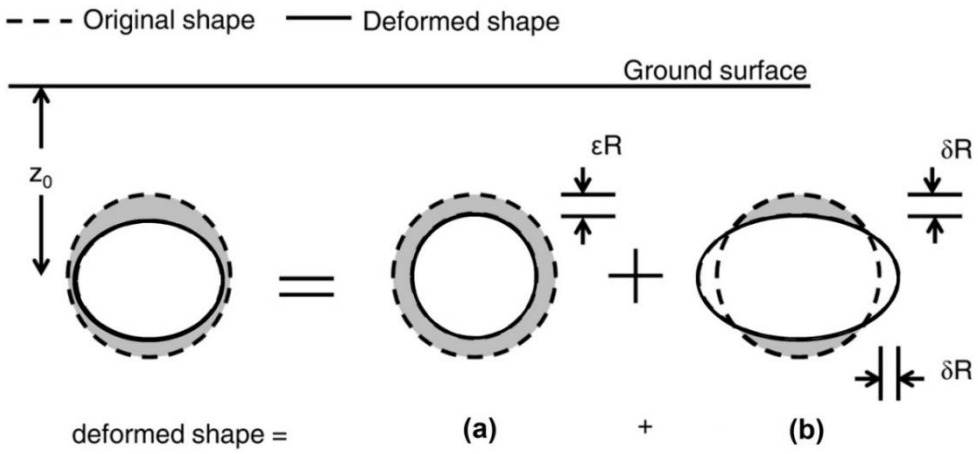

Figure 2.5. Deformed tunnel shape given by (a) ground loss and (b) ovalisation (after Verruijt and Booker, 1996)

Compressible soils require a value of Poisson's Ratio, *v*, less than 0.5. Verruijt and Booker (1996) estimate settlement by;

$$S_V = 4\varepsilon R^2(1-\vartheta)\frac{Z_0}{x^2+Z_0^2} - 2\delta R^2\frac{Z_0(x^2-Z_0^2}{(x^2+Z_0^2)^2} \quad (2.8)$$

where the radial strain was given by;

$$\varepsilon = \frac{V_s}{4(1-\vartheta)} \quad \text{Sagaseta (1987)} \quad (2.9)$$

and the ovalisation ratio was given by;

$$\delta = \frac{U_R}{R} \qquad \text{Verruijt and Booker (1996)} \qquad (2.10)$$

and U_R is the radial deformation around the tunnel diameter.

Verruijt and Booker (1996) considered the uniform radial ground movement around the tunnel for the short-term undrained condition, the predicted settlement troughs are wider and horizontal movements are larger than observed values. In practice the radial ground movement around the tunnel is not uniform but oval-shaped. Therefore the previous methods must be adjusted to incorporate the non-uniform radial ground movement around the tunnel (Park, 2004). For the short-term undrained conditions in the soft ground (k=1 and v_u=0.5), the displacements can be obtained for the deep tunnel as follows:

$$u_r = -\frac{1.5}{E_u}\frac{a_0}{r} \text{ and } u_\theta = 0 \qquad (2.11)$$

and for a shallow tunnel

$$u_r = -\frac{1.5}{E_u}\left(\frac{a_0}{r} + \frac{\gamma a_0^2}{2}\ln r\, sin\theta\right) \qquad (2.12)$$

$$u_r = -\frac{1.5}{E_u}\frac{\gamma a_0^2}{2}(1 + \ln r)cos\theta \qquad (2.13)$$

where E_u = undrained Young's modulus, r is the distance from tunnel centerline to the tunnel boundary, θ is the polar coordinate angle from tunnel centerline, a_0 is the tunnel radius.

Loganathan and Poulos (1998) proposed an analytical method based on shallow tunnel volume loss cases due to the fact that Verruijt and Booker (1996) under-predict the maximum settlement. The reasons why the authors gave for this were that soil exhibits non-linear behavior and therefore the ground movement at the tunnel soil interface was not realistic. Loganathan and Poulos (1998) considers the situation when the ovalisation, δ, had been equal to zero i.e. there is no deformation of the

lining. Loganathan and Poulos (1998), therefore, attempted to model construction conditions generated by a TBM method and compared this ground movement monitoring data taken during construction of the Heathrow Express Trial Tunnel. This method uses a 'gap' parameter (originally from Rowe et al., 1983) which defines the ground displacements prior to the installation of the lining. Gap parameter will be explained in the following paragraphs.

Consideration must be given to two key factors influencing possible deformation near the tunnel support in modeling tunnel opening. Foremost, disturbed soil zone around tunnel will be produced by tunnel induced local stresses. The limit of this zone will rely on labor and excavation factors such as rate of advance and shield performance. Consolidation of this disturbed zone will bring about a volume decrease of the soil unit, therefore supplying extra space for settlement of the overlying soil.

Secondly, soil in front of the tunnel face will move both axially and radially towards the heading with the progress of the tunnel machine (Peck, 1969). Thereby the soil that forms the final cut surface of the tunnel will have originally been placed at some greater distance from the tunnel axis. The volume between the final cut surface and the initial position of this soil represents a loss of ground. Extra loss of ground is represented by the radial void which is the difference between the tunnel diameter and the outer diameter of the support.

The final result of these factors may be almost incorporated in plane strain analysis with respect to a space containing not only the ground loss but also volume variation of disturbed soil. The extent of this space may be stated in terms of gap parameter. If the tunnel invert stand on the underlying soil, then the gap is the vertical space between the tunnel crown and initial position of the soil directly above the crown.

The 'gap' will depend on the tunneling machine, soil type, and experience and skill of the tunneling machine operators. In Figure 2.6 the 'gap' is shown to account for the physical clearance between the outer shield and the lining (Gp), allowance for out-of-plane ground movements (u_{3D}) and allowances for workmanship (ω). Rowe et

al. (1983) assumed ‘gaps’ between 90 and 160 mm. Loganathan and Poulos (1998) proposed the following expression to predict vertical settlement;

$$S_V = 4V_L(1-\vartheta)R^2\frac{z_0}{z_0^2+x^2}exp\left(-\frac{1.38x^2}{\left[z_0^2+R^2\right]^2}\right) \quad (2.13)$$

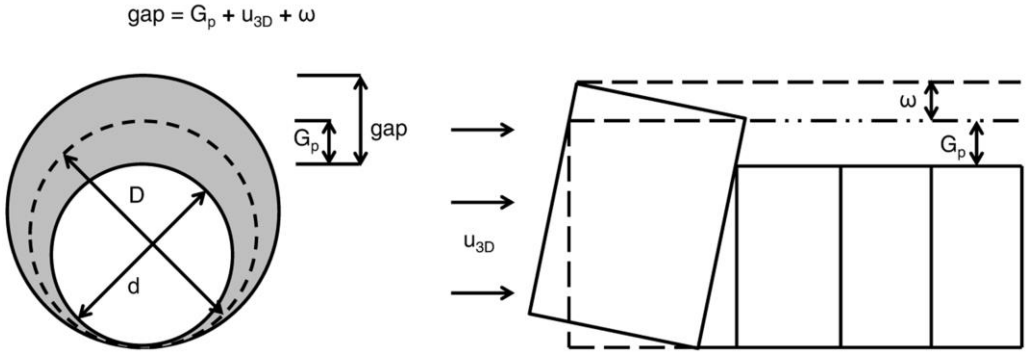

Figure 2.6. Definition of Gap parameter (after Rowe et al., 1983)

Franza and Marshall (2015) stated that the analytical solution reveals poor prediction of subsurface displacements of tunnels in sands due to the assumption of a mean compressibility parameter that neglects the complex volumetric strain mechanism above tunnels in sands.

The analytical solution is obtained for a specific case and problem. It is not suitable for all types of the case and cannot be interested in complicated condition which is a limitation of analytical method, because the ground environment, the mechanical and physical characteristics of rock and soil, the tunnel geometry are different in studied areas (Yahya and Abdullah, 2014). However, Pinto et al. (2014) showed that the analytical predictions can achieve very good representations of the distribution of far field deformations induced by tunnels.

2.2. Prediction Methods for Twin Tunnel Induced Surface Settlement

A number of prediction methods have been outlined up to this point in order to estimate the tunneling-induced movements from single tunnel arrangement. Relatively little literature documenting the behavior regarding twin tunnels and their interaction has been published. It is because of this reason perhaps that few prediction methods exist (Dival, 2013).

If tunnels are assumed to be parallel then it could be stated that, usually, three twin tunneling arrangements exist. 2D idealizations are shown in Figure 2.7. It can be seen that within these three variations "side by side" geometry means that multi-tunnels have been excavated at the same horizontal level. Stacked/Piggyback structure is composed of vertically consecutive multi-tunnels. Offset can be defined as middle of the Side-by-side and Stacked layouts (Dival, 2013).

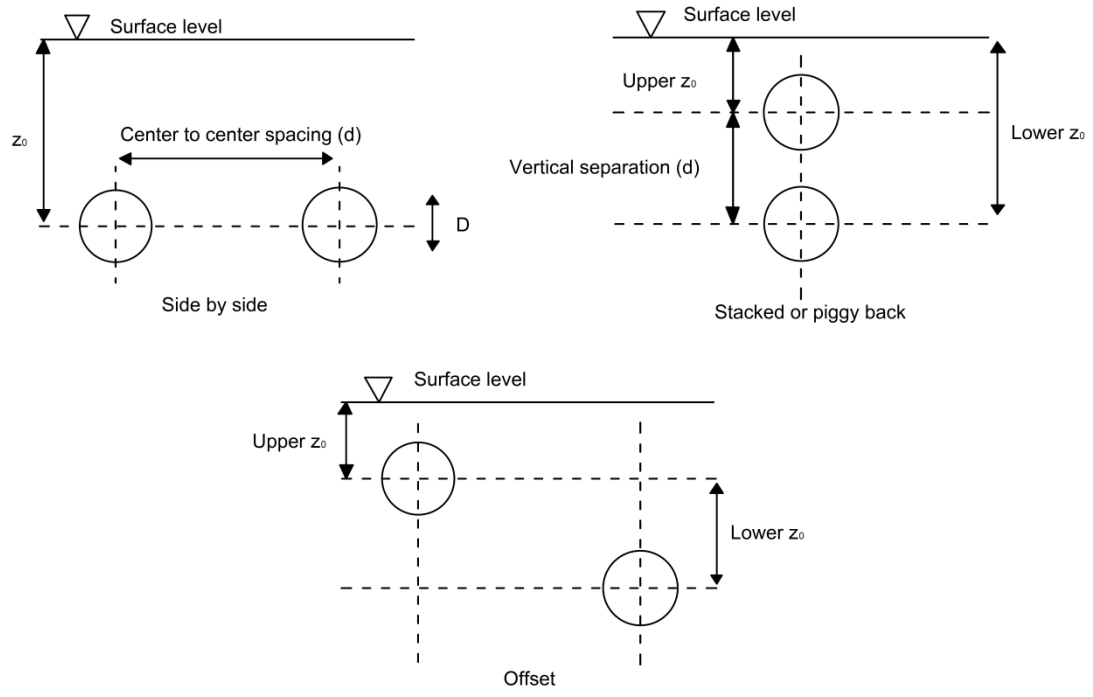

Figure 2.7. Idealizations of the three twin-tunneling cases in the y-z plane (Divall, 2013)

Empirical and analytical methods do not include the interaction effects of twin tunnels. Relative separation and soil properties are the most important parameters while analyzing the twin tunnel interaction. Wang et al. (2003) have studied on the interaction of twin parallel tunneling by using numerical analysis and concluded that for the relative separation (spacing between tunnels / tunnel depth) is larger than 3, the interaction can be ignored for shallow tunnels (tunnel depth / diameter < 5). The deeper the tunnel, the less the interaction is. Moreover, soil properties heavily affect the pattern of ground settlement.

It was stated that the excavation of the lag tunnel produces extremely larger settlements due to decreasing stress caused from the construction of the lead tunnel while considering parallel tunnel arrangement (Peck, 1969).

Mahmutoğlu (2010) proposed that fluctuations in the settlement trough due to shield tunneling are associated with not only the ground deformation but also the type and thickness of the rock above tunnel opening.

Chapman et al. (2004) stated that data coming from selective twin tunnel cases may develop the empirical methods predicting twin tunnel induced ground settlement. On the other hand, most twin tunnel cases do not generally include settlement bolt in necessary places and are commonly produced as a total settlement trough, this means that they do not present the profile for twin tunnel tunnels separately.

A number of methods are outlined in this part for the estimation of settlement due to twin tunneling. Relatively little literature documenting the behavior regarding twin tunnels and their interaction has been published. It is because of this reason perhaps that few prediction methods exist. The complexity of any twin tunnel prediction method is further exacerbated by the near infinite possible geometric arrangements (Divall, 2013).

2.2.1. Superposition Method

It is defined as a method to estimate subsidence above any twin tunnel structure. A surface settlement prediction is produced using one of the methods used for single

tunnel induced settlement. Assuming that the second tunnel is of similar size and depth then the similar settlement trough is placed over the centerline of the second opening disregarding any effect from the lead tunnel. These two overlapping curves were summed up to describe the whole settlement (Figure 2.8).

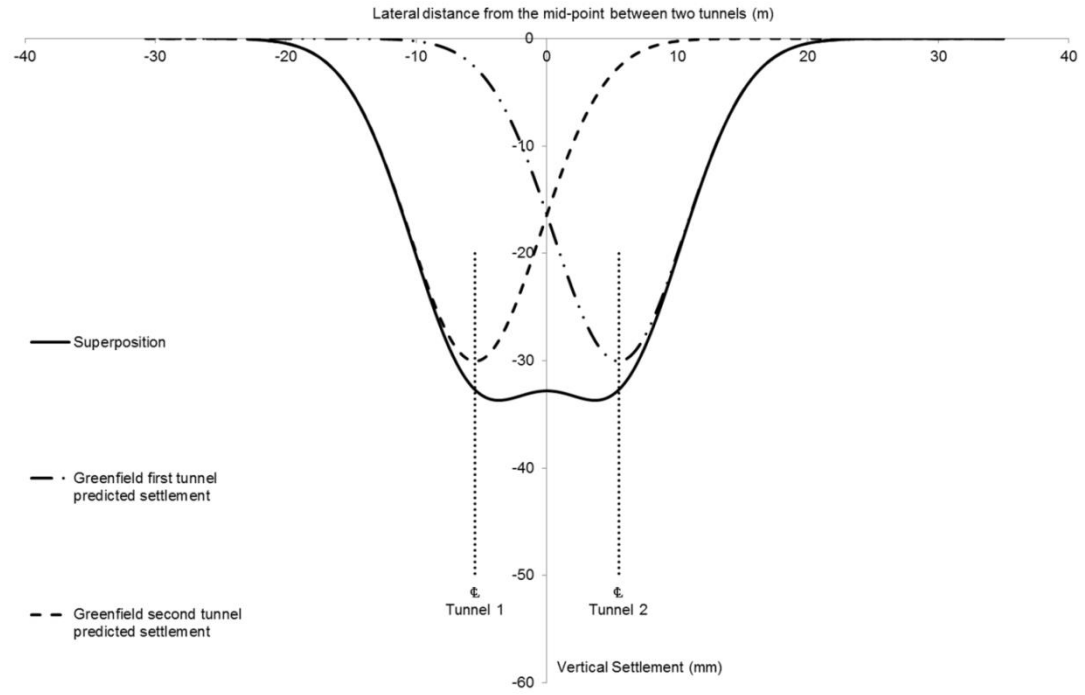

Figure 2.8. Superposition method (O'Reilly and New, 1982)

O'Reilly and New (1982) provided a formula for twin tunnels by superposition;

$$S_v = S_{max}\left[exp\left(-\frac{x_A^2}{2i^2}\right) + exp\left(\frac{(x_A-d)^2}{2i^2}\right)\right] \quad (2.14)$$

where d is the horizontal distance between the two tunnels center-lines, and x_A is the lateral distance from the center-line of the first bored tunnel.

The same tunnel diameter, volume loss and settlement trough width was considered in above mentioned equation. However, it is possible to consider different tunnel depth and width of settlement trough by widening the expression. More importantly, the tunnel interaction is indirectly disregarded in this equation.

Fang (1994) suggested that the superposition method could be used to predict the settlement trough induced by parallel tunneling if the z/D ratio is greater than 1.5 and two tunnels are spaced 1.3D apart (center to center), because the plastic zones associated with each tunnel will not overlap.

Do et al. (2014) stated that the superposition method can be used to obtain a preliminary estimation of the settlement curves above horizontal twin tunnels. Besides, they concluded that the existing tunnel is affected to a critical extent by the construction of the second tunnel. However, the existing tunnel only causes a slight impact on the new tunnel. The behavior of the new tunnel is similar to that of a single tunnel.

2.2.2. Herzog (1985)

Herzog (1985) assumed that the building site is an elastic medium, than a model would be true, which defines the volume of the settlement trough and the opening of tunnel as the same. Although the building shallow-lying tunnel in many cases is heterogeneous and anisotropic, it behaves because of the low stress - the ratio of the stress to the rock strength is generally less than 1/3 - most nearly elastic.

From the primary rock pressure (surface load p_0, unit weight γ, overburden depth $H_{ü}$ and coefficient of earth pressure λ_0=1)

$$p = p_0 + \gamma(H_{Ü} + \frac{D}{2}) \quad (2.15)$$

and the radius R=D/2 of the approximately circular opening and the deformation modulus of the rock mass E_S, in Figure 2.9 radial deformation will be assumed as

$$w = 1{,}5\, pR/E_S \quad (2.16)$$

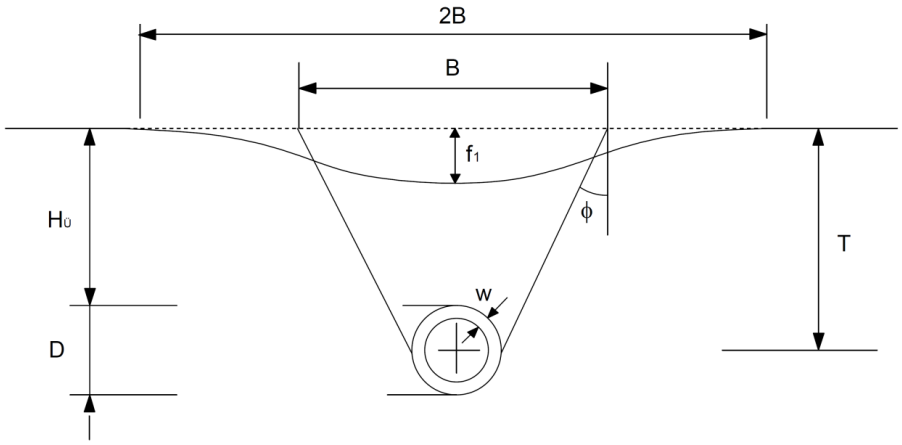

Figure 2.9. Settlement trough over a single-tube tunnel (Herzog, 1985)

With the angle of internal friction ϱ and the inclination of slip planes in the active Rankine state $=\frac{\pi}{2}-\varrho$, half of the calculated width of the settlement trough according to Figure 2.10 would be like

$$B=\frac{D}{cos\varphi}+2Ttan\varphi \tag{2.17}$$

If it is assumed that a circular path of the settlement trough and the highest value of the settlement is f, the cross-sectional area of the settlement trough would be $A_1 \approx f \cdot B$. Since it is assumed that the cross sectional area of the opening should be the same$A_2 \approx w \cdot \pi D$.

A_1=A_2 would be the expected relation between peak of the settlement trough and the ground loss at the single tunnel

$$f_1 = w \cdot \pi D/B \tag{2.18}$$

In the case of multiple tunnels with two tubes (Figure 2.10) where the spacing between tunnels is a<B, the equation for the peak of the settlement trough

$$f_2 = w \cdot \frac{2\pi D}{B+a} \tag{2.19}$$

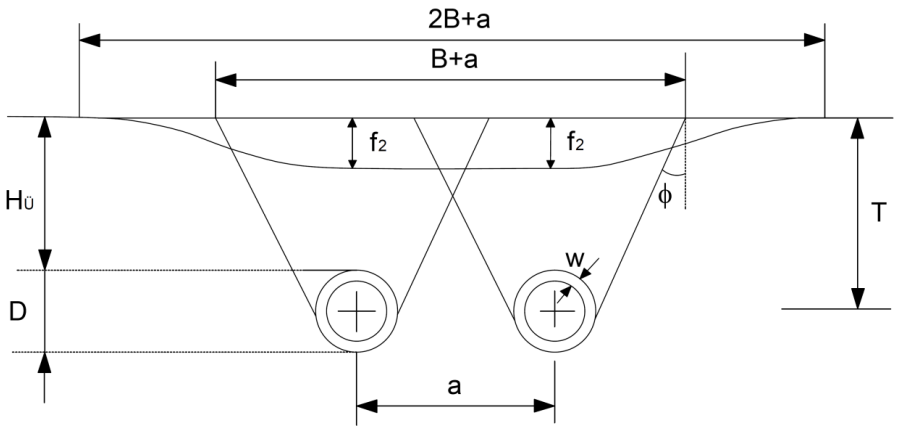

Figure 2.10. Settlement trough over a twin tunnel (Herzog, 1985)

Substituting equations (15) and (16) in equations (18) and (19), we obtain a relationship between the peak of the settlement trough and the main parameters

$$f_1 = \frac{3\pi}{4}(p_0 + \gamma T)\frac{D^2}{BE_S} \tag{2.20}$$

$$f_2 = \frac{3\pi}{2}(p_0 + \gamma T)\frac{D^2}{(B+a)E_S} \tag{2.21}$$

The largest inclination of the settlement trough is approximately (parabolic) as $n = 2f/B$.

2.2.3. Overlapping Zones

Fang et al. (1994) considered the displacements and strains associated with twin-tunneling. The work considers a disturbed zone surrounding each of the tunnels created during a construction. If the second tunnel construction generates stresses within the zone created by the first construction a 'large and irregular' volume loss could be expected. Originally from Hoyaux and Ladanyi (1970) and redrawn in Fang et al. (1994), used the finite element method to analyze the stress distribution surrounding tunnels driven through soft soils (Figure 2.11). This study indicated the plastic zone was mainly influenced by the sensitivity of the soil deposit, diameter of

tunnel and depth of tunnel. The varied sensitivity is represented by the two trends in the figure. These trends were derived from 22 twin-tunnel profiles which found the Z/R ratios varied from 3.2 to 18.1 and the d/D ratios varied from 1.3 to 2.7. However, the lag tunnel would slightly affect the lead tunnel when large spacing between tunnels exists. The authors postulated at what spacing between the tunnels can be considered large enough to avoid interaction. If the criterion of Z/R>3 has been used for insensitive clays, then the plastic zones do not overlap and the interaction is negligible. Fang et al. (1994) also state that superposition could be used to estimate settlements above parallel tunnel construction if the interaction is negligible.

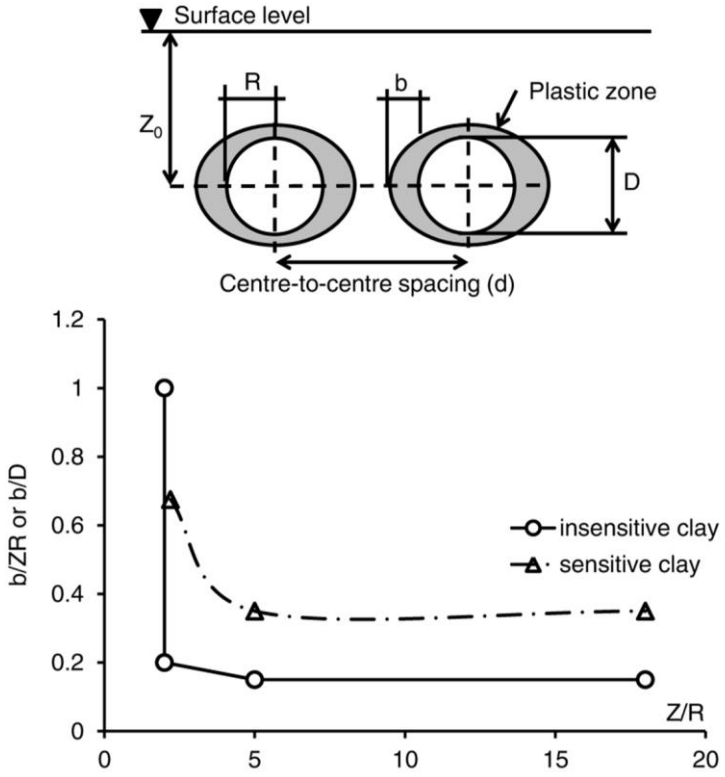

Figure 2.11. Plastic zones induced by shield tunneling in soft ground (after Fang et. al., 1994)

2.2.4. Design Plots by Addenbrooke and Potts (2001)

Addenbrooke and Potts (2001) carried out an extensive numerical study to examine the effect of a second tunnel excavation depending on an existing tunnel. A series of finite element analyses were performed using a non-linear elastic-perfectly plastic constitutive model to represent the soil. Various geometric arrangements were considered, either side by side or piggy back, and all tunnels were modeled as having equal diameters. The analysis comprised the excavation of the lead tunnel in short term and the construction of the lag tunnel in long term. When considering side by side tunnel arrangements constructed using similar methods, the form of the lag tunnel's ground settlement profile was estimated to be slightly similar to the lead tunnel. Therefore, a method to regulate the estimated settlement trough of the lag tunnel is recommended.

Two design plots were introduced to predict the twin tunnel induced settlement trough, the first one is used to get an eccentricity of the largest settlement and the second one is utilized to obtain the increment in ground loss of the lag tunnel (Figure 2.12). The charts shown that decreasing of the central spacing between the tunnels results in increasing lag tunnel induced volume loss. The increase in ground loss is presented in a multiple of ground loss from the lag tunnel construction, V_L Tunnel B, over volume loss of the first (greenfield) tunnel construction, V_L greenfield. The revised ground loss was determined to get the ground deformation for lag tunnel and then it is able to be added up with the original ground deformation for lead tunnel to estimate the whole settlement. As with the majority of the previous methods discussed, this method is only applicable to surface settlements.

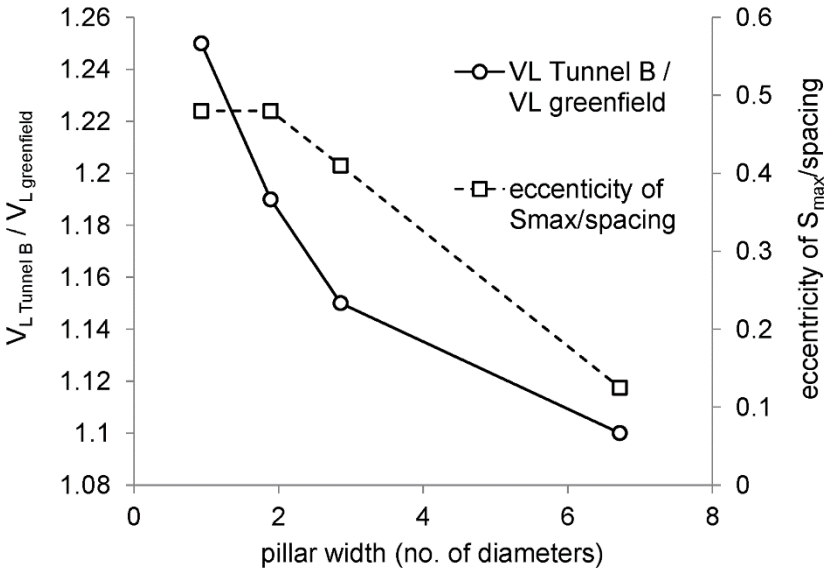

Figure 2.12. Design plots to determine an eccentricity of the maximum settlement (right) and the increment in ground loss of the second tunnel's settlement trough (left) (Divall et al., 2013 after Addenbrooke and Potts, 2001)

The design charts presented in the work are plotted in 'pillar width' parameter. Pillar width is the length of center-to-center spacing between twin tunnels and expressed as number of tunnel diameter. This allows for any possible distortion of the tunnel linings.

The chart pointed out that the lag tunnel induced volume loss becomes larger as the horizontal distance between the tunnel axes becomes smaller. The second tunnel settlements can be corrected when the modified volume loss has been found. Then, for estimating the total settlement, the revised settlements of lag tunnel can be added up with those of the original lead tunnel.

2.2.5. Modification Method by Hunt (2005)

Hunt (2005) provided a different method for predicting movements above twin-tunnel constructions. This, finite element based, study used the modeling package ABAQUS applying a small strain-stiffness model and the modified gap parameter to analyze 2D plain strain undrained tunnel constructions in London clay. Attempts

were made to examine the construction delay by involving a variation of stiffness without long-term deformation. The outcomes of these numerical analyses cause the author to propose a modification factor to the surface settlements induced by a lag tunnel. This method was confirmed by a number of case studies.

This method modified the surface settlement of the lag tunnel in an 'overlying region and this soil have been supposed to be disturbed by the lead tunnel construction. This is illustrated in Figure 2.13, taken from the study.

$$S_{mod} = F\, S_V \tag{2.15}$$

where S_{mod} is the modified settlement,

S_v is the original settlement due to the lag tunnel, and

$$F = \left\{1 + \left[M\left(1 - \frac{|d+x|}{AK_1Z^*}\right)\right]\right\} \tag{2.16}$$

where $Z^*=(z_0-z)$

A is the trough width coefficient (usually taken as 2.5 or 3)

d is the center-to-center horizontal distance of the tunnels,

K_1 is K-value in the zone of the lead tunnel, and

M is the greatest modification factor specified by Chapman et al. (2006).

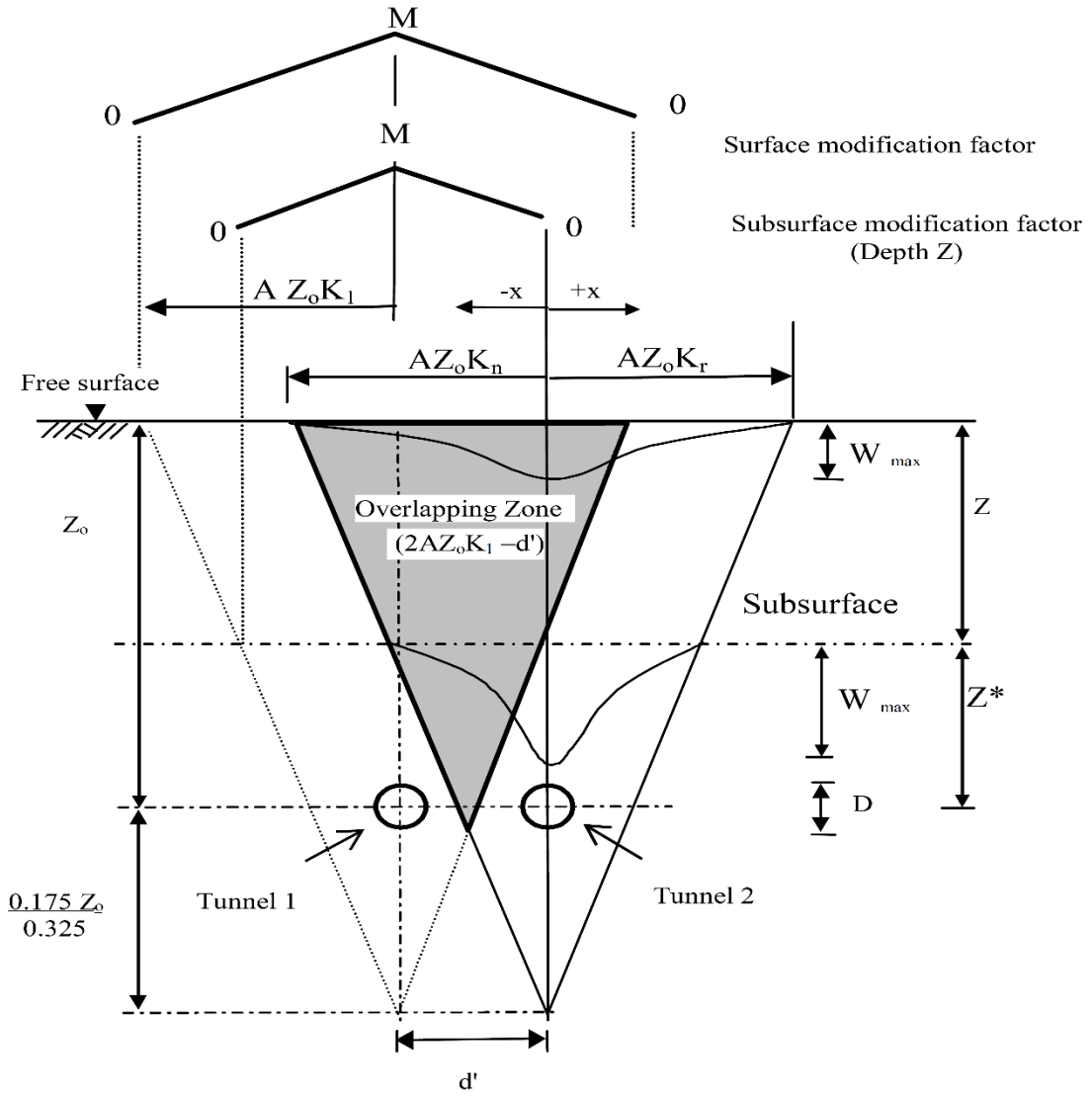

Figure 2.13. The modification factor for the settlement above the second tunnel (Hunt, 2005)

The maximum increment in settlement is stand in line with the Tunnel 1 axis and become zero at some horizontal distance from Tunnel 1.

Fang et al. (2015) stated that the maximum surface settlements induced by each of the twin tunnels generally increase with the decrease of the overburden thickness. Moreover, Zong (2014) stated that surface settlement induced by twin tunneling will be decreased due to the existence of the underground passage.

Fargnoli et al. (2015) stated that the subsidence solely induced by the second excavation is not symmetric with respect to the second tunnel axis, being the displacements higher on the side towards the first tunnel. This effect should be related to the reduced stiffness of the soil in this area due to the former accumulation of strains as a consequence of the excavation of the first tunnel.

2.2.6. Chakeri and Ünver (2013)

Three metro project constructions namely Istanbul, Tehran, Mashhad in the Middle East excavated by EPBS (Earth Pressure Balance Shields) were chosen to present better equations in estimating the maximum surface settlement-based actual data set from several tunnel projects and numerical modeling (Chakeri and Ünver, 2013). Equation for estimating the maximum surface settlement value based on numerical and observed results are given by:

$$S_{max} = (A \times S) \tag{2.17}$$

where S_{max} is the maximum surface subsidence, A is the factor associated with tunnel diameter and depth of the tunnel and S is relevant to tunnel depth, unit weight, traffic load, cohesion, face support pressure, modulus of elasticity, Poisson's ratio and internal friction angle. Relationships which require the prediction of the value of A and S are shown in equations 2.18-19.

$$A = 1.8825\left(\frac{D}{Z_0}\right) \tag{2.18}$$

$$S = 1699.2\left[\left(\frac{\gamma Z_0 + \sigma_s - (c + 0.3\sigma_T)}{E}\right)(1-\vartheta)(1-\sin\varphi)\right]^{0.8361} \tag{2.19}$$

where γ is the unit weight (kN/m^3); Z_0 is the tunnel depth (m); σ_s is the surface loading (kPa); c is the cohesion (kPa); σ_T is the required face support pressure (kPa); E is the modulus of elasticity (kPa); ν is the Poisson's ratio; φ is the internal friction angle (^{o}) and D is the tunnel diameter (m). The unit of S is assumed as mm.

Considering previously obtained parameters from relationships 2.18 and 2.19 and putting them into Eq. 2.17, one can obtain more accurate relationship for estimating maximum surface settlement value (Eq. 2.20).

$$S_{max} = 3198.744\left(\frac{D}{Z_0}\right) \times \left[\left(\frac{\gamma Z_0 + \sigma_S - (c + 0.3\sigma_T)}{E}\right)(1-\vartheta)(1-\sin\varphi)\right]^{0.8361} \quad (2.20)$$

where S_{max} is the maximum surface settlement (mm).

2.3. Numerical Methods

A simple empirical formula in predicting the tunneling induced ground movement can be used for a preliminary assessment and when there is relatively no important structure or utility around the construction area. However, in a more complex situation, it is suggested to carry out finite element analysis and perform a study on the soil structure interaction (Liong, 2005; Elmanan and Elarabi, 2015).

Nowadays, considering the sudden increase in development of computational tools and capability of solving the complicated issues, the finite element methods are widely used. Several restrictions of the analytical and empirical methods can be eliminated by the finite element method. In addition to geomechanical properties of material, depth, the stress-strain condition and geometry of the tunnel structure can influence the ground deformation depending on the excavation procedure. Finite element method can consider this excavation procedure called 'step-by-step' method (Katzenbach and Breth, 1981; Galli et al., 2004). Ground surface settlement is more sensitive to tunnel geometry rather than height of tunnel placement (Hosseini et al., 2012). Talebinejad et al. (2013) stated that since multilayer tunneling is a three-dimensional phenomenon in nature, 3D numerical solutions must be utilized for analyzing effect of perpendicularly crossing tunnels at various levels. They concluded that numerical modeling and determination of the appropriate distance between the tunnels are essential before starting excavation of another tunnel under or around existing tunnels in urban area.

The most helpful way for estimating tunnel induced surface settlement is the numerical method which composed of continuum and discontinuum modeling. Continuum model consists of Finite Element Method (FEM) and FDM (Finite Difference Method) and Discontinuum model involves Distinct Element Method (DEM). It is pointed out that a variety of parameters influencing surface subsidence can be extensively conceived by the numerical analysis, which can accurately estimate tunnel induced surface settlement (Li and Zhu, 2007). Numerical methods can handle with complicated boundary conditions, numerous rock and soil parameters, different tunnel geometries and temporal computations. They have a lots of helpful features such as colorful output of the results and plots and automatic mesh generation. It was noted that finite element program has advantages applied to any specific situations, for instance for a bedded soil with different elasticity modulus or non-circular sections or different density (Vafaeian and Mirmirani, 2003).

A comprehensive analytical solution coupled with numerical modeling is necessary to model the surface settlement. The finite element elastic-plastic analysis gave better predictions than the linear elastic model with satisfactory estimate for the displacement magnitude and slightly overestimated width of the surface settlement trough (Fattah et al., 2012). Furthermore, Fu et al. (2016) stated that the soil deformation mainly occurs in the elastic range, which further highlights the importance of considering elastic non-linearity for modeling the tunneling problem.

A realistic tunnel-deforming pattern combined with a soil model that can take account of stiffness decay at small strains can lead to a more accurate prediction of tunneling-induced settlement profiles (Whittle et al., 2003; Fu et al., 2016).

Tunnel construction is three-dimensional in nature and time dependent. However, three-dimensional coupled-consolidation analyses are still fairly rare in the literature. Constitutive model for numerical analysis can be an elastic – perfectly plastic soil model, using the Drucker–Prager failure criterion with a non-associated flow rule (Ng and Lee, 2005; Migliazza et al., 2008).

Farias et al. (2003) concluded that characterizing a NATM tunnel excavation should be performed by using 3D finite element method. Methods of settlement control during NATM tunneling are partial-face excavation, free span distance and support activation and they can be simulated appropriately by using numerical analysis. During analysis for a proper displacement forecast, an appropriate constitutive model is of utmost importance. The effect of partial face excavation will be more significant for elastoplastic models. However, a staged excavation is essentially a non-linear simulation even with an elastic linear model. Besides, Karakus and Fowell (2000) stated that sequences of excavating a NATM tunnel face must be reproduced in any numerical modeling undertaken.

Nowadays, numerical method is still limited to 2D models, since 3D modelling of tunnel excavation is highly compelling with respect to capacity and time of computer operation. There are a number of methods recommended in literature (Dragojević, 2012) for the modelling of excavation stages utilizing 2D models, namely; progressive softening method, stress reduction method, the Gap method and volume loss control method. Stress reduction method is generally used for the 2D modelling of tunnel construction. It is presented in the 2D model by relaxation factor standing for percentage of initial stress relaxation before installation of tunnel support. The relaxation factor depends on initial stress, unsupported length of tunnel, geometry of tunnel and soil properties. Smaller stress reduction factor causes smaller deformations and greater support forces (Dragojević, 2012).

When assessing the damages caused by the excavation of shallow tunnels on pre-existing buildings, it is often necessary to thoroughly study the soil-structure interaction. For this purpose, we need numerical models capable of reproducing the field of surface displacements induced in green-field condition. Altamura et al. (2007) stated that differential release technique is used to numerically reproduce the field of displacements induced by the excavation in green field conditions, as a first step to model the interaction between soil and the existing surface structures.

2.4. Pre-Support for NATM Tunneling

Inner-city ground usually composed of unconsolidated material and/or rock mass which has dense set of discontinuities. Both types of units are subject to major displacements during excavation. These deformations control the whole design stages due to the project limitations, with regard to the design necessities may require extra lining systems such as jet grouted columns, ground freezing, or pipe jacking (Volkmann and Schubert, 2007; Coulter and Martin, 2006 and Croce et al., 2004). Pre-support, pre-confinement, auxiliary method, and pre-improvement (Song et al. 2006; Lunardi, 2008; Sadaghiani and Dadizadeh, 2010, Basirat et al., 2016) are extra meaning of primary pre-support used in tunneling when support of the tunnel face is required (Oke et al., 2014).

A widespread pre-support system is the “Forepole” system, which is also assigned to in literature as Steel Pipe Umbrella (Oreste and Peila 1998), Umbrella Arch Method (Kim et al., 1996; Ocak, 2008), Pipe Forepole Umbrella (Hoek, 2003), Long-Span Steel Pipe Fore-Piling (Miura, 2003) or Steel Pipe Canopy (Gibbs et al., 2002), Pipe Roof Support (Volkmann and Schubert, 2007), Pipe Roof Umbrella, Pipe Roofing (Gamsjäger and Scholz, 2009), Steel Pile Canopy (Gibbs et al., 2007), and Spiles (Trinh et al., 2007). These terms all contain the words for describing this system. It is approved that the common term for the pre-support structure is an Umbrella Arch (Oke et al., 2014). Consequently, a standard terminology of support types is provided to guarantee that tunneling engineers and researches make conduct with each other efficiently and follow a commonly-held standard.

Furthermore, the Umbrella Arch pre-support can be separated into three distinct classes according to using support components. These components are subdivided based on their physical features (Oke et al., 2014). These subclasses composed of: Spiles (smaller than the tunnel height), Forepoles (higher than the tunnel height) and Grouted (simply consisting of grout). Grouting is commonly used in tunneling projects as a preventive measure to control water seepage. It is also used to strengthen ground material, fill voids, secure bolts, rods, and, in the case of drilled

holes, act as anchors (Warner 2004). The main contrast between spiles, forepoles and grouted are that the systems vary in their respective stiffness, costs, and time commitment (Volkmann and Schubert 2007; Tunçdemir et al. 2012).

The design parameters of the pre-support system are presented in Figure 2.14. These are the forepole element length (L_{fp}), the length of forepole overlap (L_{fpo}), the center to center spacing of the forepole elements (S_{cfp}), thickness of the forepole element (t_{fp}), outside diameter of the forepole element (ϕ_{fp}), the installation angle (α_{fp}) of the forepole element, the coverage angle of the forepole elements (α_{fpa}) (Oke et al., 2014). The parameter L_{fp} is not able to be optimized by numerical analysis because there exists too many design factors out of geotechnics. The L_{fp} relies on financial aspects, borehole precision, equipment availability and ability of ground conditions to drill. The length of forepoles is beyond of the successive plastic area around and face of the tunnel within these weak rock units (Kumar et al., 2014). The L_{fpo} is able to be optimized by utilizing related numerical analysis. This intersection area is vital to assure system stability and ground reaction. Overlap is half of the total length but varies from 1/3 to 2/3 of the total length (Oke et al., 2014). The α_{fpa} is described by the yielding process more than the instinctive reaction of the structure. For settlement controlled failure mechanisms, it is more well-known to utilize 180 coverage above the tunnel heading.

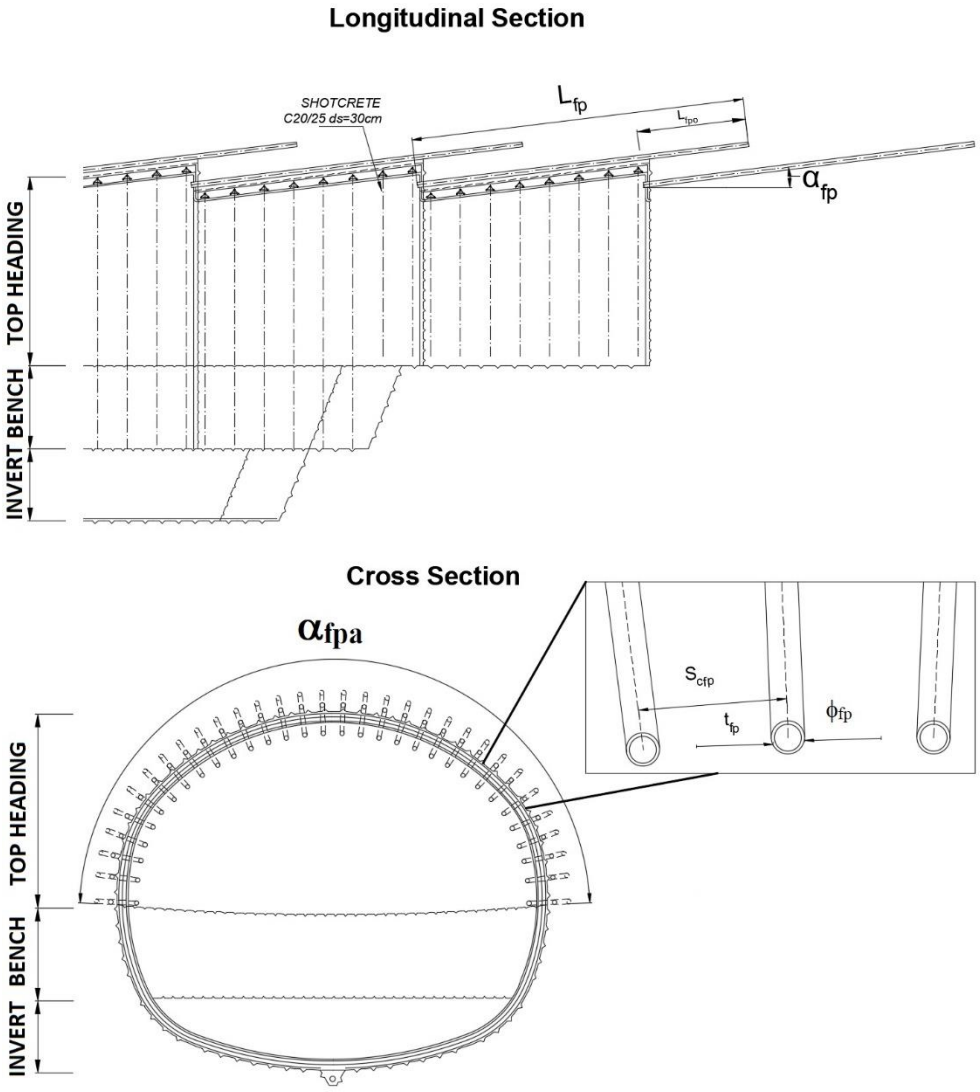

Figure 2.14. Constructional plan of the umbrella arch

The forepoles may be installed in shallow angle from the horizontal in longitudinal direction of tunnel alignment. The ideal condition of angle may vary from 3º to 8º with spacing range within 15-60 cm center to center. The spacing is based on the requirement to create the arching effect means overlapping of forepoles. The arching effect of forepoles is described by the geometry of the forepoles, which have a wall thickness of 5–10 mm and an external diameter of 60–168.3 mm (Tuncdemir et al.,

2012). Forepoling should be densely installed to reduce the influences from stress release at face and the crown (Warner, 2004).

To prevent or indeed to decrease the effect of tunnel induced settlements, some authors suggested a way that minimizes the ground deformation. Ercelebi et al. (2010) suggested that grouting of the excavation void should be performed as fast as possible after excavation of a section as a precaution against surface settlements during TBM tunneling. Moayed and Izadi (2011) presented that the application of the single-bench top heading method decrease the magnitude of surface settlements to a half of induced settlement which is found in the full-faced heading. Hasanpour et al. (2012) showed that tunnel roof formed by the pipe roofing provides a restraining effect, reducing deformation and ground surface settlement by up to 65 %. Yasitli (2012) showed that umbrella arch pipe is very effective to minimize the surface settlement during NATM tunneling. Zhao and Qi (2014) concluded that the large pipe-shed (LPS) ground stabilization can be utilized to perform ground stabilization prior to the new tunnel excavation. They also indicate that the LPS ground stabilization can significantly reduce the settlement of an existing tunnel caused by the excavation of a new tunnel, and the ground volume loss method has proven to be an effective approach to estimate the effects of LPS ground stabilization.

CHAPTER 3

GEOTECHNICAL EVALUATION OF STUDY AREA

Geotechnical investigations are essential for proper design of a tunnel. Selection of the tunnel alignment, cross section, and excavation methods is affected by the geological and geotechnical conditions, as well as the site constraints. Good knowledge of the expected geological conditions is vital. The type of the ground encountered along the alignment would affect the selection of the tunnel type and its method of construction (Hung et al., 2009).

Geology plays a dominant role in many major decisions made in designing and constructing a tunnel, from determining its feasibility and cost to assessing its performance. In tunnels, unlike other structures, the ground acts not only as the loading mechanism, but as the primary supporting medium as well. When the excavation is made, the strength of the ground keeps the hollow open until supports are installed. Even after supports are in place, the ground provides a substantial percentage of the load-carrying capacity. Thus, for the tunnel designer and builder, the rock and soil surrounding a tunnel is a construction material. Its engineering characteristics are as important as those of the concrete or steel used in other aspects of the work (Parker, 1996).

To calculate active earth pressure on tunnel support system and on lining, deformation, shear and moment forces, finite element method are used. This requires the parameters; internal friction angle, cohesion, unit weight to calculate coefficient of earth pressure, deformation modulus and Poisson's ratio to calculate retaining wall deformations and to analyze ground displacements behind earth retaining wall and base of excavation. These required parameters for soil used in FEM analysis are determined to specify settlement of the buildings originated from tunnel excavation.

Geotechnical parameters are normally obtained from laboratory and field tests. If these are not available or sufficient, various codes, standards and state-of-the-art reports are considered. In this study, there were not sufficient field test then available correlations from literature and wise engineering judgment were evaluated during determination of material parameters. Since granular soils are not suitable for sampling in routine site investigation work, field tests are used to determine engineering properties like strength and compressibility.

In the following sections final parameters were specified for the Asia NATM Tunnels of the Eurasia Tunnel project. The soil profile mainly consists of fill (made ground) (and in some boreholes completely decomposed rock layers) overlying bedrock. Standard penetration test (SPT) is the main source for correlations. Few pressuremeter tests (PMT) are available. Laboratory tests were performed on some of the samples. To determine the rock profiles, borehole logs and descriptions, core photographs, laboratory and field tests have been evaluated. The rock profiles are mostly composed of sandstone and mudstone.

3.1. Sources of Geotechnical Information

Field tests such as standard penetration tests (SPT), pressuremeter test and water pressure (Lugeon) tests, laboratory tests for soil and rock formations and wise engineering judgment were used to determine geotechnical design parameters.

3.1.1. Boreholes

In respect to NATM Tunnel Structures, the total numbers of 8 boreholes (Appendix A) that are total 415.80 m in length were carried out. Lugeon tests were carried out in S-AS-105, S-AS-106 and S-AS-107 boreholes. Pressuremeter tests carried out in NTB-1, NTB-2 and NTB-3. Borehole logs are given in Appendix B and core box photos are presented in Appendix C. The borehole numbers, elevations, coordinates and depths are tabulated in Table 3.1 and locations of boreholes are presented in Figure 3.1.

Table 3.1. Borehole Information for the Asia NATM tunnels

Borehole No.	Coordinates		Elevation (m)	Borehole Depth (m)	Groundwater Depth from Ground Surface (m)
	N	E			
S-AS-105	4541614,8	417483,6	27,81	51,00	5,00
S-AS-106	4541676,9	417764,0	43,09	50,00	7,50
S-AS-107	4541627,0	418032,6	35,75	40,00	5,70
S-AS-115	4541610,3	418128,0	27,45	25,00	8,60
NTB-1	4541568,7	417171,6	11,61	64,80	9,70
NTB-2	4541586,9	417309,8	16,25	58,30	5,50
NTB-3	4541690,1	417597,7	36,51	67,70	4,40
NTB-4	4541698,2	417867,7	39,85	59,00	1,60

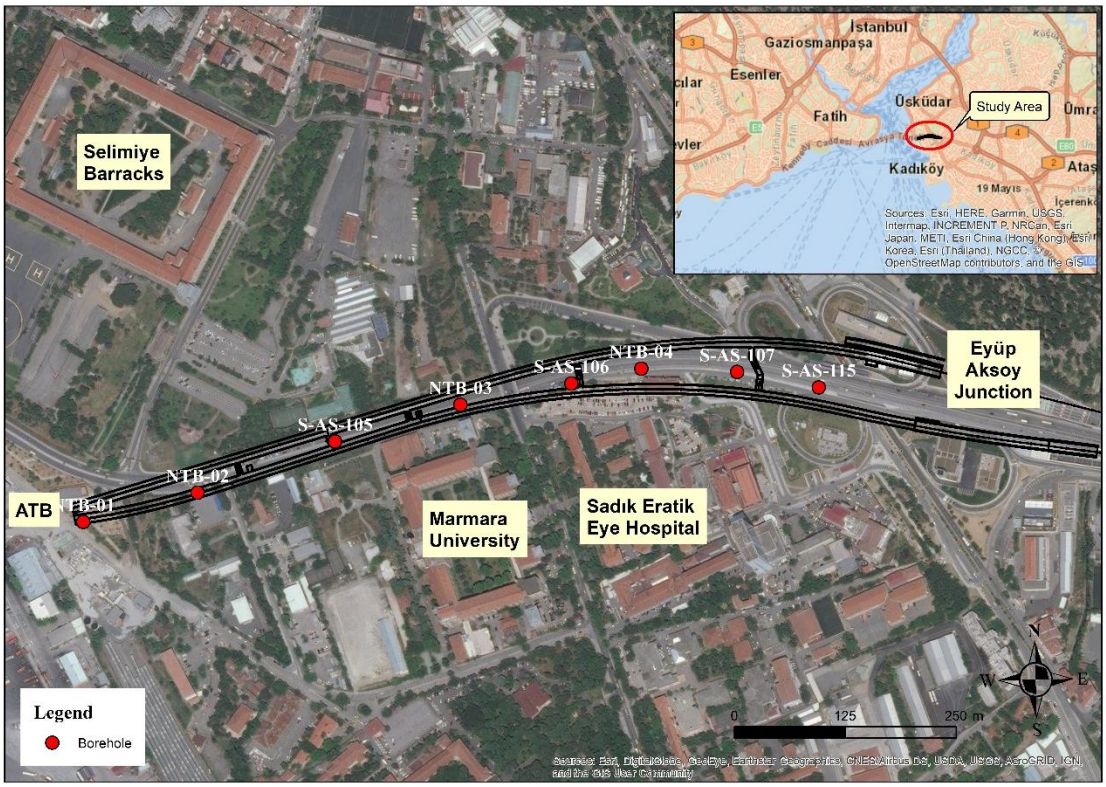

Figure 3.1. Borehole location along tunnel alignment

3.1.2. Standard Penetration Test (SPT)

Standard Penetration Test (SPT) was performed at the boreholes of S-AS-107, S-AS-115, NTB-1, NTB-2, NTB-3 and NTB-4 in soil and completely decomposed rock till the maximum depth of borehole at rough 1.50 m centers. The investigation was executed consistent with ASTM (2000). According to the energy conditions of an automatic hammer (N_{45}), the hammer energy efficiency was considered as 73%. A total of 31 SPT have accomplished at chosen levels. N_{60} values recovered according to 60% of energy of theoretical free-fall hammer. N_{60} values were calculated for these boreholes (Table 3.2).

Table 3.2. SPT-N_{45} and N_{60} Values for the boreholes open along the Asian NATM tunnels

Borehole No	**Depth (m)**	**SPT –N_{45}**	**N_{60}**
S-AS-107	1.5-1.95	21	15
	3-3.45	18	13
	4.5-4.95	18	13
	6-6.45	19	13
	7.5-7.95	16	15
NTB-1	1.50-1.95	34	24
	3.00-3.45	44	31
	4.50-4.85	>100	70
	6.00-6.45	34	24
	7.50-7.95	30	21
	9.00-9.45	70	44
	10.50-10.95	>100	59
	12.00-12.45	>100	56
NTB-2	1.50-1.95	51	36
	3.00-3.45	20	14
	4.50-4.95	16	11
	6.00-6.20	>100	70
	7.50-7.70	>100	70
	9.00-9.20	>100	70
NTB-3	1.50-1.95	63	44
	3.00-3.13	>100	70

Borehole No	Depth (m)	SPT –N_{45}	N_{60}
NTB-4	3.00-3.17	>100	70
S-AS-115	1.5-1.95	17	12
	3-3.45	8	6
	4.5-4.95	15	11
	6-6.2	>100	70
	7.2-7.55	>100	70

3.1.3. Water Pressure Test (Lugeon Test)

Fourteen Lugeon tests in borehole of S-AS-105, 6 tests in borehole of S-AS-106 and 6 tests in borehole of S-AS-107 (in total 26 Lugeon tests) were performed with single packer. An inflatable packer is set at the top of the interval to be tested. The test would be run at pressures of about 3, 6, and 9 kg/cm^2. Water intake readings are made at 5-minute intervals. The pressure is then raised to the next step. After the highest step, the process is reversed and the pressure maintained for 5 minutes at the same pressures.

Table 3.3 describes the conditions typically associated with different Lugeon values, as well as the typical precision used to report these values.

Table 3.3. Condition of rock mass discontinuities associated with different Lugeon values (after Quiñones-Rozo, 2010)

Lugeon Range	Classification	Hydraulic Conductivity Range (cm/sec)	Condition of Rock Mass Discontinuities	Reporting Precision (Lugeons)
<1	Very Low	$< 1 \times 10^{-5}$	Very tight	<1
1-5	Low	1×10^{-5}- 6×10^{-5}	Tight	± 0
5-15	Moderate	6×10^{-5}- 2×10^{-4}	Few partly open	± 1
15-50	Medium	2×10^{-4}- 6×10^{-4}	Some open	± 5
50-100	High	6×10^{-4}- 1×10^{-3}	Many open	± 10
>100	Very High	$> 1 \times 10^{-3}$	Openclosely spaced or voids	>100

Water pressure tests were carried out in accordance with terms of site (USBR, 2001). Borehole no, elevation and Lugeon values, permeability and descriptions according to Lugeon values are given in Table 3.4. Water pressure test elevations and Lugeon values for the boreholes open at transition box on Asian side. Rock mass are classified according to their permeability based on the Lugeon values. Sandstone, mudstone and diabase may be impermeable depending on their lithological characteristics. Permeability values obtained by the tests belong to the discontinuity and fault zones. Especially, Lugeon values are quite high in the related discontinuity and fault zones. Water leakage and/or seepage in the test zones are associated with directions and dips, fillings and persistence of the discontinuities. Results of the Lugeon tests indicate that the permeability values of the sandstone range from 0.61 to 32.55 Lugeon Unit (LU) and have an average value of 10 LU. Along NATM part of the Eurasia Tunnel, it is considered that the water leakage can be under the control of the fault zone and related discontinuities. Rock mass can be described as permeable and low permeable. In this section, rock mass is described as low to medium permeable according to Table 3.4. Lugeon tests results are presented in the Appendix E.

Table 3.4. Water pressure test elevations and Lugeon values for the boreholes open at transition box on Asian side

Borehole No.	Depth (m)	Lugeon Pattern	Lugeon Value	Description	Permeability (m/sec.)	Lithology
S-AS-105	3.00-4.00	Laminar	6.78	Moderate Permeable	3.14E-05	Sandstone
	6.00-7.00	Laminar	5.46	Moderate Permeable	2.43E-05	Sandstone
	9.00-10.00	Laminar	9.85	Moderate Permeable	4.11E-05	Sandstone
	12.00-13.00	Laminar	1.2	Low Permeable	4.57E-06	Sandstone
	15.00-16.00	Wash-out	21.82	Medium Permeable	9.47E-05	Sandstone
	18.00-19.00	Laminar	13.46	Moderate Permeable	5.48E-05	Sandstone
	21.00-22.00	Void Filling	0.61	Very Low Permeable	2.63E-06	Sandstone

Borehole No.	Depth (m)	Lugeon Pattern	Lugeon Value	Description	Permeability (m/sec.)	Lithology
	24.00-25.00	Void Filling	0.61	Very Low Permeable	2.63E-06	Sandstone
	27.00-28.00	Laminar	11.62	Moderate Permeable	4.41E-05	Sandstone
	30.00-31.00	Wash-out	10.91	Moderate Permeable	4.73E-05	Sandstone
	35.00-36.00	Void Filling	10.91	Moderate Permeable	4.73E-05	Sandstone
	39.00-40.00	Void Filling	14.55	Moderate Permeable	6.31E-05	Sandstone
	43.00-44.00	Laminar	12.12	Moderate Permeable	5.26E-05	Sandstone
	46.00-47.00	Laminar	3.64	Low Permeable	1.58E-05	Sandstone
S-AS-106	7.00-8.00	Wash-out	15.88	Medium Permeable	7.38E-05	Sandstone
	15.00-16.00	Wash-out	32.55	Medium Permeable	1.41E-04	Mudstone
	17.00-18.00	Void Filling	5.79	Moderate Permeable	2.51E-05	Sandstone
	21.50-22.50	Laminar	6.84	Moderate Permeable	2.97E-05	Sandstone
	41.00-42.00	Laminar	4.69	Low Permeable	2.38E-05	Sandstone
	43.00-44.00	Laminar	2.01	Low Permeable	9.79E-06	Sandstone
S-AS-107	15.00-16.00	Laminar	17.79	Medium Permeable	8.37E-05	Sandstone
	18.00-19.00	Wash-out	21	Medium Permeable	9.11E-05	Sandstone
	22.50-23.50	Laminar	9.99	Moderate Permeable	4.47E-05	Sandstone
	28.50-29.50	Laminar	7.35	Moderate Permeable	3.46E-05	Sandstone
	34.50-35.50	Wash-out	15.47	Medium Permeable	6.71E-05	Diabase
	39.00-40.00	Turbulent	9.85	Moderate Permeable	4.98E-05	Diabase

3.1.4. Pressuremeter Tests

Pressuremeter tests were carried out in various depths of NTB-1, NTB-2, NTB-3 and NTB-4 boreholes. Results of the pressuremeter tests are given in Table 3.5. Pressuremeter test reports are presented Appendix F.

Table 3.5. Pressuremeter test results

Borehole No	Depth (m)	Intact Modulus (MPa)	Lithology
NTB-1	38.50	2430.83	Sandstone
	44.50	2879.47	Mudstone
	52.60	9717.22	Mudstone
NTB-2	37.80	5780.73	Sandstone
NTB-3	38.40	1684.69	Mudstone
NTB-4	33.10	1555.60	Mudstone
	42.00	5261.60	Sandstone

3.1.5. Groundwater Levels

Groundwater levels were measured after expirations of drillings at different time intervals. Static groundwater levels were determined and these levels were assumed as groundwater levels. Groundwater depth from surface are given in Table 3.6.

Table 3.6. Groundwater depth from the surface

Borehole No.	Measurement 11.08.2011	Measurement 20.08.2011	Measurement 22.08.2011	Measurement 25.08.2011	Measurement 26.08.2011	Measurement 27.08.2011	Measurement 07-12.09.2011	Ground Water Level (GWL) (m)
S-AS-105	-	-	-	-	-	-	5,00	5,00
S-AS-106	-	4,30	4,30	7,50	-	7,50	7,50	7,50
S-AS-107	-	-	-	5,70	-	-	-	5,70
S-AS-115	8,60	-	-	-	-	-	-	8,60
NTB-1	-	-	-	-	-	-	-	9,70
NTB-2	-	-	-	-	-	-	-	5,50
NTB-3	-	-	-	-	-	-	-	4,40
NTB-4	-	-	-	-	-	-	-	1,60

3.1.6. Laboratory Tests

Rock samples collected from the boreholes were classified and identified at the Zemar Soil and Rock Mechanics Laboratory in order to determine the mechanical, index and physical properties of the rocks. Index and mechanical parameters were

calculated by using necessary tests including unit weight, uniaxial compression test (for rock) with elasticity modulus and Poisson's ratio, point load strength index test, Brazilian tensile strength and water absorption test. All tests were conducted in accordance with the ASTM D4719, TS 17025 and ISRM 2007 standards.

Laboratory tests on disturbed soil specimens obtained by field test (SPT) were carried out to obtain the index and physical characteristics of the lithological unit, these are Atterberg test, moisture content, natural unit weight and sieve analysis. Results of laboratory tests are given in Appendix D.

Laboratory Tests for Soil Units

Soil mechanical analyses were conducted and outcome of the lab-test completed by ZEMAR are presented in the Appendix D. Results belong to the soils of completely weathered sandstone and residual soil. Soil tests results are summarized in Table 3.7. The sieve analysis test is utilized to determine the size distribution of particles. Coarse-grained soils have more than 50% retained above No.200 Sieve, then this is classified as Sand like in our case present in following table. The Atterberg limits are a basic measure of the critical water contents of a fine-grained soil. If plasticity index is more than 7, then the fines are classified as clay. If plasticity index is less than 4, then the fines are classified as silt. Clayey sand (SC) indicates that fines are classified as clay and silty sand (SM) indicates that fines are classified as silt (ASTM, 2000).

Table 3.7. Soil test results of the samples taken from the boreholes

Boring No	**Depth (m)**	**Sieve Analysis**		**LL**	**PL**	**PI**	**Wn**	**Gs**	**Classification**
		+4	**-200**						
		(%)	**(%)**	**(%)**	**(%)**	**(%)**	**(%)**	**( )**	
NTB-1	9.00-12.00	54	18	26	12	14	11	2,72	SC
NTB-2	1.50-2.00	61	12	-	-	-	16	-	-
	3.00-7.50	57	22	35	18	18	13	2,62	SC
	-	0	34	NP	NP	NP	30	-	SM

Boring No	Depth (m)	Sieve Analysis		LL	PL	PI	Wn	Gs	Classification
		+4	-200	(%)	(%)	(%)	(%)	( )	
		(%)	(%)						
NTB-3	1.50-1.95	66	10	28	19	9	11	-	SC

Laboratory Tests for Rock Units

Rock mechanics tests were carried out on samples taken from various levels of the borings to determine intact rock mechanics properties. Also, unit weight and water absorption tests were carried out on the intact rock taken from various levels of the lithological units to determine their physical features. According to results of the tests, unit weight, elastic modulus, Poisson's ratio, indirect tensile strength, water absorption ratio and point load strength index for intact rock were measured. Rock test results are given in the Appendix D.

Uniaxial compressive strength shows changes depending on weathering condition and micro discontinuities of the intact rock sample. Also, uniaxial compressive strength can be affected by other conditions such as crushed, tectonic factors etc. Therefore, values of uniaxial compressive strength are ranging from 5.30 MPa to 95.14 MPa, and accordingly, values related to modulus of elasticity (E_s) ranges from 0.34 to 10.89 GPa. Values of the uniaxial compressive strength used in calculation of geotechnical design parameters were determined according to average resulting value of uniaxial compressive strength for rock material and point load index tests (Table 3.8). It is reported that for 50 mm diameter cores the uniaxial compressive strength is approximately equal to 24 times the point load index for sandstone (Broch and Franklin, 1972) and 20 times the point load index for mudstone (Rusnak and Mark, 1999). Then this average values were used in RocLab software (Rocscience, 2007) to get geotechnical design parameters of the rock masses (Appendix G). Moreover, software values depend on lithological features of rock.

Table 3.8. Average value of q_u as laboratory test results

Lithology	Uniaxial Compressive Strength		Point Load Strength Index Test			Average Value of q_u (MPa)
	q_u (MPa)	Mean q_u (MPa)	Is_{50}	$q_u=Is_{50}*k$	Mean q_u (MPa)	
Sandstone	10,04	41,08	1,43	34,32	38,54	39,81
	21,09		1,01	24,24		
	9,97		0,78	18,72		
	95,14		0,98	23,52		
	20,91		1,11	26,64		
	25,51		0,40	9,60		
	89,90		1,88	45,12		
	56,20		6,23	149,52		
	58,00		0,89	21,36		
	53,50		0,63	15,12		
	8,70		2,29	54,96		
	5,30		2,53	60,72		
	65,30		1,43	34,32		
	55,60		0,89	21,36		
Mudstone	13,51	20,70	0,37	7,40	19,66	20,18
	39,00		1,26	25,20		
	9,60		1,55	31,00		
	-		0,75	15,00		
	-		1,11	22,20		
	-		0,60	12,00		
	-		1,24	24,80		

3.2. Geotechnical Design Parameters for Soils

Unit weights (kN/m^3) used in the twin tunnel induced maximum surface settlement calculations are bulk (wet) (γ_t), saturated (γ_{sat}) and submerged (γ') unit weights. Submerged unit weight of the soil is calculated by ($\gamma'=\gamma_{sat} - \gamma_w$) where γ_w is unit weight of water (γ_w = 9.8 kN/m^3). It may be taken as 10 kN/m^3 except in calculations for uplift of underground structures.

Since granular soils cannot be normally sampled in the undisturbed state codes, standards and other references are employed in the assessment. The same is true for cohesive soils if no samples are available.

Internal friction angle of the granular soils is very difficult to determine under field loading. When drained triaxial compression test results on reconstituted coarse-grained soils or on undisturbed fine-grained soils are available their mean value are used. If no such tests are available recommended values in codes, standards and technical papers shall be used. Since standard penetration test is usually performed in the investigations, correlations that use N numbers are briefly summarized below.

Hatanaka and Uchida (1996) made comparisons of results of triaxial compression tests on undisturbed samples with SPT number N in Japan. In Turkey, donut hammer and cathead with 1.5-2 turns are used and 45 percent energy level is appropriate and the related equations are:

$$\varphi' = \sqrt{12N_{45}} + 20 \tag{3.1}$$

A lower bound for the equation 3.1 is given as

$$\varphi' = \sqrt{12N_{45}} + 15 \tag{3.2}$$

Deformation modulus in the coarse-grained soils under static loading is regarded as drained modulus. There is a wide range of values depending on grain size, uniformity, relative density, fines percent etc. Numerous equations and/or graphs proposed in the literature reflect this variation (Burland, et al., 1978, D'Appolonia et al., 1970, Bowles, 1988). Some of these mainly based on SPT-N numbers are summarized below;

$$E\ (MPa) = (0.6 \sim 3.0)*N \tag{3.3}$$

$$E\ (MPa) = 21 + 1.06*N \tag{3.4}$$

$$E\ (kPa) = 500*(N+15) \tag{3.5}$$

$$E\ (kPa) = 1200*(N+6) \quad (3.6)$$

Pressuremeter tests are also used for the measurement of in-situ moduli. Pressuremeter modulus is divided by an empirical coefficient α (0.66, 0.50 and 0.33 for clays, silts and sands respectively, all normally consolidated) (Baguelin et al., 1978).

Poisson's ratio for coarse grained soils are reported between 0.2-0.4 (AASHTO, 1995).

Measured values of shear wave velocity by PS logging shall be preferred if available. When such tests are not available standard penetration test N numbers shall be used. Some correlations given in literature for coarse grained soils are;

$V_S = 290\ (N_{60} +1)^{0.3}$ (ft/sec) (Dickenson, 1994)

$V_S = 80N^{1/3}$ (m/s) (JRA, 2002)

Based on various correlations outlined in this section geotechnical design parameters of the soils are summarized in Table 3.9.

Table 3.9. Geotechnical design parameters for the soils in the Asia NATM Tunnels area.

Type of Soil	**Label**	**$(N_{45})_{ave}$**	**γ_{sat} (kN/m^3)**	**c (kPa)**	**ϕ (°)**	**E (MPa)**	**ν**	**V_s (m/s)**
Fill (Made Ground)	F	21	20	0	35	20	0,33	240
Completely Decomposed Rock	CDR	15	21	0	33	30	0,32	200

3.3. Geotechnical Design Parameters for the Rocks

Hoek et al. (1995) states that rock mass classification can be very helpful if there is not enough data about rock mass and its strain and hydrological properties while preliminary phase of a project design. Classification of rock mass have been improved to provide rocks collecting into resemble groups. The initial well-arranged schema was presented by Dr. Karl Terzaghi (1946) and then a number of systems created by others which are more quantitative (Lauffer, 1958; Deere, 1964; Wickham et al., 1972; Bieniawski, 1973; Barton et al., 1974; Hoek and Brown 1997; Hoek et.al., 2002; Grimstad and Barton, 1993). However, three of the above classification systems have been more frequently used in correlation with parameters applicable to the design of rock foundations. These are the Geomechanics System (Rock Mass Rating, RMR), the Q-System and the GSI System.

The six factors are used to categorize a rock mass utilizing the RMR scheme: uniaxial compressive strength of rock material, Rock Quality Designation (RQD), discontinuity spacings, discontinuity conditions, groundwater conditions, discontinuity orientation.

In the Asia NATM Tunnels area due to limited data about the strike and dip directions of the rock masses, the degree of favorability is taken as favor (RMR rating of -5 for slopes) for all rock masses.

Borehole logs and descriptions, core photographs, laboratory and field tests have been studied to determine the rock profiles and the rock mass characteristics. Most profiles are composed of sandstone, sandstone/mudstone and mudstone layers. Occasionally there are diabase layers. The Geological Strength Index (GSI) system approach has been found appropriate to use in the interpretation of the geotechnical properties of the rock masses relevant to design of temporary support system for tunnel excavation and reinforced concrete lining in the long run. GSI was introduced to estimate the reduction in rock mass strength for different geological conditions. It

gives a GSI value estimated from rock mass structure (blocky, block size description etc.) and rock discontinuity surface condition.

The units in the Trakya formation at the site have been plotted with depth in all boreholes. RMR values have been estimated in all layers making use of borehole log descriptions, rock quality designation (RQD), total core recovery (TCR), core photographs and laboratory strength data.

Sandstone and mudstone sub-units have been separated in terms of RMR values. Sandstone units S0, S1, S2, S3 and mudstone units M0, M1, M2, and M3 are shown in the geological profile given in Appendix A. Range and average of RMR values for each sub-units are given in Table 3.10. RMR values found for the mudstones and sandstones generally vary from poor to fair categories.

Table 3.10. RMR and GSI values for each sub-units

RMR and GSI Values							
Sandstone				**Mudstone**			
RMR Range	**Average RMR**	**GSI**	**Label**	**RMR Range**	**Average RMR**	**GSI**	**Label**
0 - 8	8	25	S0	0 - 7	7	32	M0
12 - 21	17	29	S1	8 - 11	11	35	M1
23 - 29	27	39	S2	22 - 39	31	41	M2
30 - 67	42	42	S3	41 - 59	47	45	M3

There are several different test methods available to estimate deformation modulus of rock masses. While all methods are used in estimating modulus for design purpose, only the following seven have been standardized: the uniaxial compression tests; uniaxial-jacking (and flat-jack) tests; the pressuremeter test; plate load test; pressure-chamber tests; radial jack tests; and borehole jacking tests. In addition, there are numerous empirical methods which correlate classification scheme to deformation modulus. RMR correlation between deformation modulus and the RMR Classification scheme was produced by Serafim and Pereira (1983):

$$E_d = 10^{\frac{(RMR-10)}{40}} \quad \text{for RMR<50} \tag{3.8}$$

$$E_d = 2RMR - 100 \quad \text{for RMR>50} \tag{3.9}$$

E_d is deformation modulus of rock mass (in GPa). In both these correlations, the RMR is used without the adjustment for discontinuity orientation.

GSI approach proposes the following expression for modulus: A correlation between deformation modulus and the GSI value was produced by Serafim and Pereira (1983) by substituting GSI for RMR in equation 3.10 with reducing E_d as value of σ_{ci} falls below 100 MPa.

$$E_d(GPa) = (\sigma_{ci}/100)^{0.5} 10^{(GSI-10)/40} \tag{3.10}$$

Geomechanics rock mass classification (Bieniawski, 1989) supplies friction angles and a cohesion value interval for the in-situ rock. Hoek and Brown (1997) and Hoek et.al. (2002) provide charts and equations to estimate cohesion and angle of friction. Commercially available the RocLab program developed based on Hoek et al. (2002) gives cohesion and friction angle using GSI value, unconfined compressive strength of intact rock (σ_{ci}), parameter for rock type (m_i) together with specified type of construction (tunnel, slope, general) and disturbance factor (D) which is accepted as 0.3 in calculations since mechanical excavation causes minimal disturbance to the surrounding rock masses (Hoek, 2012).

Deformation modulus for the rock mass can also be estimated with reference to uniaxial compression of the intact rock, and degree of fracturing from the equation 3.11 (Hobbs, 1974).

$$E_m = jM_r\sigma_c \tag{3.11}$$

where j is a mass factor related to the degree of fracturing, M_r is the ratio between the deformation modulus and compressive strength of the intact rock (σ_c).

Finally Table 3.11 summarizes mechanical properties of the rock mass for eight rock units. Strength parameters are based on Hoek-Brown failure criterion presented in form of Mohr-Coulomb criterion (Hoek and Brown, 1997; Hoek et.al., 2002). The RocLab software based on Hoek et.al. (2002) yield high friction angles, and they are reduced according to Japan Highway Public Corporation (1986) recommendations.

Table 3.11. Geotechnical design parameters of rock mass

	Symbol	Unit Weight (γ) (kN/m^3)	Cohesion (c) (kPa)	Friction Angle (ϕ) (°)	Deformation Modulus (E) (MPa)	Poisson's Ratio
Mudstone 0	M0	22	65	14	95	0,32
Mudstone 1	M1	23	80	18	120	0,30
Mudstone 2	M2	24	150	28	300	0,28
Mudstone 3	M3	25	240	37	750	0,26
Sandstone 0	S0	22	90	18	160	0,30
Sandstone 1	S1	23	150	28	300	0,28
Sandstone 2	S2	24	200	36	500	0,26
Sandstone 3	S3	25	300	43	1100	0,25

3.4. Evaluation of Ground Conditions along NATM Part of the Eurasia Tunnel

Ground profile of the route was prepared according to the data obtained from borehole recordings of NTB-1, NTB-3, NTB-4, S-AS-105, S-AS-106, S-AS-107 and S-AS-108 and field observations. Along the tunnel route, sandstone and mudstone layers belonging to the Trakya formation were identified. Geological profiles belonging to the location at which boreholes were drilled are presented in Figures 3.2-3.6. It is noted that geological formations were subdivided according to their rock mass quality.

Moreover, the artificial fill at the top of the profile is observed in almost all boreholes. Its thickness varies between 0 and 7.5 m. There is a completely decomposed rock layer (CDR) under made ground in some of the boreholes (NTB-1,

NTB-2 and NTB-3). Its thickness varies between 1.2 and 8.4 m. The groundwater depth ranges between 1.6 m and 9.7 m. The Trakya formation underlies the artificial fill and CDR. The sandstones are more frequently encountered rather than the mudstones in the boreholes.

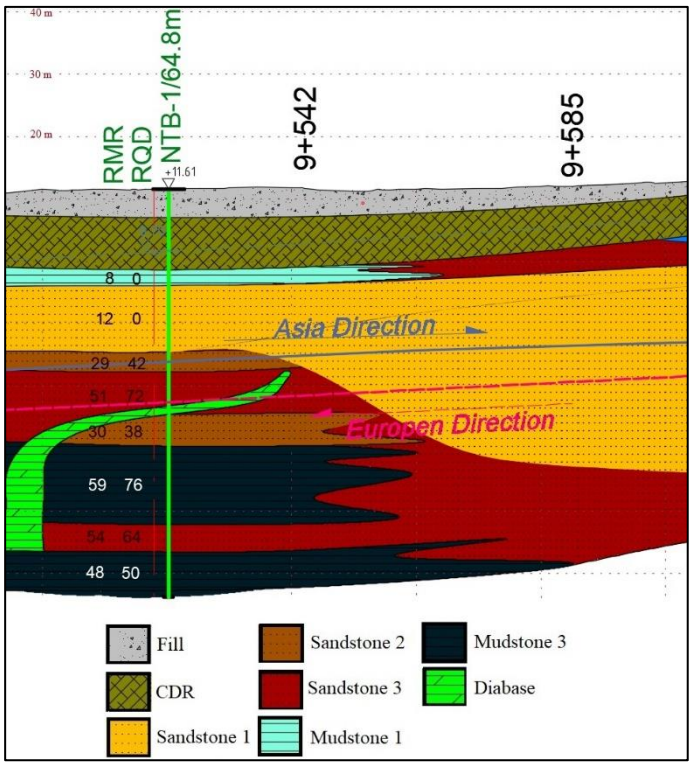

Figure 3.2. Geological profile around the borehole NTB-1

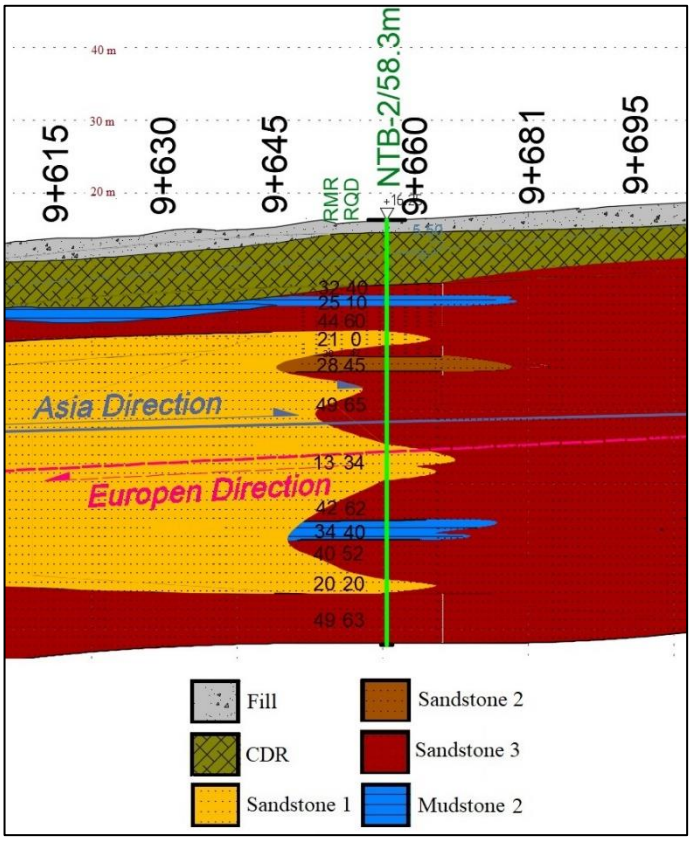

Figure 3.3. Geological profile around the borehole NTB-2

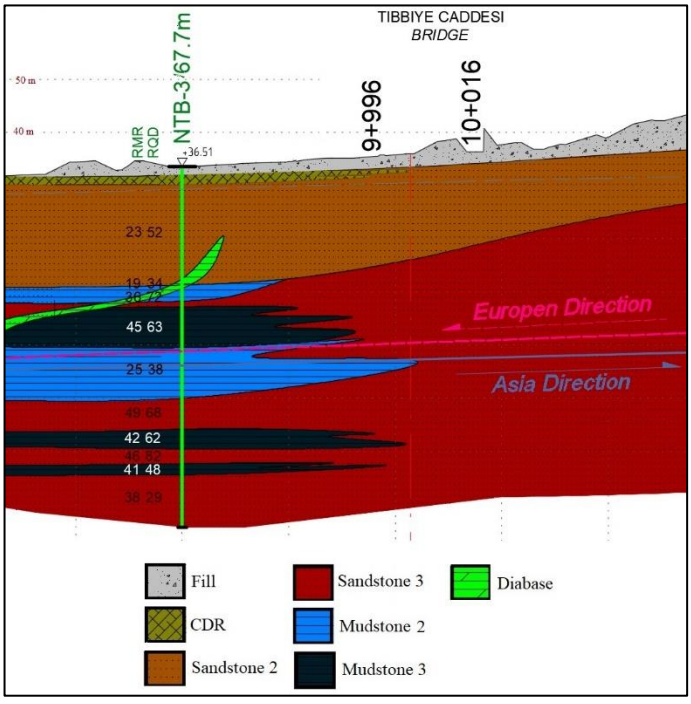

Figure 3.4. Geological profile around the borehole NTB-3

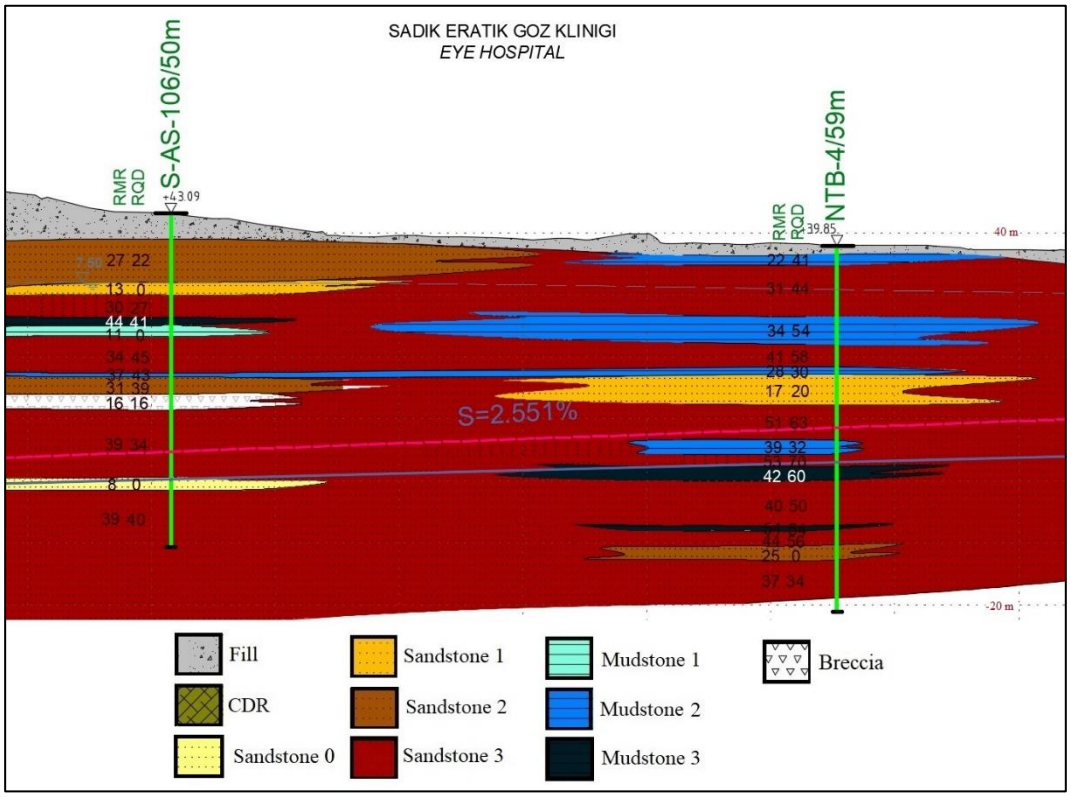

Figure 3.5. Geological profile around the borehole NTB-4 and S-AS-106

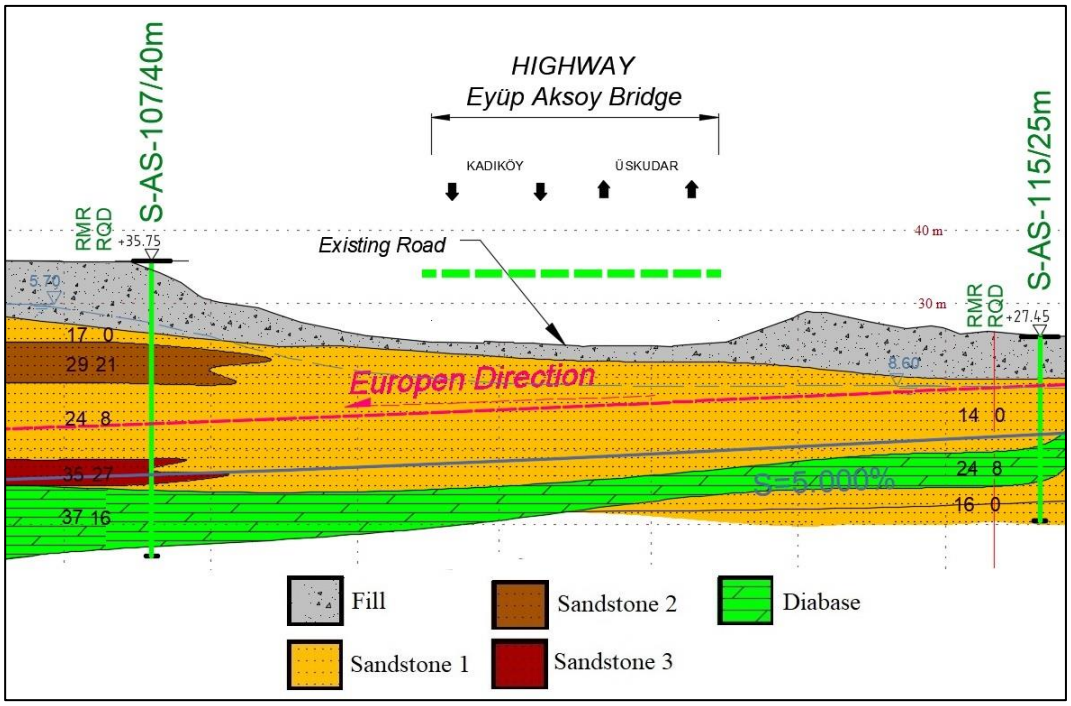

Figure 3.6. Geological profile around the borehole S-AS-107 and S-AS-115

Simplified 3D geological profile including the proper rock mass type around tunnel excavation was constructed by using borehole information and extracting much detail, thin layers of rock mass (Figure 3.7).

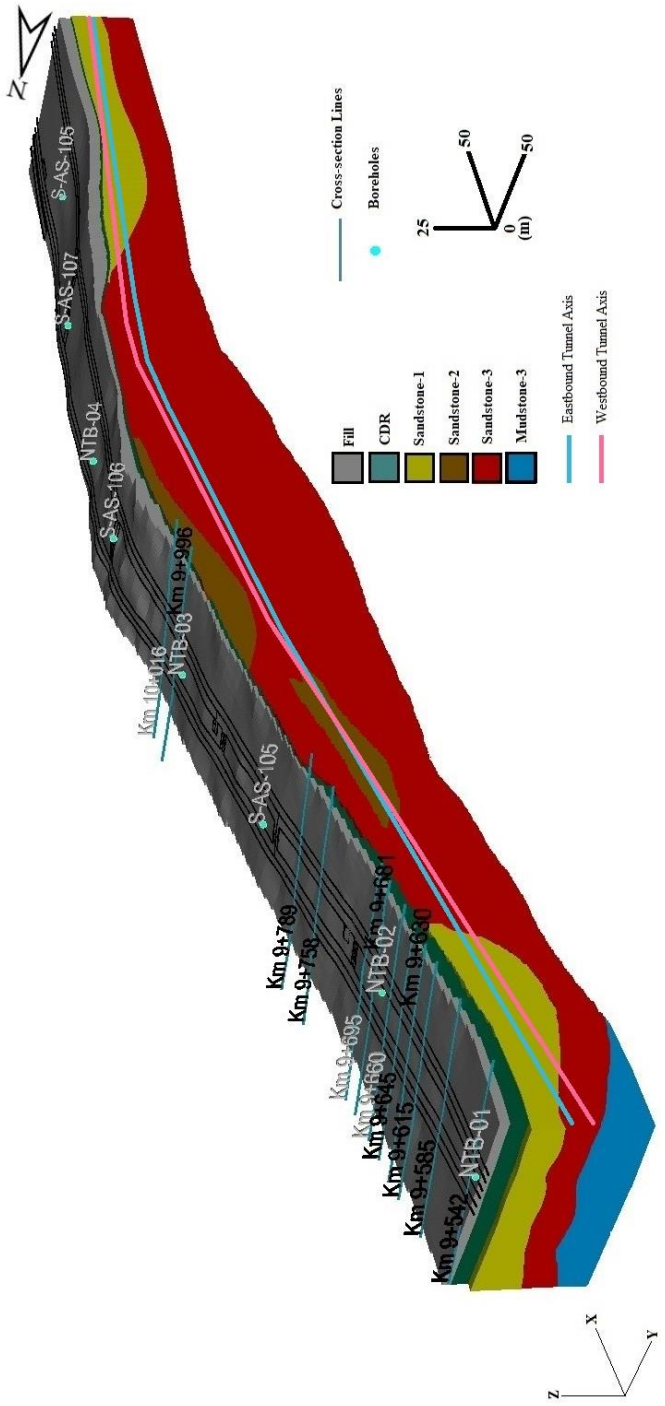

Figure 3.7. Simplified geological cross-section along tunnel alignment

3.5. Ground Settlement Bolt

Field maximum ground settlement comes from the field monitoring technique named as installation of ground settlement bolt. Ground settlement bolts are simply 1 meter long rebar inserted in ground and protected by steel covering to avoid any damage. They are measured with precision of ±1 mm (Figure 3.8). The measured data are compared to the first data; consequently vertical displacement of each unit is plotted in the form of graphics.

Figure 3.8. Ground settlement bolts and taking measurement in the study area

There are 367 settlement bolts in the scope of the Eurasia Tunnel project. However, a total of 78 settlement bolt data along all the selected cross-section lines were used for this study. Settlement data along the selected cross-section lines were given in Table 3.12. The largest value of maximum surface settlement belongs to section Km 9+630 at which there is thickest geo-material with lower rock mass quality.

Table 3.12. Settlement bolt data along the selected cross-section lines

Km 9+542		**Km 9+585**		**Km 9+615**	
Measurement Point	**Smax (mm)**	**Measurement Point**	**Smax (mm)**	**Measurement Point**	**Smax (mm)**
ATB-Z41	4,7	ASK-Z02	8,6	E5-Z05	25,4
ATB-Z38	6,6	ASK-Z01	12,6	ASK-Z03	22,6
ATB-Z35	5,1	E5-Z01	13,6	ASK-Z04	18,2
ATB-Z32	6,1	E5-Z01B	23	ASK-Z05	13,3
ATB-Z29	6	DLH-Z02	21,7	ASK-Z06	9,2
ATB-Z26	6,4	DLH-Z03	18,1	DLH-Z09	10,7
ATB-Z25	5,6	DLH-Z04	15	DLH-Z08	19,1
ATB-Z23	4,9	DLH-Z05	12,7	DLH-Z07	19,9
Smax	**6,6**	E5-P01	25,5	E5-Z04	28,2
		Smax	**25,5**	**Smax**	**28,2**
Km 9+630		**Km 9+645**		**Km 9+660**	
Measurement Point	**Smax (mm)**	**Measurement Point**	**Smax (mm)**	**Measurement Point**	**Smax (mm)**
E5-Z06	28,4	E5-Z09	22,1	E5-Z10A	17,4
ASK-Z07	26,7	ASK-Z09	23	ASK-Z11	18,5
ASK-Z08	24	ASK-Z10	21	ASK-Z12	20,1
DLH-Z10	26,3	DLH-Z11	17,6	ASK-Z13	11,3
E5-Z07	30,7	E5-Z08	25,3	ASK-Z13A	12
Smax	**30,7**	**Smax**	**25,3**	E5-Z11	11,1
				E5-Z10	18,3
				Smax	**20,1**
Km 9+681		**Km 9+695**		**Km 9+758**	
Measurement Point	**Smax (mm)**	**Measurement Point**	**Smax (mm)**	**Measurement Point**	**Smax (mm)**
ASK-Z15	11,4	E5-Z14	8,6	ASK-Z24	7,3
ASK-Z14	12,3	ASK-Z16	6,2	ASK-Z23	12,8
E5-Z13A	12,1	ASK-Z17	6	E5-Z25	13,2
E5-Z13	12,7	E5-Z16	8,6	E5-Z24	13,4
E5-Z12	10,5	E5-Z15	9,8	E5-Z23	9,3
Smax	**12,7**	**Smax**	**9,8**	**Smax**	**13,4**
Km 9+789		**Km 9+996**		**Km 10+016**	
Measurement Point	**Smax (mm)**	**Measurement Point**	**Smax (mm)**	**Measurement Point**	**Smax (mm)**
ASK-Z26	10,5	TZ34	3,7	TZ35	3,6
ASK-Z25	10,5	TZ33	4,6	TZ36	4
E5-Z26	13	TZ32	4,9	TZ37	4,2
E5-Z27	13	E503	3,5	E5-04	3,3
E5-Z28	10,9	E501	5,9	E5-02	5,9
Smax	**13**	TZ29	6,1	TZ28	2,4
		TZ30	2,8	TZ27	2,8
		TZ31	2,6	TZ26	2,7
		Smax	**6,1**	**Smax**	**5,9**

CHAPTER 4

NUMERICAL ANALYSES OF NATM PART OF THE EURASIA TUNNEL

In metropolitan areas, the enhanced request of mass transit and the shortage of horizontal space bring about an increased necessity for subway transport system.

Despite the fact that conventional analyses are easy to utilize and provide well results, they are restricted due to presence of different solution methods: stresses are usually obtained by elastic solution, movements are determined by using empirical methods. Therefore, finite element method (FEM) is preferred to handle complicated issues such as; modeling the complicated ground conditions, excavation orders, actual behavior of soil material, complicated hydrogeological environments, interaction between multiple tunnels, considering short and long term conditions, soil structure interaction (David and Zdravkovic, 2001).

Nowadays, considering the sudden increase in development of computational tools and capability of solving the complicated issues, the finite element methods are widely used. Several restrictions of the analytical and empirical methods can be eliminated by the finite element method. In addition to geomechanical properties of material, depth, the stress-strain condition and geometry of the tunnel structure can influence the ground deformation depending on the excavation procedure. Finite element method can consider this excavation procedure called ‘step-by-step’ method (Katzenbach and Breth, 1981; Galli et al., 2004; Yang et al., 2015; Panthee et al., 2016; Zhang et al., 2016).

4.1. Finite Element Method

This study is focused on introducing a detailed procedure for obtaining modification factor based on pre-support technique and rock mass quality, which are used in an existing equation as a modification factor for calculating maximum surface settlement above openings of the twin tunnel structure. A parametric study was carried out for this purpose to determine the effects of center-to-center distance between pipes in pre-support system of the tunnel on surface settlement. The finite element analyses were performed by using the software Phase^2 2D (Rocscience, 2012) geotechnical finite element package. This chapter is devoted to introduce the details of the finite element modeling, constitutive models and construction procedures used in the performed parametric study.

Despite the improvements in hardware and software, 3D modelling of tunnels is still a time-consuming task because it involves incremental phases to simulate the excavation and, most often, incorporates material non-linearity (Trinh et al., 2010; Mazek and Almannaei, 2013; Shabna and Sankar, 2016; Vitali et al., 2017; Kilany et al., 2017).

Calculation processes of modelling using FEM generally includes basic steps: determining model geometry, determination of material parameters, meshing, and delineation of boundary, external and initial loading circumstances (Boeraeve, 2010).

Tunnel opening is modeled by removing the elements inside a tunnel limit. Excavation orders (top heading, bench and invert) are applied in the plane-strain model. The tunnel support structure comprises of; pre-support (forepole and umbrella arch), the outer lining (shotcrete) and the inner lining (final shotcrete for esthetic purposes).

Jaeger (1979) pointed out that tunnels are extremely stressed in all directions, the vertical constituent of stress proportional to overburden weight over the tunnel and

there is also a horizontal constituent of this stress. The in-situ horizontal stress components are greater than the vertical ones at the mountain range.

The vertical stress can be computed by multiplying relevant depth with unit weight of overburden rock (Equation 4.2). Nonetheless, Sheorey (1994) formulate the earth stress model to recognize the mechanism of horizontal stress at near-surface and deep levels. Therefore, the ratio of horizontal stress to vertical stress (k) was proposed (Equation 4.3):

$$\sigma_v = \gamma z \tag{4.2}$$

where;

σ_v = the vertical stress

γ = the unit weight of the rock above tunnel

z = the depth measured from ground surface

$$k = 0.25 + 7E_h(0.001 + \frac{1}{z}) \tag{4.3}$$

where E_h is the mean deformation modulus of the rock above tunnel and z is the depth under surface.

It is suggested that mesh dimensions for two dimensional simulating of tunnels. It was supposed to take 3D from tunnel axis to the bottom mesh boundary, and 5D from the tunnel axis to the vertical mesh boundaries; where D is the tunnel diameter (Meissner, 1996; Möller, 2006).

It is also important to check that boundary conditions are not affecting the results. To assure that boundary effects are eliminated, plane-strain conditions should be reached. In other words, the simulation of the tunnel advancement procedure should be performed until steady state surface settlements and lining forces are observed. The mesh size is finer near the tunnel boundary and coarser at both ends to minimize mesh density while maximizing the mesh length. The simulation of the tunnel advancement is repeated until the steady state conditions are reached.

4.2. Material Parameters Used in the Analyses

There are eight numbers of borings covering the tunnel alignment of the Asia NATM Tunnels. There are generally fills and sands as soil layers on top. The Trakya formation was reported to extend along the route. Borings disclose that this information is composed of alternating layers of sandstone and mudstone almost at all sections. It is noted that they are intensely folded, fractured and weathered.

In this study, 12 cross-section lines were selected along the tunnel alignment at which interaction between tunnels are active to perform numerical analysis (Figure 4.1). The analyses were executed in these sections according to the following criteria: rock mass quality, type of pre-support and suitability of number of settlement bolts along section line. Fundamental information about the tunnel section along these selected cross section lines are given in Table 4.2.

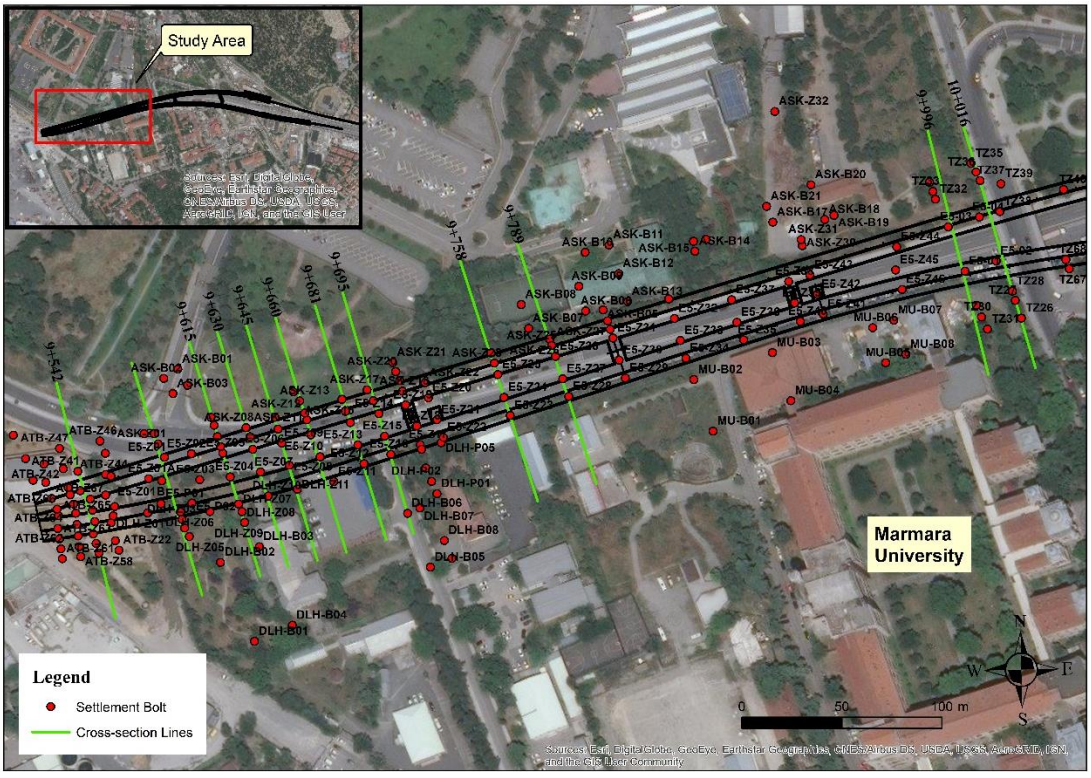

Figure 4.1. Selected twelve cross section lines along twin tunnel alignment

Table 4.1. Tunnel data along the selected cross-sections

No	Km	Spacing (m)	Overburden Depth (m)		Support Type		Tunnel Diameter (m)	GWT from surface (m)
			Westbound	Eastbound	Westbound	Eastbound		
1	9+542	17.71	33.21	26.40	ST-3	ST-3	11.2	8.90
2	9+585	22.29	31.54	25.54	ST-UA1	ST-UA1	11.6	6.40
3	9+615	24.33	33.13	26.38	ST-3	ST-UA1	11.4	5.80
4	9+630	24.90	33.28	27.20	ST-2	ST-UA1	11.4	5.80
5	9+645	25.24	33.40	27.31	ST-2	ST-UA1	11.4	6.30
6	9+660	25.40	33.55	27.78	ST-2	ST-UA1	11.4	4.80
7	9+681	25.21	33.75	28.36	ST-UA1	ST-UA1	11.6	3.90
8	9+695	25.10	33.95	28.90	ST-3	ST-3	11.2	3.30
9	9+758	24.10	34.43	31.20	ST-3	ST-3	11.2	0.45
10	9+789	23.50	34.71	32.23	ST-3	ST-3	11.2	0.10
11	9+996	25.80	38.54	35.37	ST-2	ST-2	11.2	5.20
12	10+016	27.40	38.89	35.49	ST-2	ST-2	11.2	8.00

The choice of an appropriate material strength model is a vital action in finite element analysis. Numerical analyses in this study were practiced using the finite element program Phase^2 with linearly elastic perfectly plastic constitutive model with Mohr-Coulomb failure criterion that is a common model extensively used to show shear failure in rock and soil units.

Based on various correlations outlined in Chapter 3, geotechnical design parameters of soils were presented in Table 3.9 and based on rock mass quality, RocLab results, laboratory test results, literature correlations and wise engineering interpretation, geotechnical design parameters of rocks were presented in Table 3.11.

There are there main types of support systems used in the selected 12 cross sections, namely ST-2, ST-3 and ST-UA-1. These primary support systems consist of shotcrete, lattice girder and wire mesh. Shotcrete, lattice girder and wire mesh were simulated as composite liner in the numerical analysis. The characteristics of the support cross sections are: (i) the shotcrete width is 25 cm for ST-2 and 30 cm for ST-3, ST-UA-1, (ii) 3-Bar type of lattice girder with 1 cm spacing was not applied to invert part in ST-2 and ST-3 type of support, (iii) the double layered (Q221/221 type)

wire mesh. To simulate the hardening behavior of shotcrete with time, the shotcrete's Young's modulus is increased step by step at 1 m length cycles behind the tunnel heading, then stage factor was used as 25% for the first application of shotcrete. Forepoling for ST-2, ST-3 and umbrella pipes for ST-UA-1 technique were used as a pre-support to decrease the effect of tunnel induced surface settlement through weak ground by reinforcing the ground above top heading. A complete solution needs to use 3D models but such models are infrequently utilized for ordinary feasibility project for tunneling. Two dimensional modeling of the forepoling will be explained in the following section. The cross-sections of the tunnel revealing three basic support systems and steps of excavation are shown in Figure 4.2 and Figure 4.3.

Due to tunnel excavation in the rock mass, redistribution for stresses is occurred in surrounding tunnel. By developing the plastic zone around the tunnel, radial convergence proceeds, resulting in the reduction of stresses in rock mass (Golshani et al., 2009). Disturbed zone was specified as a range of 2-3 m offset from the tunnel periphery and while determining its parameters, disturbance factor was selected as 0.7. This material has been activated after excavation.

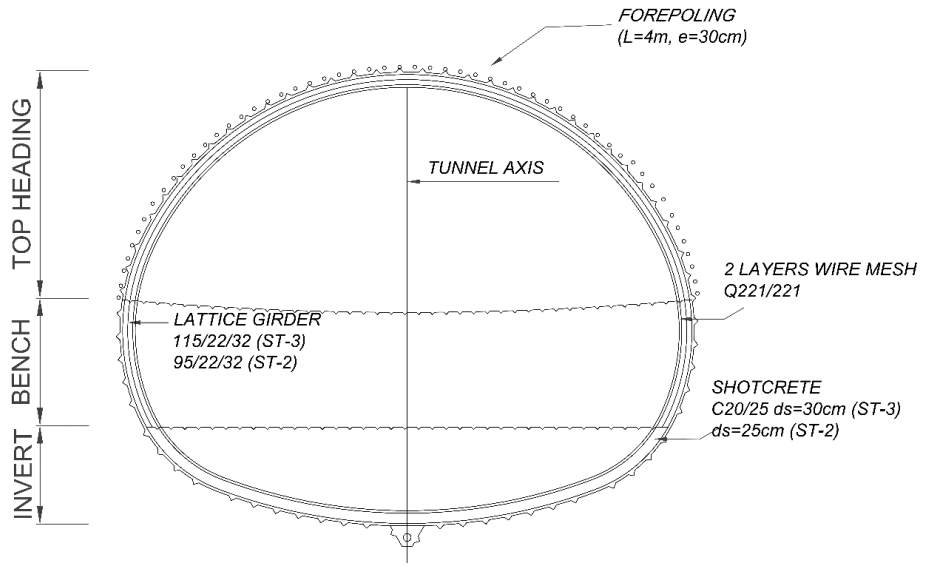

Figure 4.2. Typical tunnel section of the Asia NATM with ST-2 and ST-3 type support

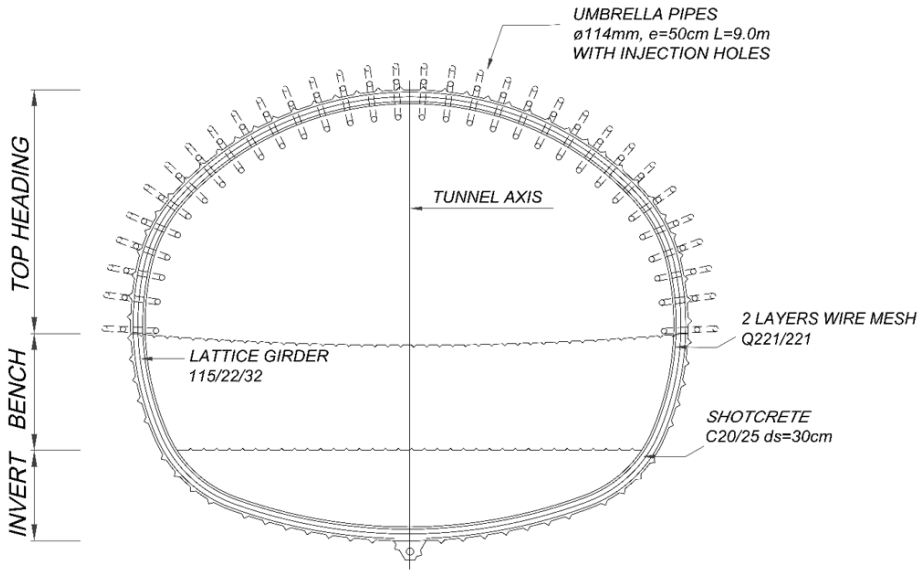

Figure 4.3. Typical tunnel section of the Asia NATM with ST-UA-1 type support

Tunnel lining was modeled using a linear elastic material model and the corresponding material properties are given in Table 4.2.

Table 4.2. Tunnel support parameters used in the numerical analyses

Support Type	**E (MPa)**	**Poisson's Ratio, ν**	**Compressive Strength (MPa)**	**Tensile Strength (MPa)**	**Dimensions**
Shotcrete	21 000	0.2	28	2.2	25-30 cm
Lattice Girder	200 000	0.25	400	400	#95 - #115 Bar Size:22-32 mm
Wire Mesh	200 000	0.25	400	400	Q221*Q221
Forepoling	Steel pipes (E= 200 000 MPa), 30 cm spacing, 70 mm diameter, 4.0 m length, angle of 9 with the tunnel longitudinal axis				
Umbrella	Steel pipes (E= 200 000 MPa), 50 cm spacing, 114 mm diameter with 6 mm thickness, 9.0 m length, angle of 7 with the tunnel longitudinal axis				

4.3. Determination of Initial Relaxation Factor

Although tunnel excavation is 3D issue, the 2D modelling of a tunnel is still preferred nowadays, because 3D modelling needs more time and cost. Initial relaxation factor used in the plane-strain analyses was determined by performing axisymmetric analyses. 2D plane-strain analysis is utilized due to simulate the tunneling whose length is too large in third dimension. In the numerical analysis, material softening method is applied to specify the deformation before rock support installment (Swoboda, 1979; Swoboda et al., 1994; Vlachopoulos and Diederichs, 2009; Mehra, 2016; Anguiano et al., 2017).

The axisymmetric model was used for determining the reduction amount of the deformation modulus of the geological formation around tunnel in the selected cross section lines. The generic case of axisymmetric model is shown in Figure 4.4. Axisymmetric analysis was required in this study for the units of sanstone-1, sandstone-2, sandstone-3 and mudstone-2 since only these units are found around tunnel present in specified cross sections. The results of the axisymmetric analysis are represented by total displacement curve (Figure 4.5-Figure 4.8).

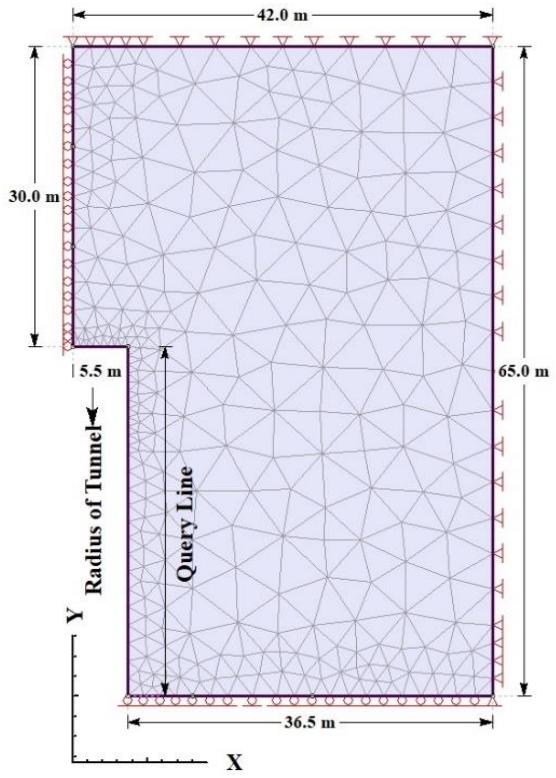

Figure 4.4. Generic model of axisymmetric analysis

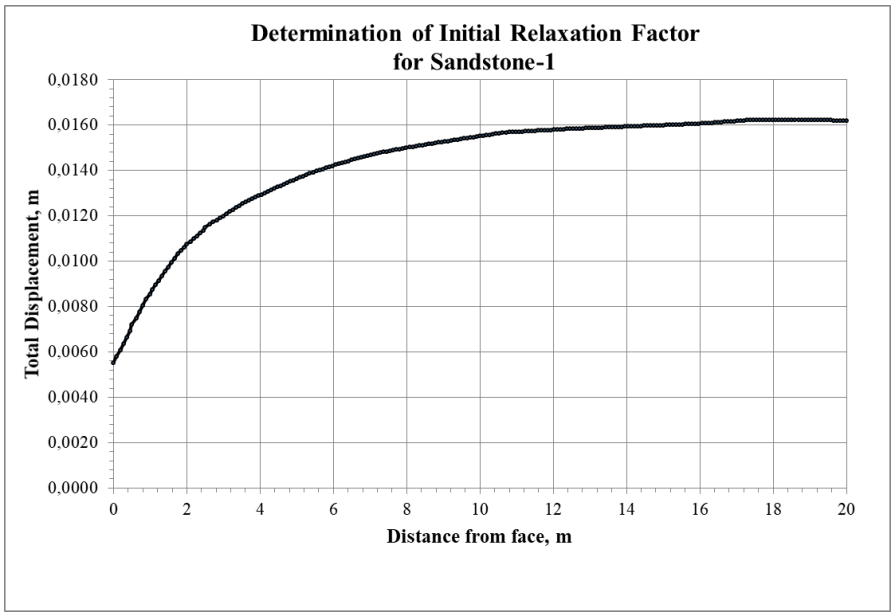

Figure 4.5. Total displacement curve of axisymmetric model for the sandstone-1

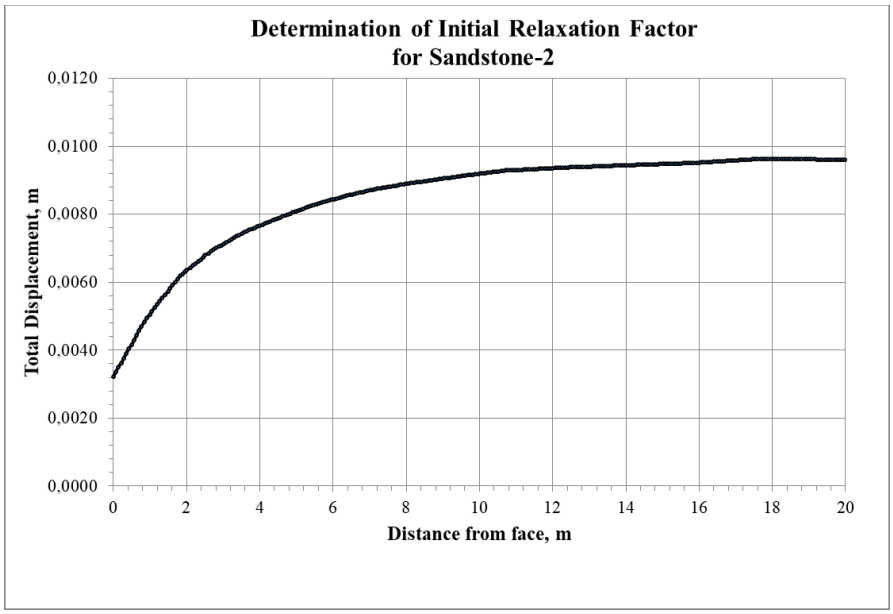

Figure 4.6. Total displacement curve of axisymmetric model for the sandstone-2

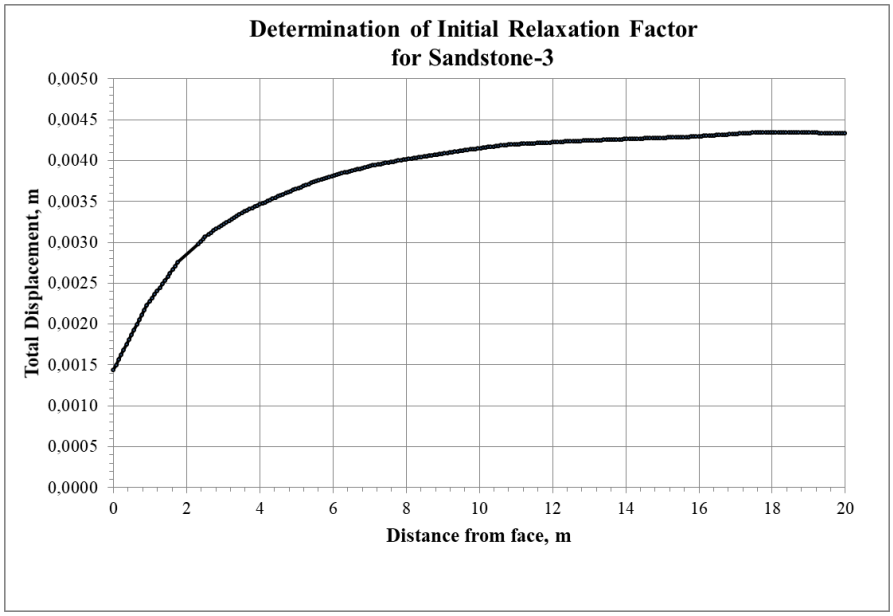

Figure 4.7. Total displacement curve of axisymmetric model for the sandstone-3

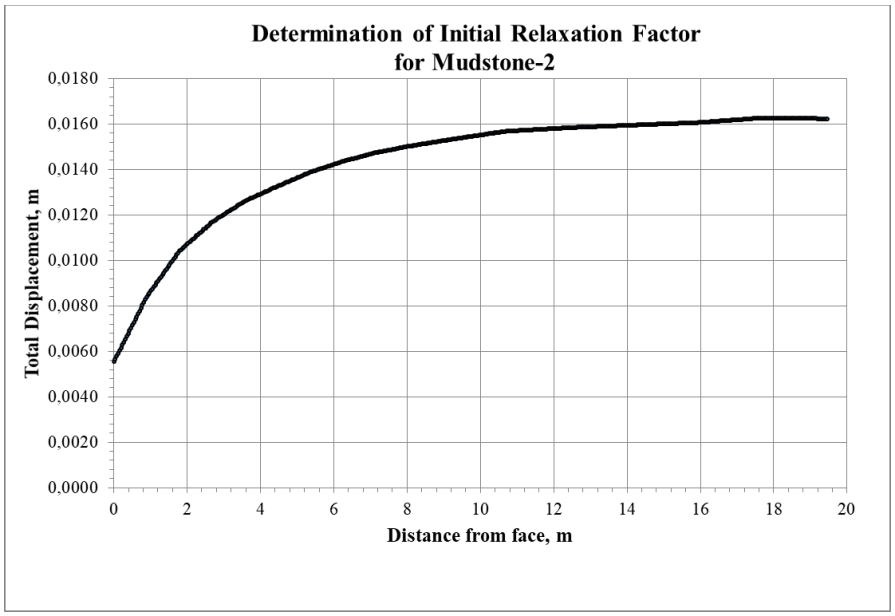

Figure 4.8. Total displacement curve of axisymmetric model for the mudstone-2

The results of the analyses for all of the geological units encountered along the tunnel axis are presented in Table 4.3. The softening ratio reaches 41.1 % for the sandstone-1, 20.8 % for the mudstone-2 and 52 % for the other geological units for the cumulative displacement at 1 m ahead of the face (round length) shown by red color. Hence, the softening ratios were multiplied with the deformation modulus of the rock mass.

Table 4.3. Axisymmetric analysis results of geological units encountered along the tunnel axis.

Geological Formation	Distance to Tunnel Face	Total Displacement	Softening Ratio	Rock Mass Deformation Modulus	
				In-situ	Induced
	m	m	%	MPa	MPa
Sandstone-1	0	0.00554	26.6%	**300**	220.1
	0.5	0.00722	34.7%		195.9
	1	0.00856	41.1%		176.7
	1.5	0.00975	46.8%		159.5
	2	0.01074	51.6%		145.2
	2.5	0.01150	55.2%		134.3
	30	0.02081	100.0%		0.0
Sandstone-2	0	0.00322	33.2%	**500**	334.2
	0.5	0.00417	42.8%		285.8
	1	0.00506	52.0%		240.0
	1.5	0.00573	58.9%		205.6
	2	0.00637	65.5%		172.7
	2.5	0.00679	69.8%		150.8
	35	0.00972	100.0%		0.0
Sandstone-3	0	0.00144	32.9%	**1 100**	737.7
	0.5	0.00187	42.7%		630.3
	1	0.00228	51.9%		528.6
	1.5	0.00258	58.9%		452.3
	2	0.00287	65.5%		379.1
	2.5	0.00307	70.0%		330.2
	30	0.00438	100.0%		0.0
Mudstone-2	0	0.00554	13.3%	**300**	260.0
	0.5	0.00716	17.2%		248.4
	1	0.00866	20.8%		237.5
	1.5	0.00981	23.6%		229.3
	2	0.01075	25.8%		222.5
	2.5	0.01142	27.5%		217.6
	35	0.04160	100.0%		0.0

4.4. Two Dimensional Modeling of the Forepoling Technique

The real process of tunnel excavation and reinforcement is very complex where the deformations of tunnel face are a 3D phenomenon (Dias et al., 1997). However, the

usual practice of tunnel calculation still relies on 2D numerical simulations to estimate both the surface settlements and structural efforts (Kitchah and Benmebarek, 2016). Moreover, maximum vertical surface settlement conditions are studied in the scope of this thesis, and settlement field measurement data are found to be reliable in the 2D sections.

Analysis of the pre-support systems like spiles is currently more complex than that of the face stability. Hoek (2003) pointed out that there is no rule of a thumb for the 2D analysis of the forepoles and therefore in the absence of such rules; a primitive equivalent model is used in this thesis. The crude model supposed that a procedure of weighted averages can be utilized to find the stress and strain of the zone of 'strengthened rock'. For instance, the uniaxial compressive strength is predicted by multiplying the strength of each element by the cross-sectional area of each element and then dividing the sum of these results by the complete area. In this case, the stages in the top heading of the tunnel was essential to establish the forepoles are nearly 0.6 m deep and hence a rock beam 1 m wide and 0.6 m deep is considered in this study. Cross-sectional area of the steel and grout can be calculated by considering the number of pipes per unit meter.

The ground around the tunnel is reinforced before the excavation using an umbrella arch system. In the scope of the project, there are two main pre-support types, namely, forepoles (ST-2, ST-3) and umbrella arch (ST-UA-1). The forepole is composed of 70 mm diameter steel pipes of 4.0 m length with an installation angle of 9° relative to the tunnel axis and the longitudinal spacing is 30 cm. The umbrella arch with injection is composed of 114 mm diameter steel pipes of 6 mm thickness, 9.0 m length with an installation angle of 7° relative to the tunnel axis and the longitudinal spacing is 50 cm. The number of pipes per unit meter can be determined by considering spacing value and 4 pipes/m and 2 pipes/m exist in the forepole and umbrella arch systems, respectively. The equivalent quantities involved in the selected 12 cross sections are given in Table 4.4.

The strength of rock material existed on the Forepoling area (Figure 4.9) was calculated by weighted average method if more than one geological unit. The resultant strength of rock mass for this reinforced concrete is Product/Area. The corresponding rock mass properties can be predicted by iteration of the Hoek-Brown failure criteria (using the program RocLab). Note that the Disturbance Factor D = 0 in this case since the forepoling is assumed to be undamaged. These parameters only apply to a strip of rock material (denoted as composite 'beam') of 600 mm around the tunnel crown (Henfy et al., 2004).

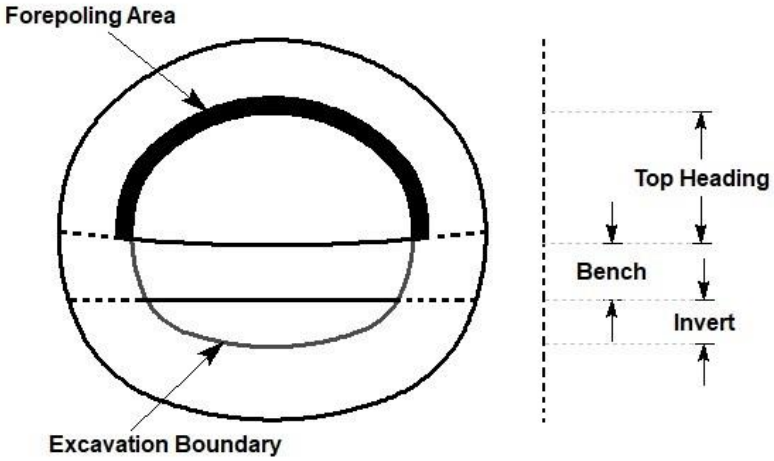

Figure 4.9. Sample 2D geometry of forepoling modeling in Phase^2 software

Table 4.4. Parameters for equivalent model to determine strength of the forepoling material

		Westbound			Eastbound		
Km	**Component**	**Area (m^2)**	**Strength (MPa)**	**Product**	**Area (m^2)**	**Strength (MPa)**	**Product**
9+542	Support Type	ST-3			ST-3		
	Rock	0,58	0,77	0,45	0,58	0,43	0,25
	Steel pipe	0,02	250	3,85	0,02	250	3,85
	Grout	0,00	28	0,00	0,00	28	0,00
	Sum	0,60		4,30	0,60		4,10
	Strength of Pre-support Area (MPa)	7,2			6,8		
	Equivalent Deformation Modulus (MPa)	9470,3			9065,3		
9+585	Support Type	ST-UA1			ST-UA1		
	Rock	0,58	0,13	0,08	0,58	0,13	0,08
	Steel pipe	0,00	250	1,02	0,00	250	1,02
	Grout	0,02	28	0,46	0,02	28	0,46
	Sum	0,60		1,55	0,60		1,55
	Strength of Pre-support Area (MPa)	2,6			2,6		
	Equivalent Deformation Modulus (MPa)	4424,2			4424,2		
9+615	Support Type	ST-3			ST-UA1		
	Rock	0,58	0,13	0,08	0,58	0,13	0,08
	Steel pipe	0,02	250	3,85	0,00	250	1,02
	Grout	0,00	28	0,00	0,02	28	0,46
	Sum	0,60		3,92	0,60		1,55
	Strength of Pre-support Area (MPa)	6,5			2,6		
	Equivalent Deformation Modulus (MPa)	11205,9			4424,2		
9+630	Support Type	ST-2			ST-UA1		
	Rock	0,58	0,13	0,08	0,58	0,13	0,08
	Steel pipe	0,02	250	3,85	0,00	250	1,02
	Grout	0,00	28	0,00	0,02	28	0,46
	Sum	0,60		3,92	0,60		1,55

		Westbound			Eastbound		
Km	**Component**	**Area (m^2)**	**Strength (MPa)**	**Product**	**Area (m^2)**	**Strength (MPa)**	**Product**
	Strength of Pre-support Area (MPa)	6,5			2,6		
	Equivalent Deformation Modulus (MPa)	11205,9			4424,2		
9+645	Support Type	ST-2			ST-UA1		
	Rock	0,58	0,13	0,08	0,58	0,13	0,08
	Steel pipe	0,02	250	3,85	0,00	250	1,02
	Grout	0,00	28	0,00	0,02	28	0,46
	Sum	0,60		3,92	0,60		1,55
	Strength of Pre-support Area (MPa)	6,5			2,6		
	Equivalent Deformation Modulus (MPa)	11205,9			4424,2		
9+660	Support Type	ST-2			ST-UA1		
	Rock	0,58	0,13	0,08	0,58	0,81	0,47
	Steel pipe	0,02	250	3,85	0,00	250	1,02
	Grout	0,00	28	0,00	0,02	28	0,46
	Sum	0,60		3,92	0,60		1,94
	Strength of Pre-support Area (MPa)	6,5			3,2		
	Equivalent Deformation Modulus (MPa)	11205,9			4293,2		
9+681	Support Type	ST-UA1			ST-UA1		
	Rock	0,58	0,88	0,51	0,58	0,88	0,51
	Steel pipe	0,00	250	1,02	0,00	250	1,02
	Grout	0,02	28	0,46	0,02	28	0,46
	Sum	0,60		1,99	0,60		1,99
	Strength of Pre-support Area (MPa)	3,3			3,3		
	Equivalent Deformation Modulus (MPa)	4452,8			4452,8		
9+695	Support Type	ST-3			ST-3		
	Rock	0,58	0,88	0,52	0,58	0,88	0,52
	Steel pipe	0,02	250	3,85	0,02	250	3,85

		Westbound			Eastbound		
Km	**Component**	**Area (m^2)**	**Strength (MPa)**	**Product**	**Area (m^2)**	**Strength (MPa)**	**Product**
	Grout	0,00	28	0,00	0,00	28	0,00
	Sum	0,60		4,36	0,60		4,36
	Strength of Pre-support Area (MPa)	7,3			7,3		
	Equivalent Deformation Modulus (MPa)	9786,1			9786,1		
9+758	Support Type	ST-3			ST-3		
	Rock	0,58	0,56	0,33	0,58	0,34	0,20
	Steel pipe	0,02	250	3,85	0,02	250	3,85
	Grout	0,00	28	0,00	0,00	28	0,00
	Sum	0,60		4,17	0,60		4,05
	Strength of Pre-support Area (MPa)	7,0			6,7		
	Equivalent Deformation Modulus (MPa)	8987,0			8912,1		
9+789	Support Type	ST-3			ST-3		
	Rock	0,58	0,45	0,26	0,58	0,34	0,20
	Steel pipe	0,02	250	3,85	0,02	250	3,85
	Grout	0,00	28	0,00	0,00	28	0,00
	Sum	0,60		4,11	0,60		4,05
	Strength of Pre-support Area (MPa)	6,9			6,7		
	Equivalent Deformation Modulus (MPa)	8881,2			8912,1		
9+996	Support Type	ST-2			ST-2		
	Rock	0,58	0,88	0,52	0,58	0,88	0,52
	Steel pipe	0,02	250	3,85	0,02	250	3,85
	Grout	0,00	28	0,00	0,00	28	0,00
	Sum	0,60		4,36	0,60		4,36
	Strength of Pre-support Area (MPa)	7,3			7,3		
	Equivalent Deformation Modulus (MPa)	9786,1			9786,1		
10+016	Support Type	ST-2			ST-2		

		Westbound			Eastbound		
Km	**Component**	**Area (m^2)**	**Strength (MPa)**	**Product**	**Area (m^2)**	**Strength (MPa)**	**Product**
	Rock	0,58	0,88	0,52	0,58	0,88	0,52
	Steel pipe	0,02	250	3,85	0,02	250	3,85
	Grout	0,00	28	0,00	0,00	28	0,00
	Sum	0,60		4,36	0,60		4,36
	Strength of Pre-support Area (MPa)	7,3			7,3		
	Equivalent Deformation Modulus (MPa)	9786,1			9786,1		

The crude equivalent model is the only one that is able to capture the expected reduction in the crown convergence when other support members are installed. Analysis of this model is found that while the crude equivalent model might capture empirical trends of reduction of the crown convergence, this method does not, however, captures the true longitudinal mechanical response of the umbrella arch. This is because when the forepole elements are installed without other supports, there is no significant reduction in the crown displacement, as denoted by the 3D analysis results (Oke et al., 2014).

On the other hand, the forepole as a structural element cannot, however, be modelled as a homogenous region due to the lack of mechanistic behavior, even though the homogeneous results are empirically acceptable (Oke et al., 2012).

Compared to the stiffness of the ground, the high stiffness of the steel pipes positively influences the stress distribution ahead of the supported section. This effect and the radial support around the heading decrease the settlement amounts (Volkmann and Schubert, 2007).

The center to center spacing of the forepole elements was considered as a key design parameter, but it is unable to be easily observed in full scale 3D numerical model.

Consequently, it is suggested that a 2D analysis should be utilized to observe the largest spacing, depending on representative size and stiffness of the forepole elements (Oke et al., 2014). Therefore, the center to center distance between pipes is selected as variable in the parametric study and presented in Chapter 5.

4.5. Modeling of the Tunnel Construction

Numerical analyses were started by creating the external boundary, delineating the different material layers and specifying noncircular excavation boundary, and then generate the finite element mesh with graded 3-noded triangle.

It is suggested that mesh dimensions for two dimensional simulating of tunnels. It was supposed to take 3D from tunnel axis to the bottom mesh boundary, and 5D from the tunnel axis to the vertical mesh boundaries; where D is the tunnel diameter (Meissner, 1996; Möller, 2006). Therefore, in this study 55 m from centerlines of both tunnels to vertical boundaries and 33 m to bottom boundary (Figure 4.10).

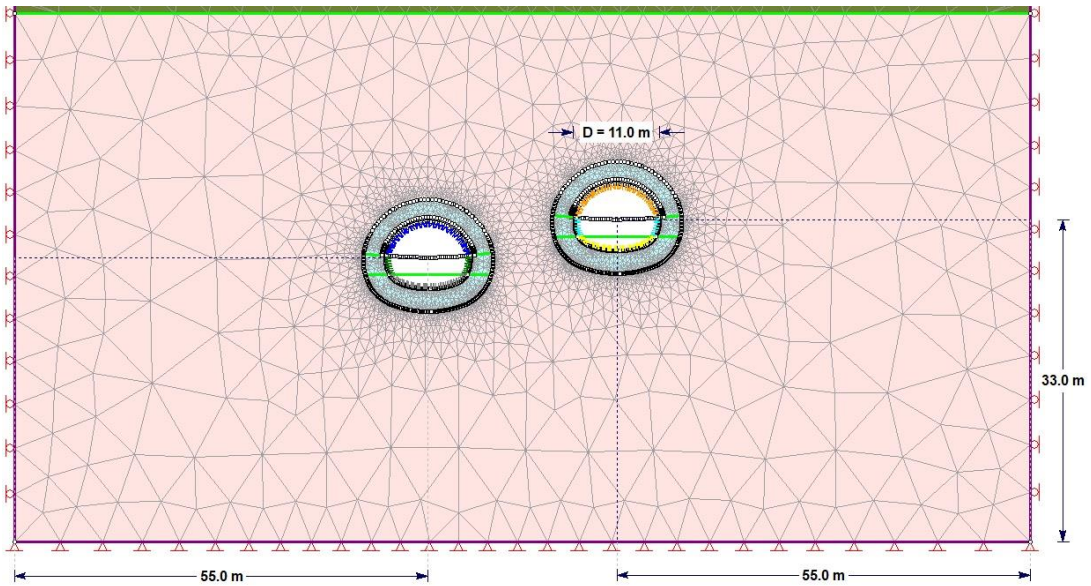

Figure 4.10. Boundary condition of the twin tunnels for this study.

Since the top of this model represents the actual ground surface, it is required to free the top surface. Boundary condition for bottom part of the model is zero displacement, i.e. fixed, and for right and left sides, roller supports which restrain only the horizontal movements and vertical displacements are left free are used.

The initial element loading is one of the most difficult concepts to grasp in Finite-Element (FE) modeling. Basically, in FE an element can have two initial internal loadings, initial stress and body force. If there is no external load on geo-material then it subsides under its own weight and the uppermost surface goes down. If the geo-material has only initial stress then it extends and the uppermost surface goes up. If both of them was defined, then the geo-material is in equilibrium and then there is no surface settlement (Rocscience, 2018). Field stress determines the initial in-situ stress conditions, prior to excavation. Gravity field stress was used, because the top of the model represents the true ground surface. The values of K_0 -total stress ratio- for out of plane and in plane were taken as 0.5 and 1.0, respectively by regarding the current geological data on the study area.

The water table is defined in view of field data coming from boreholes. A water table was created with the "Add Piezometric Line" option. Then, groundwater/hydraulic parameters for each material were specified by using "Define Hydraulic Properties" option. The Hu value is simply a factor between 0 and 1, by which the vertical distance from a point (in the soil or rock), to a Water Surface (i.e. Piezo Line) is multiplied to obtain the pressure head. Hu = 1 would indicate hydrostatic conditions, Hu = 0 would indicate a dry soil and intermediate values of Hu can be used to simulate head loss due to seepage (Rocscience, 2012).

Live loads due to highway and construction are taken into consideration with 20 kPa (AASHTO, 2002). In addition, liner properties are defined and tunnel support system is generated by using composite liner option.

It is required to define the material properties and assign the correct materials to the correct parts of the model. Because of the nature of the excavation, a distribution

zone or so-called plastic zone always develops around the excavated rock mass. Degree of the plastic zone is variable; it depends on the excavation method. While detecting the thickness of the disturbed zone, material type was selected as plastic, then performed the finite element analysis for yielded elements around tunnel periphery. The disturbed zone was specified as a range of 2-3 m offset from tunnel periphery (Table 4.5) and while determining its parameters, disturbance factor was selected as 0.7. This material has been activated after excavation.

Table 4.5. Thickness of plastic zone along the selected cross sections

No	Km	Spacing (m)	Overburden Depth (m)		Support Type		Tunnel Diameter (m)	GWT from surface (m)	Thickness of Plastic Zone (m)
			Westbound	Eastbound	Westbound	Eastbound			
1	9+542	17.71	33.21	26.40	ST-3	ST-3	11.2	8.90	2.1
2	9+585	22.29	31.54	25.54	ST-UA1	ST-UA1	11.6	6.40	2.8
3	9+615	24.33	33.13	26.38	ST-3	ST-UA1	11.4	5.80	3.3
4	9+630	24.90	33.28	27.20	ST-2	ST-UA1	11.4	5.80	3.2
5	9+645	25.24	33.40	27.31	ST-2	ST-UA1	11.4	6.30	3.4
6	9+660	25.40	33.55	27.78	ST-2	ST-UA1	11.4	4.80	2.8
7	9+681	25.21	33.75	28.36	ST-UA1	ST-UA1	11.6	3.90	2.3
8	9+695	25.10	33.95	28.90	ST-3	ST-3	11.2	3.30	2.9
9	9+758	24.10	34.43	31.20	ST-3	ST-3	11.2	0.45	2.9
10	9+789	23.50	34.71	32.23	ST-3	ST-3	11.2	0.10	3.4
11	9+996	25.80	38.54	35.37	ST-2	ST-2	11.2	5.20	1.6
12	10+016	27.40	38.89	35.49	ST-2	ST-2	11.2	8.00	1.6

General view of the finite element models for the selected cross section lines are presented in Figure 4.11- Figure 4.22. Lastly, 11 stages modeling the driving tunnel excavation order (top heading, bench and invert) are specified and presented in Figure 4.23. In the first construction stage initial stress of the ground was generated. Then pre-support was applied at the top heading of the tunnel to prevent the excessive settlement at surface and relaxation factor of the sandstone-3 was applied at top heading to represent the third dimension of the tunnel construction. Thirdly, top heading was excavated and initial liner was applied at the top heading, at the same time relaxation factor of the sandstone-3 was applied at bench of the tunnel.

Afterwards, bench of the tunnel was excavated and initial liner was applied at the bench, relaxation factor of the sandstone-3 was applied at invert of the tunnel concurrently. Later, invert part of the tunnel was excavated and liner was applied at the invert. After completion of the left tunnel of the twin tunnel structure, the same construction operations were implemented for the right tunnel (stages 7-11).

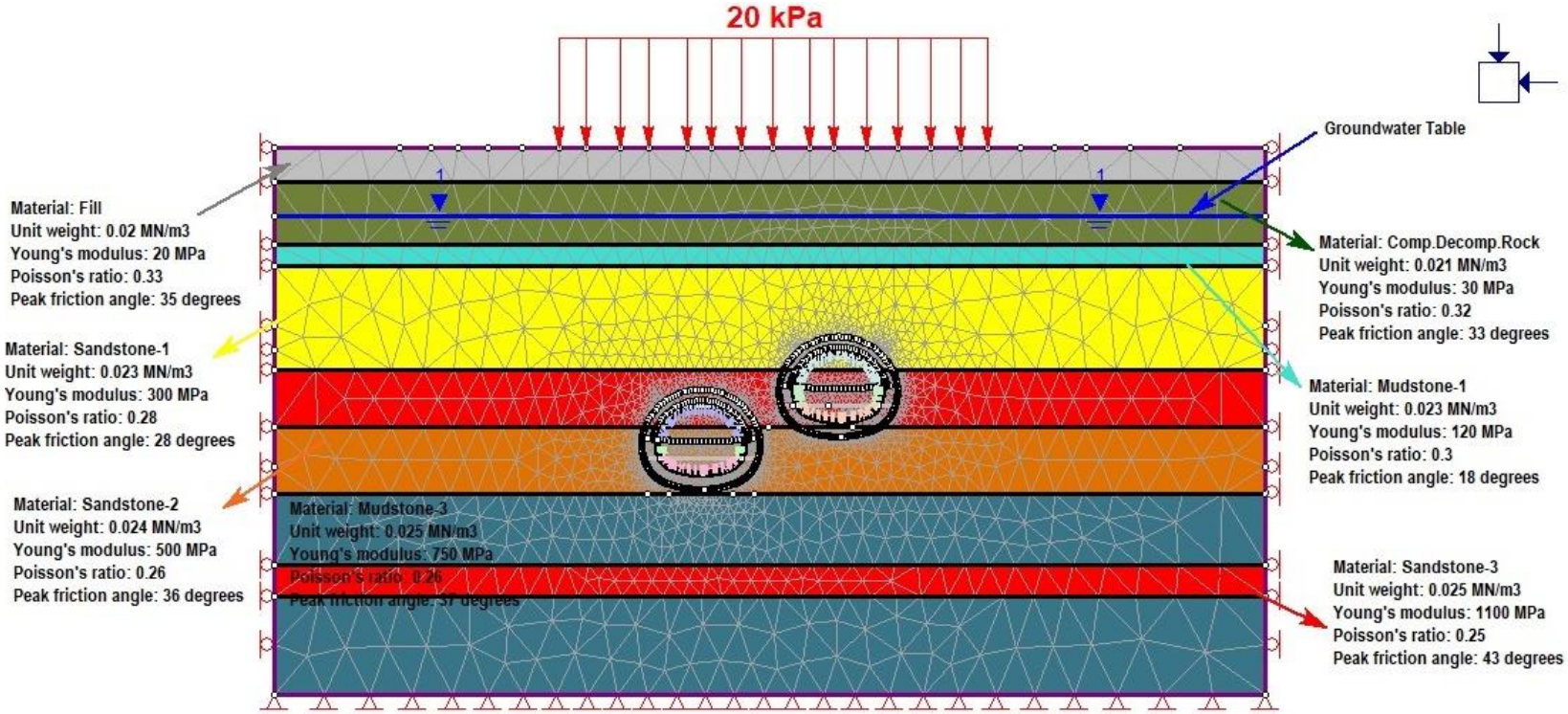

Figure 4.11. General view of the finite element model for Section Km 9+542

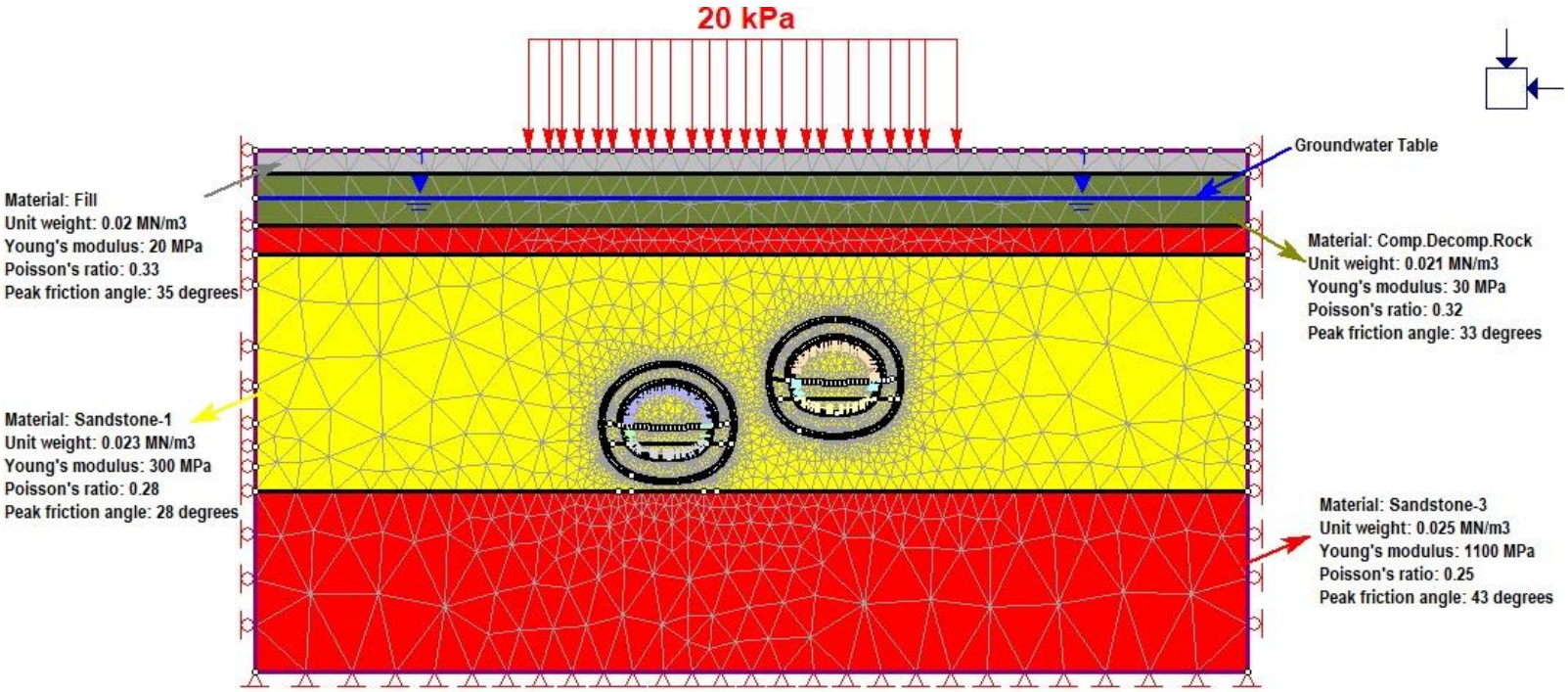

Figure 4.12. General view of the finite element model for Section Km 9+585

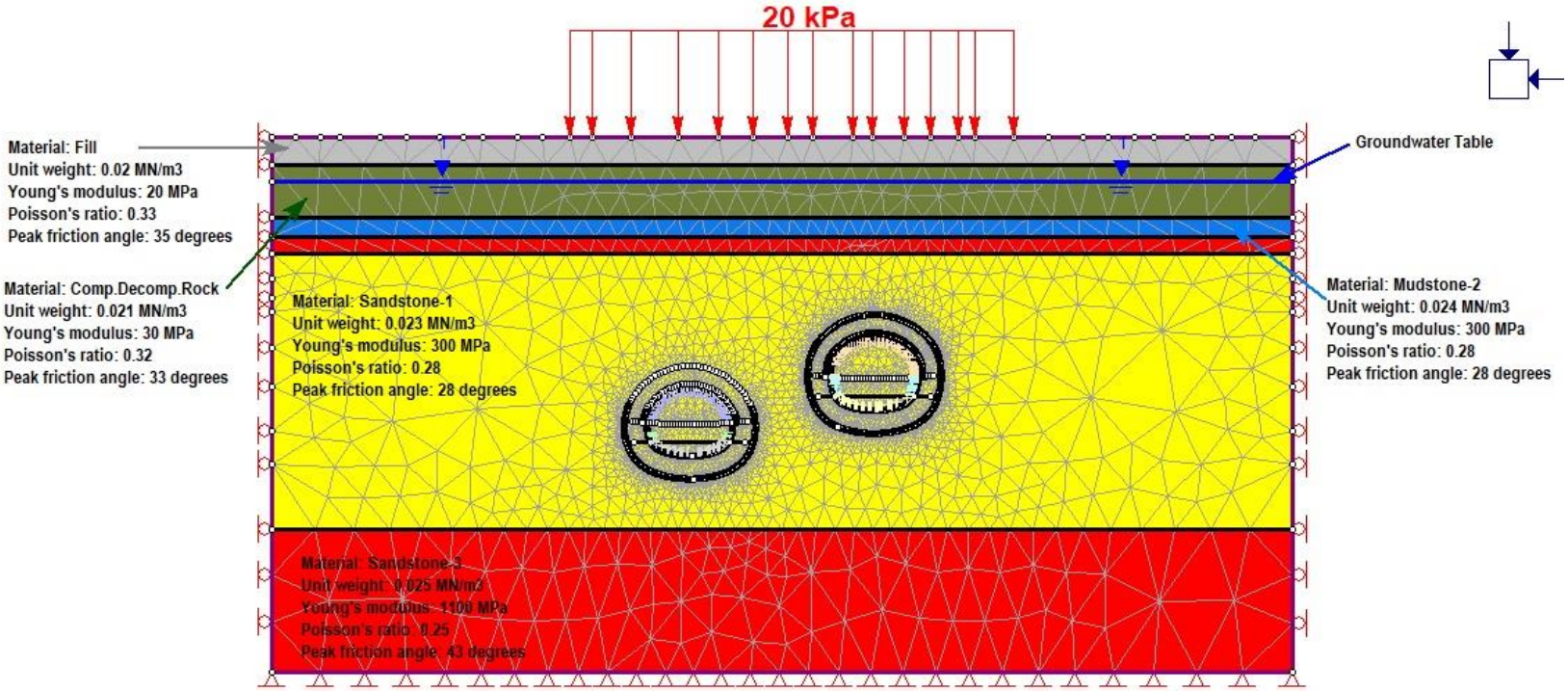

Figure 4.13. General view of the finite element model for Section Km 9+615

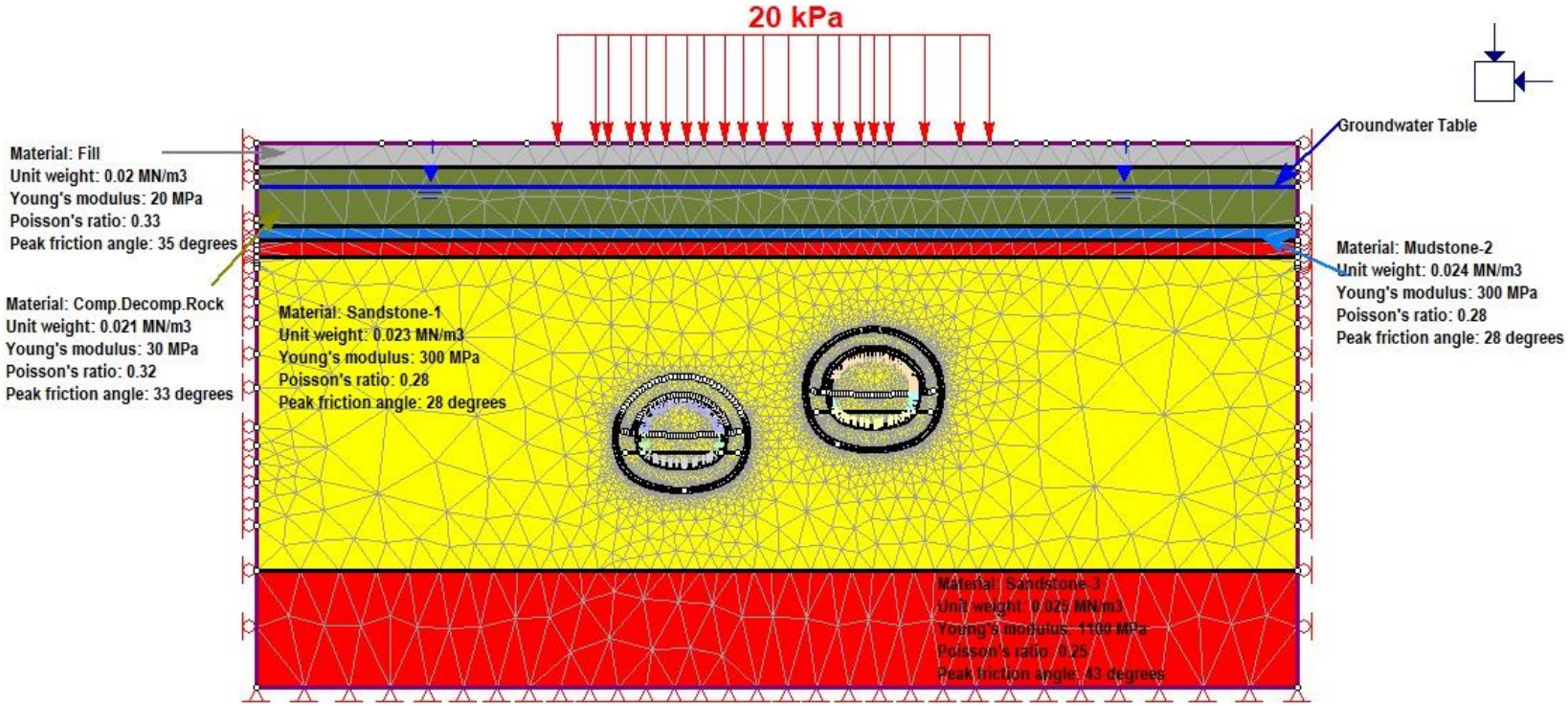

Figure 4.14. General view of the finite element model for Section Km 9+630

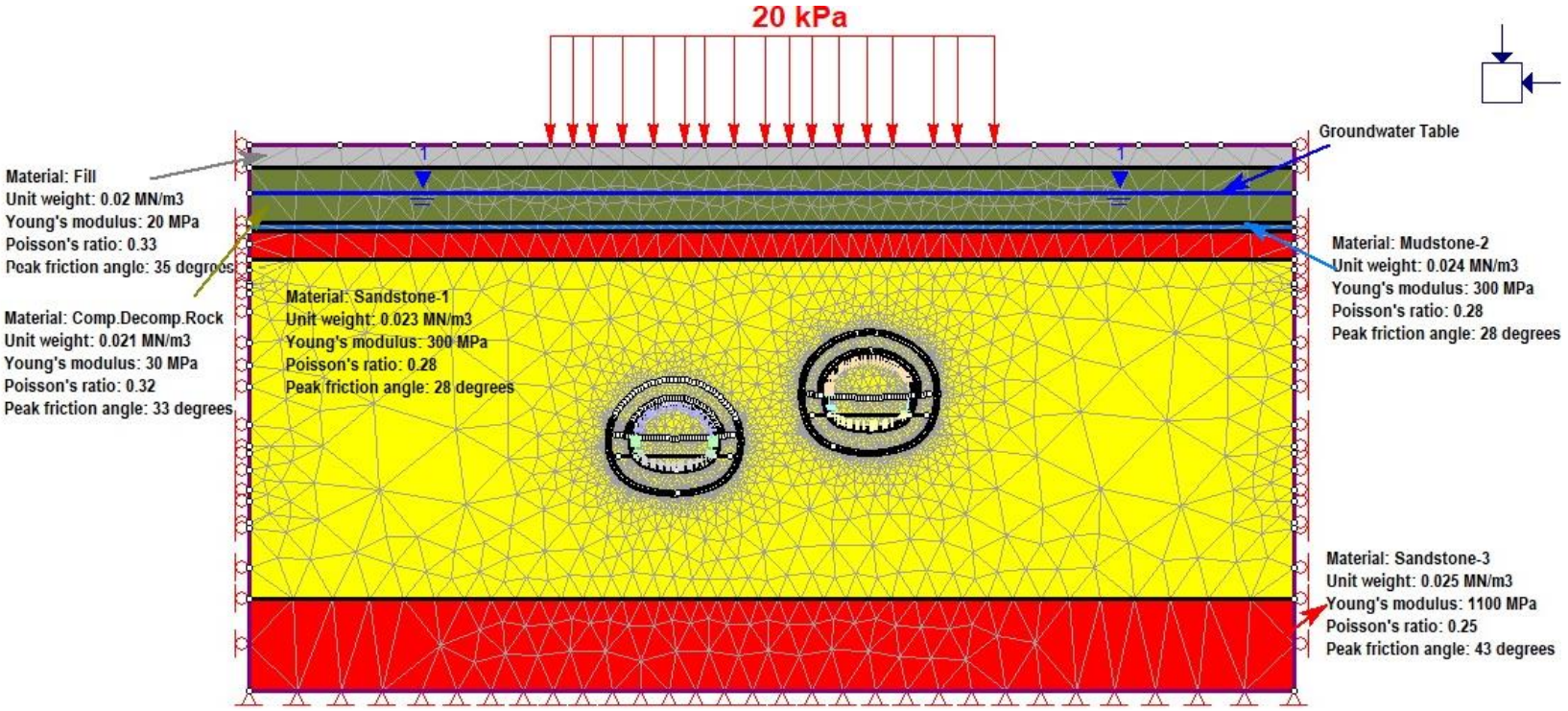

Figure 4.15. General view of the finite element model for Section Km 9+645

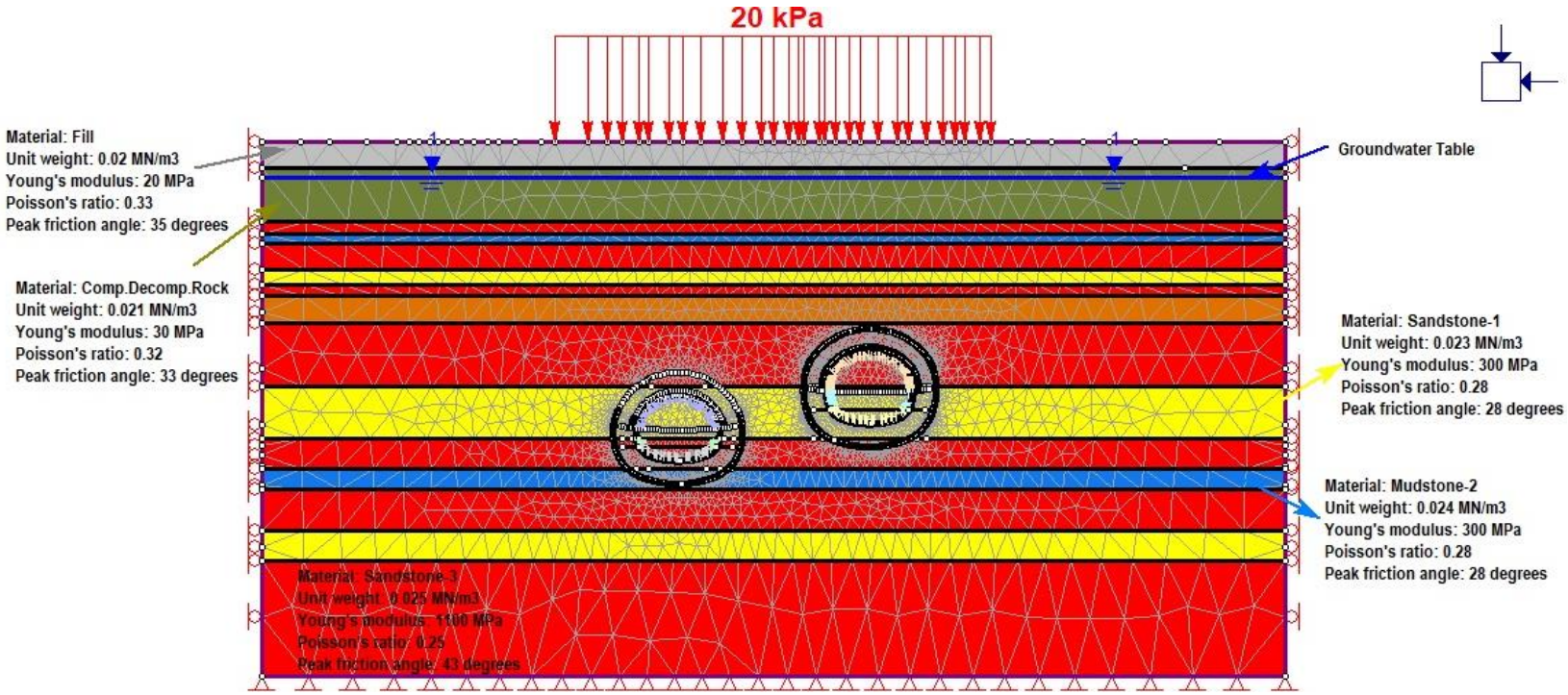

Figure 4.16. General view of the finite element model for Section Km 9+660

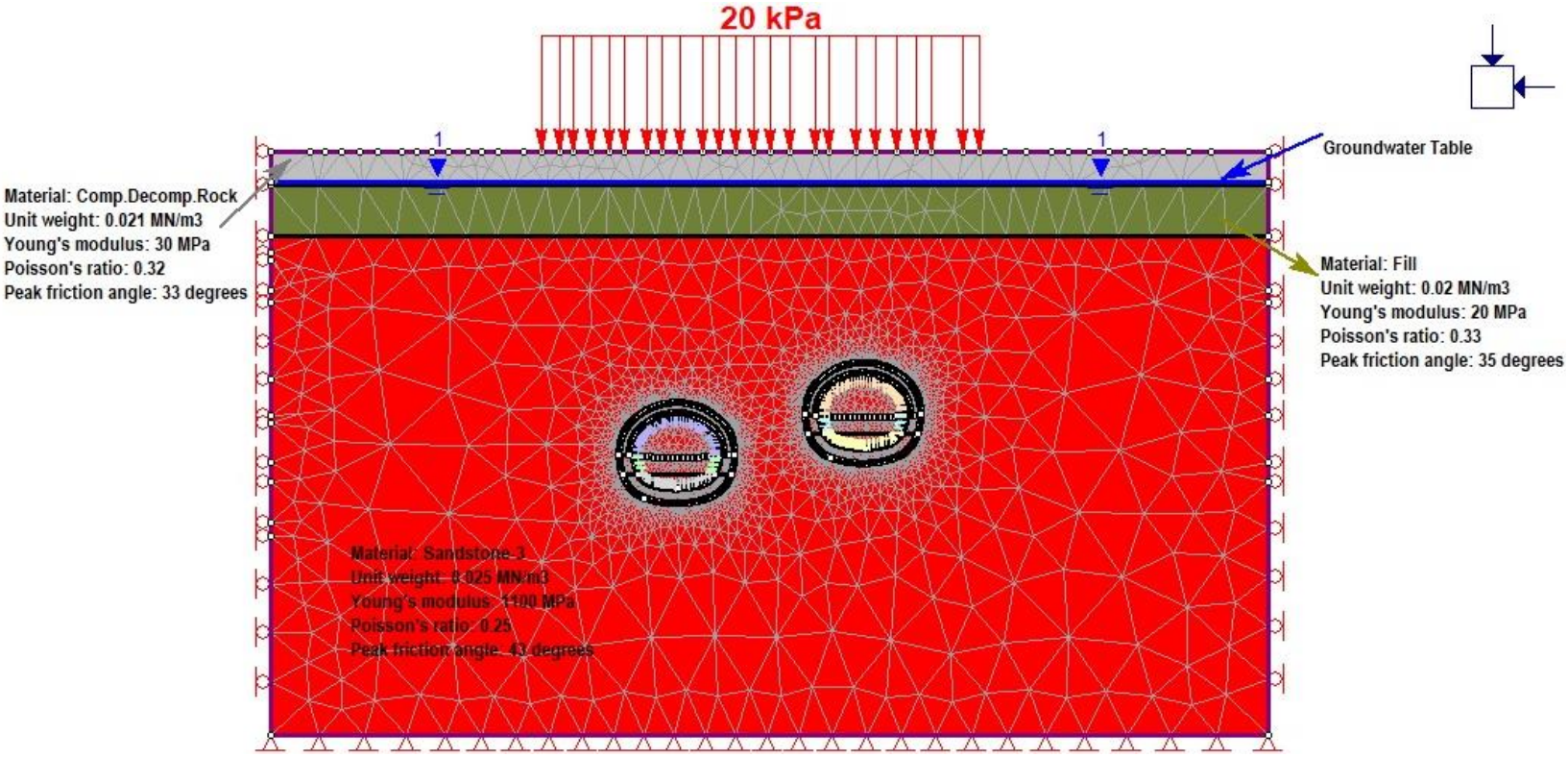

Figure 4.17. General view of the finite element model for Section Km 9+681

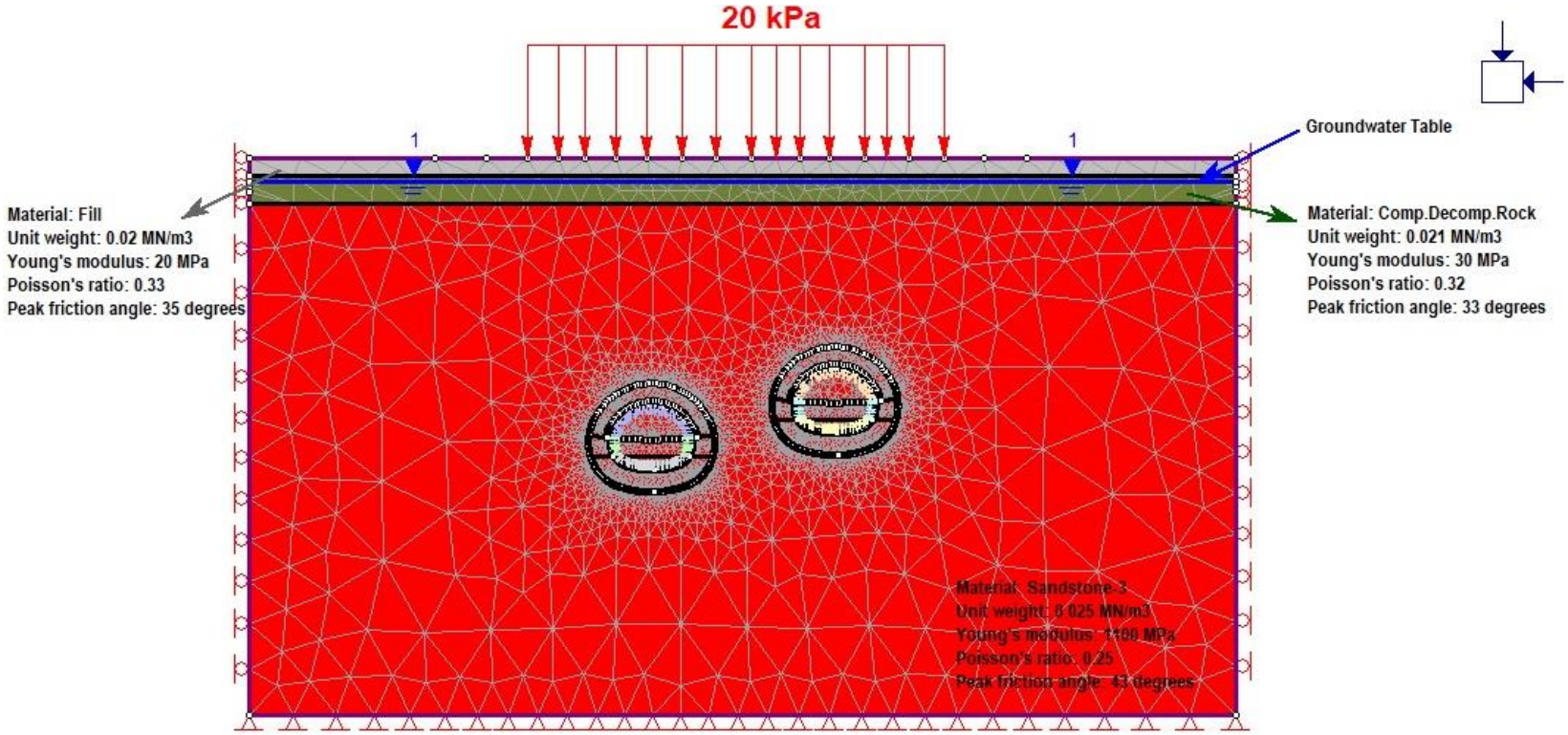

Figure 4.18. General view of the finite element model for Section Km 9+695

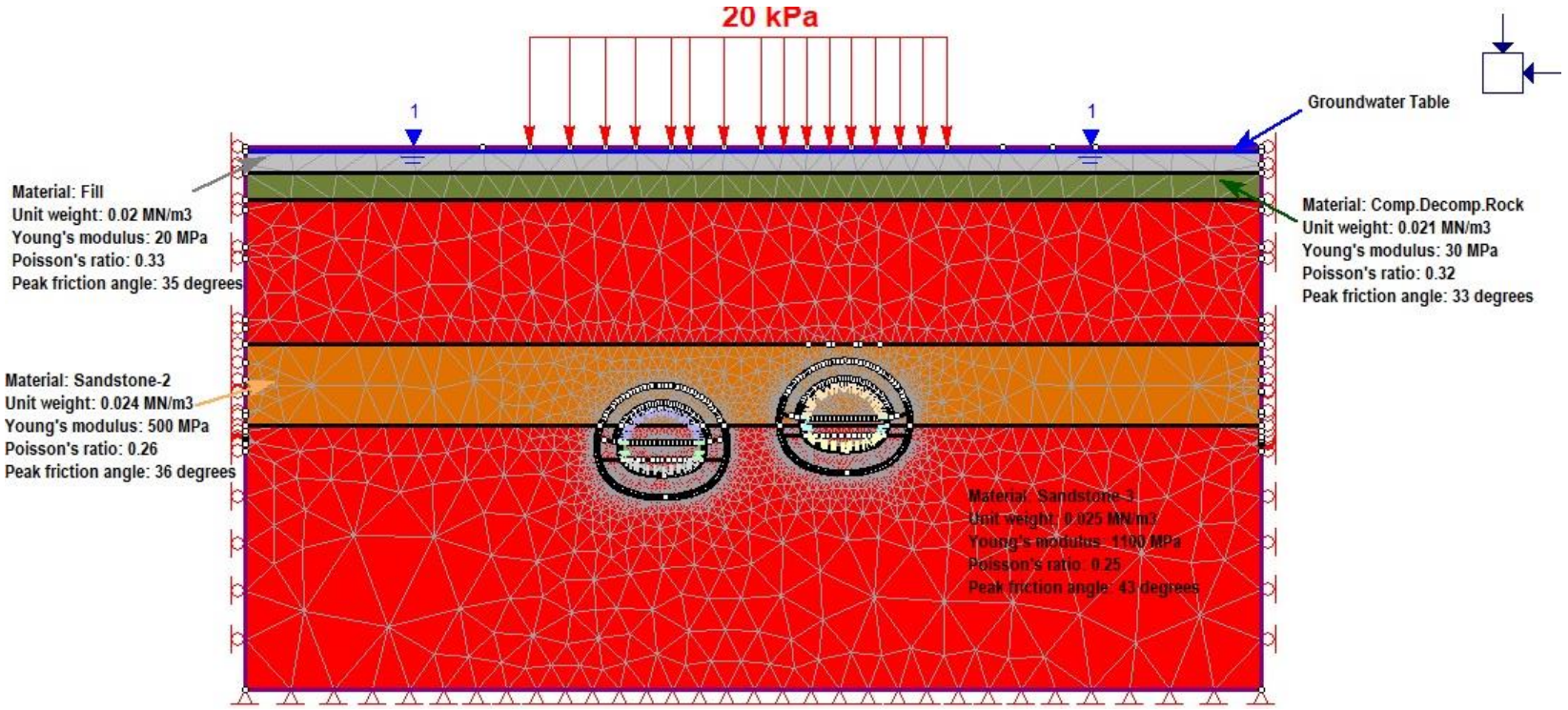

Figure 4.19. General view of the finite element model for Section Km 9+758

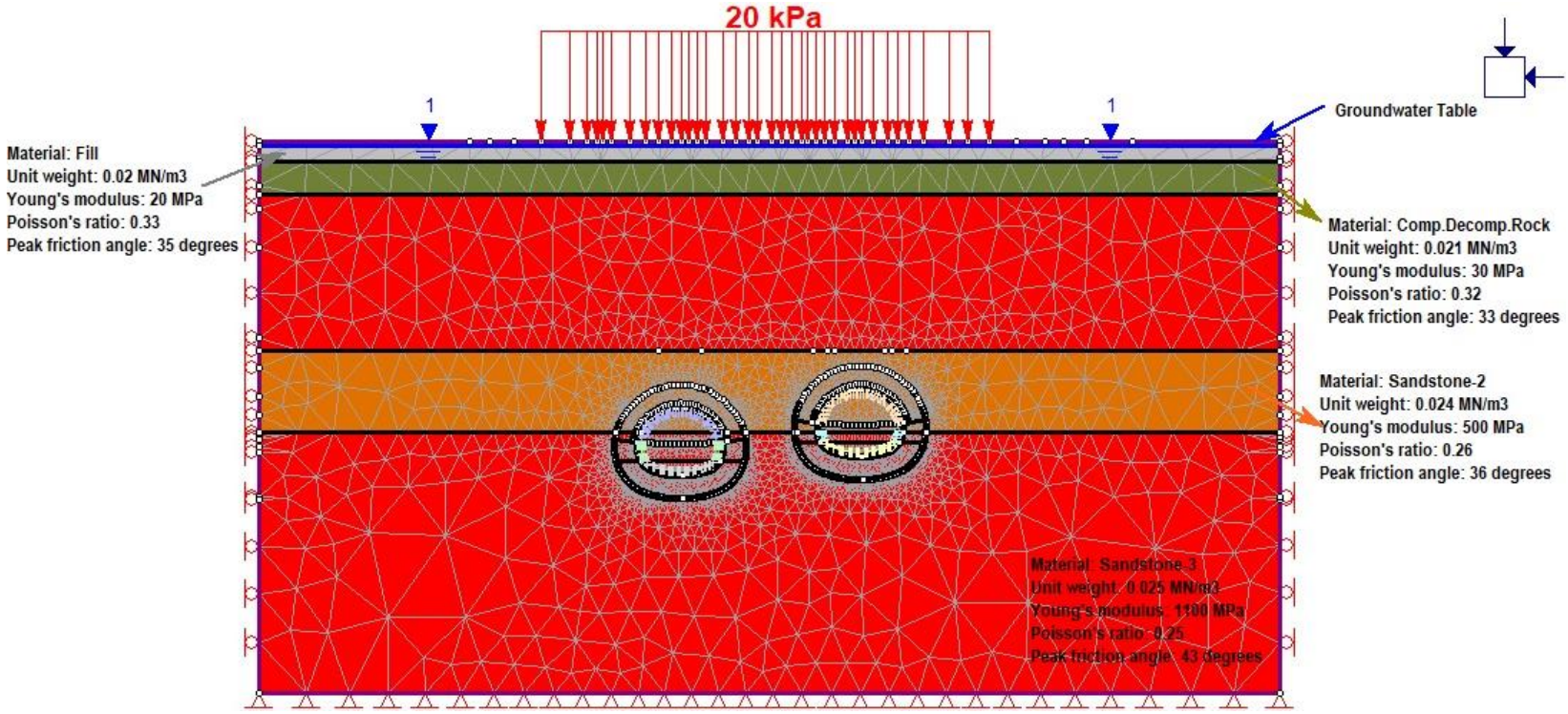

Figure 4.20. General view of the finite element model for Section Km 9+789

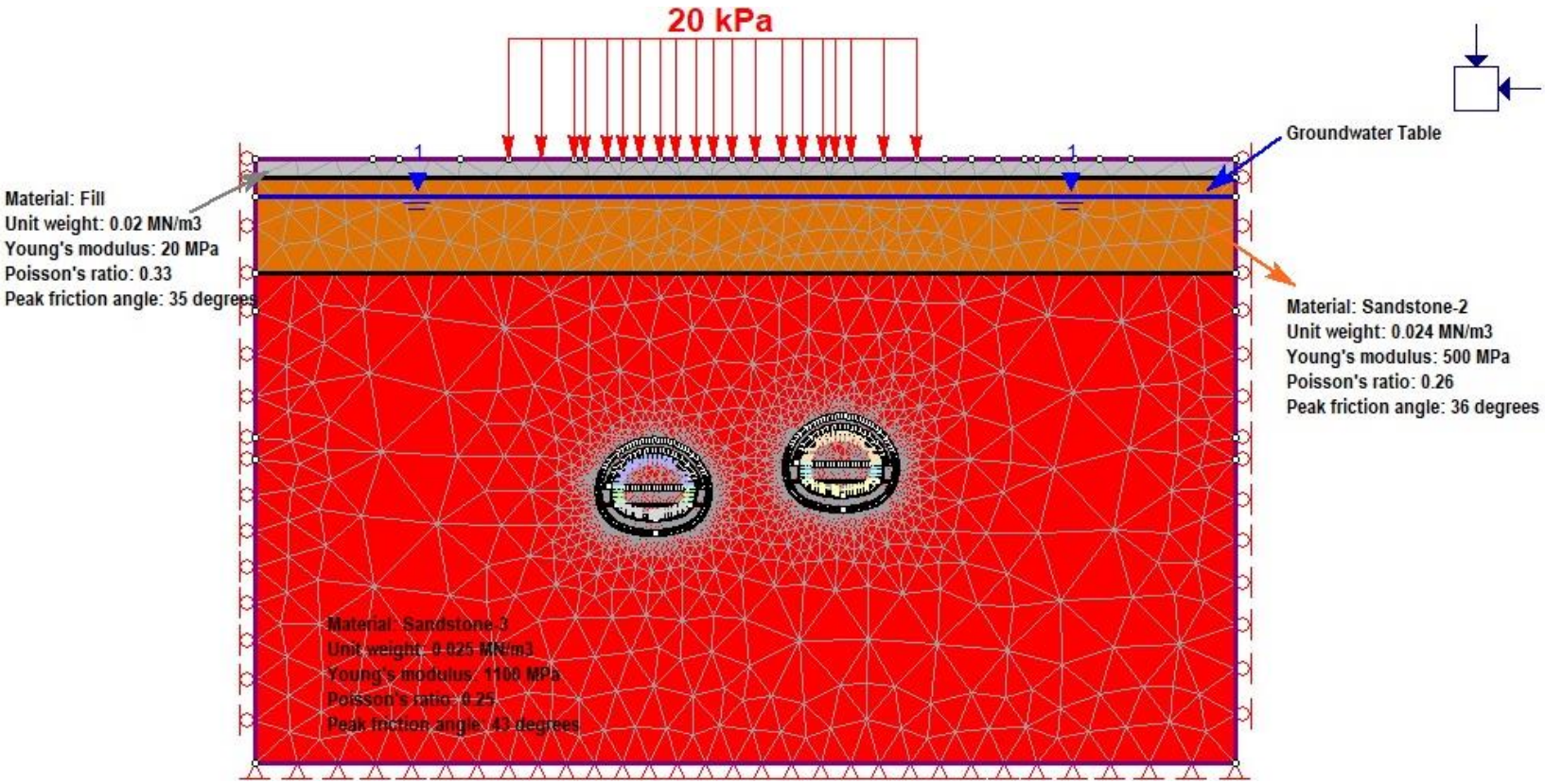

Figure 4.21. General view of the finite element model for Section Km 9+996

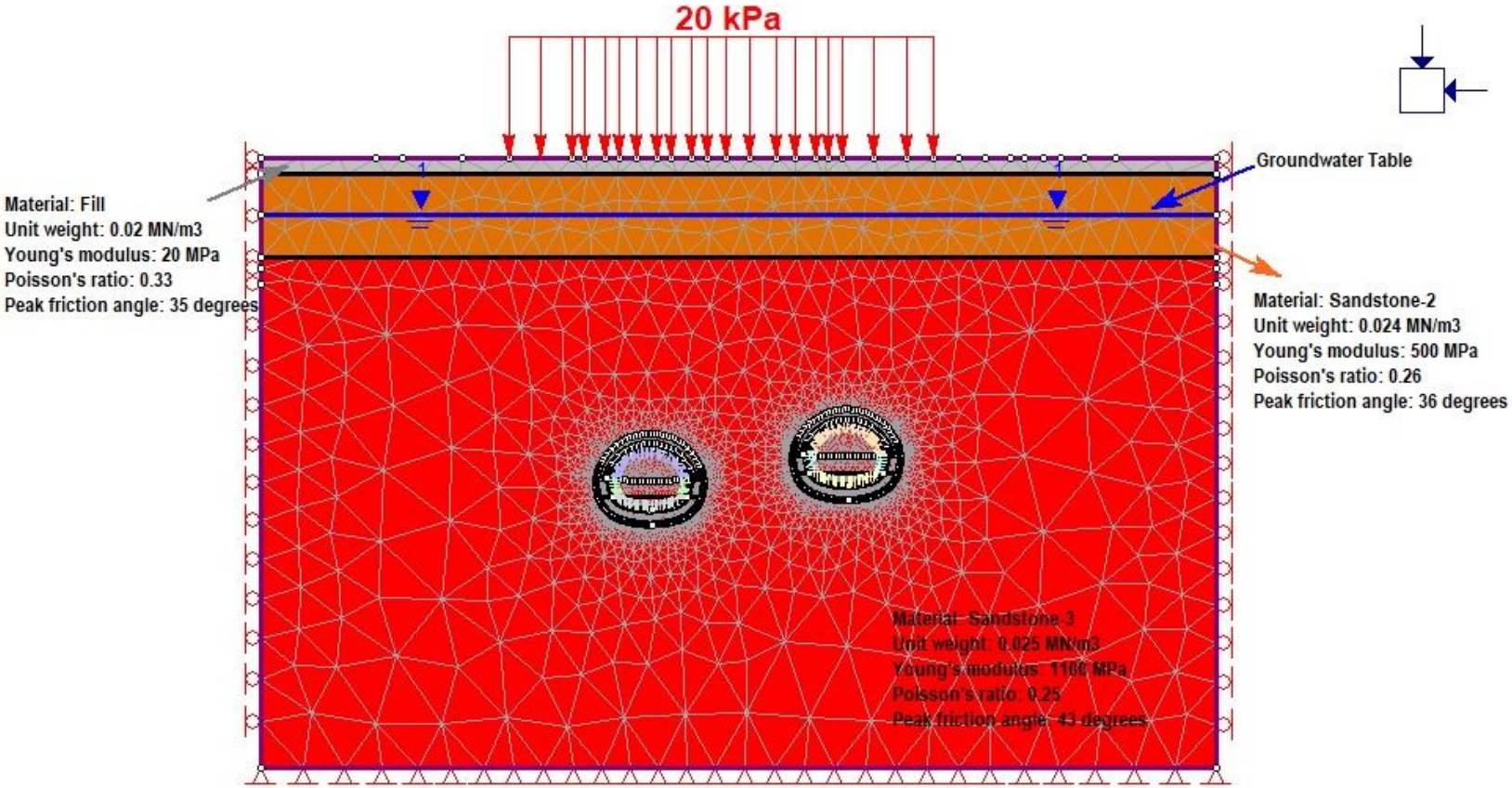

Figure 4.22. General view of the finite element model for Section Km 10+016

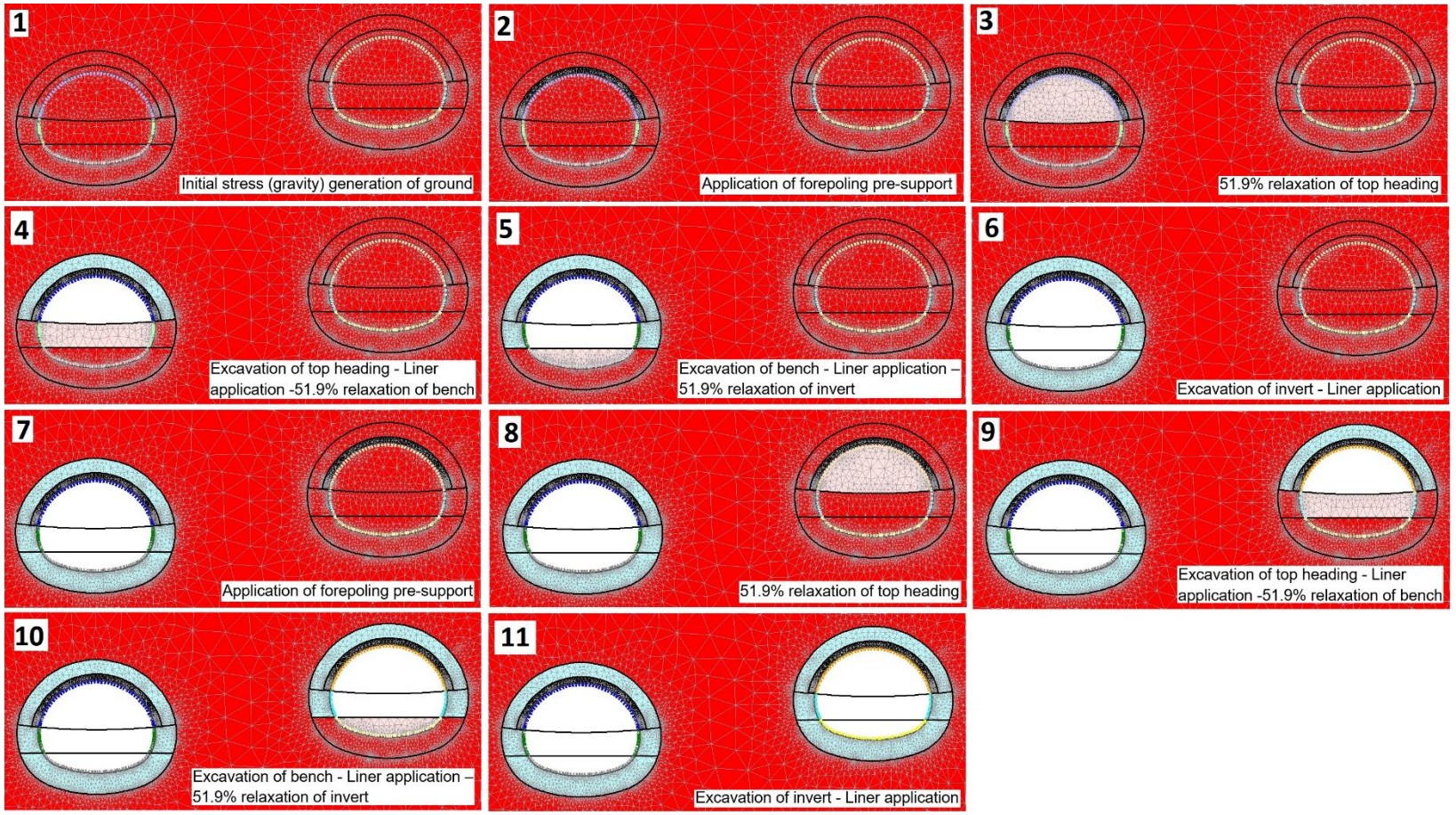

Figure 4.23. Construction of the stages

CHAPTER 5

RESULTS AND DISCUSSIONS

Up to now, it was explained what the objective of this thesis is, what was expressed in the literature about tunnel induced settlements, how finite element analysis can be performed by considering background assumptions, which geotechnical material properties can be used by applying rock mass classification. In this chapter, interpretation of finite element analyses results shall be reported with some outcomes of parametric studies.

In this study, twin tunnel induced ground settlement was investigated and so consistency between field measurement data and FEM analyses results is very crucial. Material parameters especially deformation constants; i.e., modulus and Poisson's ratio, boundary of geological formations, groundwater level, live loads, support parameters, excavation steps, mesh dimensions and field stress have effects on the results. Back analysis was applied by adapting the geological conditions at places where no borehole exists, until results of finite element analyses are close to field data, since the field measurements are reliable.

5.1. Results of the Finite Element Analysis

Finite element models given in Chapter-4 are general view for the selected cross section lines, they are computed, and results of these analyses as vertical settlement contour are presented in this chapter (Figure 5.1-Figure 5.12). The values of maximum vertical settlement obtained from the FEM analyses and field measurement for each cross section lines are listed in Table 5.1. Residuals which are computed by subtracting the measured values from the predicted values gained by the FEM analyses show how accurate model results. Residuals for this study are mostly around zero. When the residuals are zero, it means that the model wholly

represents the actual conditions. These residual values show that the FEM analyses are good enough for further evaluations.

Table 5.1. Maximum settlement values and residuals along the selected cross-sections

No	Km	Spacing (m)	Overburden Depth (m)		Support Type		Tunnel Diameter (m)	GWT from surface (m)	Field Smax (mm)	FEM Smax (mm)	Residuals
			Westbound	Eastbound	Westbound	Eastbound					
1	9+542	17.71	33.21	26.40	ST-3	ST-3	11.2	8.90	6.60	6.35	0.25
2	9+585	22.29	31.54	25.54	ST-UA1	ST-UA1	11.6	6.40	25.50	25.25	0.25
3	9+615	24.33	33.13	26.38	ST-3	ST-UA1	11.4	5.80	28.20	28.02	0.18
4	9+630	24.90	33.28	27.20	ST-2	ST-UA1	11.4	5.80	30.70	29.88	0.82
5	9+645	25.24	33.40	27.31	ST-2	ST-UA1	11.4	6.30	25.30	25.02	0.28
6	9+660	25.40	33.55	27.78	ST-2	ST-UA1	11.4	4.80	20.10	20.21	-0.11
7	9+681	25.21	33.75	28.36	ST-UA1	ST-UA1	11.6	3.90	12.70	12.92	-0.22
8	9+695	25.10	33.95	28.90	ST-3	ST-3	11.2	3.30	9.80	9.97	-0.17
9	9+758	24.10	34.43	31.20	ST-3	ST-3	11.2	0.45	13.40	13.12	0.28
10	9+789	23.50	34.71	32.23	ST-3	ST-3	11.2	0.10	13.00	12.92	0.08
11	9+996	25.80	38.54	35.37	ST-2	ST-2	11.2	5.20	6.10	5.81	0.29
12	10+016	27.40	38.89	35.49	ST-2	ST-2	11.2	8.00	5.90	5.59	0.31

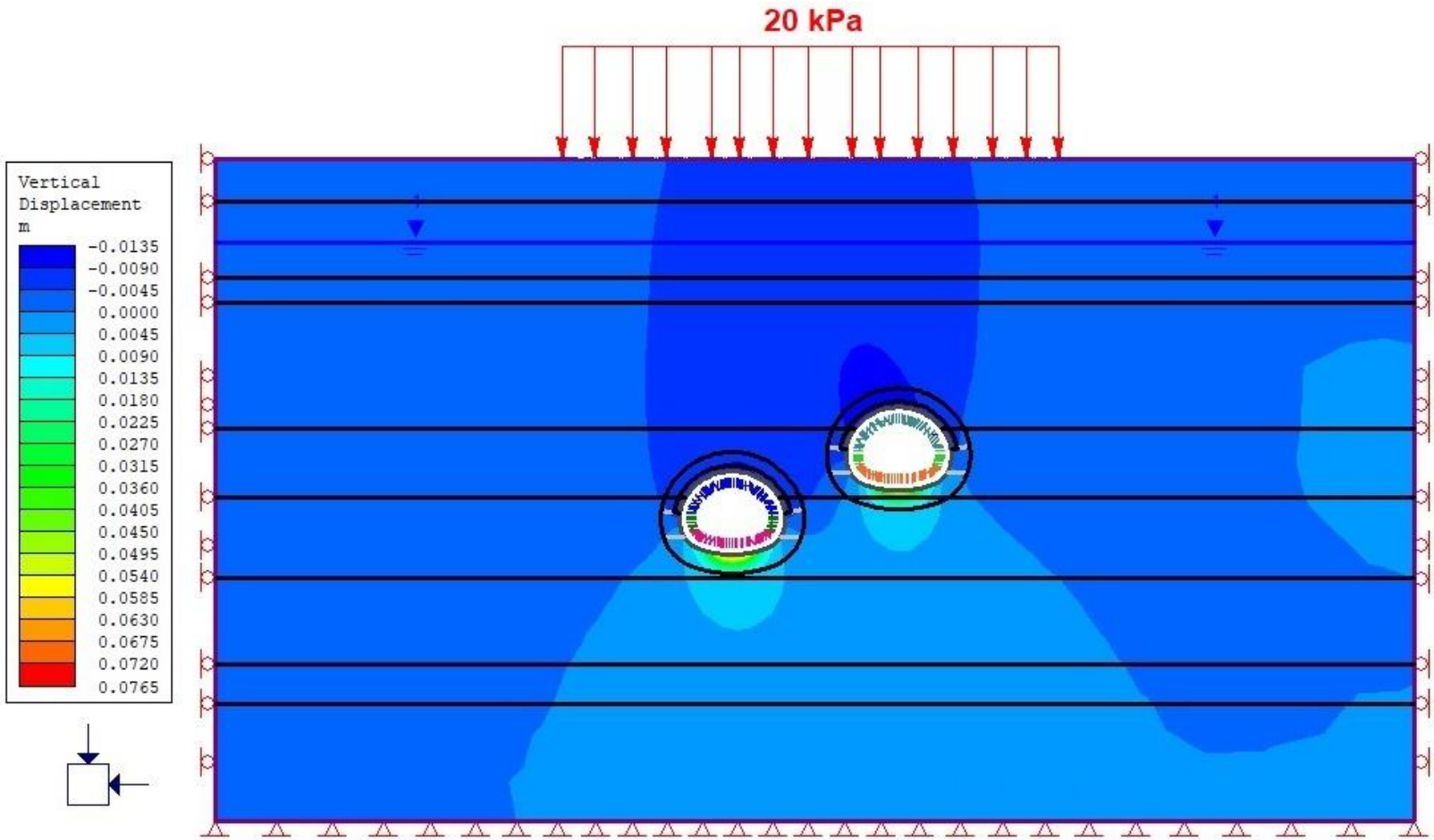

Figure 5.1. Finite element analysis result for the section Km 9+542

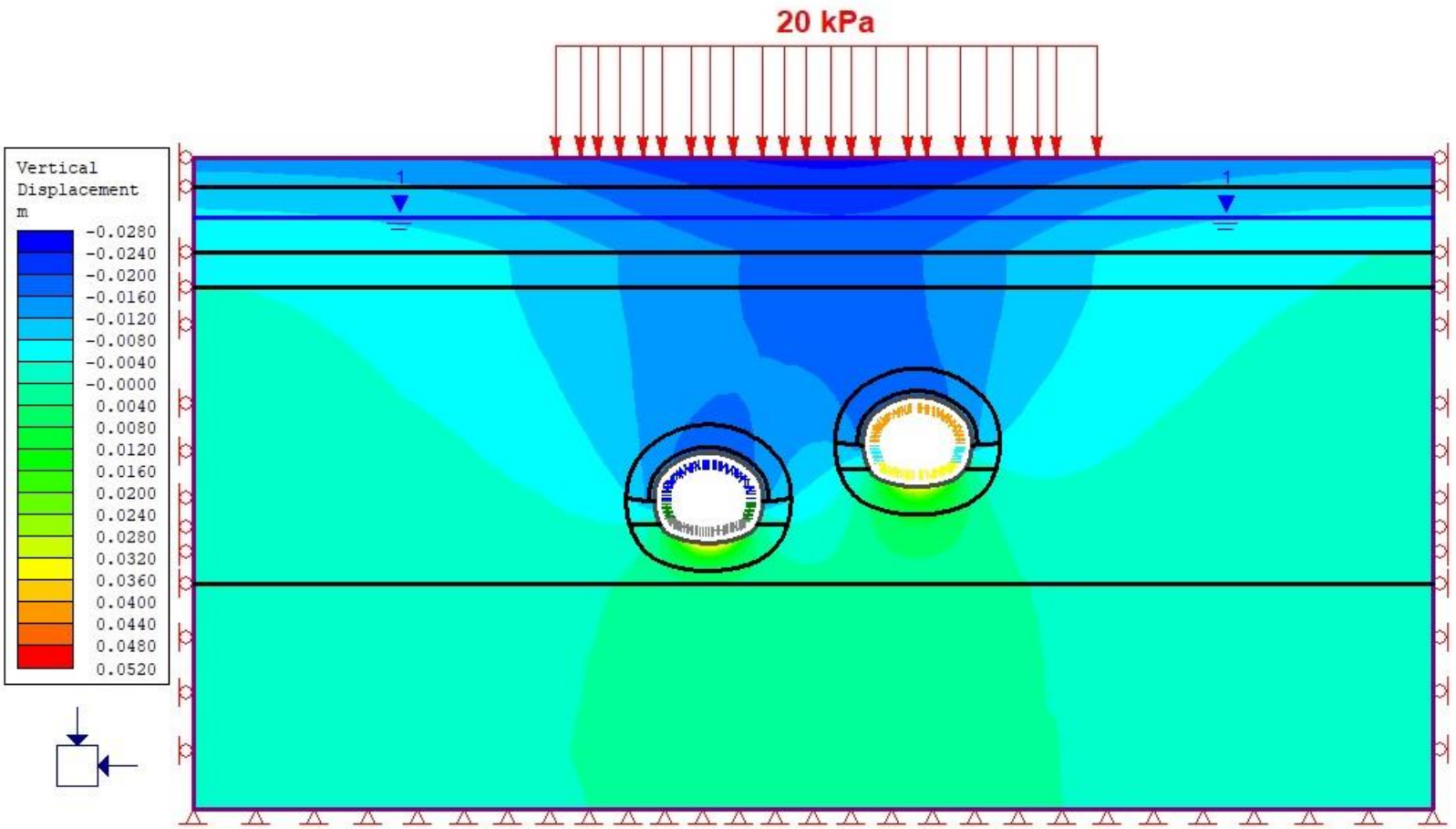

Figure 5.2. Finite element analysis result for the section Km 9+585

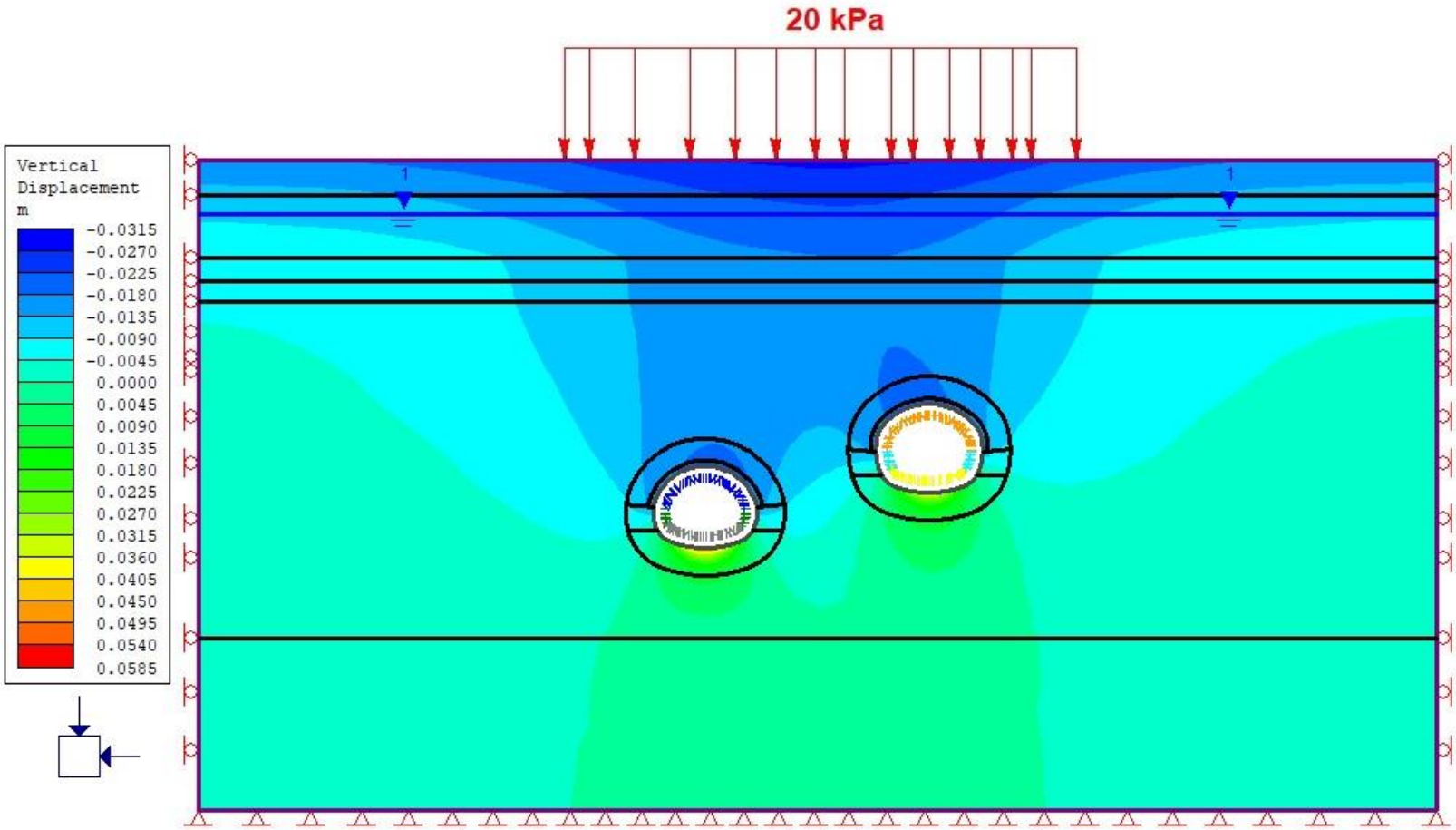

Figure 5.3. Finite element analysis result for the section Km 9+615

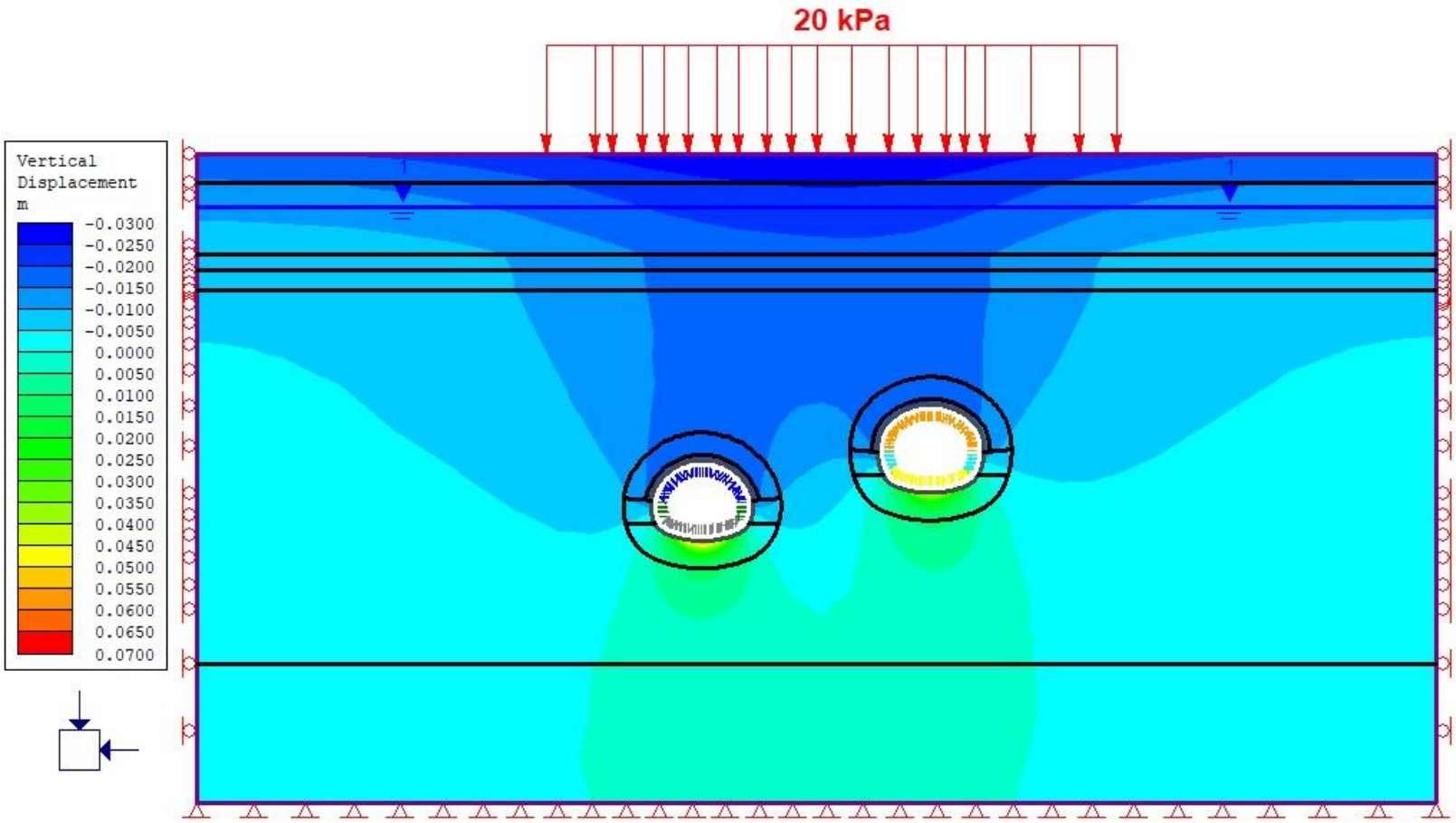

Figure 5.4. Finite element analysis result for the section Km 9+630

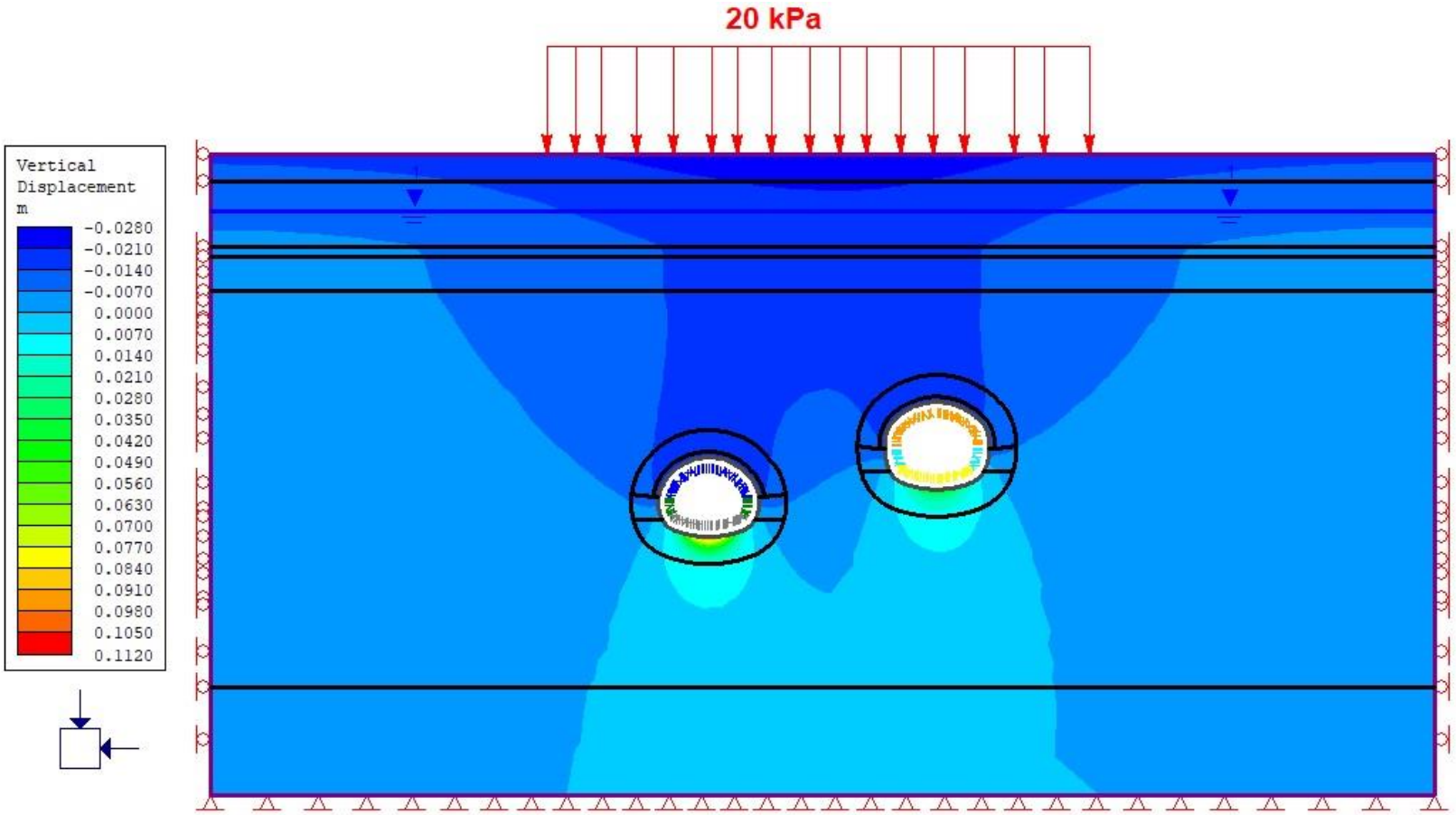

Figure 5.5. Finite element analysis result for the section Km 9+645

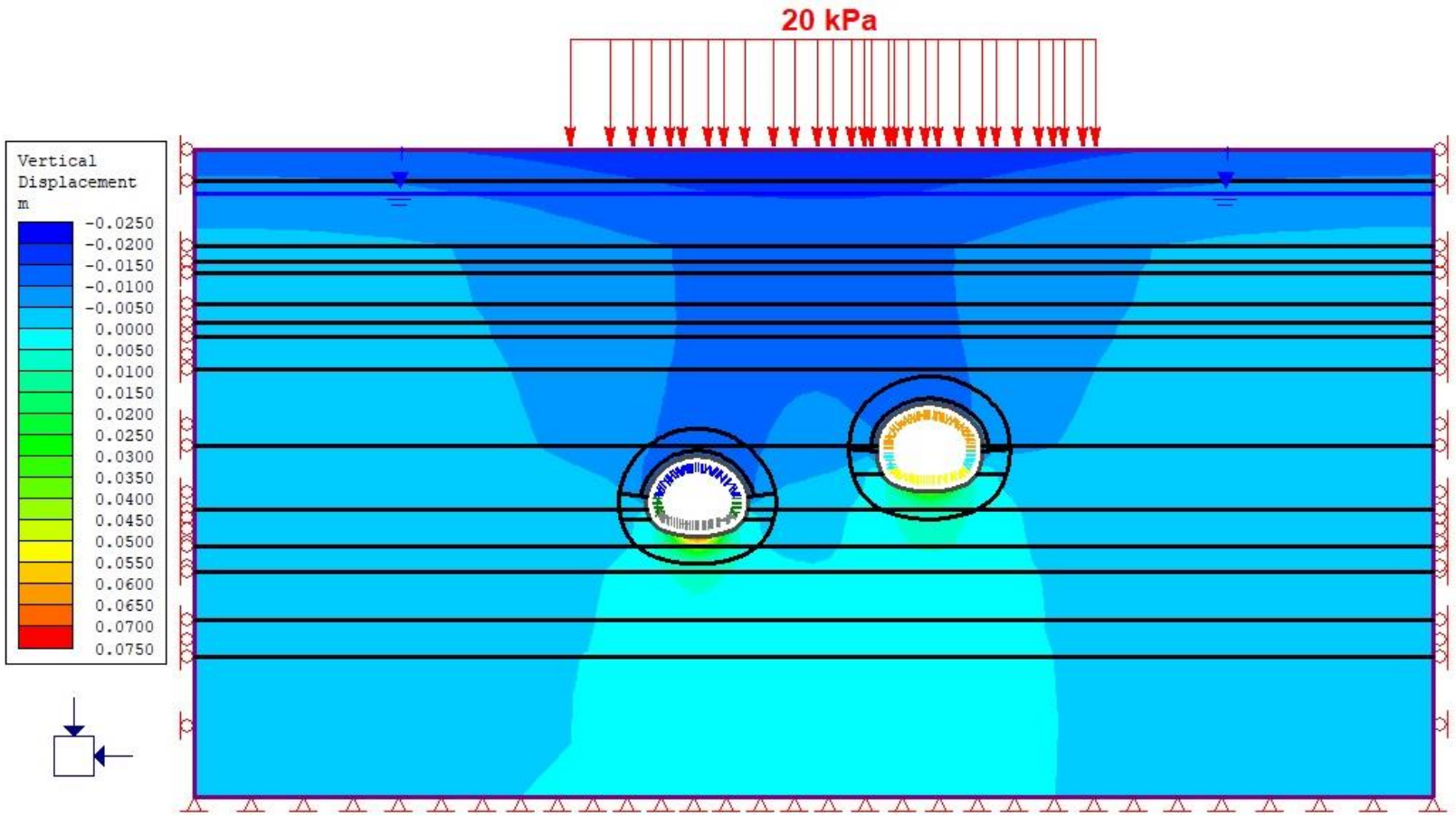

Figure 5.6. Finite element analysis result for the section Km 9+660

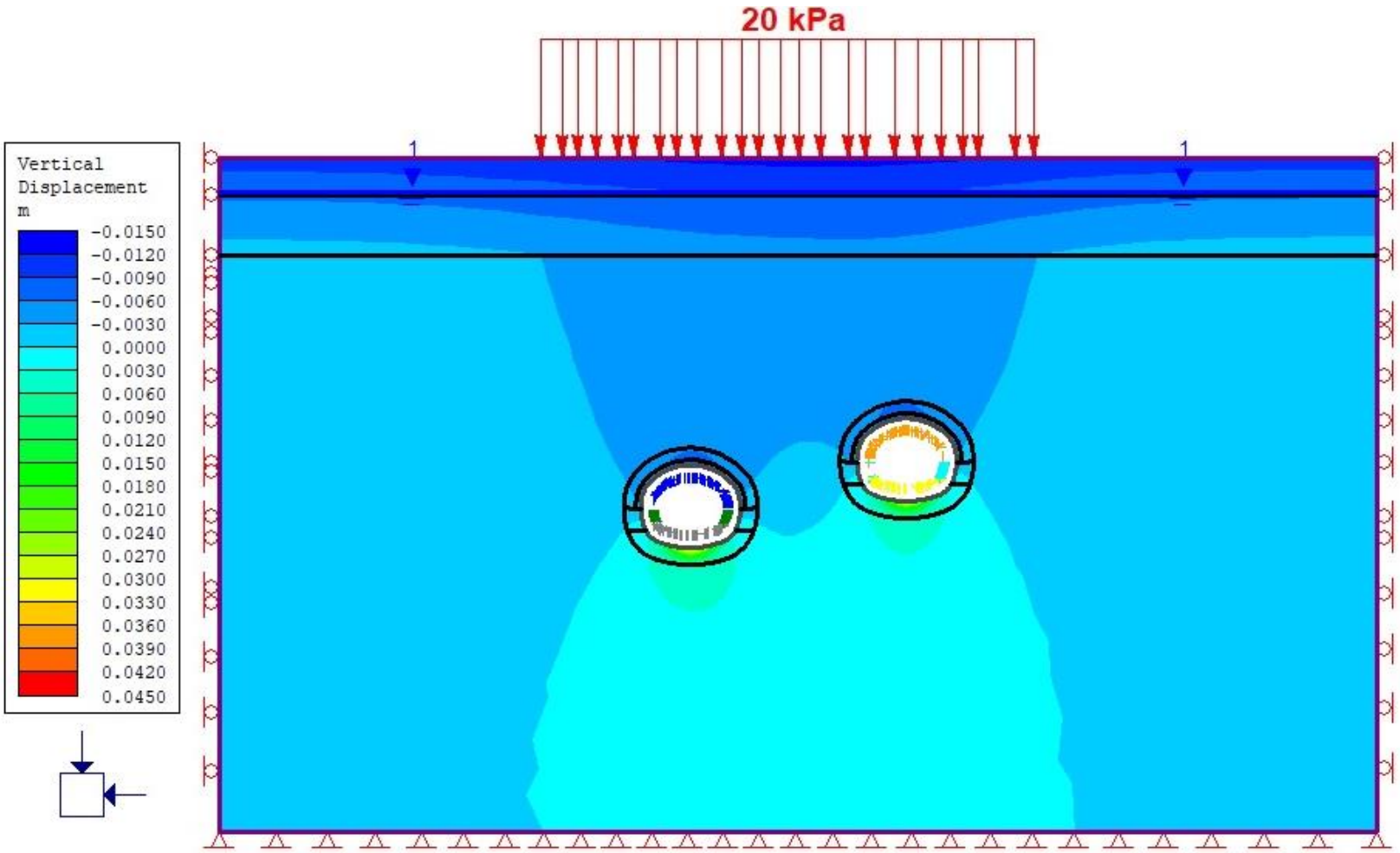

Figure 5.7. Finite element analysis result for the section Km 9+681

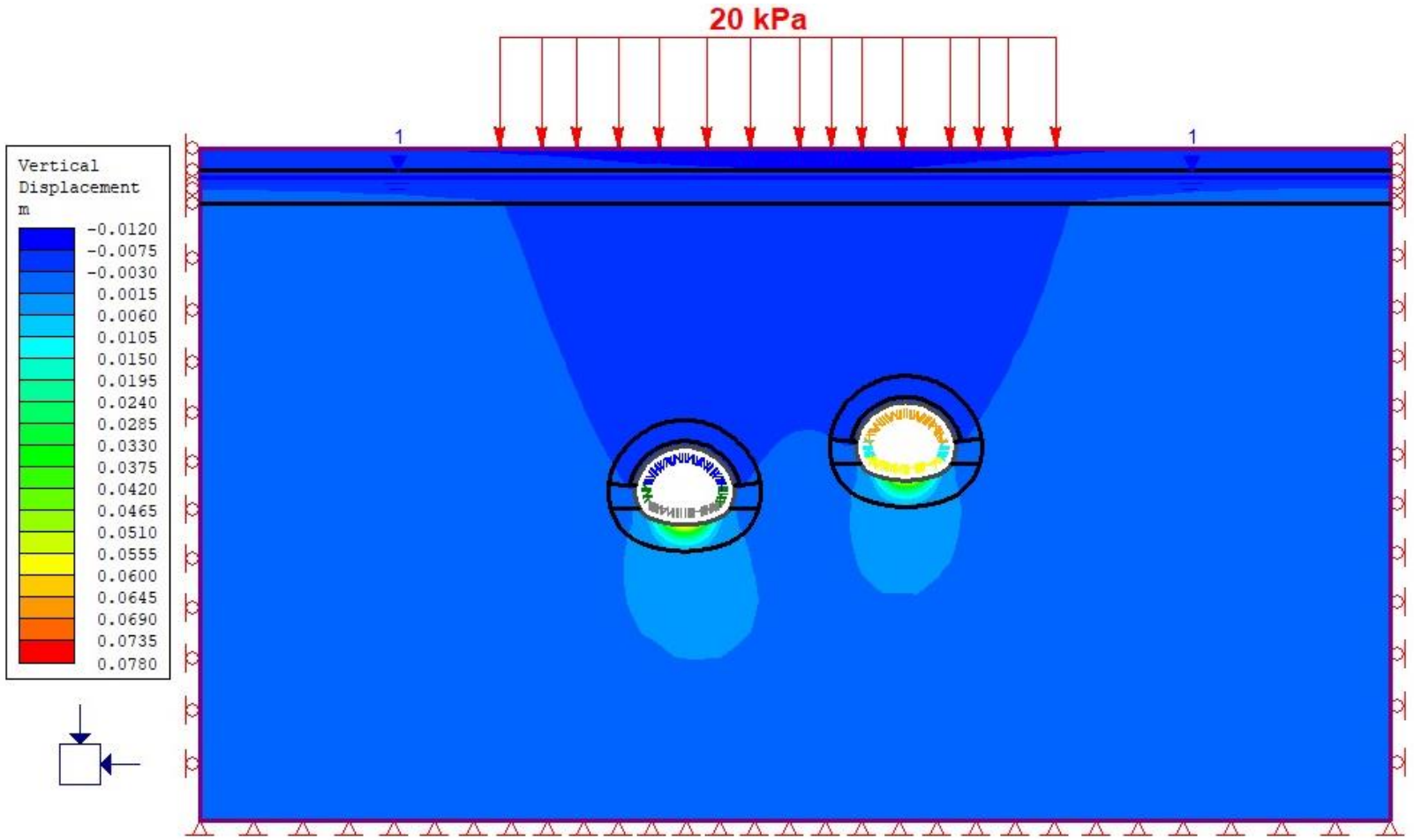

Figure 5.8. Finite element analysis result for the section Km 9+695

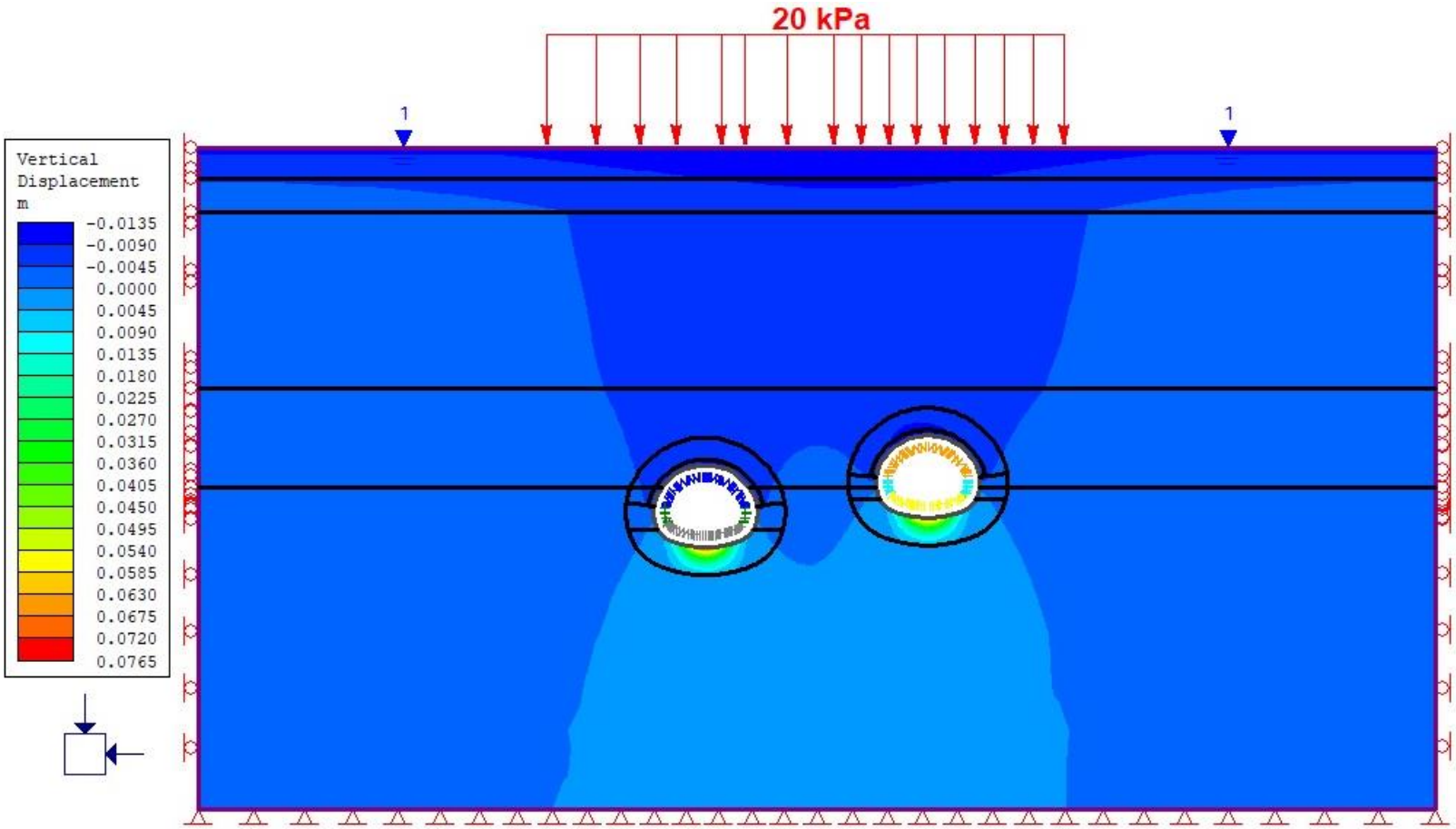

Figure 5.9. Finite element analysis result for the section Km 9+758

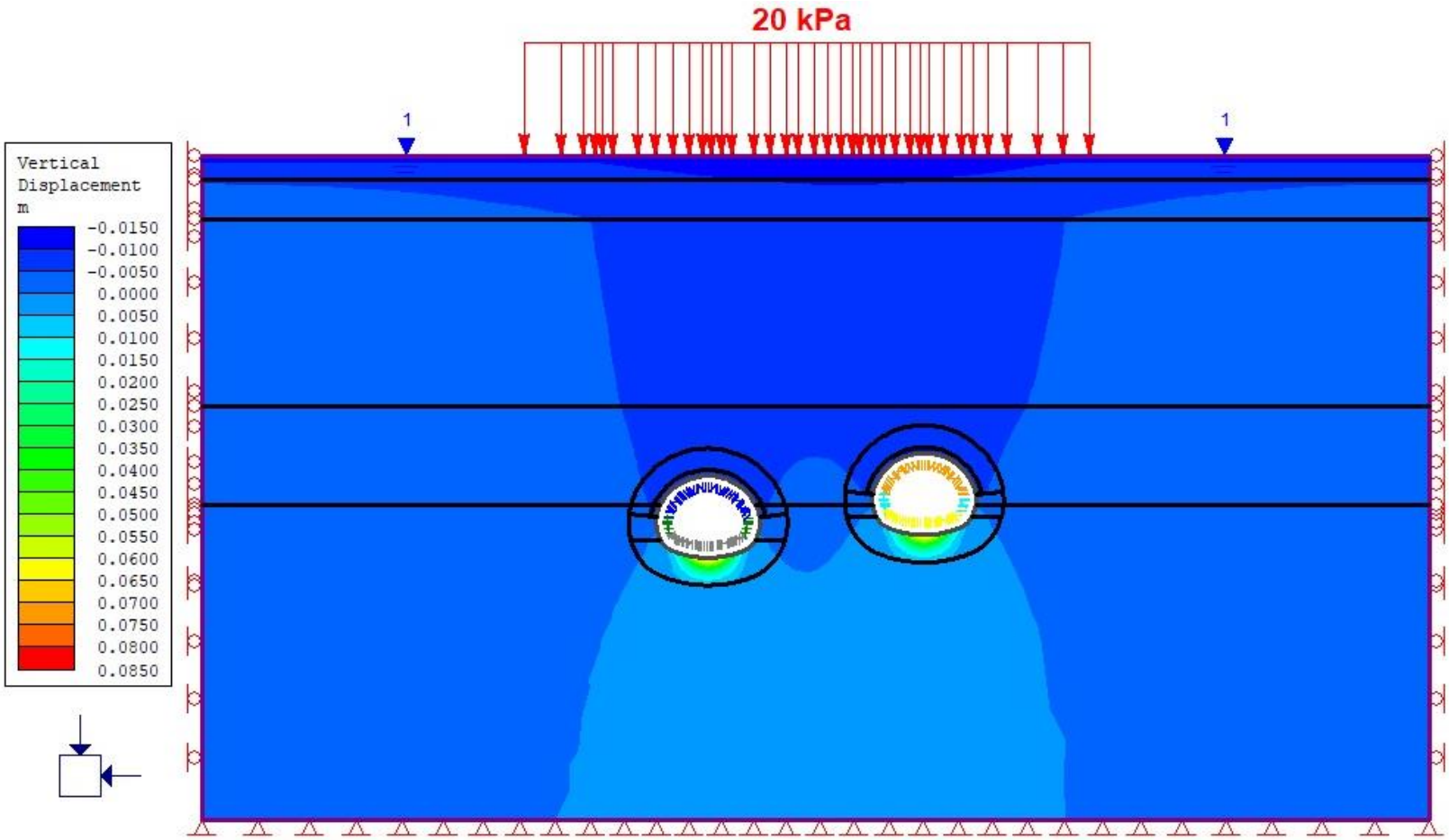

Figure 5.10. Finite element analysis result for the section Km 9+789

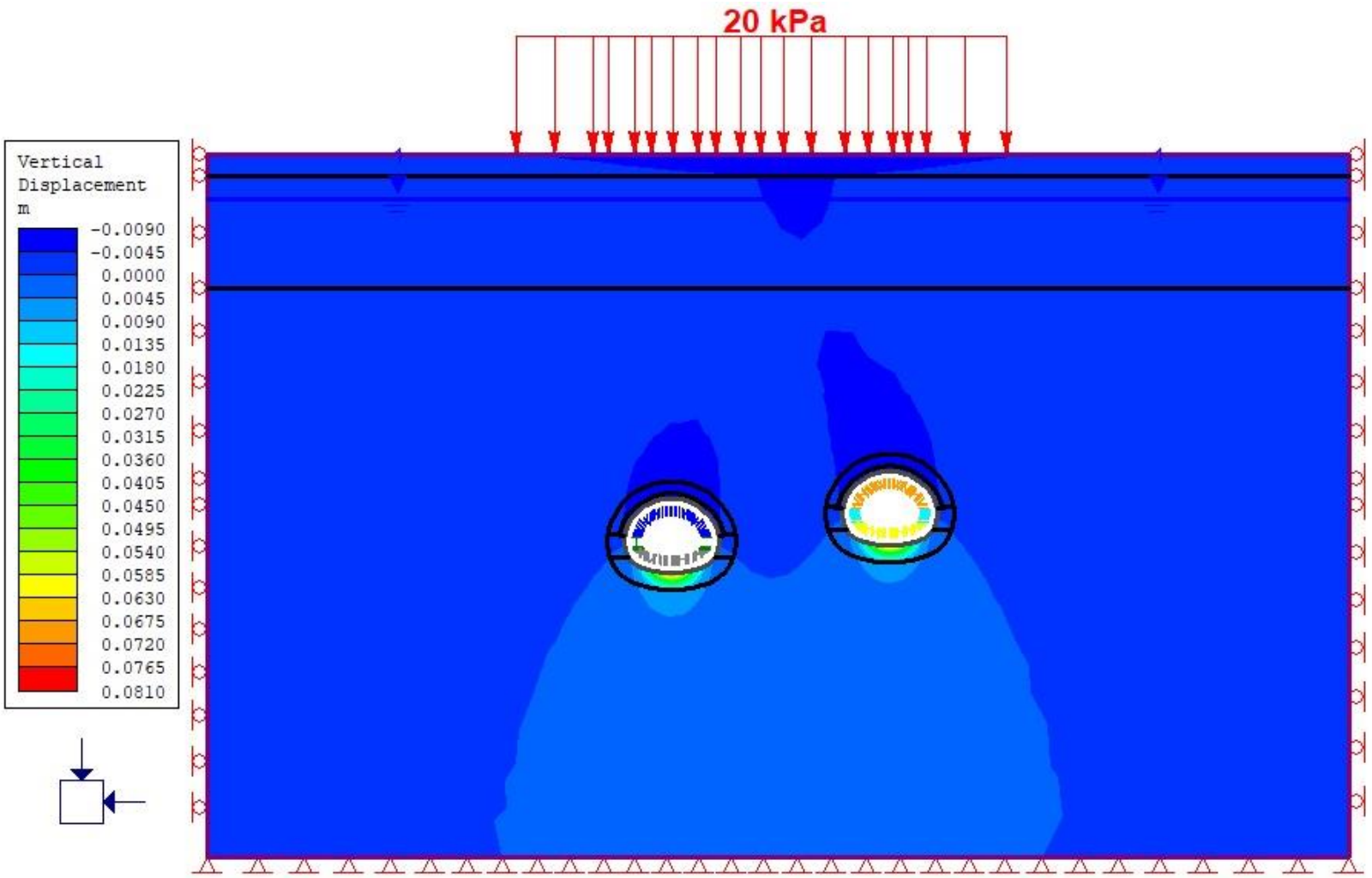

Figure 5.11. Finite element analysis result for the section Km 9+996

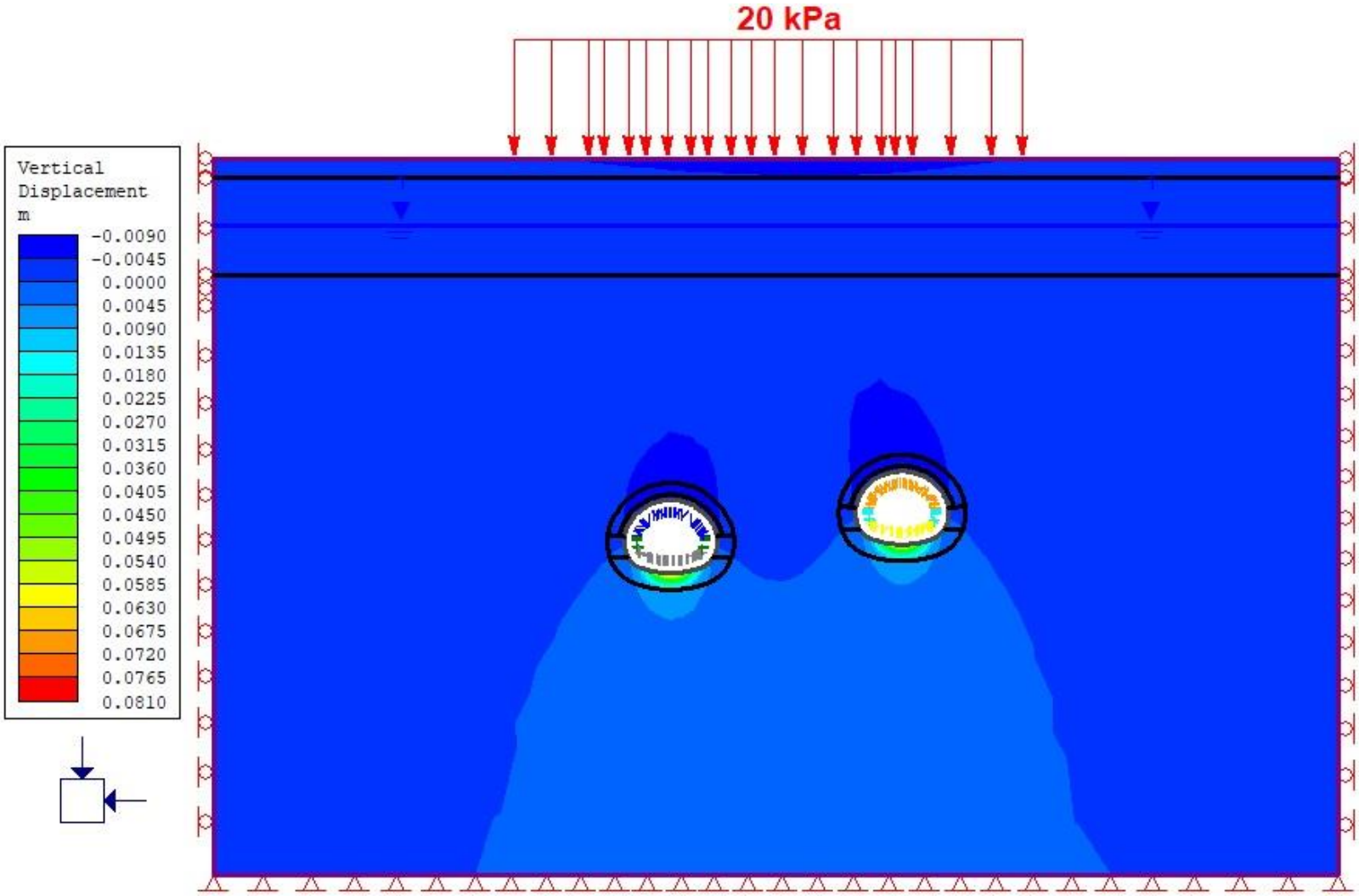

Figure 5.12. Finite element analysis result for the section Km 10+016

It is obvious that both the settlement pattern and amplitude depend on the spacing between twin tunnels. According to Chakeri et al. (2014), shape of ground surface settlement curve for spacing from 0 to 3D (D is tunnel diameter) is similar to the shape of ground surface settlement curve for single tunnel excavation. In the scope of this thesis, the spacing and tunnel diameter are between 17.71 m and 27.4 m, 11.2 m and 11.6 m, respectively. This means that settlement trough is similar to single tunnel one and they are following the Gaussian distribution (Equation 5.1).

$$S_V = S_{max} exp\left(-\frac{x^2}{2i^2}\right) \tag{5.1}$$

Where, S_v = the theoretical settlement at a given lateral distance from the tunnel centerline,

S_{max} = the theoretical maximum settlement at the tunnel centerline

x = the horizontal distance from the tunnel centerline

i = the horizontal distance from the tunnel centerline to the point of inflection in the Normal distribution curve

Logarithmic transformation of Gaussian distribution was applied to get the representative Gaussian curve for settlement bolt data along the selected cross section lines. Resulted curve is presented with the field data and resulting settlement troughs of FEM analyses for all cross section lines.

Equation 5.1 was transformed into logarithmic functions;

$$\ln(S_v) = Y \text{ and } x^2 = X \tag{5.2}$$

$$\left(-\frac{1}{2i^2}\right) = A, \ln(S_{max}) = B \tag{5.3}$$

$$Y = AX + B \tag{5.4}$$

Equations 5.2 and 5.3 were applied to data of the selected cross section lines, and slope and constant term of linear regression (Equation 5.4) are summarized in Table 5.2. Then, they were used to get the Gaussian curves by considering transformation of linear regression terms into settlement trough width and maximum settlement value. Field settlement measurement data, predicted Gaussian curves and resulting settlement troughs of the FEM analyses are all together presented in Figure 5.13-Figure 5.18.

Table 5.2. Regression analysis results belonging to settlement profile of the selected section lines

Section Km	Z_0 (m)	Slope of Regression Line, A	B	i (m)	S_{max} (mm)	Correlation Constant, r
Km 9+542	35.405	-0.0003	1.7998	40.82	6.05	0.56
Km 9+585	34.34	-0.0011	3.1752	21.32	23.93	0.88
Km 9+615	35.455	-0.0014	3.3716	18.90	29.13	0.97
Km 9+630	35.94	-0.0006	3.4033	28.87	30.06	0.90
Km 9+645	36.055	-0.0006	3.1965	28.87	24.45	0.77
Km 9+660	36.365	-0.0007	2.9444	26.73	19.00	0.77
Km 9+681	36.855	-0.0005	2.537	31.62	12.64	0.79
Km 9+695	37.025	-0.0011	2.2162	21.32	9.17	0.67
Km 9+758	38.415	-0.0021	2.7061	15.43	14.97	0.94
Km 9+789	39.07	-0.001	2.5844	22.36	13.26	0.91
Km 9+996	42.555	-0.0003	1.7156	40.82	5.56	0.61
Km 10+016	42.79	-0.0002	1.419	50.00	4.13	0.38

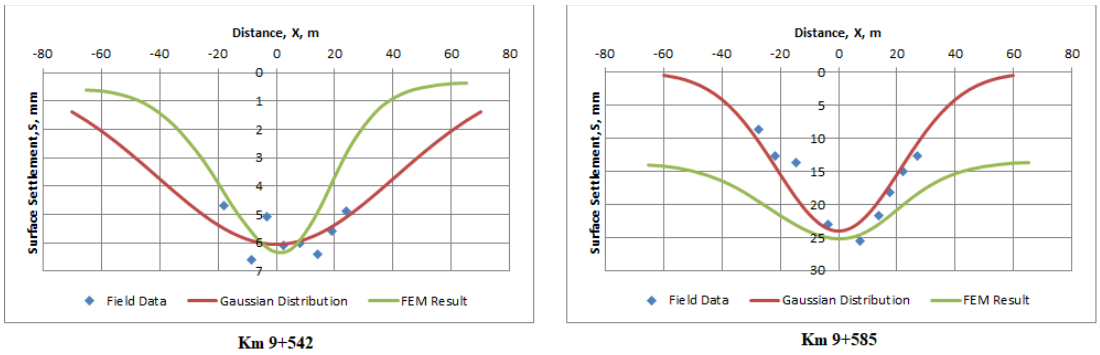

Figure 5.13. Settlement troughs and measurement data for the sections of Km 9+542 and Km 9+585

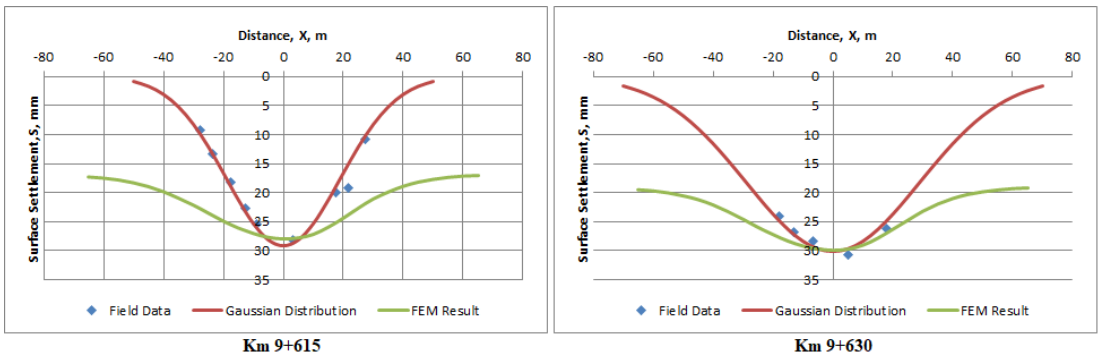

Figure 5.14. Settlement troughs and measurement data for the sections of Km 9+615 and Km 9+630

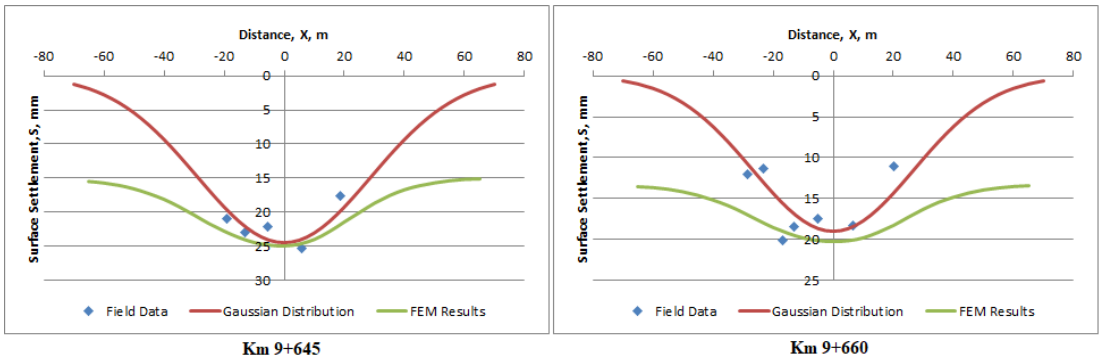

Figure 5.15. Settlement troughs and measurement data for the sections of Km 9+645 and Km 9+660

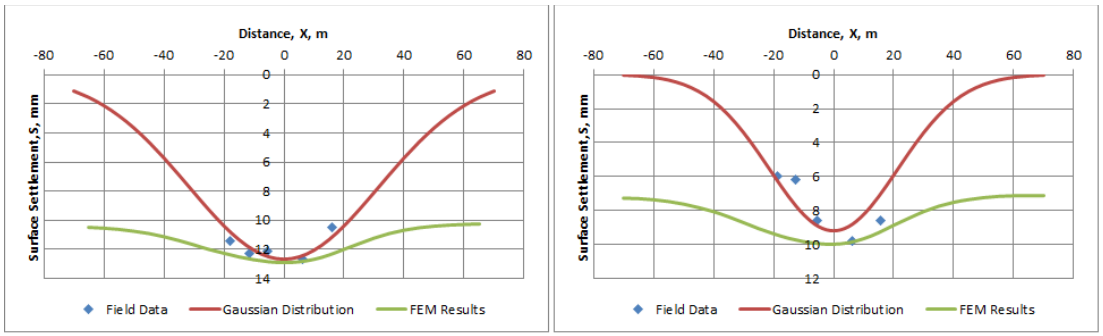

Figure 5.16. Settlement troughs and measurement data for the sections of Km 9+681 and Km 9+695

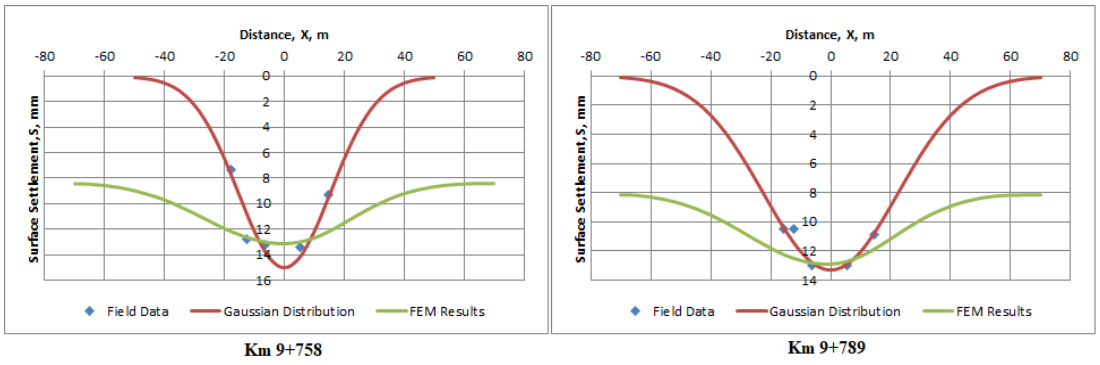

Figure 5.17. Settlement troughs and measurement data for the sections of Km 9+758 and Km 9+789

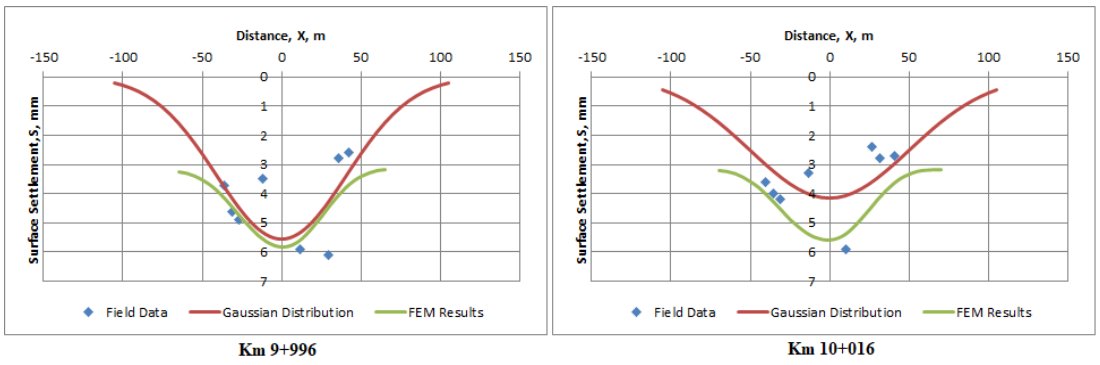

Figure 5.18. Settlement troughs and measurement data for the sections of Km 9+996 and Km 10+016

There are 367 settlement bolts in the scope of the Eurasia Tunnel project. However, a total of 78 settlement bolt data along all the selected cross-section lines were used for this study. Maximum settlement value was interpolated statistically by using ArcGIS 10 Spatial Analyst in which Kriging interpolation method -geostatistical interpolation technique- was used. Contour map of the maximum surface settlement along the studied tunnel is presented in Figure 5.19.

Maximum surface settlement has the largest value around 30 mm and the smallest value around 2.5 mm along the center of the twin tunnel structure. The reason behind this result may be about support type used, geological conditions and spacing between the twin tunnels. Figure 5.20 shows the maximum surface settlement profile along the center of the twin tunnel structure and rock mass profile around the tunnel boundary. It is concluded that dominant factor on maximum surface settlement is the rock mass quality since there is a strict relationship between maximum surface settlement value and deformation modulus of the rock mass. Moreover, it is noticed that the other effective factor on surface settlement is the distance between tunnels. Thicker sandstone-1 unit with lower rock mass quality was found on two locations, one of them is at the beginning of the tunnel structure and other is at the end of tunnel alignment, Smax value of former one is higher than that of latter. Since, the distance between tunnels increases with progress of tunneling.

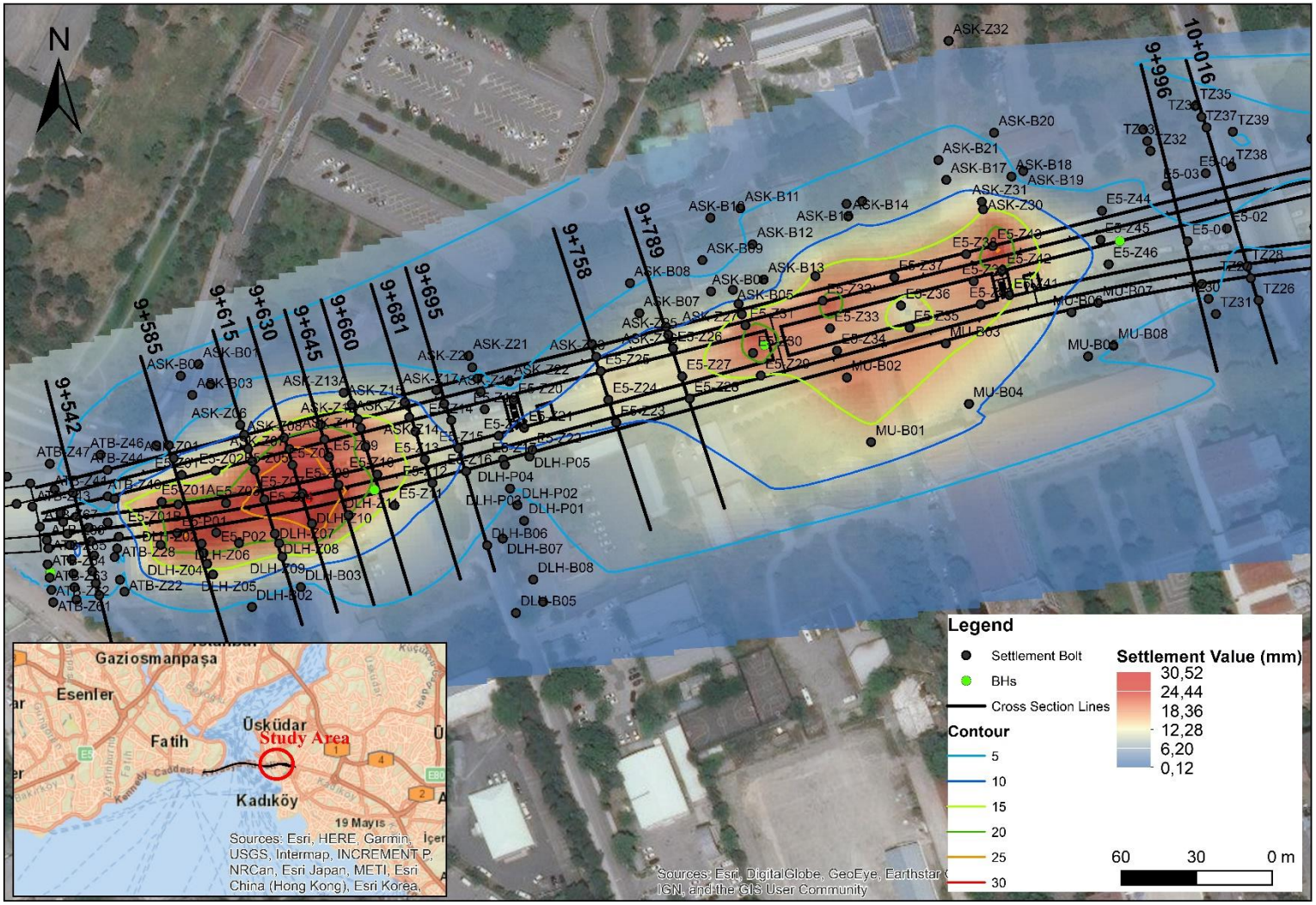

Figure 5.19. Maximum surface settlement contour map along the tunnel

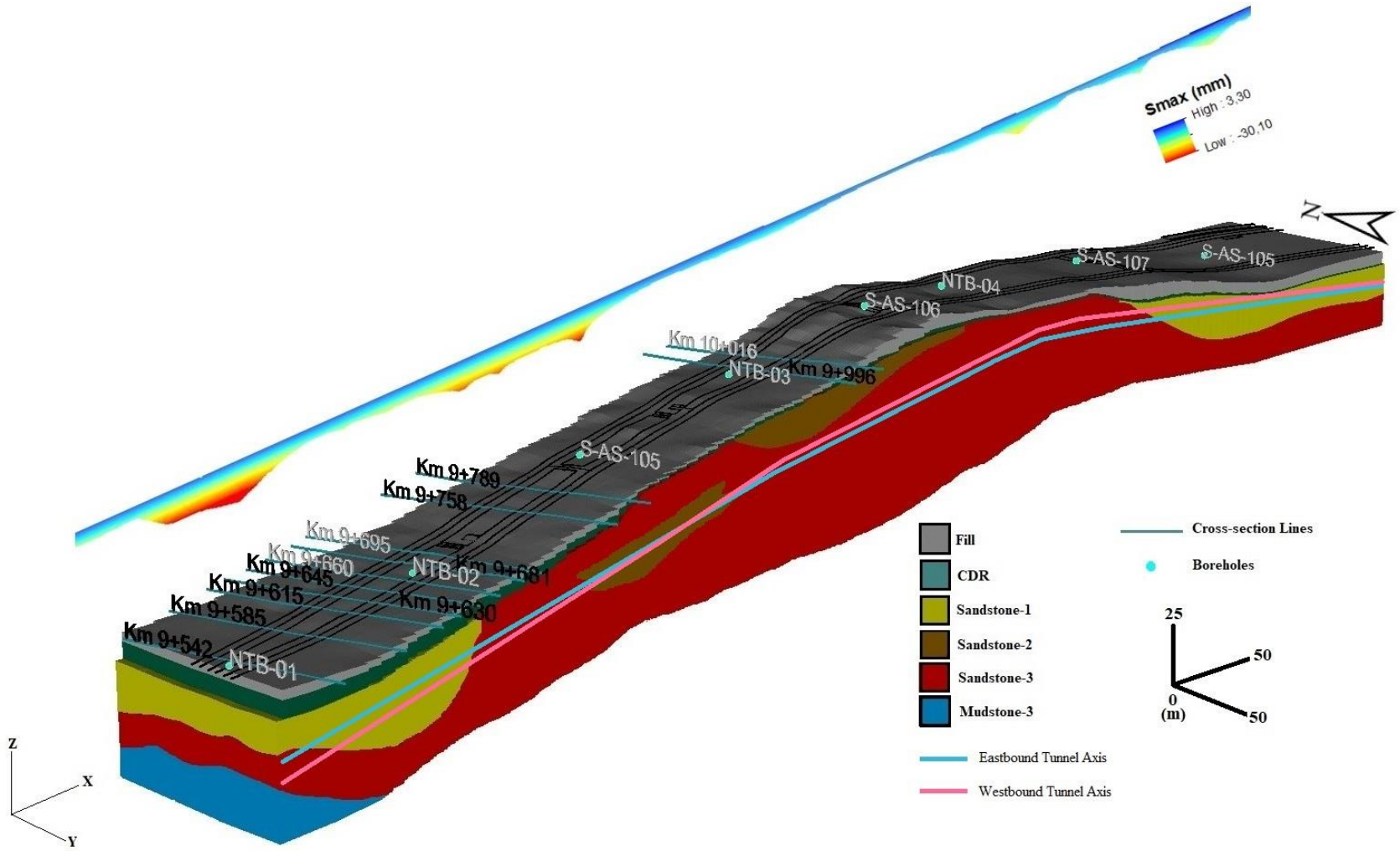

Figure 5.20. Maximum settlement profile and simplified rock mass around tunnel

Tunnel construction involves the removal of ground and the installation of a support system. The removal of the ground induces ground stress relief and its redistribution around the tunnel opening, resulting in a decrease in radial stress and an increase in tangential stress. The installation of the support system provides some internal support stress around the tunnel periphery. The change in ground stresses induces ground settlements above the tunnel. The higher the ground stress relief, the higher the ground settlements are. The critical strain values (percentage ratio of the tunnel closure to tunnel radius) around tunnel should be controlled for tunnel stability and its limit have to be smaller than %1 (Hoek, 2001). Finite element analyses for all cross-section lines of the studied twin tunnels satisfy the stability (Table 5.3).

Table 5.3. Strain values around the tunnel periphery

No	Km	Spacing (m)	Overburden Depth (m)		Support Type		Tunnel Diameter (m)	GWT from surface (m)	Field Smax (mm)	FEM Smax (mm)	<%1 Strain
			Westbound	Eastbound	Westbound	Eastbound					
1	9+542	17.71	33.21	26.40	ST-3	ST-3	11.2	8.90	6.60	6.35	0.73
2	9+585	22.29	31.54	25.54	ST-UA1	ST-UA1	11.6	6.40	25.50	25.25	0.45
3	9+615	24.33	33.13	26.38	ST-3	ST-UA1	11.4	5.80	28.20	28.02	0.55
4	9+630	24.90	33.28	27.20	ST-2	ST-UA1	11.4	5.80	30.70	29.88	0.64
5	9+645	25.24	33.40	27.31	ST-2	ST-UA1	11.4	6.30	25.30	25.02	0.98
6	9+660	25.40	33.55	27.78	ST-2	ST-UA1	11.4	4.80	20.10	20.21	0.73
7	9+681	25.21	33.75	28.36	ST-UA1	ST-UA1	11.6	3.90	12.70	12.92	0.36
8	9+695	25.10	33.95	28.90	ST-3	ST-3	11.2	3.30	9.80	9.97	0.64
9	9+758	24.10	34.43	31.20	ST-3	ST-3	11.2	0.45	13.40	13.12	0.73
10	9+789	23.50	34.71	32.23	ST-3	ST-3	11.2	0.10	13.00	12.92	0.73
11	9+996	25.80	38.54	35.37	ST-2	ST-2	11.2	5.20	6.10	5.81	0.73
12	10+016	27.40	38.89	35.49	ST-2	ST-2	11.2	8.00	5.90	5.59	0.73

Excavating underground openings undoubtedly violates the equilibrium state of the pre-existing initial stresses in the rock mass. Therefore, rock mass tends to readjust its behavior until a new equilibrium state is attained. Otherwise, collapse may result due to high stress concentration in some regions (Abdellaha, et al., 2018). Accordingly, there will be several indicators and precursors which will lead to local damage and subsequently regional failure. An indicator is defined as a sign, a state or a contributing factor that points out or suggest that the rock mass may be prone to

damage or failure. In general potential failure is indicated by geotechnical and operational factors. A geotechnical precursor is a state or behavior suggesting that the structure of the rock mass has been damaged prior to possible failure. Precursors, including results from instrumentation, warn the development of excess ground deformations or high stress. Local damage is manifested by the following precursors e.g. spalling, squeezing, bursting, roof sagging, local falls, slabbing, joint dilation, creep, floor heaving, support damage etc. (Rao, 2012). In this study, roof sagging can be prevented by using pre-support and the dominant failure type is floor heaving. Sample figure of stress-strain graph for the cross section at Km 9+542 was given in Figure 5.21 and those for the others are presented in Appendix H.

Stress strain curve shows the complete picture of mechanical behavior of material. It gives us the value of load for a particular material up to which it is under elastic limit and also gives us the ultimate point stress and corresponding strain. In this way it tells us how much we can load a material. It is concluded from figures of stress-strain graph that material around the tunnel is elastoplastic which exhibits both elastic and plastic properties.

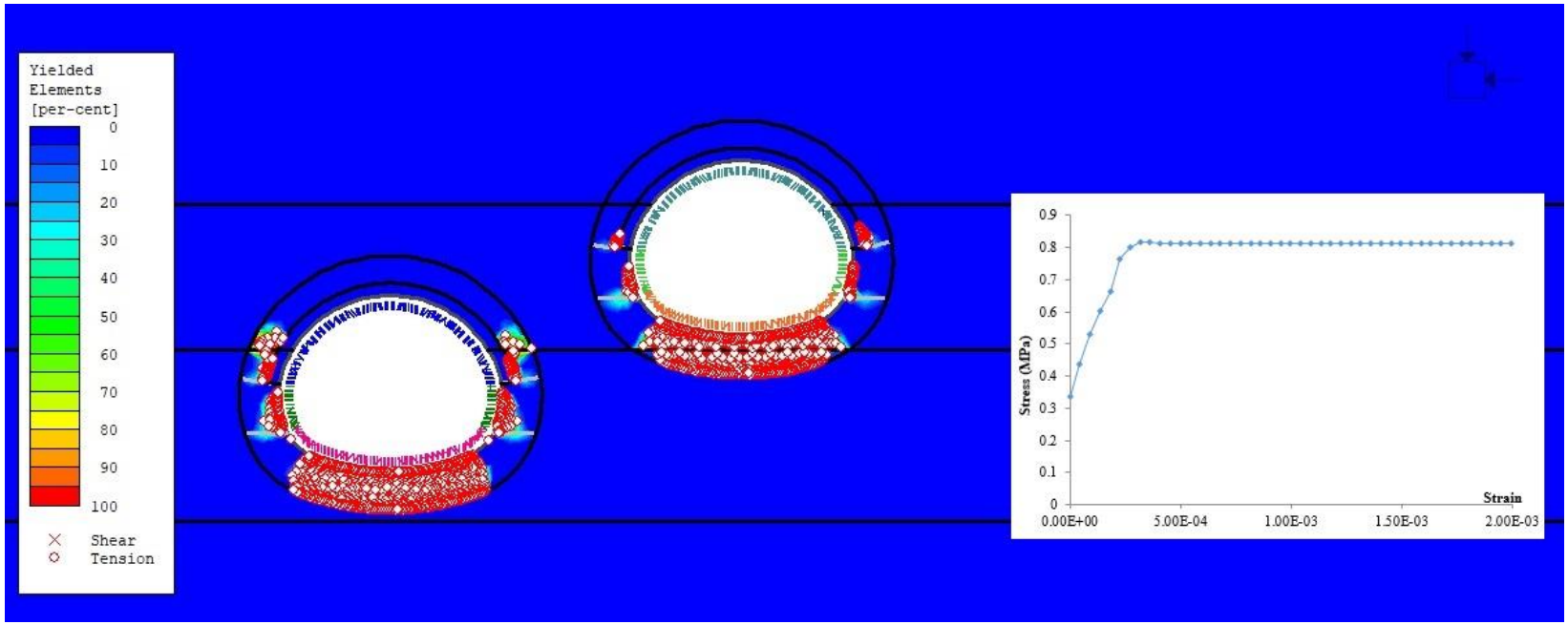

Figure 5.21. Closer view of the yielded elements and stress-strain graph of the cross section at Km 9+542

5.2. Numerical Parametric Study of Maximum Surface Settlement

This study is focused on the prediction of the maximum surface settlement due to twin NATM tunnels in the Trakya formation. Magnitude of maximum settlement depends on factors like soil/rock stiffness, excavation method, tunnel cover to diameter ratio, groundwater conditions. A parametric study was performed by using finite element analysis to determine the effects of geo-material parameters such as cohesion, friction angle, deformation modulus and Poisson's ratio, the effects of groundwater levels and surface surcharge.

One of the cross section lines at Km 9+789 was selected for numerical modeling in parametric analysis. The original geo-material parameters used in the parametric study are presented in Table 5.4.

Table 5.4. Original geo-material parameters used in the parametric study

	Friction Angle (°)	Cohesion (KPa)	Elastic Modulus (MPa)	Poisson's Ratio	GWT Depth from Surface (m)
Fill	35	0	20	0.33	0.1
CDR	33	0	30	0.32	
Sandstone-1	28	150	300	0.28	
Sandstone-2	36	200	500	0.26	

The parametric study was carried out for three different cases of geomechanical properties of the ground, namely; 50% less than, 50% more than and 100% more than the original value of geo-material parameters in order to observe explicit variation on the resulting settlement values. For Poisson's ratio 100% increase was limited to 0.40 due to its nature (Gercek, 2007). While one of the material parameters is changed, other geomechanical properties of the ground are all kept constant during the parametric analyses. Five and four different values of groundwater level and

surface surcharge respectively were used for parametric studies. Results of the parametric studies are presented in Figure 5.22-Figure 5.27.

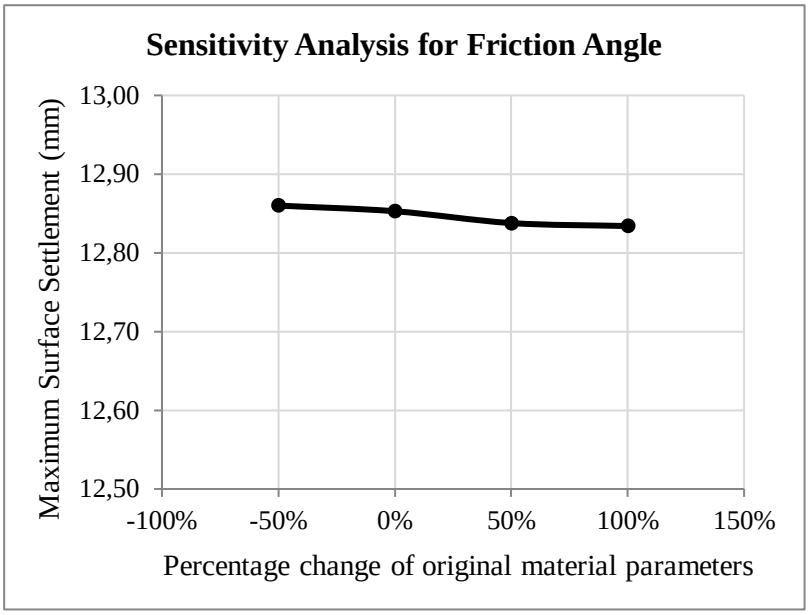

Figure 5.22. Results of parametric studies for friction angle

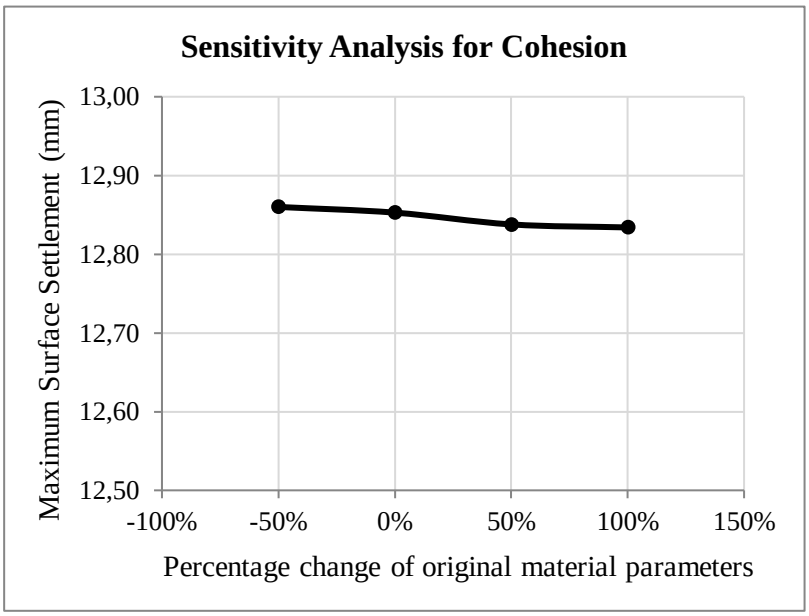

Figure 5.23. Results of parametric studies for cohesion

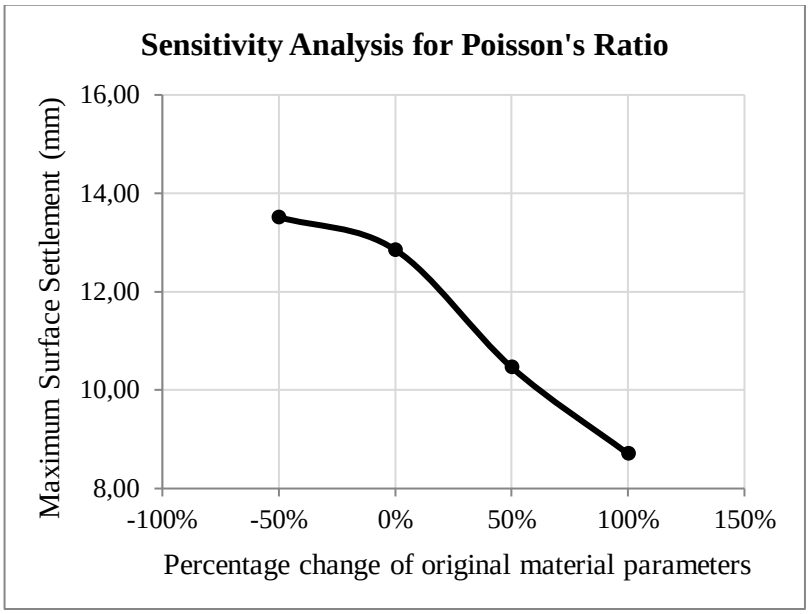

Figure 5.24. Results of parametric studies for Poisson's ratio

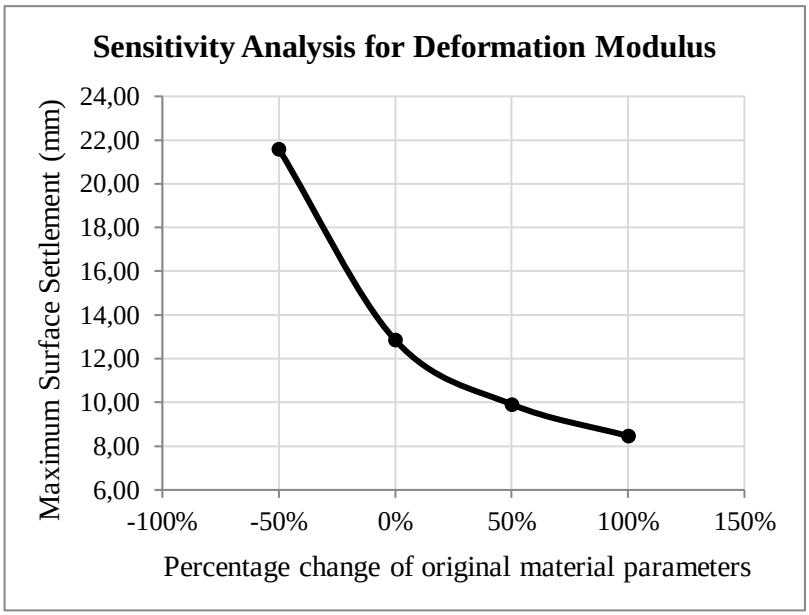

Figure 5.25. Results of parametric studies for deformation modulus

It is concluded that friction angle and cohesion parameters have less effect on the surface settlement. However, deformation modulus and Poisson's ratio of the ground causes the highest change in settlement values, since settlement is mainly controlled by stress-strain states of surrounding medium of the tunnel.

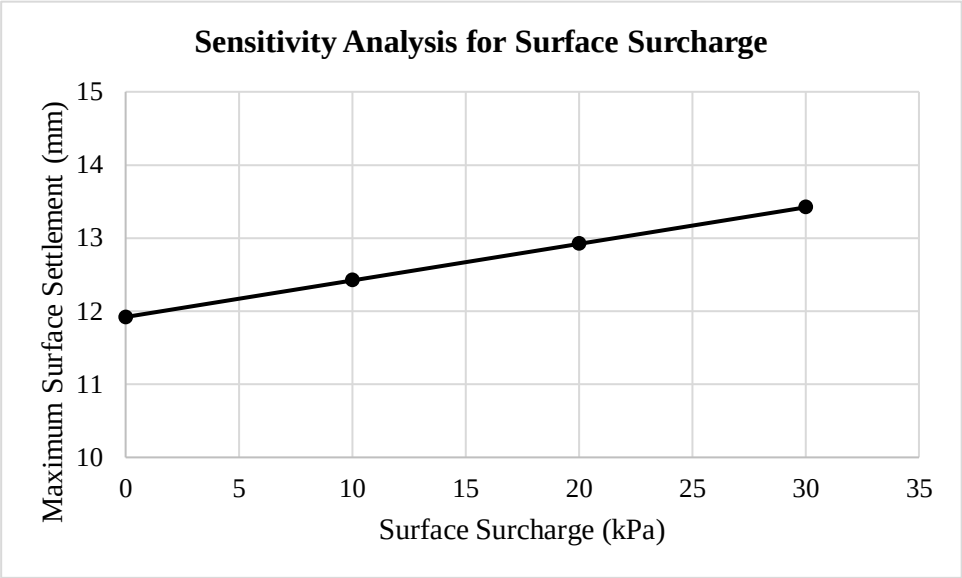

Figure 5.26. Results of parametric studies for surface surcharge

Numerical analysis shows that an increase in the amount of surface surcharge from zero to 30 kPa resulted in an increment of approximately 1.5 mm in maximum surface settlement value (Figure 5.26). This situation reveals that surface surcharge has not a significant effect on the amount of surface settlement.

Scientific investigations for surface subsidence caused by groundwater drawdown date go back to 1890's. Technological and industrial developments have rapidly increased the demand for groundwater and this resulted heavily use of groundwater resources. This phenomenon, observed in industrial areas and causing damage to infrastructures, has been related to heavy production of water-oil-and gas (Karahanoğlu, 2018). Groundwater drawdown causes consolidation settlement. The excessive withdrawal of groundwater and the consequent settlement has been

recognized as a geological and geotechnical hazard, and extensively investigated (Poland and Davis, 1969; Galloway et al., 1999; Ortega-Guerrero et al., 1999; Shi et al., 2007). Tunneling activity in water-bearing ground may result in unwanted groundwater inflow into the excavated area, thus causing some groundwater drawdown. Tunneling-induced groundwater drawdown has been known to induce associated ground settlements in addition to the settlements caused by the unloading effect due to excavation (Yoo, 2005, Yoo and Kim, 2006).

In Figure 5.27, it is observed that maximum settlement slightly increases while groundwater level decreases and finally get dry. This result reveals that groundwater table has ignoring effect on surface settlement. In the scope of this study, there is no groundwater drawdown induced settlement by tunneling, since there was no high quantities of groundwater and impermeable support was applied immediately ensuring the hydrostatic head.

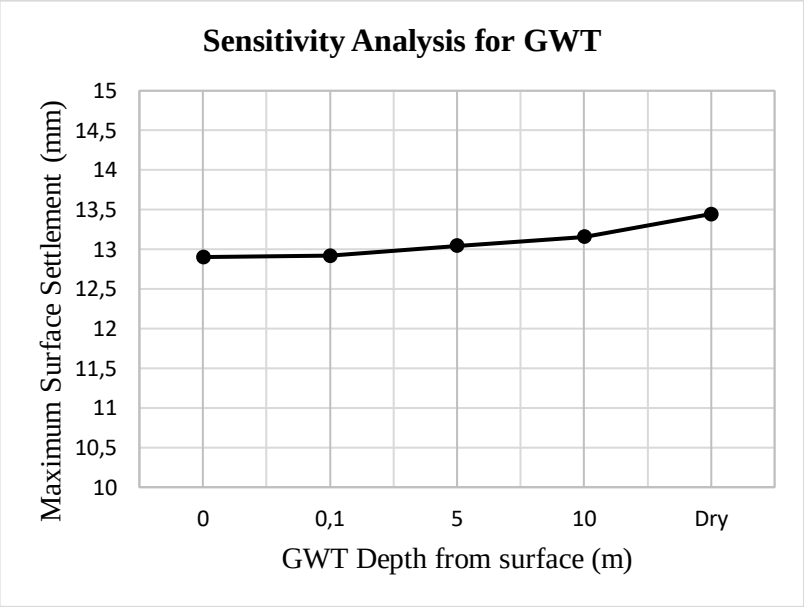

Figure 5.27. Results of parametric studies for depth of groundwater table from the surface

5.3. Maximum Surface Settlement from Previous Formulas

The maximum of monitoring settlement data recorded during the tunneling were compared to the maximum settlement determined by applying empirical and analytical methods for twin tunnel structure referred to in the technical literature. These empirical and analytical methods are presented in Chapter 2, literature review.

There are five widely used formulas to calculate maximum settlement for twin tunnel structure, namely; Superposition Method (O'Reilly and New, 1982), Addenbrooke and Potts (2001), Hunt (2005), Herzog (1985) and Chakeri and Unver (2013). The first three methods require the settlement value obtained by equations for single tunnels.

To estimate single tunnel induced surface settlement, the ground settlements are expected to be compatible a Normal distribution given previously in equation 2.1. Moreover, maximum settlement value was derived from above mentioned equation as given previously in equation 2.4. The settlement trough widths were calculated by using equations given previously in Table 2.1 and they were used in Gaussian distribution formula to get the maximum settlement values (Table 5.5.)

A closed-form solution by using isotropic, homogeneous elastic half space equations is derived by some researches as analytical methods for single tunnel induced settlement. The widely used formulas were presented previously in Chapter 2. These formulas are valid for single tunnels and they are used in twin tunnel induced settlement equations. Results of single tunnel equations are presented in Table 5.5.

Table 5.5. Maximum settlement values calculated by using equations for single tunnel

Km Point	D (m)	Z_0 (m)	E (MPa)	Poisson's Ratio	Unit Weigth (kN/m^3)	i (Peck, 1964)	i (Attkinson, 1977)	i (O'Reilly, 1982)	i (Mair, 1993)	i (Clough, 1981)	i (Arioğlu et al., 2002)	i (Arioğlu et al., 2002)	i (Arioğlu et al., 2002)	i_{avg} (Arioğlu et al., 2002)
Km 9+542	11.2	35.31	775	0.26	24.4	15.74	13.94	16.28	17.65	14.03	16.04	13.42	16.19	15.22
Km 9+585	11.6	34.04	300	0.28	23.0	15.28	13.49	15.74	17.02	13.72	15.54	12.94	15.86	14.78
Km 9+615	11.4	35.26	300	0.28	23.0	15.75	13.93	16.26	17.63	14.06	16.02	13.40	16.24	15.22
Km 9+630	11.4	35.74	300	0.28	23.0	15.94	14.12	16.47	17.87	14.22	16.22	13.58	16.41	15.40
Km 9+645	11.4	35.86	300	0.28	23.0	15.99	14.16	16.52	17.93	14.26	16.26	13.62	16.45	15.45
Km 9+660	11.4	36.17	640	0.27	23.9	16.11	14.27	16.65	18.08	14.35	16.39	13.74	16.57	15.56
Km 9+681	11.6	36.56	1100	0.25	25.0	16.30	14.43	16.82	18.28	14.53	16.54	13.89	16.77	15.73
Km 9+695	11.2	36.93	1100	0.25	25.0	16.39	14.55	16.98	18.46	14.54	16.69	14.03	16.77	15.83
Km 9+758	11.2	38.32	860	0.25	24.6	16.94	15.07	17.58	19.16	14.98	17.25	14.56	17.26	16.36
Km 9+789	11.2	38.97	830	0.25	24.6	17.20	15.31	17.86	19.49	15.18	17.51	14.81	17.49	16.60
Km 9+996	11.2	42.46	1100	0.25	25.0	18.58	16.62	19.36	21.23	16.26	18.90	16.13	18.70	17.91
Km 10+016	11.2	42.69	1100	0.25	25.0	18.67	16.71	19.46	21.35	16.33	19.00	16.22	18.78	18.00

Km Point	u	V_L (%)	Smax (Peck, 1964)	Smax (Attkinson, 1977)	Smax (O'Reilly, 1982)	Smax (Mair, 1993)	Smax (Clough, 1981)	Smax (Arioğlu et al., 2002)	Smax (Arioğlu et al., 2002)	Smax (Arioğlu et al., 2002)	Verruijt & Booker (1996)	Loganathan & Poulos (1998)
Km 9+542	0.008	0.003	7.02	7.93	6.79	6.26	7.88	6.89	8.24	6.83	4.93	7.43
Km 9+585	0.020	0.007	19.95	22.61	19.38	17.92	22.22	19.63	23.58	19.23	15.13	20.61
Km 9+615	0.020	0.007	18.70	21.13	18.10	16.70	20.93	18.37	21.97	18.13	13.61	19.21
Km 9+630	0.020	0.007	18.72	21.14	18.12	16.69	20.98	18.40	21.97	18.18	13.61	19.20
Km 9+645	0.021	0.007	18.72	21.14	18.12	16.69	20.99	18.40	21.96	18.19	13.61	19.20
Km 9+660	0.010	0.004	9.01	10.17	8.71	8.02	10.11	8.86	10.56	8.76	6.54	9.39
Km 9+681	0.006	0.002	5.80	6.55	5.62	5.17	6.50	5.71	6.80	5.63	4.36	6.19
Km 9+695	0.006	0.002	5.06	5.70	4.88	4.49	5.70	4.97	5.91	4.94	3.53	5.38
Km 9+758	0.008	0.003	6.41	7.21	6.18	5.67	7.25	6.30	7.46	6.29	4.46	6.75
Km 9+789	0.008	0.003	6.64	7.46	6.40	5.86	7.52	6.52	7.71	6.53	4.61	6.98
Km 9+996	0.007	0.002	5.12	5.72	4.91	4.48	5.85	5.03	5.89	5.08	3.52	5.37
Km 10+016	0.007	0.002	5.12	5.72	4.91	4.48	5.85	5.03	5.89	5.09	3.52	5.37

Analytical and empirical methods for twin tunnel induced settlements are explained in Chapter 2. The equations for twin tunnel induced settlement are Superposition Method (1982) (Equation 2.14), Addenbrooke and Potts (2001) (Figure 2.12), Hunt (2005) (Equation 2.15) and they require the settlement value for single tunnel. The equations formed by Herzog (1985) (Equation 2.21) and Chakeri and Unver (2013) (Equation 2.27) derived the analytical solution for twin tunnel structure (Equations 5.13-5.14).

Here, the results of equations are presented (Table 5.6 and Table 5.7) and unit of settlement values is mm.

Table 5.6. Maximum settlement values calculated by using Superposition and Addenbrooke and Potts methods for twin tunnel

							Superposition Method									
Km Point	**D (m)**	**Z_0 (m)**	**Spacing (m)**	**E (MPa)**	u	V_L (%)	Smax (Peck, 1964)	Smax (Attkinson, 1977)	Smax (O'Reilly, 1982)	Smax (Mair, 1993)	Smax (Clough, 1981)	Smax (Arioğlu et al., 2002)	Smax (Arioğlu et al., 2002)	Smax (Arioğlu et al., 2002)	Verruijt & Booker (1996)	Loganathan & Poulos (1998)
Km 9+542	11.2	35.31	17.71	775	0.008	0.0028	14.05	15.86	13.58	12.52	15.76	13.78	16.48	13.65	9.85	14.85
Km 9+585	11.6	34.04	22.29	300	0.020	0.0072	39.91	45.21	38.76	35.84	44.45	39.26	47.15	38.45	30.25	41.22
Km 9+615	11.4	35.26	24.33	300	0.020	0.0072	37.39	42.26	36.21	33.40	41.86	36.75	43.95	36.25	27.23	38.41
Km 9+630	11.4	35.74	24.90	300	0.020	0.0073	37.43	42.27	36.23	33.39	41.96	36.79	43.93	36.35	27.22	38.40
Km 9+645	11.4	35.86	25.24	300	0.021	0.0074	37.44	42.27	36.24	33.39	41.99	36.81	43.93	36.37	27.22	38.40
Km 9+660	11.4	36.17	25.40	640	0.010	0.0036	18.01	20.33	17.43	16.05	20.22	17.71	21.12	17.52	13.08	18.79
Km 9+681	11.6	36.56	25.21	1100	0.006	0.0022	11.59	13.09	11.23	10.34	13.01	11.42	13.60	11.27	8.73	12.39
Km 9+695	11.2	36.93	25.10	1100	0.006	0.0021	10.12	11.40	9.77	8.98	11.40	9.94	11.82	9.89	7.07	10.76
Km 9+758	11.2	38.32	24.10	860	0.008	0.0028	12.82	14.41	12.36	11.34	14.50	12.59	14.92	12.58	8.92	13.51
Km 9+789	11.2	38.97	23.50	830	0.008	0.0029	13.28	14.92	12.79	11.72	15.04	13.05	15.42	13.06	9.22	13.96
Km 9+996	11.2	42.46	25.80	1100	0.007	0.0024	10.23	11.44	9.82	8.96	11.69	10.06	11.79	10.17	7.05	10.73
Km 10+016	11.2	42.69	27.40	1100	0.007	0.0024	10.24	11.44	9.83	8.96	11.70	10.06	11.78	10.18	7.05	10.73

								Addenbrooke & Potts (2001)											
Km Point	**Support Type**	**D (m)**	**Z_0 (m)**	**Spacing (m)**	**E (MPa)**	u	V_L (%)	Pillar Width (# of D)	V_{L2}/V_L	V_{L2}	Smax (Peck, 1964)	Smax (Attkinson, 1977)	Smax (O'Reilly, 1982)	Smax (Mair, 1993)	Smax (Clough, 1981)	Smax (Arioğlu et al., 2002)	Smax (Arioğlu et al., 2002)	Smax (Arioğlu et al., 2002)	Verruijt & Booker (1996)	Loganathan & Poulos (1998)
Km 9+542	ST-3/ST-3	11.2	35.31	17.71	775	0.008	0.0028	0.599107	1.26	0.003547	8.85	9.99	8.55	7.89	9.93	8.68	10.38	8.60	6.21	9.36
Km 9+585	ST-UA1/ST-UA1	11.6	34.04	22.29	300	0.020	0.0072	0.973276	1.242	0.008993	24.78	28.08	24.07	22.25	27.60	24.38	29.28	23.88	18.79	25.60
Km 9+615	ST-3/ST-UA1	11.4	35.26	24.33	300	0.020	0.0072	1.169298	1.23	0.008901	23.00	25.99	22.27	20.54	25.74	22.60	27.03	22.30	16.75	23.63
Km 9+630	ST-2/ST-UA1	11.4	35.74	24.90	300	0.020	0.0073	1.219298	1.225	0.008984	22.93	25.89	22.19	20.45	25.70	22.54	26.91	22.27	16.67	23.52
Km 9+645	ST-2/ST-UA1	11.4	35.86	25.24	300	0.021	0.0074	1.249123	1.223	0.008998	22.89	25.85	22.16	20.42	25.67	22.51	26.86	22.24	16.64	23.48
Km 9+660	ST-2/ST-UA1	11.4	36.17	25.40	640	0.010	0.0036	1.263158	1.221	0.004356	11.00	12.41	10.64	9.80	12.34	10.81	12.89	10.70	7.99	11.47
Km 9+681	ST-UA1/ST-UA1	11.6	36.56	25.21	1100	0.006	0.0022	1.225	1.223	0.002743	7.09	8.01	6.87	6.32	7.95	6.98	8.32	6.89	5.34	7.57
Km 9+695	ST-3/ST-3	11.2	36.93	25.10	1100	0.006	0.0021	1.258929	1.222	0.002581	6.18	6.97	5.97	5.49	6.97	6.07	7.22	6.04	4.32	6.57
Km 9+758	ST-3/ST-3	11.2	38.32	24.10	860	0.008	0.0028	1.169643	1.233	0.00341	7.90	8.89	7.62	6.99	8.94	7.76	9.20	7.76	5.50	8.33
Km 9+789	ST-3/ST-3	11.2	38.97	23.50	830	0.008	0.0029	1.116071	1.241	0.00361	8.24	9.26	7.94	7.27	9.33	8.10	9.57	8.10	5.72	8.66
Km 9+996	ST-2/ST-2	11.2	42.46	25.80	1100	0.007	0.0024	1.321429	1.23	0.002978	6.29	7.04	6.04	5.51	7.19	6.19	7.25	6.25	4.33	6.60
Km 10+016	ST-2/ST-2	11.2	42.69	27.40	1100	0.007	0.0024	1.464286	1.215	0.002958	6.22	6.95	5.97	5.44	7.11	6.11	7.16	6.18	4.28	6.52

Table 5.7. Maximum settlement values calculated by using Hunt, Herzog and Chakeri and Unver methods for twin tunnel

									Hunt (2005)								
Km Point	**Support Type**	**D (m)**	**Z_0 (m)**	**Spacing (m)**	**E (MPa)**	u	V_L	V_L (%)	Smax (Attkinson, 1977)	Smax (O'Reilly, 1982)	Smax (Mair, 1993)	Smax (Clough, 1981)	Smax (Arioğlu et al., 2002)	Smax (Arioğlu et al., 2002)	Smax (Arioğlu et al., 2002)	Verruijt & Booker (1996)	Loganathan & Poulos (1998)
Km 9+542	ST-3/ST-3	11.2	35.31	17.71	775	0.008	0.282	0.0028	10.89	9.33	8.60	10.82	9.47	11.32	16.19	6.77	10.20
Km 9+585	ST-UA1/ST-UA1	11.6	34.04	22.29	300	0.020	0.724	0.0072	27.08	23.21	21.46	26.62	23.51	28.24	15.86	18.12	24.69
Km 9+615	ST-3/ST-UA1	11.4	35.26	24.33	300	0.020	0.724	0.0072	24.77	21.22	19.58	24.54	21.54	25.76	16.24	15.96	22.52
Km 9+630	ST-2/ST-UA1	11.4	35.74	24.90	300	0.020	0.733	0.0073	24.66	21.13	19.48	24.48	21.46	25.63	16.41	15.88	22.40
Km 9+645	ST-2/ST-UA1	11.4	35.86	25.24	300	0.021	0.736	0.0074	24.56	21.05	19.39	24.39	21.38	25.52	16.45	15.81	22.31
Km 9+660	ST-2/ST-UA1	11.4	36.17	25.40	640	0.010	0.357	0.0036	12.74	10.92	10.06	12.67	11.10	13.23	16.57	8.20	11.77
Km 9+681	ST-UA1/ST-UA1	11.6	36.56	25.21	1100	0.006	0.224	0.0022	8.69	7.46	6.86	8.63	7.58	9.03	16.77	5.79	8.22
Km 9+695	ST-3/ST-3	11.2	36.93	25.10	1100	0.006	0.211	0.0021	7.58	6.49	5.97	7.58	6.61	7.86	16.77	4.70	7.15
Km 9+758	ST-3/ST-3	11.2	38.32	24.10	860	0.008	0.277	0.0028	9.18	7.87	7.22	9.24	8.02	9.51	17.26	5.68	8.61
Km 9+789	ST-3/ST-3	11.2	38.97	23.50	830	0.008	0.291	0.0029	9.51	8.15	7.47	9.59	8.32	9.83	17.49	5.88	8.90
Km 9+996	ST-2/ST-2	11.2	42.46	25.80	1100	0.007	0.242	0.0024	7.57	6.50	5.93	7.74	6.65	7.80	18.70	4.66	7.10
Km 10+016	ST-2/ST-2	11.2	42.69	27.40	1100	0.007	0.243	0.0024	7.48	6.42	5.85	7.65	6.58	7.70	18.78	4.61	7.01

Km Point	**Support Type**	**D (m)**	**Z_0 (m)**	**Spacing (m)**	**E (MPa)**	**Poisson's Ratio**	**Unit Weigth (kN/m^3)**	**Cohesion (kPa)**	**Friction Angle (°)**	i_{avg}	Smax (Herzog,1985)	Smax (Chakeri& Unver, 2013)
Km 9+542	ST-3/ST-3	11,2	35,31	17,71	775	0,26	24,4	243,8	39,3	15,41	10,59	9,01
Km 9+585	ST-UA1/ST-UA1	11,6	34,04	22,29	300	0,28	23,0	150,0	28,0	14,95	43,85	28,98
Km 9+615	ST-3/ST-UA1	11,4	35,26	24,33	300	0,28	23,0	150,0	28,0	15,41	42,59	28,48
Km 9+630	ST-2/ST-UA1	11,4	35,74	24,90	300	0,28	23,0	150,0	28,0	15,60	46,08	28,48
Km 9+645	ST-2/ST-UA1	11,4	35,86	25,24	300	0,28	23,0	150,0	28,0	15,65	42,03	28,48
Km 9+660	ST-2/ST-UA1	11,4	36,17	25,40	640	0,27	23,9	213,8	34,4	15,77	31,34	12,49
Km 9+681	ST-UA1/ST-UA1	11,6	36,56	25,21	1100	0,25	25,0	300,0	43,0	15,94	19,21	5,99
Km 9+695	ST-3/ST-3	11,2	36,93	25,10	1100	0,25	25,0	300,0	43,0	16,05	17,93	5,80
Km 9+758	ST-3/ST-3	11,2	38,32	24,10	860	0,25	24,6	260,0	40,2	16,60	22,93	8,06
Km 9+789	ST-3/ST-3	11,2	38,97	23,50	830	0,25	24,6	255,0	39,9	16,86	23,86	8,43
Km 9+996	ST-2/ST-2	11,2	42,46	25,80	1100	0,25	25,0	300,0	43,0	18,22	9,19	5,93
Km 10+016	ST-2/ST-2	11,2	42,69	27,40	1100	0,25	25,0	300,0	43,0	18,31	9,02	5,94

Now, twin tunnel induced maximum settlement values are compared with field measurement data to observe the precision of the literature equations for twin tunnels (Figure 5.28-Figure 5.33).

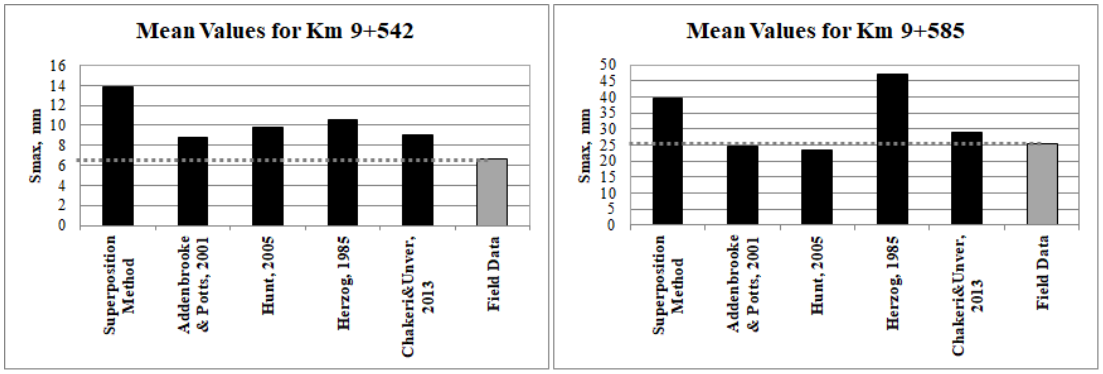

Figure 5.28. Average of maximum settlement values obtained by using the literature formulas for twin tunnel and the field data for section Km 9+542 and Km 9+585

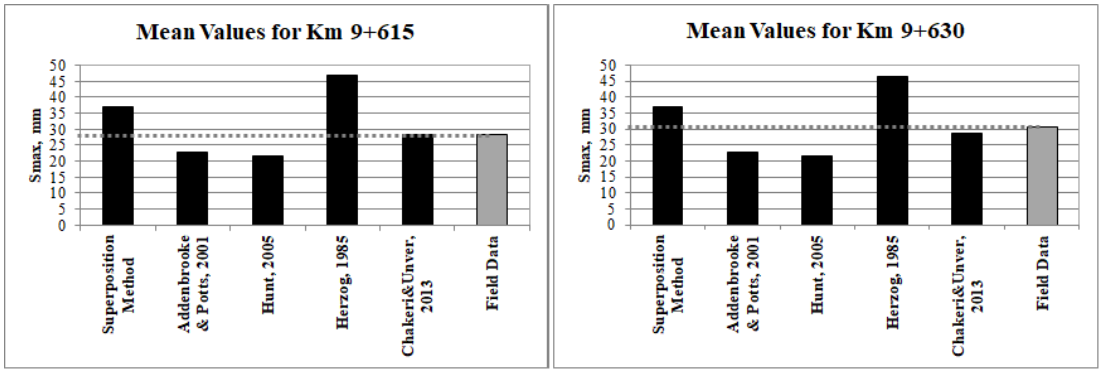

Figure 5.29. Average of maximum settlement values obtained by using the literature formulas for twin tunnel and the field data for section Km 9+615 and Km 9+630

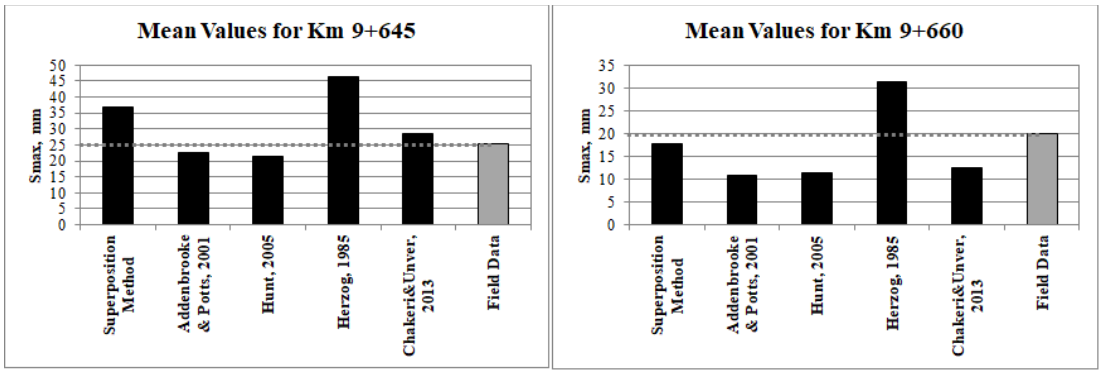

Figure 5.30. Average of maximum settlement values obtained by using the literature formulas for twin tunnel and the field data for section Km 9+645 and Km 9+660

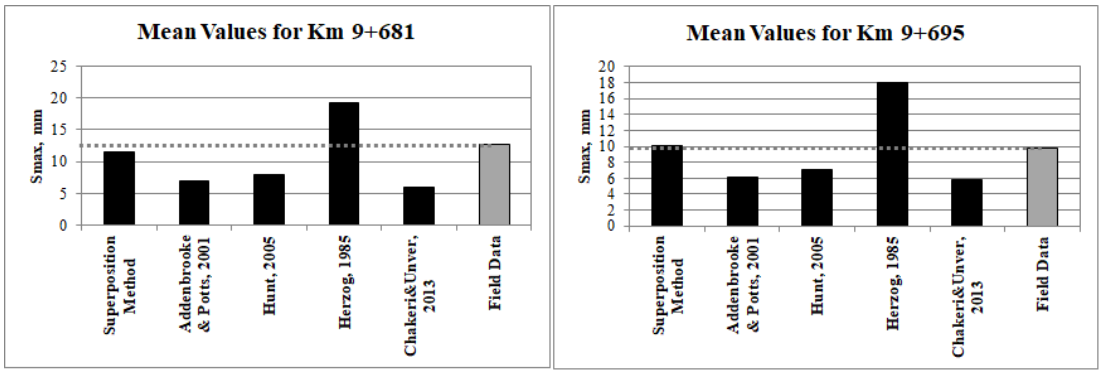

Figure 5.31. Average of maximum settlement values obtained by using the literature formulas for twin tunnel and the field data for section Km 9+681 and Km 9+695

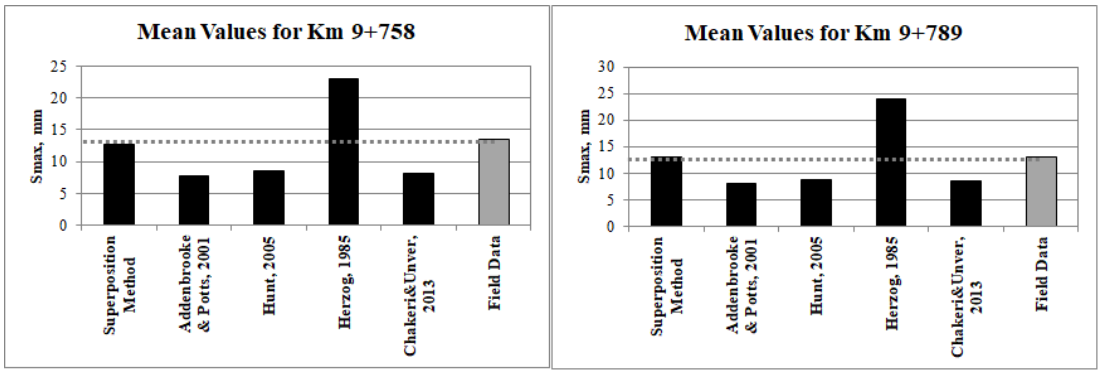

Figure 5.32. Average of maximum settlement values obtained by using the literature formulas for twin tunnel and the field data for section Km 9+758 and Km 9+789

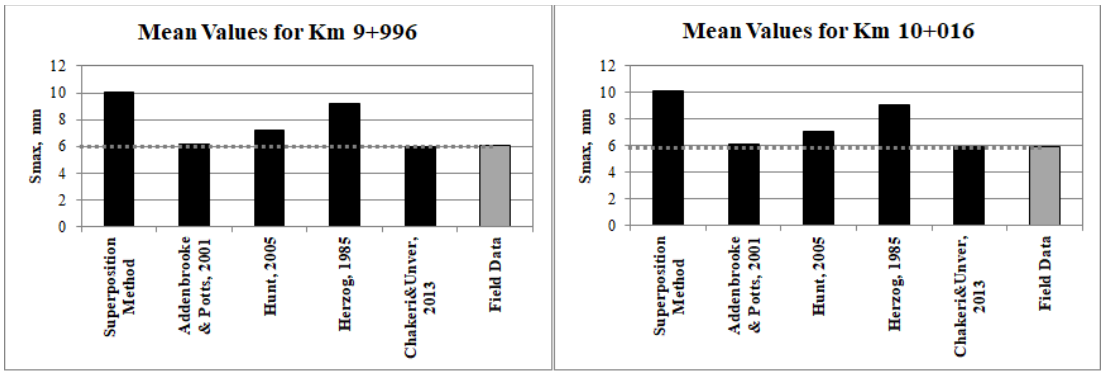

Figure 5.33. Average of maximum settlement values obtained by using the literature formulas for twin tunnel and the field data for section Km 9+996 and Km 10+016

The most precise equation is found to be Chakeri and Unver (2013) for section Km 9+542, Km 9+585, Km 9+615, Km 9+630, Km 9+645, Km 9+996, Km 10+016, Superposition method for section Km 9+660, Km 9+681, Km 9+695, Km 9+758, Km 9+789. The least precise method is Herzog (1985) for most of the sections. Prediction equations of maximum twin tunnel ground settlement utilize the methods for single tunnel which derived from the data coming from tunnel excavated through soil units. Herzog and Chakeri and Unver do not use the single tunnel data, they consider the twin tunnel structure as a whole. Data to construct the Chakeri and Unver equation comes from numerical analysis. Therefore Herzog equation have modified in this thesis.

5.4. Determination of Modification Factor

Pre-support effect is not considered in all literature formulas, however, the results of Herzog equation are so far from field measurement data since the original Herzog model does not consider the pre-support which relieves the ground deformation. As a result, it is vital to modify the Herzog equation in terms of the effect of forepoling. Therefore, the field measurements from twin NATM tunnel part of the Eurasia tunnel with forepoling pre-support have been utilized and assessed with respect to center-to-center distance between pipes in pre-support system statistically.

2D modeling of the forepoling system was addressed in Chapter 4.4. One of the parameters using to calculate the deformation modulus of the material in forepoling area is number of pipes in unit meter which is dependent on spacing between pipes. Then six different spacing size was specified, however, for ST-2 and ST-3 support type, spacing of 25 cm and 30 cm have the same number of pipes per unit meter. Pre-support deformation modulus with respect to different spacing values is presented in Table 5.8.

Table 5.8. Summary of the pre-support deformation modulus with respect to different spacing values

Km	Support Type		Original Spacing		Spacing = 15cm		Spacing = 20 cm		Spacing = 25cm	
	Westbound	Eastbound	Pre-Support Deformation Modulus, MPa		Pre-Support Deformation Modulus, MPa		Pre-Support Deformation Modulus, MPa		Pre-Support Deformation Modulus, MPa	
			Westbound	Eastbound	Westbound	Eastbound	Westbound	Eastbound	Westbound	Eastbound
9+542	ST-3	ST-3	9470.3	9065.31	15804.61	15435.56	11581.73	11188.09	-	-
9+585	ST-UA1	ST-UA1	4424.15	4424.15	14512.84	14512.84	10731.15	10731.15	8628.06	8628.06
9+615	ST-3	ST-UA1	11205.86	4424.15	19433.38	14512.84	13943.42	10731.15	11200.15	8628.06
9+630	ST-2	ST-UA1	11205.86	4424.15	19433.38	14512.84	13943.42	10731.15	11200.15	8628.06
9+645	ST-2	ST-UA1	11205.86	4424.15	14717.87	14512.84	10579.53	10731.15	8509.78	8628.06
9+660	ST-2	ST-UA1	11205.86	4293.21	19433.38	12018.86	13943.42	9120.41	11205.86	7509.92
9+681	ST-UA1	ST-UA1	4452.8	4452.8	11887.81	12146.59	9008.12	9050.49	7409.91	7329.92
9+695	ST-3	ST-3	9786.1	9786.1	16236.37	16236.37	11937.03	11937.03	-	-
9+758	ST-3	ST-3	8986.99	8912.07	19433.38	19433.38	13943.42	13943.42	-	-
9+789	ST-3	ST-3	8881.21	8912.07	19433.38	19433.38	13943.42	13943.42	-	-
9+996	ST-2	ST-2	9786.1	9786.1	16236.37	16236.37	11937.03	11937.03	-	-
10+016	ST-2	ST-2	9786.1	9786.1	16236.37	16236.37	11937.03	11937.03	-	-

Km	Support Type		Spacing = 30cm		Spacing = 40cm		Spacing = 50cm	
	Westbound	Eastbound	Pre-Support Deformation Modulus, MPa		Pre-Support Deformation Modulus, MPa		Pre-Support Deformation Modulus, MPa	
			Westbound	Eastbound	Westbound	Eastbound	Westbound	Eastbound
9+542	ST-3	ST-3	9470.3	9065.31	7358.86	6942.54	5247.01	4818.8
9+585	ST-UA1	ST-UA1	8209.26	8209.26	6527.24	6527.24	4424.15	4424.15
9+615	ST-3	ST-UA1	11205.86	8208.12	8454.6	6527.24	5711.34	4424.15
9+630	ST-2	ST-UA1	11205.86	8208.12	8454.6	6527.24	5711.34	4424.15
9+645	ST-2	ST-UA1	8509.78	8208.12	6440.02	6527.24	4371.45	4424.15
9+660	ST-2	ST-UA1	11205.86	7187.39	8455.75	5899.43	5711.34	4293.21
9+681	ST-UA1	ST-UA1	7090.03	6984.87	5809.34	5609.34	4249.3	3963.38
9+695	ST-3	ST-3	9786.1	9786.1	7637.68	7637.68	5488.27	5488.27
9+758	ST-3	ST-3	11205.86	11205.86	8455.75	8455.75	5710.2	5710.2
9+789	ST-3	ST-3	11205.86	11205.86	8455.75	8455.75	5710.2	5710.2
9+996	ST-2	ST-2	9786.1	9786.1	7637.68	7637.68	5487.76	5487.76
10+016	ST-2	ST-2	9786.1	9786.1	7637.68	7637.68	5487.76	5487.76

After determining the pre-support deformation modulus, FEM analysis was performed for each one. In FEM analysis, liner (lattice girder and wire mesh) was removed in order to observe clear pre-support effect on the ground settlement. It can

be seen from Table 5.9 that there are FEM results (maximum settlement values in mm) without liner and pre-support effect and they are much more than FEM results with liner and pre-support.

Table 5.9. Summary of the parametric study for spacing between pipes in pre-support system

			NO LINER (LATTICE GIRDER - WIRE MESH)						
	Support Type	Smax Field Result (mm)	FEM Result (no liner-no forepole)	FEM Result (with 15cm spacing)	FEM Result (with 20cm spacing)	FEM Result (with 25cm spacing)	FEM Result (with 30cm spacing)	FEM Result (with 40cm spacing)	FEM Result (with 50cm spacing)
9+542	ST-3, ST-3	6.60	23.29	17.09	17.12		17.15	17.18	17.23
Decreasing Smax (%)				26.62	26.50		26.35	26.22	26.03
9+585	ST-UA1, ST-UA1	25.50	69.56	46.50	46.71	46.84	46.94	47.05	47.17
Decreasing Smax (%)				33.14	32.85	32.66	32.51	32.35	32.18
9+615	ST-3, ST-UA1	28.20	67.46	45.00	45.10	45.18	45.30	45.47	45.58
Decreasing Smax (%)				33.29	33.14	33.02	32.84	32.60	32.43
9+630	ST-2, ST-UA1	30.70	70.67	47.27	47.32	47.38	47.43	47.52	47.64
Decreasing Smax (%)				33.12	33.04	32.96	32.89	32.76	32.59
9+645	ST-2, ST-UA1	25.30	57.86	38.61	38.79	38.86	38.93	39.02	39.12
Decreasing Smax (%)				33.27	32.96	32.84	32.72	32.56	32.38
9+660	ST-2, ST-UA1	20.10	38.08	26.40	26.49	26.56	26.65	26.79	26.88
Decreasing Smax (%)				30.67	30.43	30.25	30.01	29.64	29.41
9+681	ST-UA1, ST-UA1	12.70	22.88	18.85	17.02		17.06	17.09	17.11
Decreasing Smax (%)				25.73	25.60		25.43	25.31	25.21
9+695	ST-3, ST-3	9.80	17.46	15.51	13.00		13.05	13.07	13.08
Decreasing Smax (%)				25.60	25.55		25.30	25.18	25.09
9+758	ST-3, ST-3	13.40	36.86	28.87	27.40		27.44	27.51	27.55
Decreasing Smax (%)				25.85	25.65		25.56	25.35	25.25
9+789	ST-3, ST-3	13.00	34.77	26.33	25.89		26.00	26.03	26.08
Decreasing Smax (%)				25.78	25.54		25.22	25.13	25.00
9+996	ST-2, ST-2	6.10	11.13	9.10	8.28		8.30	8.31	8.32
Decreasing Smax (%)				25.82	25.63		25.46	25.34	25.21
10+016	ST-2, ST-2	5.90	10.63	8.69	7.93		7.94	7.97	7.99
Decreasing Smax (%)				25.66	25.46		25.28	25.02	24.90

Then, only pre-support was applied with different spacing conditions to obtain pre-support effect solely. In order to calculate the percent decrease in S_{max}, difference

between FEM results without liner and pre-support and FEM results with pre-support pipes having different spacing sizes were utilized.

All data of percent decrease in S_{max} with respect to spacing between pipes in pre-support system itemized in Table 5.10 and plotted in Figure 5.34. It can be seen from graph, data points are separated into four groups named as 1, 2, 3, and 4. Group 2 and 3 are composed of only one cross-section data which are Km 9+660 and Km 9+542 respectively. Group 1 includes the data coming from cross-sections Kms 9+585, 9+615, 9+630, 9+645. Group 4 includes the data coming from cross-sections Kms 9+681, 9+695, 9+758, 9+789, 9+996, 10+016. Group 2 and 3 were deselected for further statistical analysis due to lack of data points according to cross-section variation. Moreover, Group 2 data are more close to Group 1 data and Group 3 data are more close to Group 4 data, and so these cross section lines were used to verify the modified Herzog equation restricted according to deformation modulus by utilizing the equation whichever is closer to which.

Table 5.10. Summary of percent decrease in S_{max} with respect to spacing for all selected cross-sections

	Decrease in Smax (%)											
Spacing between pipes in Forepole (cm)	9+542	9+585	9+615	9+630	9+645	9+660	9+681	9+695	9+758	9+789	9+996	10+016
15	26.62	33.14	33.29	33.12	33.27	30.67	25.73	25.60	25.85	25.78	25.82	25.66
20	26.50	32.85	33.14	33.04	32.96	30.43	25.60	25.55	25.65	25.54	25.63	25.46
25		32.66	33.02	32.96	32.84	30.25						
30	26.35	32.51	32.84	32.89	32.72	30.01	25.43	25.30	25.56	25.22	25.46	25.28
40	26.22	32.35	32.60	32.76	32.56	29.64	25.31	25.18	25.35	25.13	25.34	25.02
50	26.03	32.18	32.43	32.59	32.38	29.41	25.21	25.09	25.25	25.00	25.21	24.90

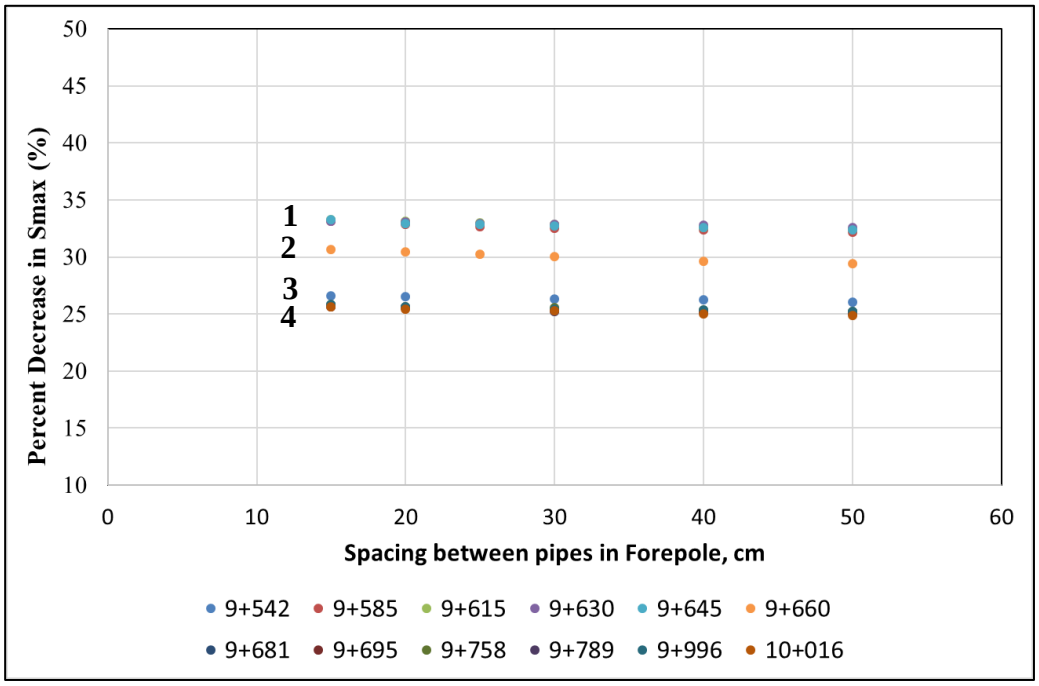

Figure 5.34. Graph of percent decrease in S_{max} versus spacing between pipes in pre-support system for all cross-section lines

If available data are interval or ratio scales parametric statistics can be used. If data are supposed to take parametric statistics it should be checked that the distributions are approximately normal. In other words, an evaluation of the normality of data is a prerequisite for many statistical tests because normal data are an underlying assumption in parametric testing. The result of a normal Q-Q Plot can be utilized to obtain normality graphically. If the data are normally distributed, the data points will be close to the diagonal line. If the data points diverge from the line in an obvious non-linear fashion, the data are not normally distributed (Ghasemi and Zahediasl, 2012). As it is seen from the normal Q-Q plot in Figure 5.35 and Figure 5.36, the data are normally distributed.

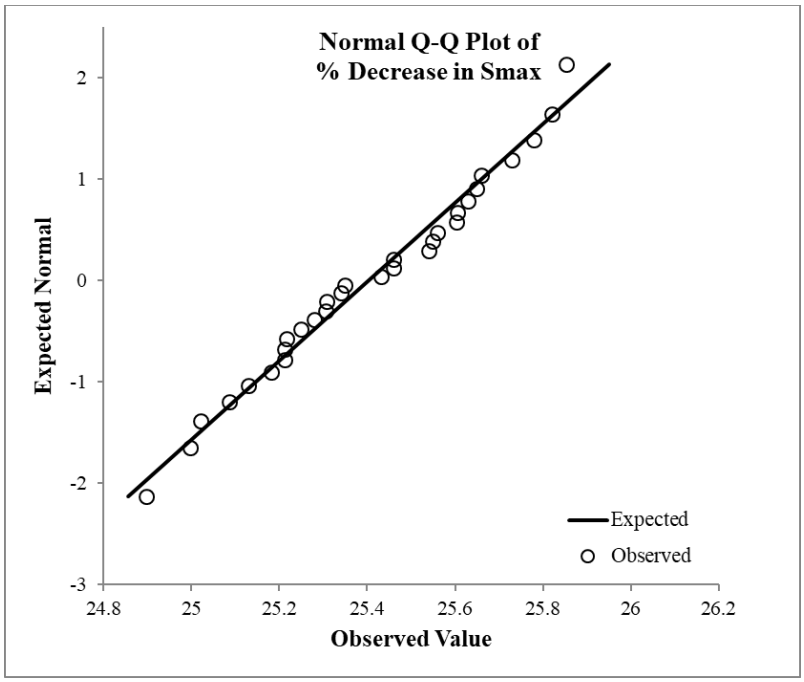

Figure 5.35. Test of normality of percent decrease in S_{max} for the cross-section Kms 9+681, 9+695, 9+758, 9+789, 9+996, 10+016

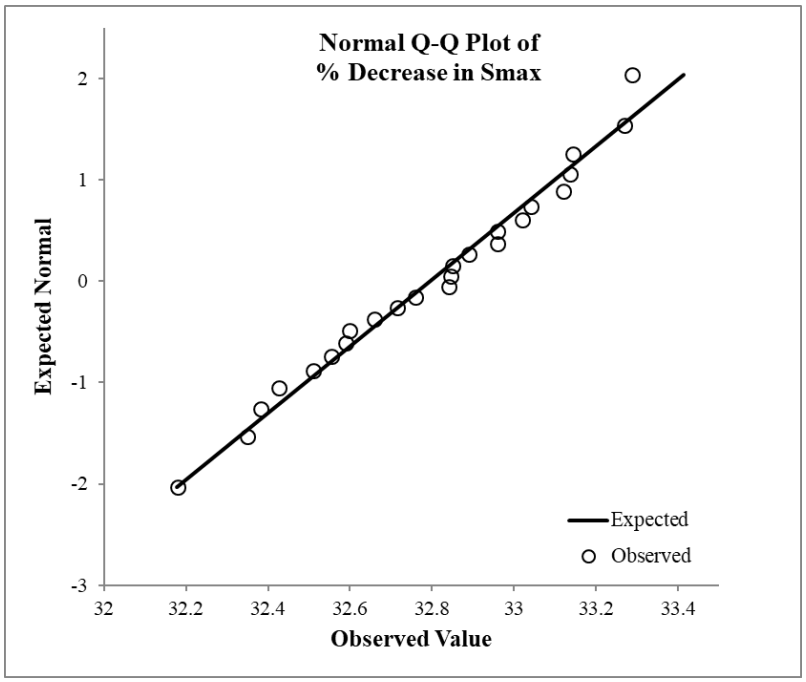

Figure 5.36. Test of normality of percent decrease in S_{max} for the cross-section Kms 9+585, 9+615, 9+630, 9+645

Therefore, parametric regression analysis can be used for the data coming from the parametric study for spacing between pipes in pre-support system. Regression analysis is a form of predictive modelling technique which investigates the relationship between a dependent (target) and independent variables (predictor) (IBM, 2018). According to Figure 5.37 and Figure 5.38, data points do not show a linear relationship and it is concluded that ground settlement reduces with decreasing center-to-center distance between pipes for same geo-mechanical conditions. Therefore, curve estimation regression models should be performed in this study. The curve estimation procedure produces curve estimation regression statistics and related plots for 11 different curve estimation regression models, namely; linear, logarithmic, inverse, quadratic, cubic, power, compound, S-curve, logistic, growth, and exponential (IBM, 2018). In Figure 5.37-Figure 5.38, power, exponential, linear, logarithmic curve estimations and related R^2 values are presented. It is found that the logarithmic curve relations fit the points with higher correlations than all the other relationships.

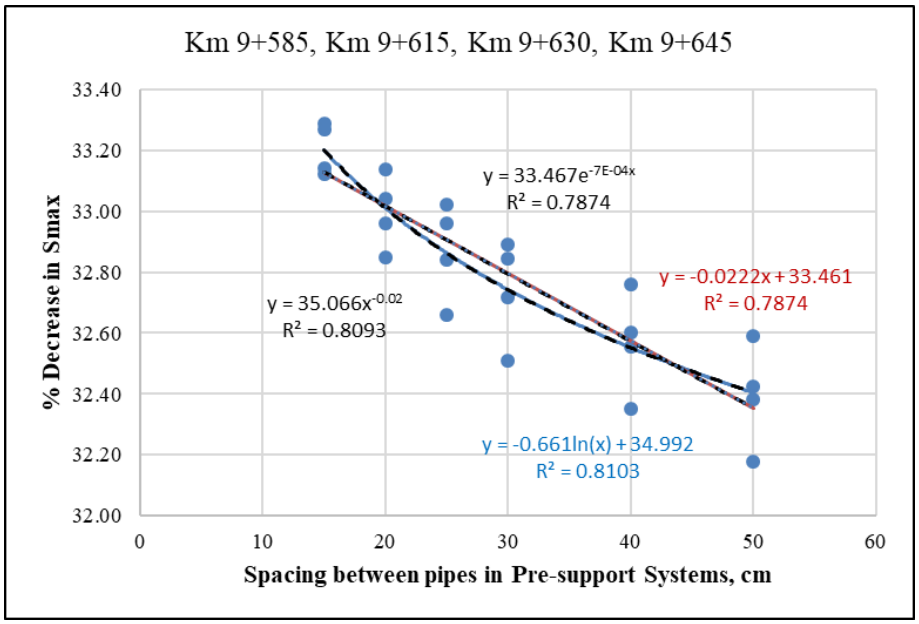

Figure 5.37. Graph of percent decrease in S_{max} versus spacing between pipes in pre-support system for the cross-section Kms 9+585, 9+615, 9+630, 9+645

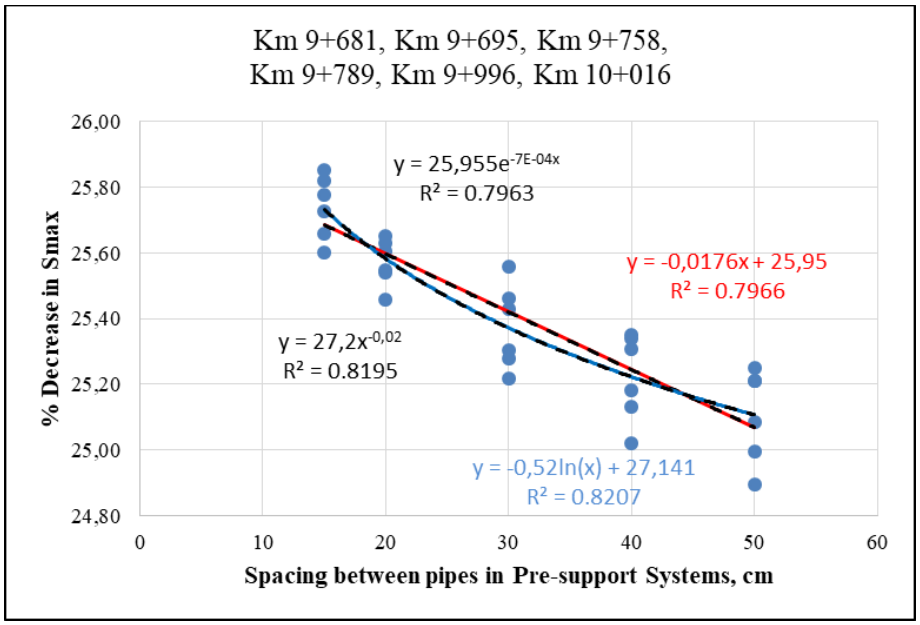

Figure 5.38. Graph of percent decrease in S_{max} versus spacing between pipes in pre-support system for the cross-section Kms 9+681, 9+695, 9+758, 9+789, 9+996, 10+016

Now, it should be clarified whether these relationships are statistically significant or not. For this purpose, F-test was applied to two groups of data points in this study. There are two hypotheses in F-test, namely; null hypothesis which is insignificant relation between x and y and alternative hypothesis which is significant relation between x and y. F-test can be used when deciding to support or reject the null hypothesis (Archdeacon, 1994). Results of the F-test were given in Table 5.11 and note that significance level is 0.05, the corresponding confidence level is 95% (Cowles and Davis, 1982). Variable 1 is spacing between pipes in pre-support system and Variable 2 is percent decrease in S_{max}.

Table 5.11. Results of the F-test for two groups of the data points

F-Test for Km 9+681, Km 9+695, Km 9+758, Km 9+789, Km 9+996, Km 10+016		
	Variable 1	***Variable 2***
Mean	31	25.40354837
Variance	169.6551724	0.066188207
Observations	30	30
df	29	29
F	2563.223588	
P(F<=f) one-tail	1.45827E-42	
F Critical two-tail	1.860811435	

F-Test for Km 9+585, Km 9+615, Km 9+630, Km 9+645		
	Variable 1	***Variable 2***
Mean	30	32.79571778
Variance	147.826087	0.092267357
Observations	24	24
df	23	23
F	1602.149368	
P(F<=f) one-tail	9.53232E-32	
F Critical two-tail	2.014424842	

F critical value is also called the F statistic and other F in the resulting table calculated from current data. The calculated F value in a test is larger than the F statistic, so you can reject the null hypothesis (Archdeacon, 1994). As it is seen from Table 5.11 null hypothesis is rejected for this study, i.e., current relationships are statistically significant. The F statistic must be used in combination with the p value when you are deciding if your overall results are significant. If the p value is less than the alpha level, you can reject the null hypothesis (Archdeacon, 1994). It is also seen from Table 5.11 null hypothesis is also rejected with respect to p value. It is concluded that current relationships are statistically significant and can be used to forecast the settlements.

Therefore, the logarithmic functions given in Figure 5.39 was used for adjusting the Herzog equation, as given in Equations 5.15-5.16 which are restricted according to deformation modulus.

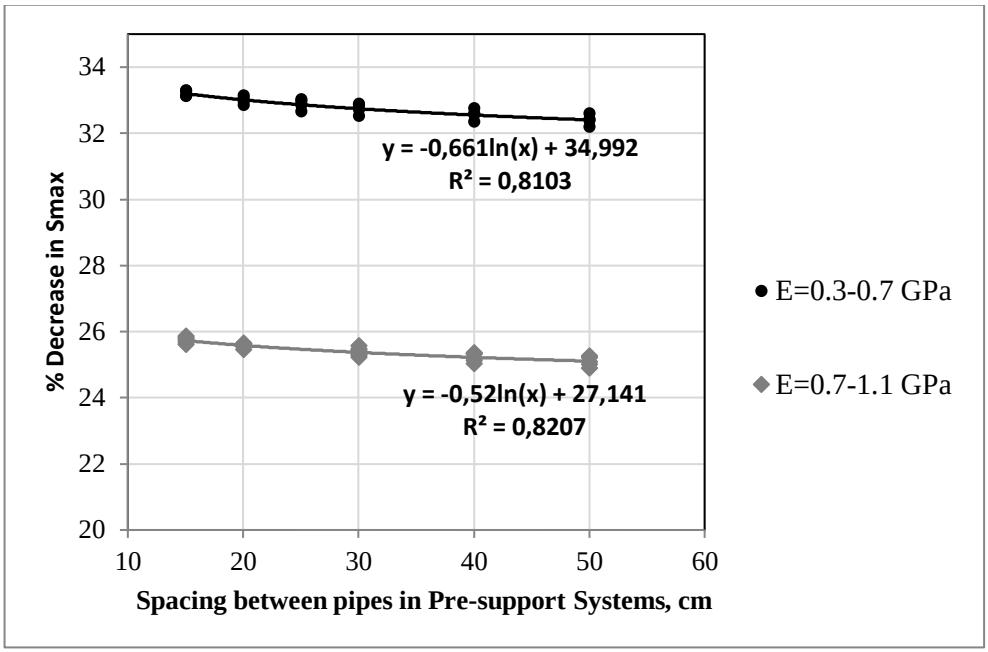

Figure 5.39. Final graph of percent decrease in S_{max} versus spacing between pipes in pre-support system for the cross-section Kms 9+585, 9+615, 9+630, 9+645, 9+681, 9+695, 9+758, 9+789, 9+996, 10+016

Modification of the Herzog equation is given below:

$$S_{max} = M \times 4.71 \times (\gamma_n Z_0 + \sigma_s)\left(\frac{D^2}{(3i+a)E}\right) \tag{5.15}$$

where, M is the modification factor and

$$M = \begin{Bmatrix} [1-(-0.00661 \times \ln(x) + 0.34992)] & for\ E = 0.3 - 0.7\ GPa \\ [1-\ (-0.0052 \times \ln(x) + 0.27141)] & for\ E = 0.7 - 1.1\ GPa \end{Bmatrix} \tag{5.16}$$

Where x is the spacing between pipes in forepole and umbrella arch systems.

Herzog equation are so far from field measurement data since the original Herzog model does not consider the pre-support which relieves the ground deformation. The Herzog equation was adjusted in terms of the center-to-center distance between pipes and the pre-support impact on the ground settlement value. Data obtained from all selected cross section lines and coming from literature (Thessaloniki metro and

Nerchowck Tunnel) (Koukoutas and Sofianos, 2015; Das et al., 2017) were used in verification of the modified Herzog equation and literature data are presented in Table 5.12. It is concluded that the results of the modified Herzog equation approach to the measured data (Figure 5.40). Note that this modification factor, M can be only used for rock mass which has the deformation modulus between 0.3-1.1 GPa.

Table 5.12. Tunnel data of Nerchowck and Thessaloniki tunnels

	Nerchowck Tunnel	**Thessaloniki Metro**
D (m)	12	6,19
$\mathbf{Z_0}$ (m)	30	27
E (GPa)	1,0	0,4
σ (kPa)	-	20
γ (MN/m^3)	0,024	0,023
a (m)	13	6
i (m)	15	11,95
$\mathbf{S_{max,field}}$ (mm)	3,14	6,42

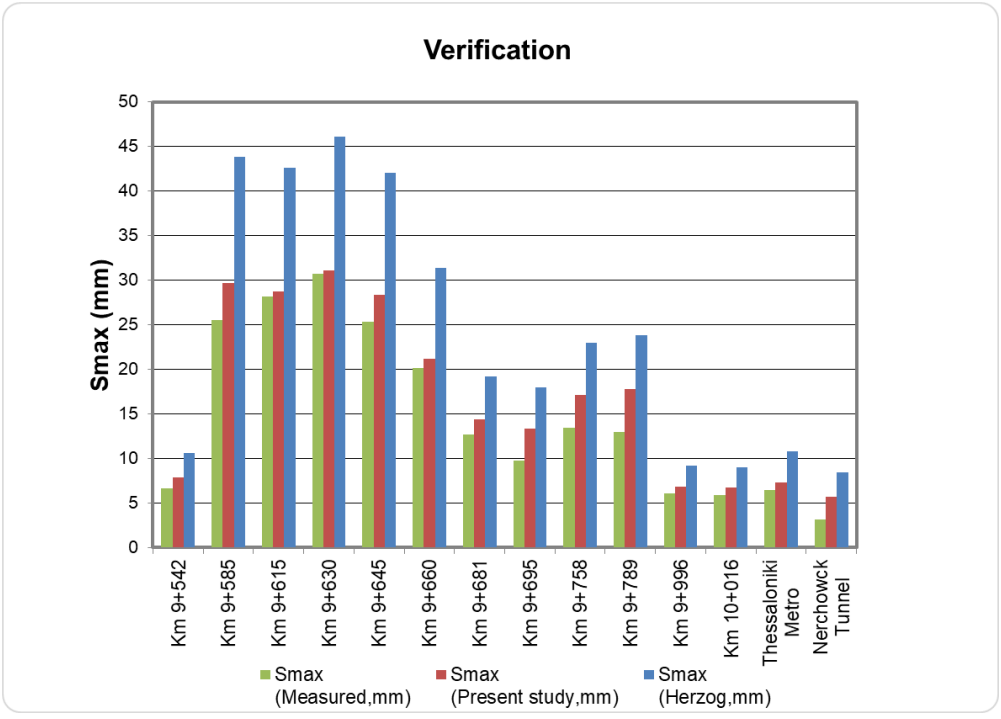

Figure 5.40. Verification of the modified Herzog equation

In the regression analysis, the difference between the observed value of the dependent variable and the predicted value is called the residual (Residual = Observed value - Predicted value). Each data point has one residual (IBM, 2018). In this study the observed value is the monitoring field data of maximum settlement, and the predicted value was calculated from the original and modified Herzog equations. Residual graphs were presented in Figure 5.41. It can be stated that the modified Herzog equation produce less residuals than the original Herzog equation.

The primary essential discrepancy between the original Herzog equation and the modified Herzog equation is that the modified Herzog equation includes the center-to-center distance between pipes and so the pre-support impact.

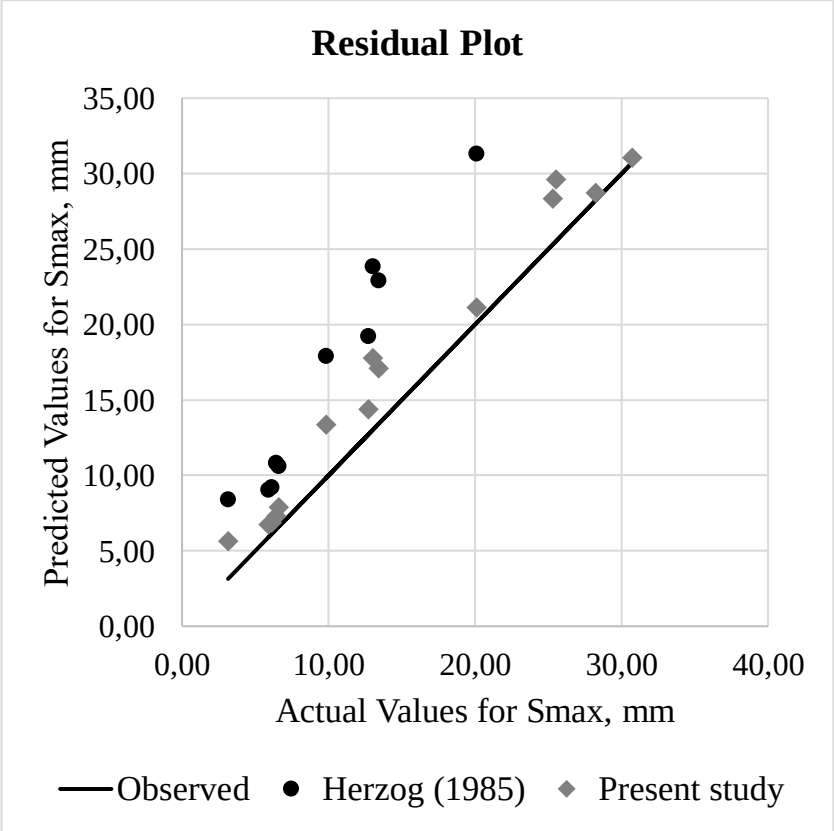

Figure 5.41. Residual plot showing the results of the modified Herzog equation

CHAPTER 6

CONCLUSIONS AND RECOMMENDATIONS

Twin tunnel induced surface settlement is mainly controlled by geomechanical factors (deformation modulus representing rock mass quality, Poisson's ratio) and engineering factors (tunnel depth, tunnel diameter, the distance between tunnels). Hence, determination of rock mass parameters is a vital step during numerical analysis of tunnel structure. This study covers the tunnel data coming from NATM part of Eurasia tunnel and including installation of settlement bolt in accordance with the procedure.

Trakya formation and volcanics are observed in the investigation site. Borehole logs and descriptions, core photographs, laboratory and field tests have been studied to determine the rock profiles and the rock mass characteristics. Most profiles are composed of sandstone, sandstone/mudstone and mudstone layers. Sandstone and mudstone sub-units namely; Sandstone units S0, S1, S2, S3 and mudstone units M0, M1, M2, and M3, have been differentiated on the basis of RMR and GSI values. It is observed that most of the cohesion values of the rock masses are below 65 and 300 kPa, friction angles are between 14^{o} and 43^{o}, deformation modulus vary between 95 and 1100 MPa.

In this study, roof sagging can be prevented by using pre-support and the dominant failure type is floor heaving. Material around the tunnel has stress strain curve showing the elastoplastic behavior which exhibits both elastic and plastic properties.

From numerical parametric analysis, it is concluded that friction angle and cohesion parameters have less effect on the surface settlement. However, deformation modulus and Poisson's ratio of the ground causes the highest change in settlement

values, since settlement is mainly controlled by stress-strain states of surrounding medium of the tunnel. Numerical analysis shows that an increase in the amount of surface surcharge from zero to 30 kPa resulted in an increment of approximately 1.5 mm in maximum surface settlement value. This situation reveals that surface surcharge has not a significant effect on the amount of surface settlement. It is observed that maximum settlement slightly increases while groundwater level decreases and finally get dry. This result reveals that groundwater table has ignoring effect on surface settlement. In the scope of this study, there is no groundwater drawdown induced settlement by tunneling, since there was no high quantities of groundwater and impermeable support was applied immediately ensuring the hydrostatic head.

The 2D-FE numerical predictions of the surface settlement were found to be compatible with field measurements.

Maximum surface settlement has the largest value around 30 mm and the smallest value around 2.5 mm along the center of the twin tunnel structure. The reason behind this result is mainly rock mass quality and the distance between the twin tunnels. Effects of interaction between twin tunnels is significant factor on the surface settlement and decreasing spacing between tunnels results in increasing twin tunnel induced ground settlement. It is concluded that the most dominant factor is the rock mass quality since there is a strict relationship between maximum settlement value and rock mass quality represented by deformation modulus (decreasing deformation modulus causes increasing surface settlement).

In the parametric analysis, the data from twin NATM part of the Eurasia tunnel using forepoling pre-support were utilized and assessed in terms of center-to-center distance between pipes in pre-support system statistically.

The most precise equation is found to be Chakeri and Unver (2013) for seven sections, Superposition method for five sections. The least precise method is Herzog (1985) for most of the sections. Prediction equations of maximum twin tunnel ground

settlement utilize the methods for single tunnel which derived from the data coming from tunnel excavated through soil units. Herzog and Chakeri and Unver do not use the single tunnel data, they consider the twin tunnel structure as a whole. Data to construct the Chakeri and Unver equation comes from numerical analysis. Therefore Herzog equation have modified in this thesis.

A modification factor (i.e. reduction ratio) was implemented into the Herzog (1985) equation to attain maximum settlement above pre-supported twin tunnel structure which gets through some part of the Trakya formation with the deformation modulus between 0.3 and 1.1 GPa. Since, Herzog (1985) gives higher maximum surface settlement along tunnels which are NATM part of Eurasia tunnel, Thessaloniki Metro and Nerchowck Tunnel.

Modification of the Herzog equation is given below:

$$S_{max} = M \times 4.71 \times (\gamma_n Z_0 + \sigma_s)\left(\frac{D^2}{(3i+a)E}\right) \tag{6.1}$$

where, M is the modification factor and

$$M = \begin{Bmatrix} [1 - (-0.00661 \times \ln(x) + 0.34992)] & for\ E = 0.3 - 0.7\ GPa \\ [1 - (-0.0052 \times \ln(x) + 0.27141)] & for\ E = 0.7 - 1.1\ GPa \end{Bmatrix} \tag{6.2}$$

Where x is the spacing between pipes in forepole and umbrella arch systems.

The F-test used in combination with the p value indicate that the current relationships were found to be statistically significant.

The primary essential discrepancy between the original Herzog equation and the modified Herzog equation is that the modified Herzog equation includes the center-to-center distance between pipes and so the pre-support impact.

Data obtained from all selected cross section lines and coming from literature (Thessaloniki metro and Nerchowck Tunnel) (Koukoutas and Sofianos, 2015; Das et al., 2017) were used in verification of the modified Herzog equation and it is

concluded that the results of the modified Herzog equation have good agreement with the actual results.

The results presented within this thesis are limited by the Eurasia tunnel data. Further investigations should include the different tunnel data with different rock mass quality. Moreover, effect of pre-support may be extended by considering the third dimension of pipes in the forepole and umbrella arch systems such as length and angle of application. In order to achieve this, 3D FEM analysis should be performed.

Although the standard practice to examine the tunnel behavior via 2D plane-strain finite element analysis, the availability of 2D plane-strain modeling of the selected cross section lines along NATM part of the Eurasia tunnel can be examined by using 3D analysis in future studies.

REFERENCES

AASHTO (1995). *Standard specifications for transportation materials and methods of sampling and testing- part II: tests*. Sixteenth Edition, Washington, D.C.

AASHTO (2002). *Guide Manual for Condition Evaluation and Load and, Resistance Factor Rating of Highway Bridges*. AASHTO publications, 1-9.

Abdellaha, W. R., Alib, M. A. and Yangca, H. S. (2018). *Studying the effect of some parameters on the stability of shallow tunnels*. Journal of Sustainable Mining v.17 p.20-33.

Addenbrooke, T. I. and Potts, D.M. (2001). *Twin tunnel interaction: surface and subsurface effects*. Int J Geomec 1(2):249–271.

Ahmed, M. and Iskander, M. (2011). *Analysis of tunneling-induced ground movements using transparent soil models*. Journal of Geotechnical and Geoenvironmental Engineering, Vol. 137, 525–535.

Altamura, G., Burghignoli, A. and Miliziano, S. (2007). *Modelling of surface settlements induced by tunnel excavation using the differential stress release technique.* Rivista Italiana Di Geotecnica, pp. 33-46.

Archdeacon, T. (1994). *Correlation and Regression Analysis: A Historian's Guide*. Univ. of Wisconsin Press.

Arıoğlu, B., Yüksel, A. and Arıoğlu, E. (2002). *Determination of the inflection point of surface settlement curves at Mevhibe İnönü Tunnel of İstanbul*. Yapı Merkezi İnş. San. A. Ş.

ASTM Standard D2487. (2000). *Standard Practice for Classification of Soils for Engineering Purposes (Unified Soil Classification System).* ASTM International, West Conshohocken, PA, 2000,DOI: 10.1520/D2487-00.

ASTM. D 1586-08a (2000). *Standard Test Method for Standard Penetration Test (SPT) and Split-Barrel Sampling of Soils*. West Conshohocken, PA: ASTM International.

Atkinson, J.H. and Potts, D. (1977). *Subsidence above shallow tunnels in soft ground*. Journal of the Geotechnical Engineering Division, 103(4), 307-325.

Attewell, P.B. (1977). *Ground movements caused by tunnelling in soil*. Cardiff J.D. In Geddes (Ed.), 1st Conf. on Large Ground Movements and Structures. Pentech Press, London pp. 812–948.

Attewell, P.B. and Yeates, J.B. (1984). *Ground movements and their effects on structures. In: tunnelling in soil*. Attewell, P. B. and Taylor, R. K. (Eds), Surrey University Press, London, pp 132-215.

Baguelin, F., Jezequel, J.F. and Shlields, D.H. (1978). *The Pressuremeter and Foundation Engineering*. Transtech Pub., p. 590

Barton, N. (2002). *Some New Q-value Correlations to Assist in Site Characterization and Tunnel Design*. Int. J. Rock Mech. And Mining Sciences, 39, 185-216.

Barton, N., Lien, R. and Lunde, J. (1974). *Engineering Classification of Masses for the Design of Tunnel Support*. Rock Mechanics, Vol.6, No.4, pp.189-236.

Basirat, R., Hassani, R. and Mahmoodian N. (2016). *Forepoling Design in Weak Medium based on the Convergence Confinement Method*. International Conference on Civil Engineering. DOI:10.13140/RG.2.2.23716.68481.

Bieniawski, Z.T. (1973). *Engineering Classification on Jointed Rock Masses*. Trans. South African Inst. Civil Engineering, Vol.15, pp. 335-344.

Bieniawski, Z.T. (1976). *Rock Mass Classifications in Rock engineering*. Proceedings Symposium on Exploration for rock Engineering, (ed. Z.T. Bieniawski), A.A. Balkema, Rotterdam, pp. 97-106.

Bieniawski, Z.T. (1989). *Engineering rock mass classifications.* John Wiley and Sons, Inc., New Yowk, 251 pages.

Boeraeve, I. P. (2010). *Introduction to the Finite Element Method (FEM)*. Institut Gramme – Liege.

Bowles, J.E. (1988). *Foundatıon Analyses and Design*. Mc- Graw- Hill. Book Co.

Broch, E. and Franklin, J. (1972). *The point-load strength test*. J. Rock Mech. Min. Sci. 9(6) 669-697.

Burland, J.B., Broms, B.B. and Mello, V.F.B. (1978). *Behaviour of Foundations and Structures.* In Proc. 9th Int. Conf. SMFE, Tokyo, Vol. 2, Jap. Society SMFE, pp. 495-538.

Chakeri, H. (2012). *Investigation of face stability and surface settlement at earth pressure balance (EPB) tunneling method* (Ph.D.), Hacettepe University.

Chakeri, H. and Ünver, B. (2013). *A new equation for estimating the maximum surface settlement above tunnels excavated in soft ground*. Environ Earth Sci (2014) 71:3195–3210. DOI 10.1007/s12665-013-2707-2.

Chakeri, H., Ozcelik, Y. and Unver, B. (2014). *Investigation of ground surface settlement in twin tunnels driven with EPBM in urban area*. Arab J Geosci.

Chapman, D. N., Rogers, C. D. F. and Hunt, D. V. L. (2004). *Predicting the settlements above twin tunnels constructed in soft ground*. School of Engineering, Civil Engineering, the University of Birmingham, U.K

Chapman, D.N., Ahn, S.K., Hunt, D.V.L. and Chan, A.H.C. (2006). *The use of model tests to investigate the ground displacements associated with multiple tunnel construction in soil.* Tunn.Undergr. Space Technol. 21 (3–4), 413.

Clough, G. W. and Schmidt, B. (1981). *Design and performance of excavations and tunnels in soft clay*. In Brand E. W. and Brenner R. P. (Eds.), Soft Clay Engineering (Chapter 8), Elsevier.

Cording, E. J. (1991). *Control of ground movements around tunnels in soil*. Proc., 9th Pan American Conf. on Soil Mechanics and Foundation Engineering, Sociedad Chilena de Geotecnia (Chilean Society of Geotechnics), Santiago, Chile.

Coulter, S. and Martin, C.D. (2006). *Effect of jet-grouting on surface settlements above the Aeschertunnel, Switzerland*. Tunn Undergr Sp Technol 21:542–553

Cowles, M. and Davis, C. (1982). *On the origins of the .05 level of statistical significance*. American Psychologist, Vol. 37, No. 5, 553-558.

Croce P., Modoni G. and Russo G. (2004). *Jet-grouting performance in tunneling*. Geo-Support. American Society of Civil Engineers, Florida

D'Appolonia, D. J., D'Appolonia, E. and Brissette, R. F. (1970). *Settlement of Spread Footings on Sand*. Journal Soil Mechanics and Foundations Division, American Society of Civil Engineers, Vol 95, No. SM2, pp 754-762.

Das, R., Singh, P.K., Kainthola A., Panthee S. and Singh, T.N. (2017). *Numerical analysis of surface subsidence in asymmetric parallel highway tunnels*. Journal of Rock Mechanics and Geotechnical Engineering 9, 170-179.

Date, K., Mair, R.J. and Soga K. (2009). *Reinforcing effects of forepoling and facebolts in tunnelling*. Geotechnical Aspects of Underground Construction in Soft Ground. Taylor & Francis Group, London, ISBN 978-0-415-48475-6.

Deere, D. U. (1964). *Technical Description of Rock Cores for Engineering Purposes.* Rock Mechanics and Engineering Geology, Vol. 1, No. 1, pp. 17-22.

Dias D., Kastner R. and Dubois P. (1997). *Tunnel face reinforcement by bolting: strain approach using 3D analysis*. In: Tunnelling under Difficult Conditions and Rock Mass Classification, Proceedings of One Day Seminar and International Conference. Basel. p. 163e74.

Dickenson, S.E. (1994). *Dynamic Response of Soft and Deep Cohesive Soils During the Loma Prieta Earhtquake of October 17, 1989.* Dissertation Submitted in Partial Satisfaction for the Degree of Doctor of Philosophy, University of California at Berkeley.

Divall, S. (2013). *Ground movements associated with twin-tunnel construction in clay*. (Ph.D.), City University London. Retrieved from http://openaccess.city.ac.uk/4785/

Do, N.A., Dias, D. and Oreste, P. (2015). *3D numerical investigation on the interaction between mechanized twin tunnels in soft ground*. Environ Earth Sci, pp. 2101–2113

Do, N.A., Dias, D., Oreste, P. and Maigre, I.D. (2014). *Three-dimensional numerical simulation of a mechanized twin tunnels in soft ground*. Tunnelling and Underground Space Technology, pp.40–51.

Dragojević, S.M. (2012). *Analysis of ground settlement caused by tunnel construction*. Gradevinar, pp. 573-581.

Elmanan, A.M.A. and Elarabi H. (2015). *Analysis of surface settlement due to tunneling in soft ground by using empirical and numerical methods*. The

Fourth African Young Geotechnical Engineer's Conference (4AyGEC'15), Casablanca, Morocco.

Equihua-Anguiano, L. N., Viveros-Viveros, F., Pérez-Cruz, J. R., Chávez-Negrete, C. and Arreygue-Rocha, E. (2017). *Displacement nomograph from two (2D) to three (3D) dimensions applied to circular tunnels in clay using finite element.* Proceedings of the 19th International Conference on Soil Mechanics and Geotechnical Engineering, Seoul.

Ercelebi, S. G., Copur, H. and Ocak, I. (2010). *Surface settlement predictions for Istanbul metro tunnels excavated by EPB-TBM*. Environ Earth Sci.

Eroskay, S.O. (1985). *Greywackes of Istanbul region, proceedings of international symposium on design of supports to deep excavations*. Turkish Group of Soil Mechanics, Bosphorus University, 41-44.

Fang, Q., Tai, Q., Zhang D. and Wong, L. N. Y. (2015). *Ground surface settlements due to construction of closely-spaced twin tunnels with different geometric arrangements.* Tunnelling and Underground Space Technology, pp.144–151.

Fang, Y. S., Lin, L. S. and Su, C. S. (1994). *An estimation of ground settlement due to shield tunnelling by the Peck-Fujita method*. Canadian Geotechnical Journal, Vol. 31, No. 3, pp. 431-443.

Fargnoli, V., Boldini, D. and Amorosi, A. (2015). *Twin tunnel excavation in coarse grained soils: observations and numerical back-predictions under free field conditions and in presence of a surface structure*. Tunnelling and Underground Space Technology, pp. 454–469.

Farias, M.M., Junior, A. H. M. and Assis, A.P. (2004). *Displacement control in tunnels excavated by the NATM: 3-D numerical simulations*. Tunnelling and Underground Space Technology 19, pp. 283–293.

Fattah, M.Y., Shlash, K. T. and Salim, N.M. (2012). *Prediction of settlement trough induced by tunneling in cohesive ground*. ActaGeotechnica.

Fowell, M. (2003). *Effects of different tunnel face advance excavation on the settlement by FEM*. Tuneling and Underground Space Technology, pp 513-523.

Franza, A. and Marshall, A. M. (2015). *Analytical investigation of soil deformation patterns above tunnels in sandy soil*. Proceedings of the XVI ECSMGE Geotechnical Engineering for Infrastructure and Development.

Fu J., Klapperich, H., Azzam, R. and Yang, J. (2016). *Modelling of surface settlements induced by a non-uniformly deforming tunnel*. Ernst&Sohn Verlagfür Architektur und technische Wissenschaften GmbH & Co. KG, Berlin, Geotechnik.

Galli, G., Grimaldi, A. and Leonardi, A. (2004). *Three-dimensional modelling of tunnel excavation and lining*. Computers and Geotechnics, 31(3), 171-183.

Galloway, D., Jones, D. R. and Ingebritsen, S. E. (1999). *Land subsidence in the United States, In U.S.* Geological Survey Circular 1182. ASCE, New York.

Gamsjäger, H. and Scholz, M. (2009). *Pipe Roofing – Features & Application*.

Gercek, H. (2007). *Poisson's ratio values for rocks.* International Journal of Rock Mechanics and Mining Sciences Volume 44, Issue 1, Pages 1-13.

Ghasemi, A. and Zahediasl, S. (2012). *Normality Tests for Statistical Analysis: A Guide for Non-Statisticians*. Int J Endocrinol Metab. 10(2):486-489

Gibbs, P. W., Lowrie, J. Keiffer, S. and McQueen, L. (2002). *M5 East – Design of a shallow soft ground shotcrete motorway tunnel*. In Proceedings of the 28th ITA-AITES World Tunneling Congress, Sydney, Australia.

Golshani, A, Oda M, Okui Y, Takemura T. and Munkhtogoo E. (2009). *Numerical simulation of the excavation damaged zone around an opening in brittle rock*. Int J Rock Mech Min Sci, 44:835–45

Grimstad, E. and Barton, N. (1993). *Updating of the Q-system for NMT*. Int. Symposium on Sprayed Concrete - Modern use of wet mix sprayed concrete for underground support, Fagernes. Eds: Kompen, Opsahll and Berg, Norwegian Concrete Association, Oslo.

Hajihassani, M., Armaghani, D. J. and Faizi, K. (2013). *Effects of geotechnical conditions on surface settlement induced by tunneling in soft grounds*. Ejge, Vol. 18, pp. 1163-1170.

Hasanpour, R., Chakeri, H., Ozcelik, Y. and Denek, H. (2012). *Evaluation of surface settlements in the Istanbul metro in terms of analytical, numerical and direct measurements*. Bull Eng Geol Environ., pp.499–510.

Hatanaka, M. and Uchida, A. (1996). *Empirical correlation between penetration resistance and internal friction angle of sandy soils*. Soils and Foundations, Vol. 36, No. 4, pp. 1-9.

Herzog, M. (1985). *Surface subsidence above shallow tunnels*. Bautechnik 62(11):375–377 (in German)

Hobbs, N.B. (1974). *General Report on Rocks*. Proc. British Geotech. Society Conf. on Settlement of Structures. Cambridge, pp.579-610.

Hoek, E and Brown E.T. (1988). *The Hoek-Brown failure criterion - a 1988 update*. Proc. 15th Canadian Rock Mech. Symp. (ed. J.H. Curran), pp. 31-38. Toronto:Civil Engineering Dept., University of Toronto

Hoek, E. (1983). *Strength of jointed rock masses*. 23rd. Rankine Lecture. Géotechnique 33(3), pp.187-223.

Hoek, E. (1990). *Estimating Mohr-Coulomb friction and cohesion values from the Hoek-Brown failure criterion*. Intnl. J. Rock Mech. and Mining Sci. and Geomechanics Abstracts. 12(3), 227-229.

Hoek, E. (1994). *Strength of rock and rock masses*. ISRM News Journal, 2(2), pp.4-16.

Hoek, E. (1999). *Putting Numbers to Geology – An Engineer's Viewport*. Quarterly Journal of Engineering Geology, Vol. 32, pp. 1-19.

Hoek, E. (2003). *Numerical modelling for shallow tunnels in weak rock*. Rocscience.

Hoek, E. (2007). *Practical rock engineering*. Rocscience Inc, North Vancouver

Hoek, E. (2007). *Rock-support interaction analysis for tunnels in weak rock masses*. In: Evert H, editor. Practical Rock Engineering. Rocscience.

Hoek, E. (2012). *Blast Damage Factor D*. Technical note for Rocscience.

Hoek, E. and Brown E.T. (1980). *Underground Excavations in Rock*. The Institution of Mining and Metallurgy, London, pp.31-34.,

Hoek, E. and Brown, E.T. (1997). *Practical estimates of rock mass strength*. Int. Journal of Rock Mechanics and Mining Sciences and Geomechanics Abstracts, Vol.34, No.8, pp.1165-1186.

Hoek, E., Carranza-Torres, C. and Corkum, B. (2002). *Hoek-Brown failure criterion*. Proc. NARMS-TAC Conference, Toronto, Vol.1, pp. 267-273.

Hoek, E., Carter, T.G. and Diederichs, M.S. (2013). *Quantification of the Geological Strength Index Chart*. 47th US Rock Mechanics /Geomechanics Symposium held in San Francisco, CA, USA.

Hoek, E., Kaiser, P.K. and Bawden, W.F. (1995). *Support of Underground Excavations in Hard Rock*. A.A. Balkema, Roterdam, Brookfield, pp. 27-47.

Hoek, E., Wood, D. and Shah, S. (1992). *A modified Hoek-Brown criterion for jointed rock masses*. Proc. rock characterization, symp. Int. Soc. Rock Mech.:Eurock '92, (J. Hudson ed.), pp. 209-213.

Hosseini, S. A. A., Mohammadnejad, M., Hoseini, S.M., Mikaeil, R. and Tolooiyan, A. (2012). *Numerical and analytical investigation of ground surface settlement due to subway excavation*. Geosciences, pp.185-191.

Hung, C. J., Monsees, J., Munfah, N. and Wisniewski, J. (2009). *Technical Manual for Design and Construction of Road Tunnels - Civil Elements*. U.S. Department of Transportation Federal Highway Administration.

Hunt, D.V.L. (2005). *Predicting the ground movements above twin tunnels constructed in London clay*. (Ph.D.), University of Birmingham. Retrieved from https://www.researchgate.net/publication/259745292.

IBM (2018). *IBM SPSS Statistics V24.0 documentation.* Retrieved from https://www.ibm.com/support/knowledgecenter/en/SSLVMB_24.0.0/statistics_mainhelp_ddita-gentopic3.html

Jaeger, C. (1979). *Rock mechanics and engineering* (2nd edition). Cambridge University Press, Cambridge, London.

Japan Highway Public Corporation. (1986). *Numerical Analysis and Construction Reference Analysis-Study Report Relating to Standard Design for Tunnels.*

Japan Road Association (JRA). (2002). *Design Specifications For Highway Bridges.*

Kapsampeli, A.S. and Sakellariou, M.G. (2012). *Use of artificial neural networks for the prediction of tunnelling induced ground movements in urban area*. In "Underground Space: Expanding the Frontiers", 11th ACUUS (Associated Research Centers for Urban Underground Space) conference, Athens

Karahanoğlu, N. (2018). *Yeraltısuyu Çekimi Sonucu Oluşan Yüzey Çökmesi Problemi; Bilimsel Araştırmaların Tarihsel Gelişimi*. Journal of Geological Engineering 42 77-106.

Karakus, M. and Fowell, R.J. (2000). *FEM analysis for the effects of the NATM construction technique on settlement above shallow soft ground tunnels*. In M. C. Ervin (Ed.), GeoEng2000. Melbourne, Australia.

Katzenbach, R. and Breth, H. (1981). *Nonlinear 3-D analysis for NATM in Frankfurt clay*. Paper presented at the Proceedings of the International Conference on Soil Mechanics and Foundation Engineering, 10th.

Kim, C.Y., Bae, G.J., Hong, S.W., Park, C.H., Moon, H.K. and Shin, H.S. (2001). *Neural network based prediction of ground surface settlements due to tunnelling*. Computers and Geotechnics 28, pp. 517–547.

Kim, C.Y., Kim, K.Y., Hong, S.W., Bae, G.J. and Shin, H.S. (2004). *Interpretation of Field Measurements and Numerical Analyses on Pipe Umbrella Method in Weak Ground Tunneling*. Proceedings of the 53rd Geomechanics Colloquium & EUROCK 2004. Copyright VGE, October 2004, Salzburg, Austria

Kim, C.Y., Koo, H.B. and Bae, G.J. (1996). *A Study on the Three Dimensional Finite Element Analysis and Field Measurements of the Tunnel Reinforced by Umbrella Arch Method*. Proc. of the Korea-Japan Joint Symposium on Rock Engineering. ISBN 89-950028-0-8, pp. 395–402.

Kimura, H., Itoh, T., Iwata, M., Fujimoto, K. (2005). *Application of new urban tunneling method in Baikoh tunnel excavation*. Tunn Undergr Sp Technol 20:151–158

Kirsch, G. (1989). *Die Theorie der Elastiziat and die Bedürfnisse der Festigkeitslehre.* Z. Vereines Deutscher Ing. 42, pp. 797-807.

Kitchah, F. and Benmebarek, S. (2016). *Finite difference analysis of an advance core pre-reinforcement system for Toulon's south tube*. Journal of Rock Mechanics and Geotechnical Engineering, 703-713.

Koukoutas, S. P. and Sofianos, A. I. (2015). *Settlements due to single and twin tube urban EPB shield tunnelling*. Geotech Geol Eng, pp.487–510.

Kumar, M. and Prasad, J. (2016). *Classification and selection methodology for temporary support systems for underground structure*. Recent Advances in Rock Engineering.

Kumar, M., Jain, P., Singh, L.G. and Naithani, A. K. (2014). *Rock support assessment for a unit-1 of underground strategic crude oil storage cavern project Padur, India*", In: Proceeding of National Seminar on Innovative Practices in Rock Mechanics, Bengaluru, pp. 94-102.

Kumar, N. (2002). *Rock Mass Characterization and Evaluation of Supports for Tunnels in Himalaya.* PhD thesis, WRDTC, IIT Roorkee, 289.

Lai, J., Qiu, J., Feng, Z., Chen, J. and Fan, H. (2016). *Prediction of soil deformation in tunnelling using artificial neural networks*. Hindawi Publishing Corporation Computational Intelligence and Neuroscience.

Lauffer, H. (1958). *Gebirgsklassifizierung für den Stollenbau*. Geol. Bauwesen, Vol. 24, pp. 46-51.

Leca, E. and Barry, N. (2007). *Settlements induced by tunneling in Soft Ground*. Tunn. and Undergr. Sp. Technology: 119–149

Lee, K. M. and Rowe, R. K. (1989). *Deformations caused by surface loading and tunnelling: the role of elastic anisotropy*. Géotechnique, 39: 125-140.

LEI-Kilany, M. E., EL-Sayed, T. A. and Mohab R. A. (2017). *Numerical analysis of tunnel boring machine in soft ground*. Jökull Journal, ISSN: 0449-0576, Vol 67, No.5.

Li, X.Q. and Zhu, C.-c. (2007). *Numerical analysis on the ground settlement induced by shield tunnel construction*. Journal of Highway and Transportation Research and Development (English Edition), 2(2), 73-79.

Liong, G.T. (2005). *Tunneling induced ground movement and soil structure interactions*. Seminar on Tunnel technology in civil engineering.

Loganathan, N. and Poulos, H. (1998). *Analytical prediction for tunneling-induced ground movements in clays*. Journal of Geotechnical and Geoenvironmental Engineering, 124(9), 846-856.

Lunardi, P. (2008). *Design and construction of tunnels*. Springer, Berlin Heidelberg

Mahmutoğlu, Y. (2010). *Surface subsidence induced by twin subway tunnelling in soft ground conditions in Istanbul*. Bull Eng Geol Environ 70, pp.115–131.

Mair, R. J. (1993). *Developments in geotechnical engineering research: application to tunnels and deep excavation*. Unwin Memorial Lecture, Proceedings of the ICE - Civil Engineering, 97, 27-41.

Mair, R. J. and Taylor, R. N. (1997). *Bored tunneling in the urban environment*. Proceedings of the 14th International Conference on Soil Mechanics and Foundation Engineering, Hamburg, pp. 2353–2385.

Mair, R.J. and Taylor, R.N. (1996). *Geotechnical aspect of design criteria for bored tunneling in soft ground*. UK: Taylor & Francis.

Mair, R.J., Taylor, R.N. and Bracegirdle, A. (1993). *Subsurface settlement profiles above tunnels in clay*. Geotechnique 43, 2, 315-320.

Marto, A., Abdullaha, M.H., Makhtarb, A.M., Sohaeia, H. and Tana, C. S. (2015). *Surface settlement induced by tunneling in greenfield condition through physical modelling*. JurnalTeknologi (Sciences & Engineering) 76:2, pp. 1–7.

Martos, F. (1958). *Concerning an approximate equation of the subsidence trough and its time factors*. In: International Strata Control Congress, Leipzig. Deutsche Akademie der Wissenschaftenzu Berlin, Section fur Bergbau. Berlin, pp. 191–205

Mazek, S.A. and Almannaei, H.A. (2013). *Finite element model of Cairo metro tunnel-Line 3 performance*. Ain Shams Engineering Journal, v4, 709–716.

Meissner, H. (1996). *Tunnelbau unter Tage - Empfehlungen des Arbeitskreises.* 1.6 Numerik in der Geotechnik. Geotechnik , 99-108.

Migliazza, M., Chiorboli, M. and Giani, G.P. (2009). *Comparison of analytical method, 3d finite element model with experimental subsidence measurements resulting from the extension of the Milan underground*. Computers and Geotechnics 36, pp. 113-124.

Miura, K. (2003). *Design and construction of mountain tunnels in Japan*. Tunneling and Underground Space Technology, 18 (2003): 115-126

Moayed, R.Z. and Izadi, E. (2011). *A numerical investigation on the top heading method and induced surface settlements*. IACMAG-Melbourne, Australia.

Moldovan, A. R. and Popa, A. (2012). *Finite element modelling for tunneling excavation*. Acta Technica Napocensis: Civil Engineering and Architecture, 55(1), 98-113.

Möller, S. (2006).*Tunnel induced settlements and structural forces in linings PhD thesis*. Stuttgart: Institute of Geotechnical Engineering, Univer-sitat of Stuttgart.

Ng, C.W.W. and Lee, G. T.K. (2005). *Three-dimensional ground settlements and stress transfer mechanisms due to open-face tunneling*. Can. Geotech. J. Vol. 42, pp. 1015-1029.

O'Reilly, M.P. and New, B.M. (1982). *Settlements above tunnels in the United Kingdom – their magnitude and prediction*. Proceedings of the International Conference Tunnelling '82Institution of Mining and Metallurgy, London pp. 55–64.

Ocak, I. (2008). *Control of surface settlements with umbrella arch methods in second stage excavations of Istanbul Metro*. TUST , 674-681.

Oke, J., Vlachopoulos, N. and Diederichs, M. S. (2012). *Sensitivity numerical analysis of orientations and sizes of forepoles for underground excavations in weak rock*. 46th US Rock Mechanics / Geomechanics Symposium held in Chicago.

Oke, J., Vlachopoulos, N. and Diederichs, M. S. (2016). *Semi-analytical model for umbrella arch systems employed in squeezing ground conditions*. Tunnelling and Underground Space Technology, 136–156.

Oke, J., Vlachopoulos, N. and Diederichs, M.S. (2012). *Determination of the mechanistic behaviour of a forepole support element when tunneling within weak rock masses*. ISRM International Symposium – EUROCK.

Oke, J., Vlachopoulos, N. and Diederichs, M.S. (2014). *Numerical analyses in the design of umbrella arch systems*. Journal of Rock Mechanics and Geotechnical Engineering, 546-564.

Oke, J., Vlachopoulos, N. and Marinos, V. (2014). *Umbrella arch nomenclature and selection methodology for temporary support systems for the design and*

construction of tunnels. Geotech Geol Eng 32:97–130 DOI 10.1007/s10706-013-9697-4

Oreste, P.P. and Peila, D. (1998). *A New Theory for Steel Pipe Umbrella Design in Tunneling*. World Tunnel Congress ’98, Sao Paulo, Brasilien, ISBN 905410936X, p 1033–1039.

Ortega-Guerrero, A., Rudolph, D. L. and Cherry, J. A. (1999). *Analysis of long-term land subsidence near Mexico City: Field investigations and predictive modeling*. Water Resour. Res., Vol. 35, No. 11, 3327-3341, DOI: 10.1029/1999WR900148.

Owen, D.R.J. and Hinton, E. (1980). *Finite Elements in plasticity- theory and practice*. Pineridge Press, Swansea.

Panthee, S., Singh, P.K., Kainthola, A. and Singh, T.N. (2016). *Control of rock joint parameters on deformation of tunnel opening.* Journal of Rock Mechanics and Geotechnical Engineering, 8(4):489-98.

Parikshit, M. (2016). *Three-dimensional simulation of tunnel excavation using 2D finite element software*. Recent Advances in Rock Engineering (RARE).

Park, K.H. (2004). *Elastic solution for tunneling-induced ground movements in clays*. International Journal of Geomechanics, pp. 310-318.

Parker, H.W. (1996). *Tunnel Engineering Handbook – Chapter 4: Geotechnical Investigations*. An International Thomson Publishing Company, New York, pp. 46-79.

Peck, R.B. (1969). *Deep excavations and tunnelling in soft ground*. In: Seventh international conference on soil mechanics and foundation engineering, state-of-the-art volume, Mexico, pp. 225–290

Pietruszczak, S. (2010). *Fundamentals of plasticity in geomechanics*. CRC Press.

Pinto F., Zymnis, D.M. and Whittle, A.J. (2014). *Ground movements due to shallow tunnels in soft ground: analytical interpretation and prediction*. Journal of Geotechnical and Geoenvironmental Engineering.

Poland, J. F. and Davis, G. H. (1969). *Land subsidence due to withdrawal of fluids*. Reviews in Engineering Geology, Vol. 2, pp. 187-270, DOI: 10.1130/REG2.

Potts, D. M. and Zdravkovic, L. (1999). *Finite element analysis in geotechnical engineering. Theory*. Imperial College of Science, Technology and Medicine.

Potts, D. M. and Zdravkovic, L. (2001). *Finite element analysis in geotechnical engineering. Application*. Imperial College of Science, Technology and Medicine: Thomas Telford Publishing.

Quiñones-Rozo, C. (2010). *Lugeon Test Interpretation*. Collaborative Management of Integrated Watersheds- 30th Annual USSD Conference, April-12-16, 2010: 405-414.

Rao, K.S. (2012). *Ground response and support measures for as railway tunnel in the Himalayas*. Workshop on emerging trends in geotechnical engineering (ETGE).

Rocscience (2007). *RocLab Program*. Rock Engineering Group, University of Toronto.

Rocscience (2012). *Phase^2 Program*. Rock Engineering Group, University of Toronto.

Rocscience (2018). Retrieved from https://www.rocscience.com/help/rs2/phase2_model/Initial_Element_Loading.htm

Rowe, R. K., Lo, K. Y., and Kack, G. J. (1983). *A method of estimating surface settlement above tunnels constructed in soft ground*. Canadian Geotechnical Journal, 20(1), 11-22.

Rusnak, J. A. and Mark, C. (1999). *Using the point load test to determine the uniaxial compressive strength of coal measure rock*. Proceedings of 19th international conference on ground control in mining, 362-371.

Sadaghiani, M. and Dadizadeh, S. (2010). *Study on the effect of a new construction method for a large span metro underground station in Tabriz-Iran*. Tunn Undergr Sp Technol 25:63–69

Sagaseta, C. (1987). *Analysis of undrained soil deformation due to ground loss*. Géotechnique, 37(3), 301-320.

Serafim, S.,J. and Pereria, J. (1983). *Considerations of the Geomechanics classification of Bieniawski*. Proc Int. Symp. on eng. geol. and Undergroung Constr., LNEC, Lisbon, Portugal, vol. 1, 33-42

Shabna, P.S. and Dr. Sankar, N. (2016). *Numerical analysis of shallow tunnels in soft ground using plaxis2d*. International Journal of Scientific & Engineering Research, Volume 7, Issue 4, 161 ISSN 2229-5518.

Sheory, P. R. (1994*). A theory for in situ stresses in isotropic and transversely isotropic rock*. Int. Jrn. Rock Mech. Min. Sci. and Geomech. Abstr. 31(1), pp. 23-34.

Shi, X. Q., Xue, Y. Q. Ye, S. J., Wu, J. C., Zhang, Y. and Yu, J. (2007). *Characterization of land subsidence induced by groundwater withdrawals in Su-Xi-Chang area, China*. Environ. Geol., Vol. 52, pp. 27-40, DOI: 10.1007/s00254-006-0446-3.

Singh, B. and Goel, R. K. (1999). *Rock Mass Classification - A Practical Approach in Civil Engineering*. Elsevier Science Ltd., U.K., 268.

Singh, B. and Goel, R.K. (2006). *Tunneling in weak rocks*. Elsevier Geo-Engineering book series, Volume 5.

Song, K., Cho, G., Sim, Y., Lee, I. (2006). *Optimization of a pre-improvement support system for large underground excavation*. Tunn Undergr Sp Technol 21:374

Sugiyama, T., Hagiwara, T., Nomoto, T., Nomoto, M., Ano, Y., Mair, R.J., Bolton, M. D. and Soga, K. (1999). *Observations of ground movements during tunnel construction by slurry shield method at the Docklands light railway Lewisham extension-east London*. In: Soil and foundations Vol. 39, No.3, pp. 99-112.

Swoboda, G. (1979). *Finite element analysis of the New Austrian Tunnelling Method (NATM)*. In: Proceedings of the 3rd International Conference on Numerical Methods in Geomechanics, Aachen, 2: 581–586.

Swoboda, G., Marence, M. and Mader, I. (1994). *Finite element modelling of tunnel excavation*. International Journal of Engineering Modelling 6: 51–63.

Talebinejad, A., Chakeri, H., Moosavi, M., Özçelik, Y., Ünver, B. and Hindistan, M.A. (2013). *Investigation of surface and subsurface displacements due to multiple tunnels excavation in urban area*. Arab J Geosci, pp.3913–3923.

Terzaghi, K. (1946). *Rock Tunneling with Steel Supports.* R.V. Practor and T. White (ed), Commercial Sheving Co., Youngstown, Ohio. 296 p.

Topsakal, E. (2012). *An investigation of landslide at km: 12+200 of Artvin-Savsat junction-meydancik provincial road*. (M.Sc.), Middle East Technical University.

Trinh, Q.N., Broch, E. and Lu, M. (2007). *Three dimensional modelling of spiling bolts for tunnelling at weakness zones*. In: Eberhardt E, Stead D, Morrison T (eds) Rock mechanics: meeting society's challenges and demands. Taylor and Francis, London, pp 427–432

Trinh, Q.N., Broch, E. and Lu, M. (2010). *2D versus 3D modelling for tunneling at a weakness zone*. Rock Engineering in Difficult Ground Conditions – Soft Rocks and Karst – Vrkljan (ed), Taylor & Francis Group, London, ISBN 978-0-415-80481-3.

Tuncdemir, H., Aksoy, C.O., Guclu, E. and Ozer, S.C. (2012). *Umbrella arch and forepoling support methods: a comparison.* EUROCK, Stockholm, pp 515–527.

Türkoğlu, M. (2013). *Two-dimensional numerical analysis of tunnel collapse driven in poor ground conditions*. (M.Sc.), Middle East Technical University.

USBR. (2001). *Engineering geology field manual*. U.S. department of the interior Bureau of reclamation. Chapter 17 Water Testing and Permeability, Vol2 (2), pp. 107-182.

Vafaeian, M., and Mirmirani, S. (2003). *Applicability of elastic analysis for predicting the settlement distribution around tunneling in soft ground* (technical note). IJE Transactıons B: Applications, 16(3), 217-234.

Verruijt, A. (1998). *Deformations of an elastic half plane with a circular cavity*. In: J. Solids Structures Vol 35. No. 21. pp 2795-2804.

Verruijt, A., and Booker, J. (1996). *Surface settlements due to deformation of a tunnel in an elastic half plane*. Géotechnique, 46(4), 753-756.

Vitali, O.P.M., Celestino, T.B. and Bobet, A. (2017). *3D finite element modelling optimization for deep tunnels with material nonlinearity*. Underground Space 3, 125–139.

Vlachopoulos, N. and Diederichs, M.S. (2009). *Improved longitudinal displacement profiles for convergence confinement analysis of deep tunnels*. Journal of rock mechanics and rock engineering, vol 42, pp 131–146.

Vlachopoulos, N. and Diederichs, M.S. (2014). *Appropriate uses and practical limitations of 2D numerical analysis of tunnels and tunnel support response*. Geotechnical and Geological Engineering, 32(2):469-88.

Volkmann, G. and Schubert, W. (2006). *Contribution to the Design of Tunnels with Pipe Roof Support*. In Proc. of 4th Asian Rock Mechanics Symposium, ISRM International Symposium.

Volkmann, G. M. and Schubert, W. (2011). *Advantages and Specifications for Pipe Umbrella Support Systems*. 14th Australasian Tunneling Conference, Auckland, New Zealand.

Volkmann, G.M. and Schubert, W. (2007). *Geotechnical model for pipe roof supports in tunneling*. Underground Space – the 4th Dimension of Metropolises – Barták, Hrdina, Romancov & Zlámal (eds). Taylor & Francis Group, London, ISBN 978-0-415-40807-3.

Wang, J.G., Kong, S.L. and Leung, C.F. (2003). *Twin tunnels-induced ground settlement in soft soils*. Proceedings of the sino-japanese symposium on geotechnical engineering Beijing, china, Geotechnical engineering in urban construction, pp. 241-244.

Wang, Z., Wong, R.C.K. and Qiao, L. (2012). *Finite element analysis of long-term surface settlement above a shallow tunnel in soft ground*. Tunnelling and Underground Space Technology, pp. 85–92.

Warner, J. (2004). *Practical handbook of grouting: Soil, Rock & Structures*. John Wiley & Sons, lnc, New Jersey, pp. 720.

Whittle, A.J., Hsieh, Y.M., Pinto, F. and Chatzigiannelis, Y. (2003). *Numerical and analytical modeling of ground deformations due to shallow tunneling in soft soils*. Massachusetts Institute of Technology, Department of Civil & Environmental Engineering, Cambridge.

Wickham, G.E., Tiedeman, H.R. and Skinner, E.H. (1972). *Ground Support Prediction Model (RSR Concept)*. Proc., 1st Rapid Excavation and Tunneling Conference, American Institute of Mining Engineers, New York, pp. 43-64.

Wu, D.R. and Lee, C.J. (2003). *Ground movements and collapse mechanisms induced by tunneling in clayey soil*. International journal of physical modelling in geotechnics 4, pp. 15-29.

Yahya, S.M. and Abdullah, R. A. (2014). *A review on methods of predicting tunneling induced ground settlements*. Ejge, Vol. 19, pp. 5813-5826.

Yang, F., Zhang J., Yang, J., Zhao, L. and Zheng, X. (2015).*Stability analysis of unlined elliptical tunnel using finite element upper-bound method with rigid translator moving elements.* Tunnelling and Underground Space Technology, 50:13-22.

Yasitli, N.E. (2012). *Numerical modeling of surface settlements at the transition zone excavated by New Austrian Tunneling Method and Umbrella Arch Method in weak rock.* Arab J Geosci, pp. 2699–2708.

Yoo, C. (2005). *Interaction between tunneling and groundwater-numerical investigation using three dimensional stress–pore pressure coupled analysis*. Journal of Geotechnical and Geoenvironmental Engineering, ASCE, 131 (2), pp. 240-250.

Yoo, C. and Kim, S.B. (2006). *Stability analysis of an urban tunneling in difficult ground condition.* Tunnelling and Underground Space Technology, 21 (3–4) , pp. 351-352.

Zhang, Z.X., Liu C., Huang, X., Kwok, C.Y. and Teng, L. (2016). *Three-dimensional finite-element analysis on ground responses during twin-tunnel construction using the URUP method*. Tunnelling and Underground Space Technology. 58:133-46.

Zhao, Y. and Qi, T. (2014). *Tunneling-induced settlement evaluation for underneath existing tunnel*. Tunneling and Underground Construction.

Zong, W. (2014). *The ınfluence of underpass on surface subsidence caused by double-tube shield tunneling*. Advanced Materials Research, Vols. 915-916, pp 108-113.

APPENDIX A

GEOLOGICAL-GEOTECHNICAL GROUND PROFILE

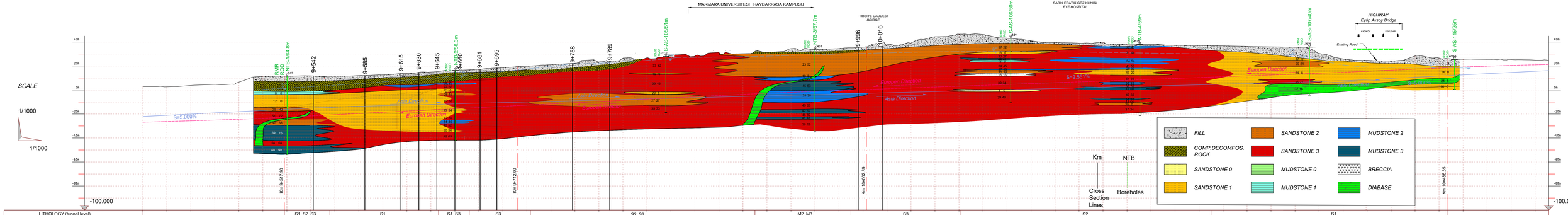
MARMARA UNIVERSITESI HAYDARPASA KAMPUSU
TIBBIYE CADDESI BRIDGE
SADIK ERATIK GOZ KLINIGI EYE HOSPITAL
HIGHWAY Eyup Aksoy Bridge
Existing Road
SCALE
1/1000
1/1000
S=5.000%
S=2.551%
Axis Direction
European Direction
Km 9+517.90
Km 9+712.00
Km 10+002.69
Km 10+486.65
-100.000
Km
Cross Section Lines
NTB
Boreholes
FILL
COMP.DECOMPOS. ROCK
SANDSTONE 0
SANDSTONE 1
SANDSTONE 2
SANDSTONE 3
MUDSTONE 0
MUDSTONE 1
MUDSTONE 2
MUDSTONE 3
BRECCIA
DIABASE
LITHOLOGY (tunnel level)
S1, S2, S3
S1
S1, S3
S3
S2, S3
M2, M3
S3
S2
S1
PARAMETERS
FILL
ROCK
DECOMPOSED ROCK (CDR)
ROCK (S, M)
NO FILL
NO CDR
EXCAVATION + SUPPORT TYPES
ST-UA 2
ST-3
ST-UA 1, ST-2, ST-3
ST-3
ST-2
ST-3, ST-UA 1

APPENDIX B

BOREHOLE LOGS

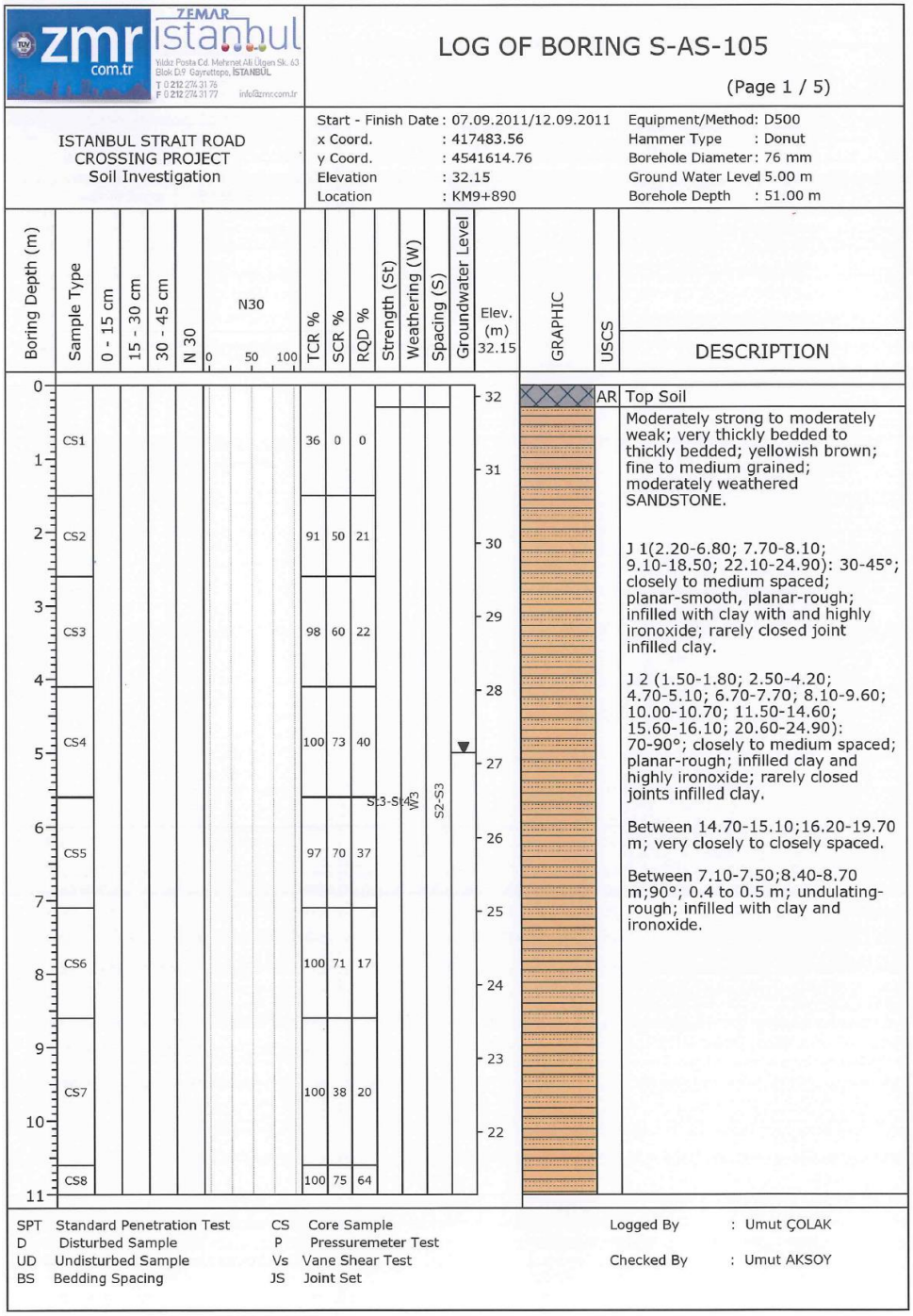

Figure B.1. Borehole No.S-AS-105 (Page 1/5)

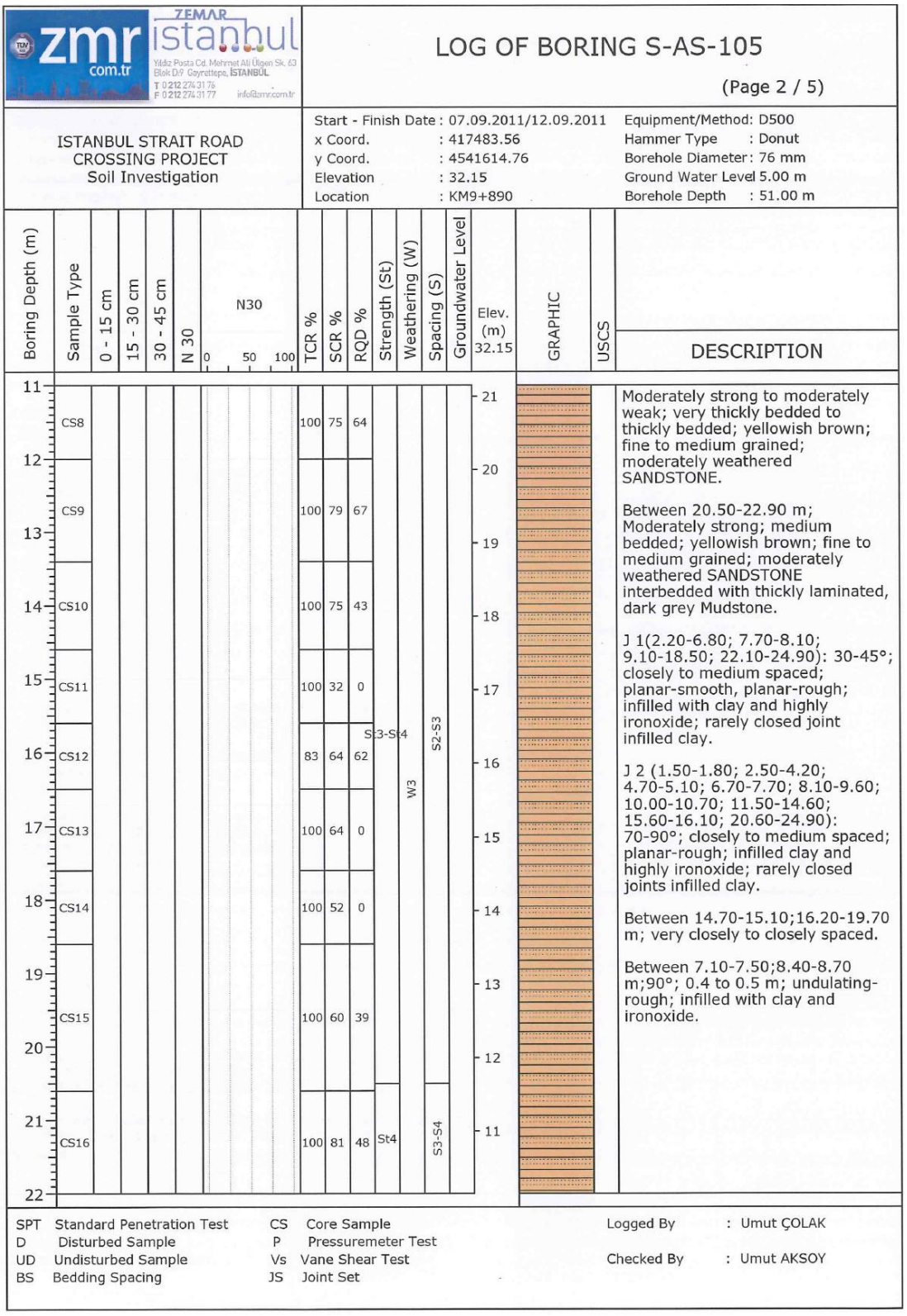

Figure B.2. Borehole No.S-AS-105 (Page 2/5)

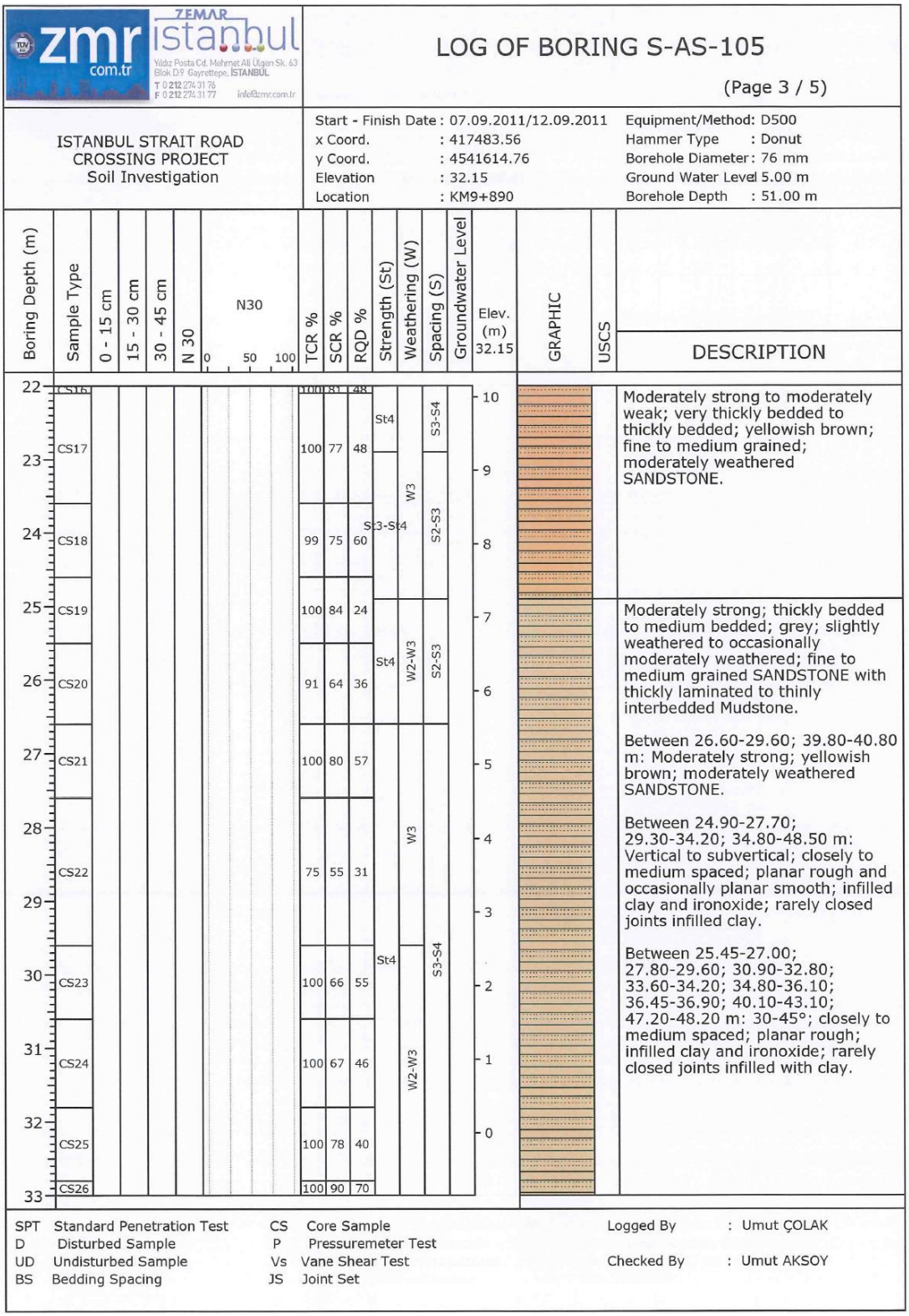

Figure B.3. Borehole No.S-AS-105 (Page 3/5)

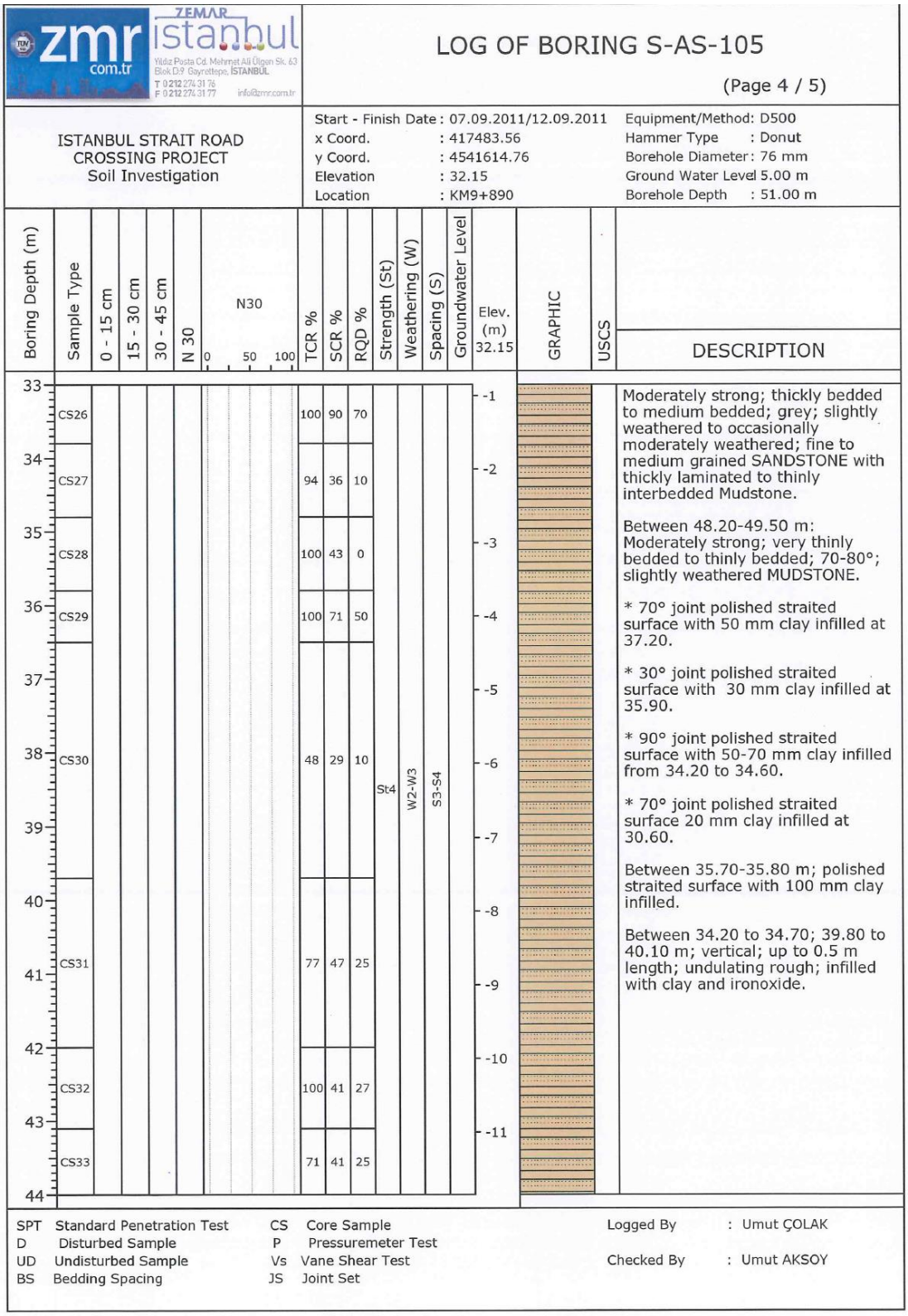

Figure B.4. Borehole No.S-AS-105 (Page 4/5)

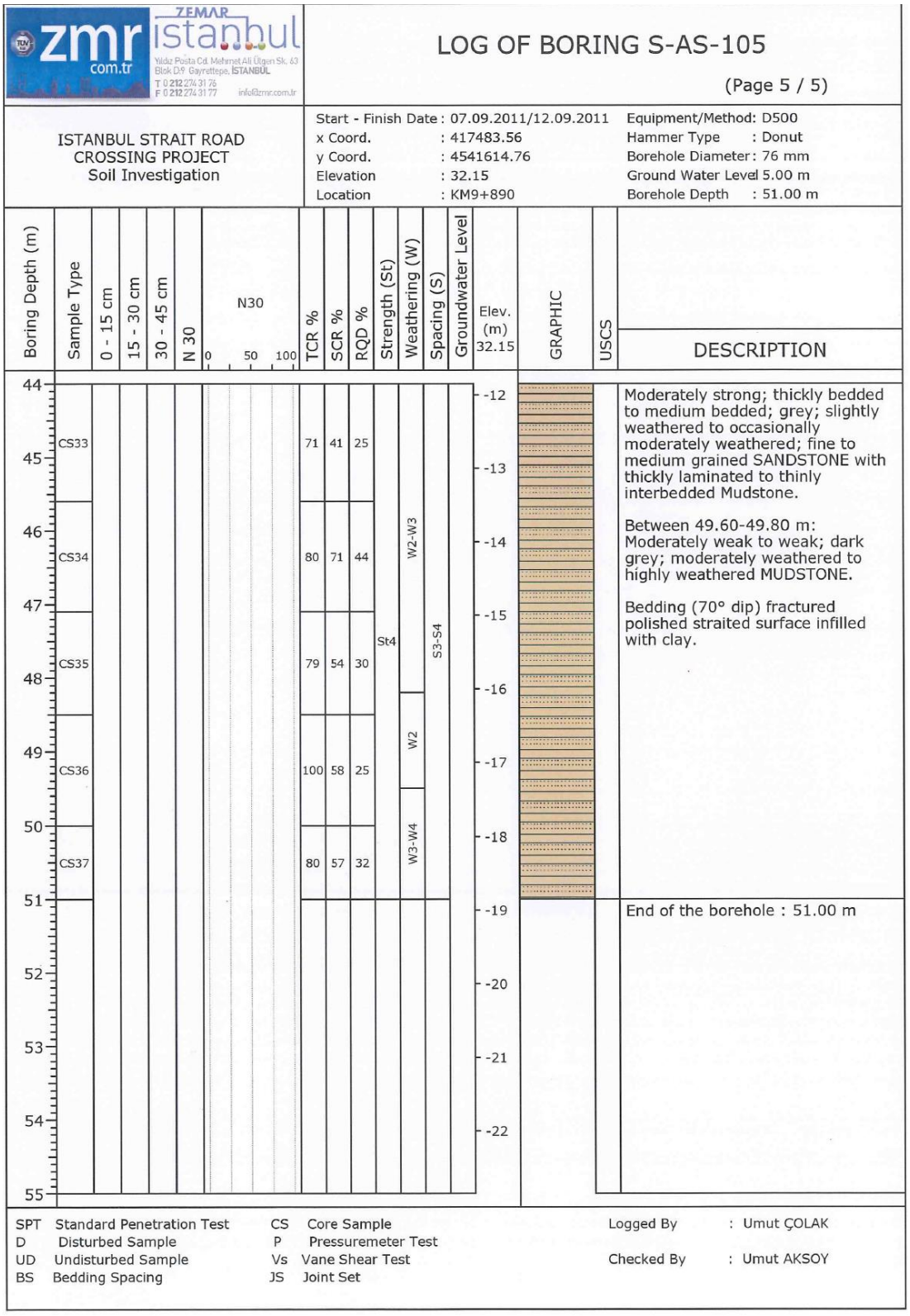

Figure B.5. Borehole No.S-AS-105 (Page 5/5)

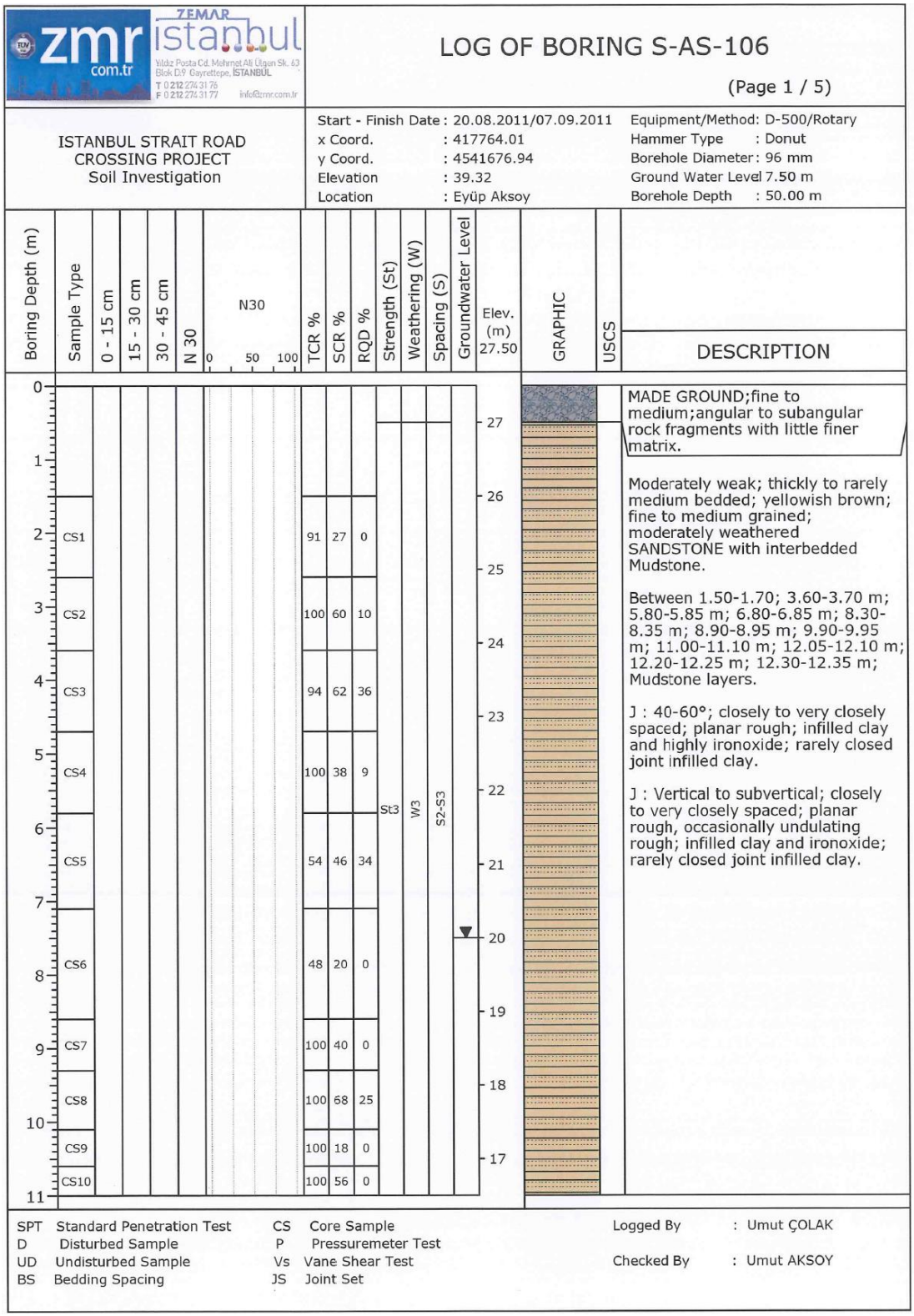

Figure B.6. Borehole No.S-AS-106 (Page 1/5)

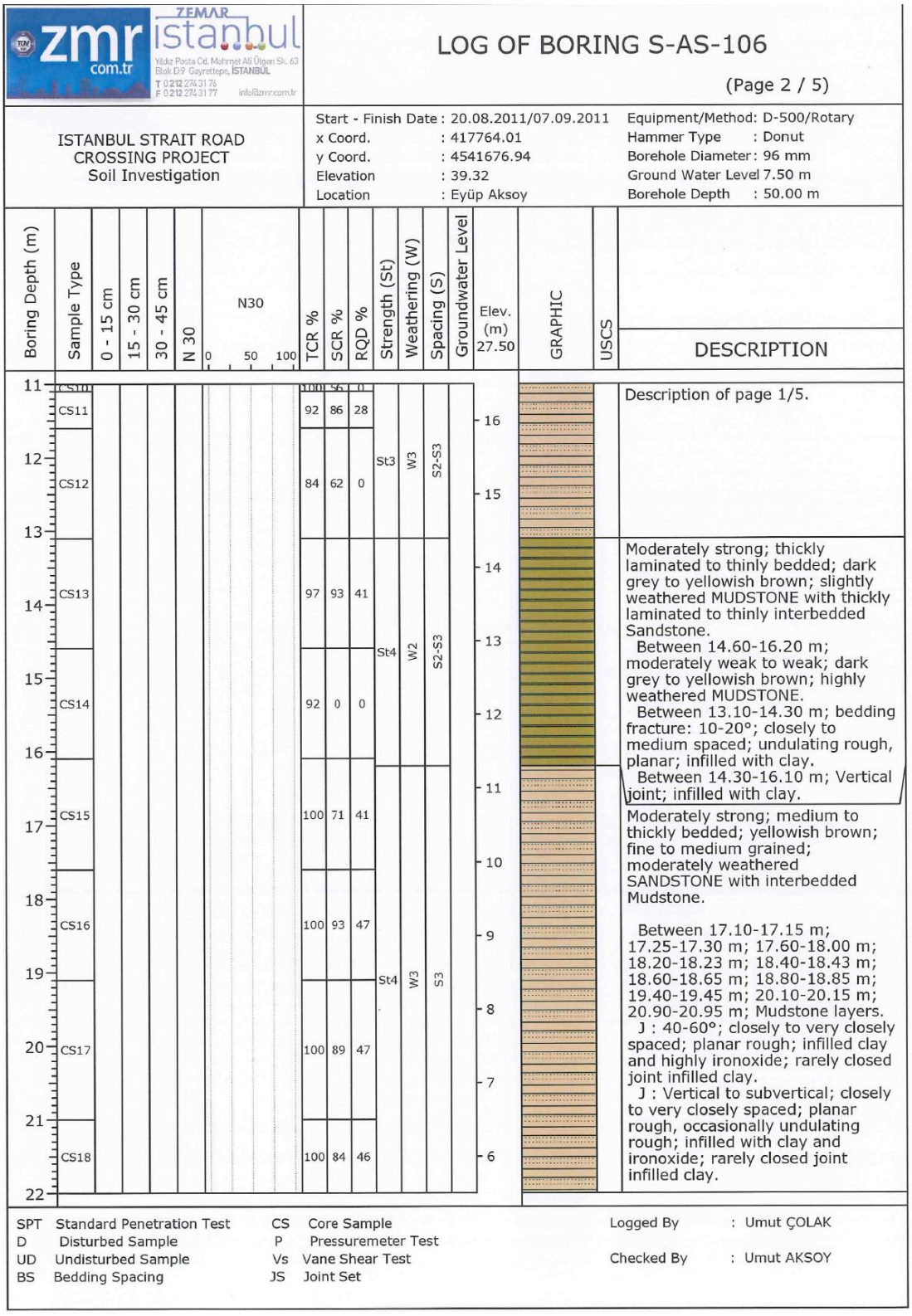

Figure B.7. Borehole No.S-AS-106 (Page 2/5)

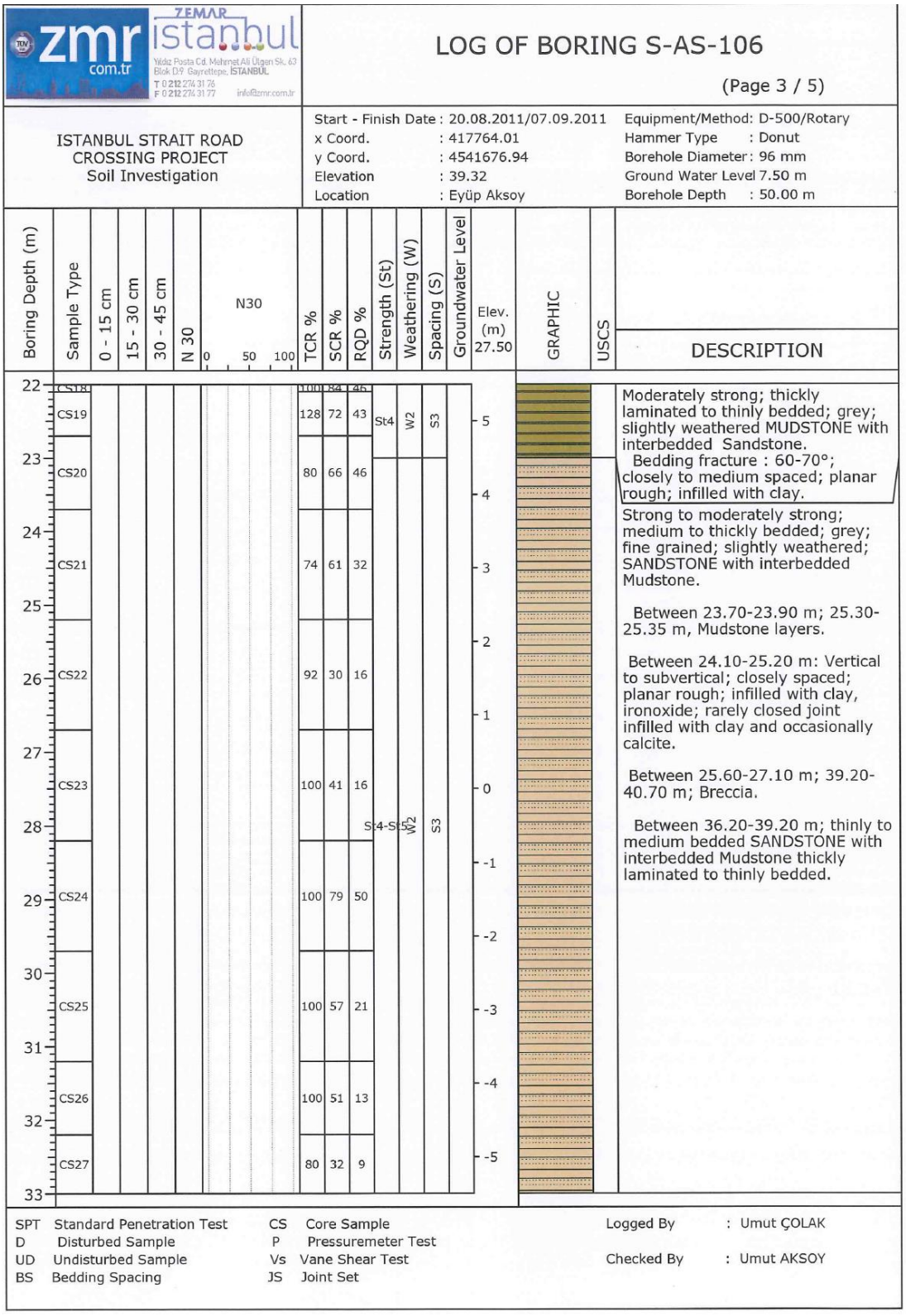

Figure B.8. Borehole No.S-AS-106 (Page 3/5)

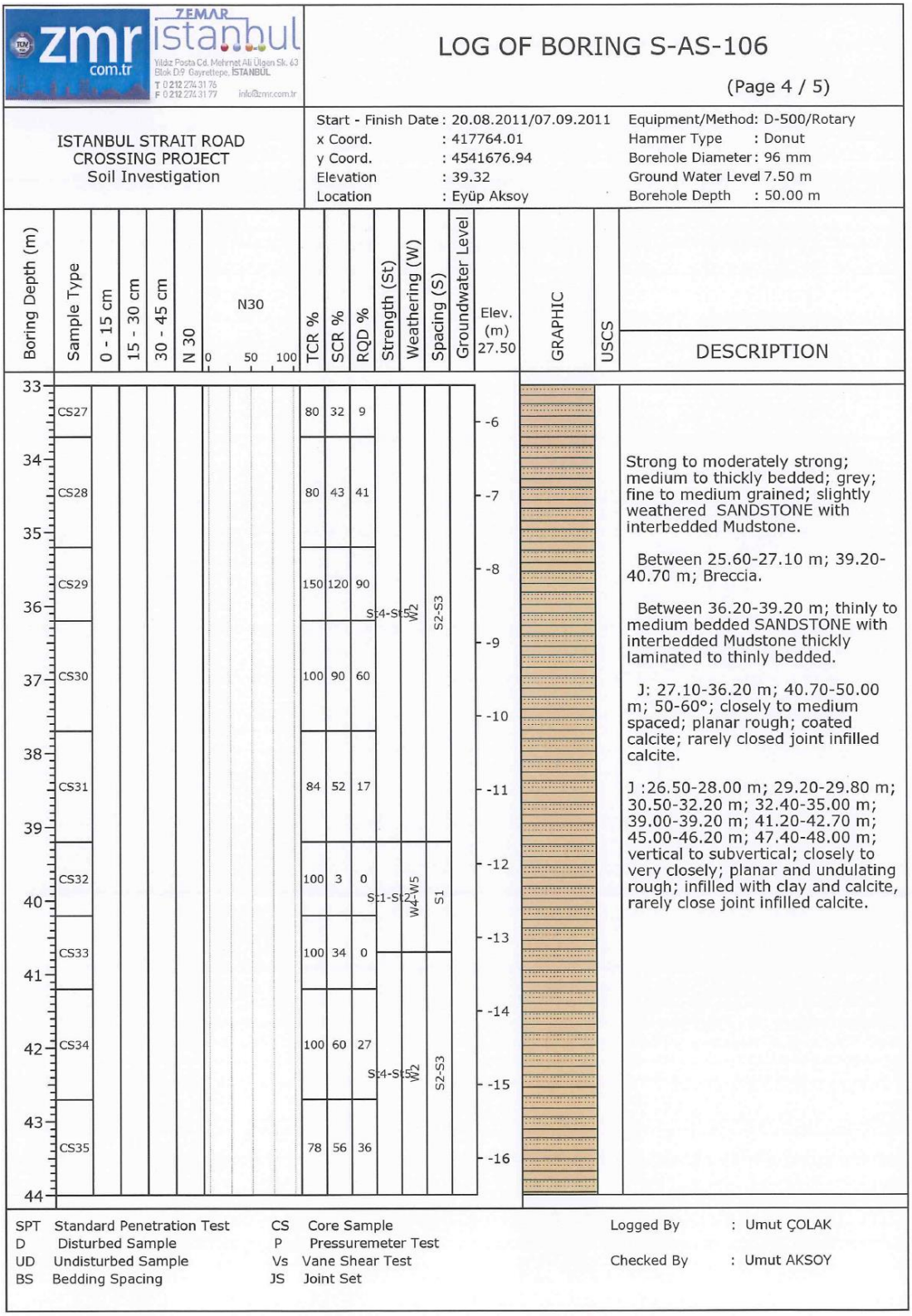

Figure B.9. Borehole No.S-AS-106 (Page 4/5)

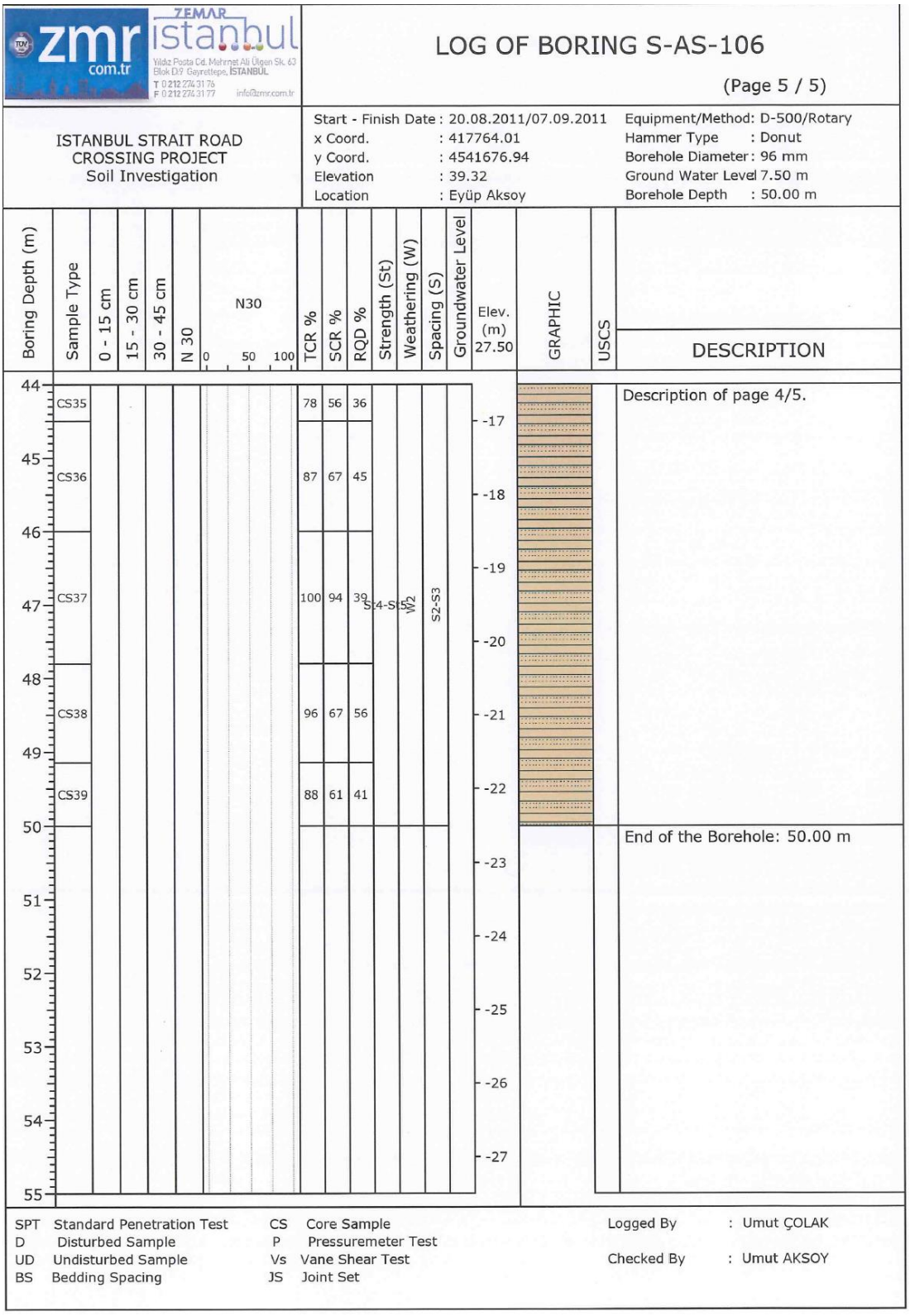

Figure B.10. Borehole No.S-AS-106 (Page 5/5)

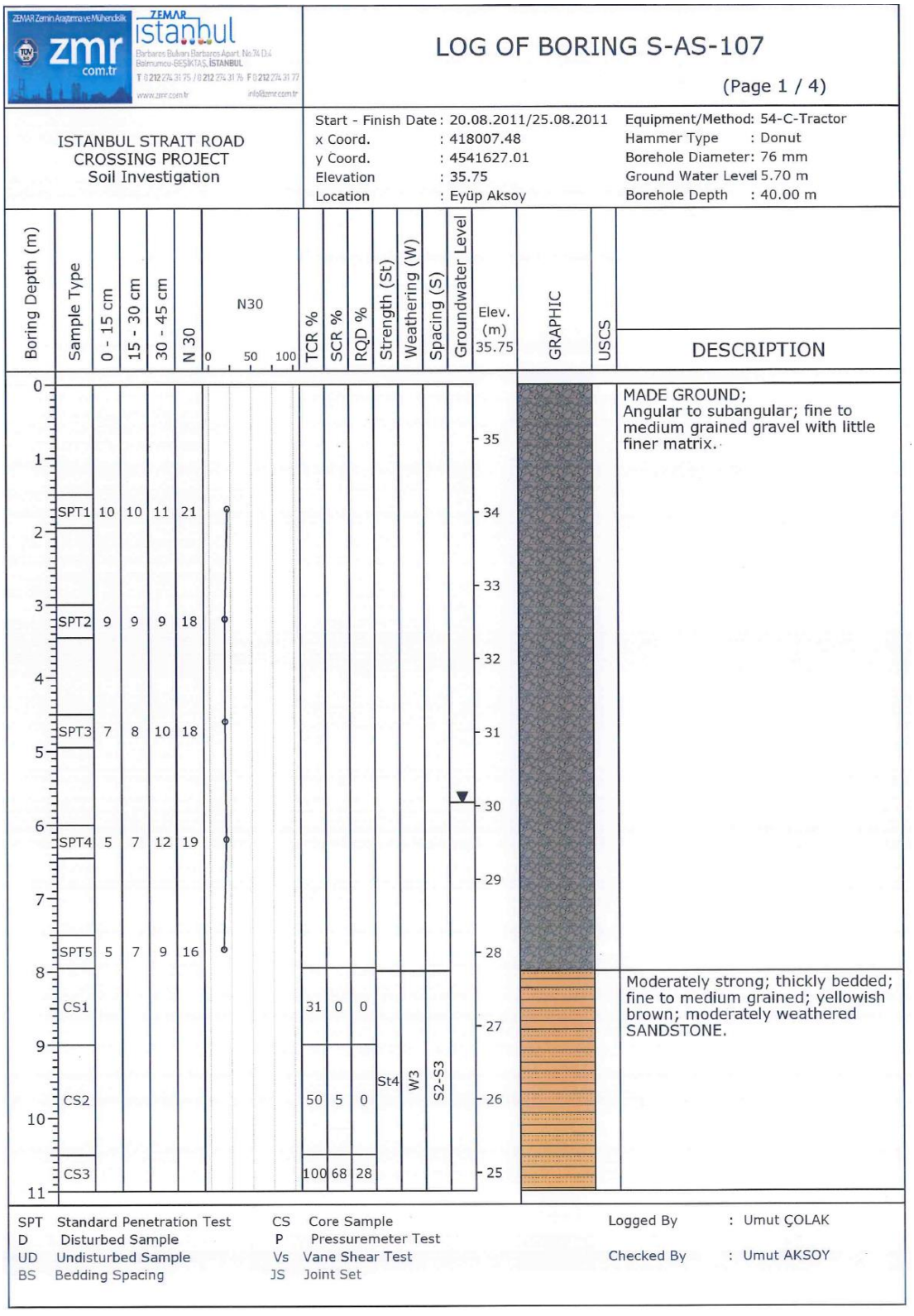

Figure B.11. Borehole No.S-AS-107 (Page 1/4)

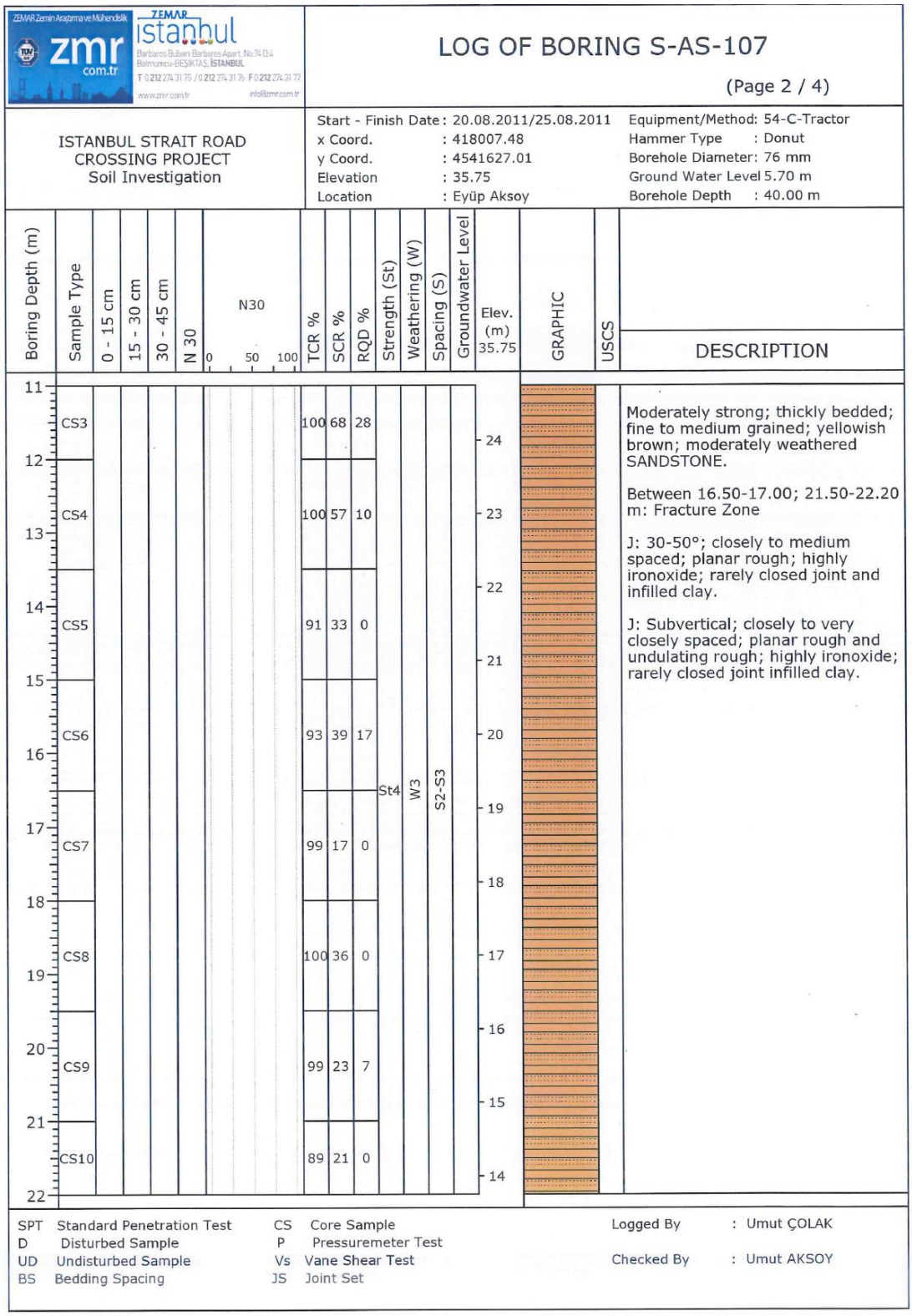

Figure B.12. Borehole No.S-AS-107 (Page 2/4)

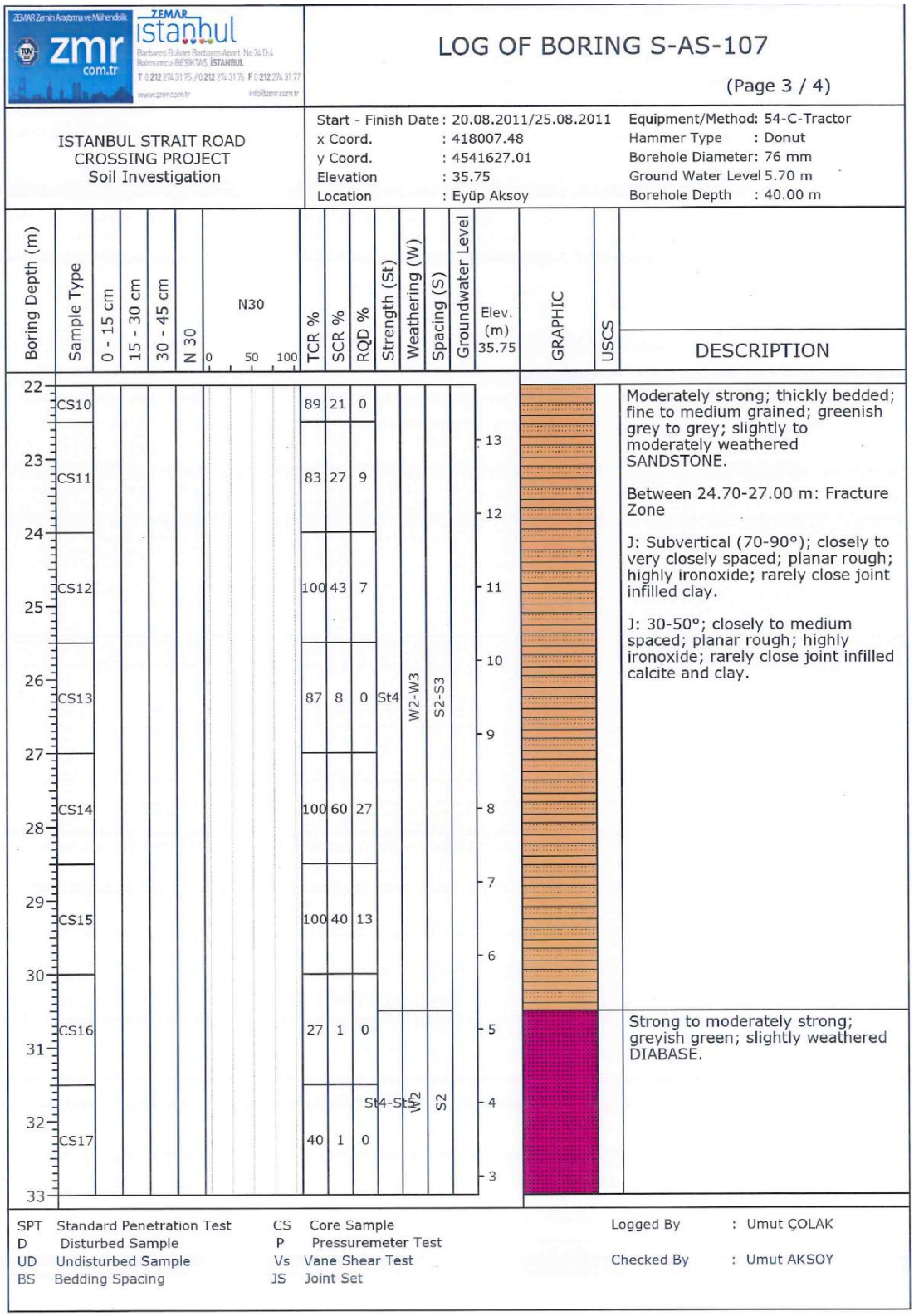

Figure B.13. Borehole No.S-AS-107 (Page 3/4)

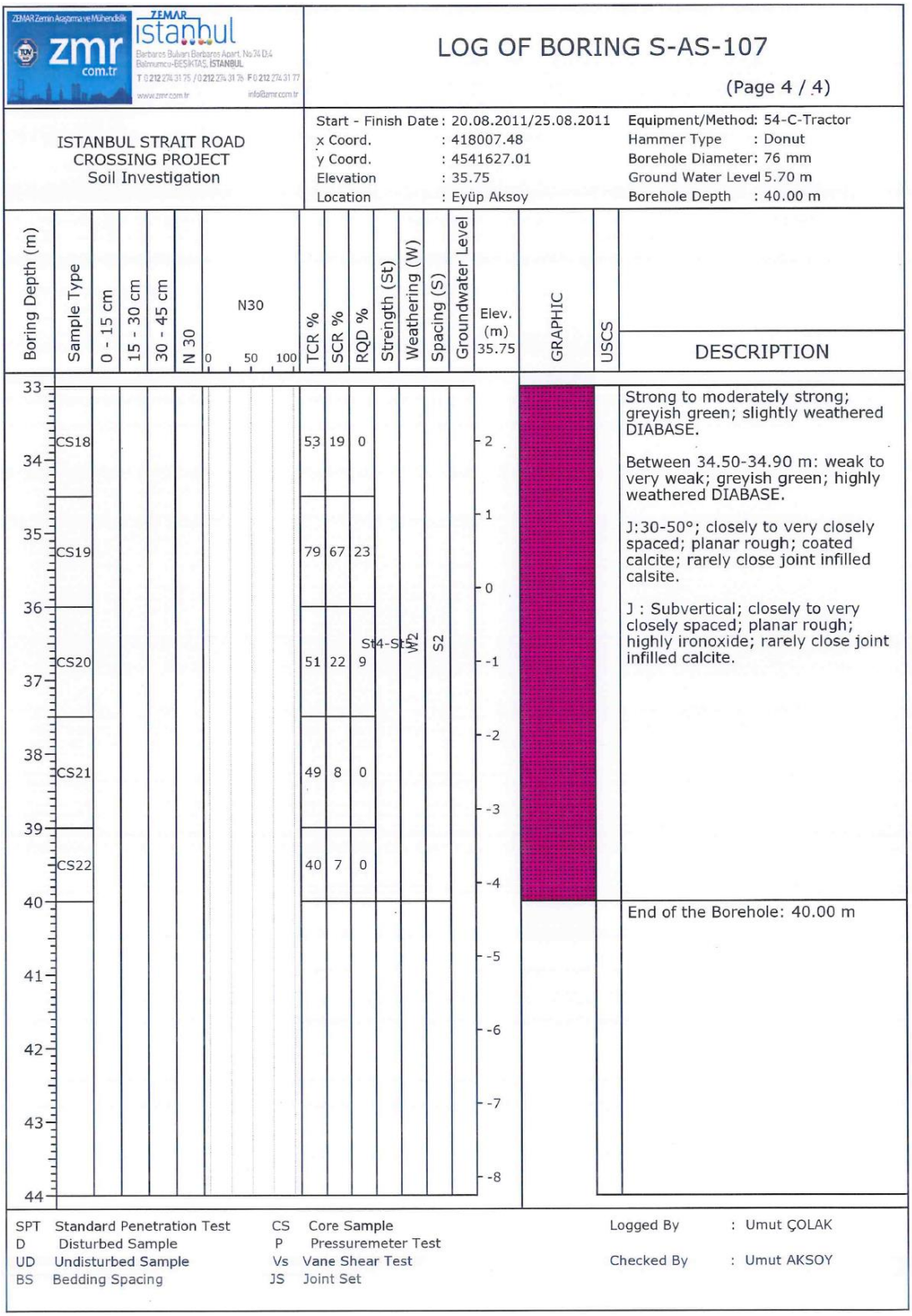

Figure B.14. Borehole No.S-AS-107 (Page 4/4)

temel investigation inc.

ISTANBUL STRAIT ROAD TUNNEL CROSSING PROJECT
GEOTECHNICAL INVESTIGATIONS

Sheet 1 of 4

LOCATION : HAREM PARK	BOREHOLE NO : NTB-01
EQUIPMENT : DIAMEC	GROUND LEVEL : 0.00 m. C.D.
BORING METHOD : Rotary Drilling from 0.00 to 12.35m. Rotary Core Drilling from 12.35 to 64.80m.	COORDS. : N : E :
BOREHOLE DIAMETER : from 0.00 to 24.00m - 114mm.	STARTED ON : 02.02.2010 FINISHED ON : 19.02.2010

SAMPLES AND IN SITU TESTS		S.P.T. blows in cm			Casing Depth (m) Date	Water Depth (m)	TCR %	RQD %	SCR %	Depth (m)	DESCRIPTION OF STRATA	C.D. (m)	LEGEND
DEPTH (M)	TYPE	15	15	15									
					02.02.20					0.50	Cobblestone with Lean Concrete.	-0.50	
1.50	D1	14	16	18							MADE GROUND Recovered as; Gravel with Sand and Cobbles, locally clay.		
1.95			N =	34									
3.00	D2	10	14	30	3.00	2.00							
3.45			N =	44	04.02.10	2.20				4.00		-4.00	
4.50	D3	15	37	50/5									
4.85													
6.00	D4	10	12	22									
6.45			N =	34									
7.50	D5	7	12	18							Very weak, highly crushed, dark grey, highly weathered SANDSTONE. Recovered as; Clayey Gravel(GC)-Aproximately 60-65 % subangular,fine gravel of sandstone orgin; 15-20 % fines with no plasticity, none dry strength,rapid dilatancy; 5-10 % fine sand; dark grey, wet.		
7.95			N =	30									
9.00	D6	16	29	41									
9.45			N =	70		G W L							
9.70	W1					9.70							
10.50	D7	25	42	50/5									
10.85													
12.00	D8	25	43	50/5									
12.40	12.35									12.35		-12.35	
12.90							80	0	0		Very weak, crushed, grey and dark grey, highly weathered MUDSTONE. Belween 12.35-13.65m and 14.05-14.85m Highly weathered. Recovered as; fine to medium gravel sized mudstone fragments and clay. (Crushed Zone)		
13.40							80	0	0				
13.90							85	0	10				
14.40							90	0	18				
14.85					12.00	2.40	60	0	0	14.85		-14.85	
14.90					06.02.10	2.50	40	0	0				
15.00							35	0	0				
15.50							30	0	0				
15.80							35	0	0		Weak, crushed, grey and dark grey, highly weathered, fine to medium grained SANDSTONE.		
16.20							45	0	0				
16.70							40	0	0		Closely, very closely spacing, smooth and rough stepped, open and close discontilies calcite coated.		
17.20							35	0	10				
17.70							50	0	20		Between 15.00-17.45m, 17.70-18.00, 19.20-21.30m, 22.30-24.80m, 25.30-26.70m		
18.10							40	0	0				
18.50							60	0	34		26.90-27.60m and 28.30-28.55m; recovered as highly fruclered and fine to coarse angular gravel and cobble sized fragments.		
19.00							65	0	14				
19.50							30	0	0		(Crushed Zone)		
19.80							40	0	0				

REMARKS :

OPERATOR : Y.YAZGU LOGGED BY : S.DEMIRBAS

Figure B.15. Borehole No.NTB-01 (Page 1/4)

temel investigation inc.

ISTANBUL STRAIT ROAD TUNNEL CROSSING PROJECT
GEOTECHNICAL INVESTIGATIONS

Sheet 2 of 4

LOCATION : HAREM PARK	BOREHOLE NO : NTB-01
EQUIPMENT : DIAMEC	GROUND LEVEL : 0.00 m. C.D.
BORING METHOD : Rotary Core Drilling from 12.35 to 64.80m.	COORDS. : N : E :
BOREHOLE DIAMETER : from 0.00 to 24.00m - 114mm.from 39.10 to 64.80m - 86mm from 24.00 to 39.10m - 98mm.	STARTED ON : 02.02.2010 FINISHED ON : 19.02.2010

SAMPLES AND IN SITU TESTS		S.P.T. blows in cm			Casing Depth (m) Date	Water Depth (m)	TCR %	RQD %	SCR %	Depth (m)	DESCRIPTION OF STRATA	C.D. (m)	LEGEND
DEPTH (M)	TYPE	15	15	15									
20.30					06.02.10		40	0	0				
20.80							35	0	0				
21.30							40	0	12				
21.80							55	0	0		Weak, crushed, grey and dark grey, highly weathered, fine to medium grained SANDSTONE.		
22.30							80	0	16		Closely, very closely spacing, smooth and rough stepped, open and close discontilies calcite coated.		
22.80							65	0	10		Between 15.00-17.45m, 17.70-18.00, 19.20-21.30m, 22.30-24.80m, 25.30-26.70m		
23.30							60	0	0		26.90-27.60m and 28.30-28.55m; recovered as highly fructered and fine to coarse angular gravel and cobble sized fragments.		
23.90							80	0	0		(Crushed Zone)		
24.40							65	0	16				
24.80							90	0	15				
25.30							95	0	16				
26.00							85	0	19				
26.20							95	0	30				
26.70							75	0	0	26.70		-26.70	
27.20							85	30	42		Moderately strong, light grey to dark gray, moderately weathered SANDSTONE. Closely spaced, sub horizontal, open, stepped rough discontinuities calcite coated.		
27.60					25.50	5.50	50	50	50				
28.30					09.02.10	5.30	90	46	57		28.55-28.70m: Moderately weak,crushed,light greenish grey, moderately weathered DIABASE. Few vertical, tight upto 1cm thick calcite vains.		
28.70							85	0	0	28.70	Between 26.90-27.10m, 28.30-28.70m:Recovered as fine to medium gravel sized angular fragments.	-28.70	
30.00							95	66	71		Strong to very strong, grey and dark grey, slightly weathered fine grained SANDSTONE.		
30.50							95	40	56		Thinly interbeded with dark grey Mudstone.		
31.20							90	41	41		Closely and very closely spacing, smooth stepped and smooth planar, open and close discontinuties with coated calsit.		
31.90							90	46	53		Joint set 1 ; Vertical, subvertical, closely and very closely, open and close, infilled with calsit.		
32.65					30.00	5.00	95	64	83		Joint set 2 ; Horizontal,subhorizotal, closely and very closely,open and close, infilled with calsit.		
32.70					10.02.10	4.00							
33.00							95	31	70				
33.70							95	95	95	34.05		-34.05	
34.10							95	60	63		Strong to very strong, grey, slightly weathered DIABASE. Closely and very closely spacing, smooth stepped, open and close with coated calsit. Subvertical and vertical,closely and very closely spacing, open and close joints, infilled with calsit.		
35.30							85	47	59	35.55		-35.55	
36.00							95	29	50		Strong to very strong, grey, slightly weathered fine to course grained SANDSTONE. Closely and very closely spacing, smooth and rough stepped, open and close discontities with coated calsit.		
36.90							90	0	20				
37.30					34.50	4.80	90	0	37		Vertical, subvertical, closely and very closely spacing, open and close joints infilled with casil.		
37.50					12.02.10	4.60							
37.90							95	38	53		Between 35.55-35.75m Highly weathered; Recovered as; fine to coarse gravel sized sandstone fragments, sand and clay.		
38.50							95	0	48				
39.00							80	58	58		Between 36.60-37.20m; Highly fructures; Recovered as; fine to course gravel sized sandstone fragments.		
39.40							90	0	13				
39.80							90	20	44				

REMARKS : P.T.1 was made at 38.50 m.

OPERATOR : Y.YAZGU LOGGED BY : S.DEMIRBAS

Figure B.16. Borehole No.NTB-01 (Page 2/4)

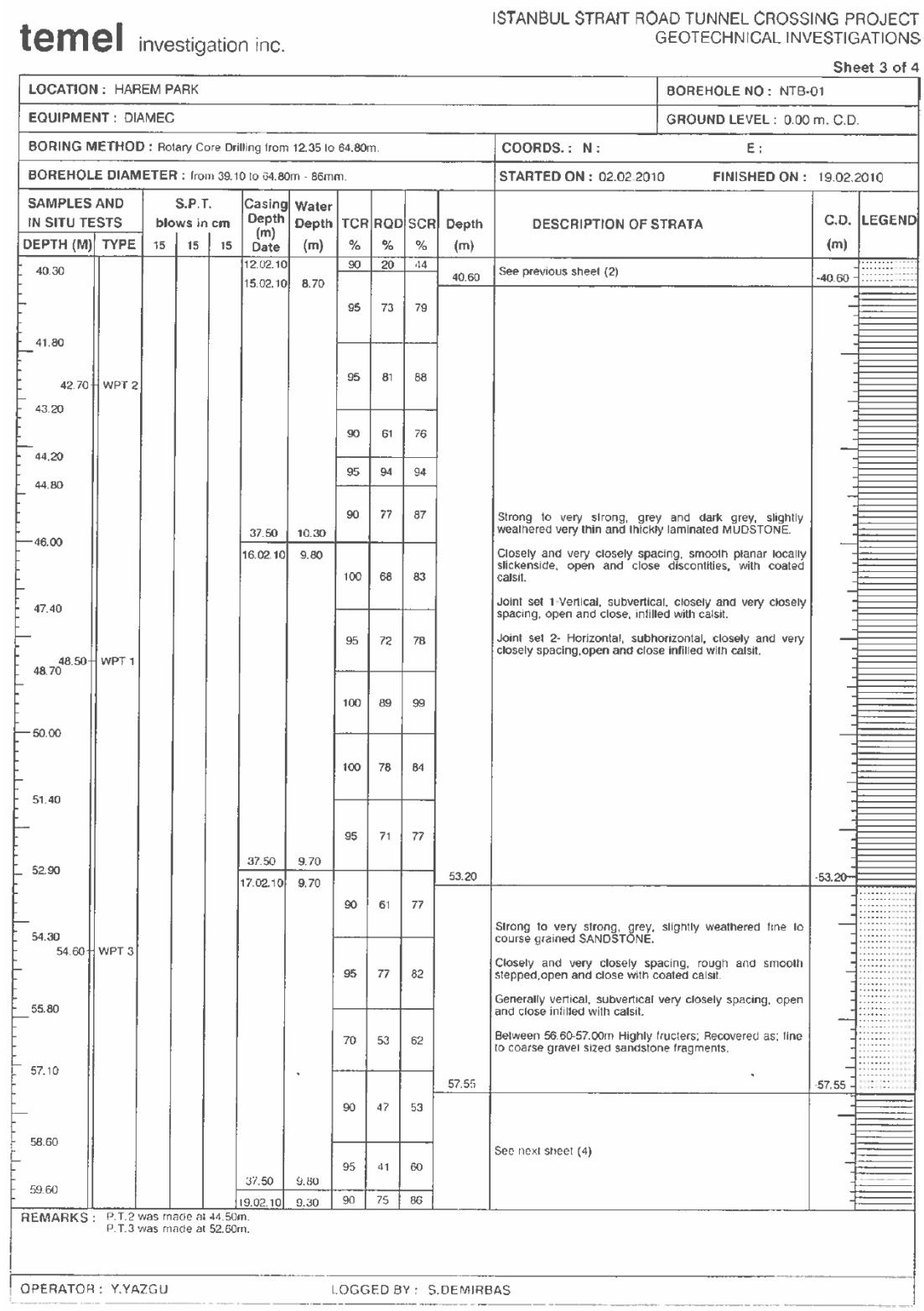

temel investigation inc.

ISTANBUL STRAIT ROAD TUNNEL CROSSING PROJECT
GEOTECHNICAL INVESTIGATIONS

Sheet 3 of 4

LOCATION : HAREM PARK	BOREHOLE NO : NTB-01
EQUIPMENT : DIAMEC	GROUND LEVEL : 0.00 m. C.D.
BORING METHOD : Rotary Core Drilling from 12.35 to 64.80m.	COORDS. : N : E :
BOREHOLE DIAMETER : from 39.10 to 64.80m - 86mm.	STARTED ON : 02.02.2010 FINISHED ON : 19.02.2010

SAMPLES AND IN SITU TESTS		S.P.T. blows in cm			Casing Depth (m)	Water Depth	TCR	RQD	SCR	Depth	DESCRIPTION OF STRATA	C.D.	LEGEND
DEPTH (M)	TYPE	15	15	15	Date	(m)	%	%	%	(m)		(m)	
40.30					12.02.10		90	20	44				
					15.02.10	8.70	95	73	79	40.60	See previous sheet (2)	-40.60	
41.80							95	81	88				
42.70	WPT 2												
43.20							90	61	76				
44.20							95	94	94				
44.80							90	77	87		Strong to very strong, grey and dark grey, slightly weathered very thin and thickly laminated MUDSTONE.		
46.00					37.50	10.30							
					16.02.10	9.80	100	68	83		Closely and very closely spacing, smooth planar locally slickenside, open and close discontities, with coated calsit.		
47.40							95	72	78		Joint set 1-Vertical, subvertical, closely and very closely spacing, open and close, infilled with calsit.		
48.50	WPT 1										Joint set 2- Horizontal, subhorizontal, closely and very closely spacing,open and close infilled with calsit.		
48.70							100	89	99				
50.00							100	78	84				
51.40							95	71	77				
52.90					37.50	9.70							
					17.02.10	9.70	90	61	77	53.20		-53.20	
54.30											Strong to very strong, grey, slightly weathered fine to course grained SANDSTONE.		
54.60	WPT 3						95	77	82		Closely and very closely spacing, rough and smooth stepped,open and close with coated calsit.		
55.80											Generally vertical, subvertical very closely spacing, open and close infilled with calsit.		
57.10							70	53	62		Between 56.60-57.00m Highly fructers; Recovered as; fine to coarse gravel sized sandstone fragments.		
58.60							90	47	53	57.55		57.55	
59.60					37.50	9.80	95	41	60		See next sheet (4)		
					19.02.10	9.30	90	75	86				

REMARKS : P.T.2 was made at 44.50m.
P.T.3 was made at 52.60m.

OPERATOR : Y.YAZGU LOGGED BY : S.DEMIRBAS

Figure B.17. Borehole No.NTB-01 (Page 3/4)

temel investigation inc.

ISTANBUL STRAIT ROAD TUNNEL CROSSING PROJECT
GEOTECHNICAL INVESTIGATIONS

Sheet 4 of 4

LOCATION : HAREM PARK	BOREHOLE NO : NTB-01
EQUIPMENT : DIAMEC	GROUND LEVEL : 0.00 m. C.D.
BORING METHOD : Rotary Core Drilling from 12.35 to 64.80m.	COORDS. : N : E :
BOREHOLE DIAMETER : from 39.10 to 64.80m - 86mm.	STARTED ON : 02.02.2010 FINISHED ON : 19.02.2010

SAMPLES AND IN SITU TESTS		S.P.T. blows in cm			Casing Depth (m) Date	Water Depth (m)	TCR %	RQD %	SCR %	Depth (m)	DESCRIPTION OF STRATA	C.D. (m)	LEGEND
DEPTH (M)	TYPE	15	15	15									
					19.02.10		90	75	86		Strong to very strong, grey and dark grey, slightly weathered very thin and thickly laminated MUDSTONE.		
61.00							95	50	50		Closely and very closely spacing, smooth planar, open and close discontities with coated calsit.		
61.40							90	45	61		Joint set 1 ; Subvertical, vertical, closely and very closely spacing, open and close infilled with calsit.		
62.50							95	14	50		Joint set 2 ; Subhorizontal, horizontal, closely and very clsely spacing, opena and close infilled with calsit.		
63.20							90	50	52	63.70	Between 59.40-59.60m Highly weathered.	-63.70	
64.20											Strong to very strong, grey slighlty weathered fine to medium grained SANDSTONE.		
64.80					37.50	9.70	90	62	62	64.80	Closely spacing, rough stepped, open and close discontities with coated calsit. Joint set 1; Horizontal, subhorizontal, closely spacing, open and close infilled with calsit. Joint sel 2; Vertical, subvertical, closely spacing, open and close infilled calsit. Between 64.70-64.80m Highly fructures; Recovered as; fine to medium gravel sized mudslone fragments.	-64.80	
											END OF BOREHOLE		

REMARKS :

OPERATOR : Y.YAZGU LOGGED BY : S.DEMIRBAS

Figure B.18. Borehole No.NTB-01 (Page 4/4)

temel investigation inc.

İSTANBUL STRAIT ROAD TUNNEL CROSSING PROJECT
GEOTECHNICAL INVESTIGATIONS

Sheet 1 of 3

LOCATION : DLH AREA	**BOREHOLE NO :** NTB-02
EQUIPMENT : ACER ACE	**GROUND LEVEL :** 0.00 m C.D.
BORING METHOD : Rotary Drilling, from 0.00 to 9.20m. Rotary Core Drilling, from 9.20 to 58.30m.	**COORDS. :** N : E :
BOREHOLE DIAMETER : from 0.00 to 37.50m - 98mm	**STARTED ON :** 18.01.2010 **FINISHED ON :** 15.02.2010

SAMPLES AND IN SITU TESTS		S.P.T. blows in cm			Casing Depth (m)	Water Depth	TCR	RQD	SCR	Depth	DESCRIPTION OF STRATA	C.D.	LEGEND
DEPTH (M)	TYPE	15	15	15	Date	(m)	%	%	%	(m)		(m)	
0.00					18.01.20						MADE GROUND		
1.50	D1	14	21	30							Concrete, Cobbles with Sand and gravel.		
1.95			N =	51						2.00		-2.00	
3.00	D2	5	6	12									
3.45			N =	20									
4.50	D3	6	7	9									
4.95			N =	16	3.00	KURU							
5.50	W1				19.01.10	KURU					Weak to moderately weak, light brown, highly weathered MUDSTONE.		
6.00	D4	25	50/5	-		5.50							
6.20													
7.50	D5	30	50/5	-									
7.70													
9.00	D6	48	50/5	-									
9.20										9.20		-9.20	
							75	40	49		Medium strong to strong, yellowish brown, brown, moderately weathered, fine to medium grained SANDSTONE.		
10.00							40	22	22		Closely to very closely spacing, smooth and rough		
10.50							50	56	56		stepped, closed and gaped discontinuities, ironoxide		
10.80							80	43	43	10.65	coated.	-10.65	
							60	0	25		Joint set 1; Subvertical to vertical, close spacing, smooth and rough stepped, open and close, infilled with ironoxide.		
11.40							60	20	20		Joint set 2; Subhorizontal to horizontal, close spacing, smooth and rough stepped, open and close, infilled with		
11.90							90	44	70	11.90	ironoxide.	-11.90	
12.70					9.00	5.00					Moderately strong to strong, yellowish brown, moderately weathered thinly laminated MUDSTONE.		
13.00					20.01.10	6.20	100	80	100		Close spacing, rough planar, open and close discontinuities ironoxide coated.		
13.70							100	77	80		Between 11.55-11.90m: Recovered as; fine to course gravel sized fragments and clay coated.		
14.00							100	74	89		Strong to very strong, brown and brownish grey,		
14.50							80	52	72		moderately to slightly weathered fine to course grained SANDSTONE.		
15.00					13.50	5.00	95	66	66				
15.50					21.01.10	6.00	90	30	40		(11.90-13.85m fine to medium grained) (13.85-18.00m medium to course grained)		
16.00							55	0	14		Closely to very closely spacing, rough stepped, open		
16.50							60	0	0		and close discontinuities ironoxide coated.		
17.00							60	0	0		Joint set 1; Subvertical to vertical, close space, rough		
17.50							65	0	0		steped open and close, infilled with ironoxide.		
18.00							80	28	50	18.00	Joint set 2; Subhorizontal to horizontal,very closely to closely, rough stepped, open and closed, infilled with ironoxide.	-18.00	
18.50							70	28	28		Between 14.50-14.60m, 16.00-17.60m Recovered as; fine to course gravel sized angular fragments.		
19.00					18.00	4.00	90	86	96		Between 15.08-15.20m Recovered as; Mudstone		
19.50					22.01.10	6.00	90	40	40	19.00	lamination.	-19.00	
20.00							80	50	64		Strong to very strong, grey, slighlty weathered fine grained SANDSTONE.		
											Very thinly bedded with dark grey Mudstone. Close spacing, rough and smooth stepped, open and close, calcite coated.		

REMARKS :

OPERATOR : A.ÜSTÜNDAĞ **LOGGED BY :** S.DEMİRBAS

Figure B.19. Borehole No.NTB-02 (Page 1/3)

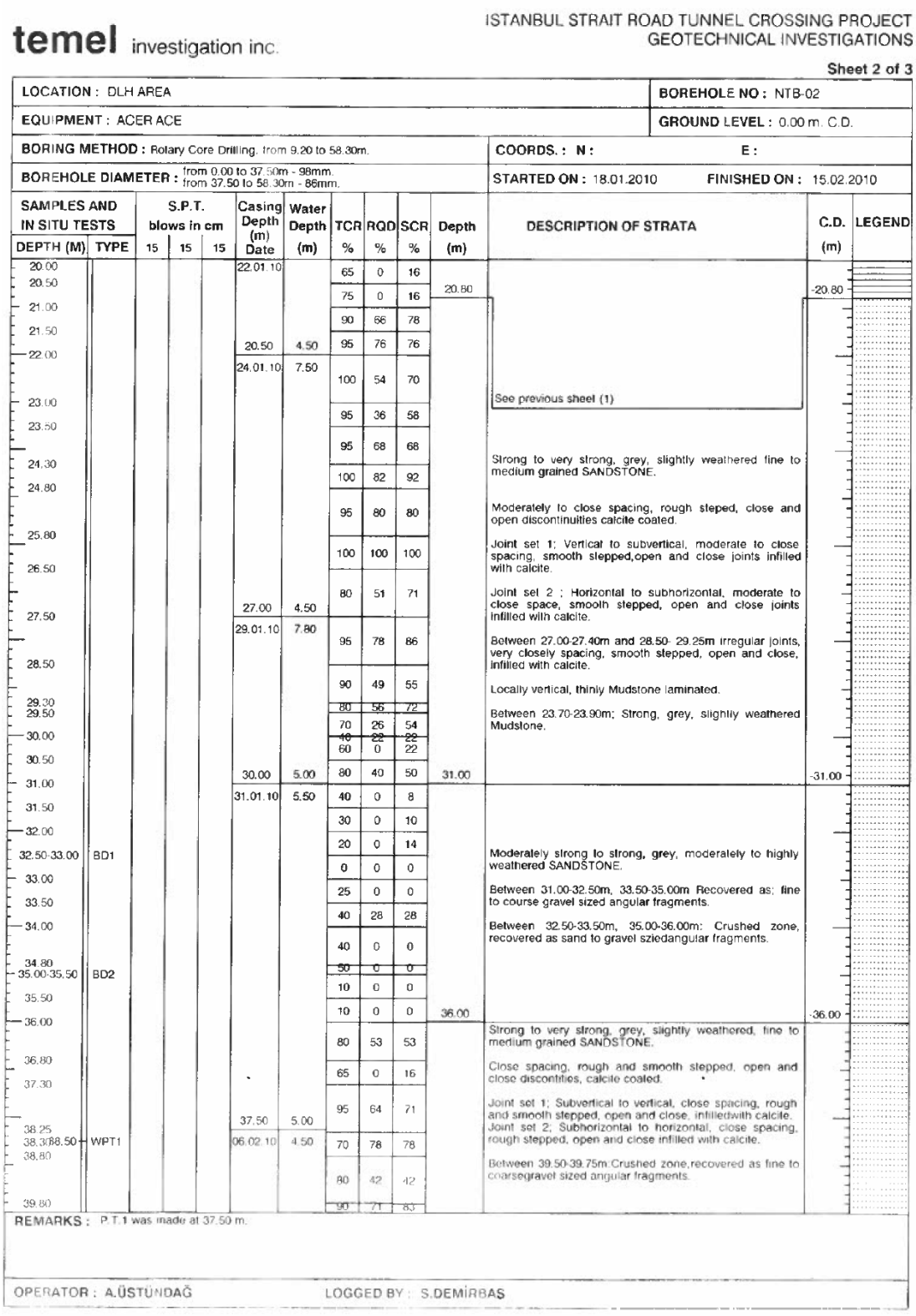

Figure B.20. Borehole No.NTB-02 (Page 2/3)

temel investigation inc.

ISTANBUL STRAIT ROAD TUNNEL CROSSING PROJECT
GEOTECHNICAL INVESTIGATIONS

Sheet 3 of 3

LOCATION : DLH AREA	**BOREHOLE NO :** NTB-02
EQUIPMENT : ACER ACE	**GROUND LEVEL :** 0.00 m. C.D.
BORING METHOD : Rotary Core Drilling from 9.20 to 58.30m.	**COORDS. : N :** **E :**
BOREHOLE DIAMETER : from 37.50 to 58.30m - 86mm.	**STARTED ON :** 18.01.2010 **FINISHED ON :** 15.02.2010

SAMPLES AND IN SITU TESTS		S.P.T. blows in cm			Casing Depth (m) Date	Water Depth (m)	TCR %	RQD %	SCR %	Depth (m)	DESCRIPTION OF STRATA	C.D. (m)	LEGEND
DEPTH (M)	TYPE	15	15	15									
38.50	WPT1				06.02.10		90	71	83				
40.50							60	30	30		See previous sheet (2)		
41.00							95	86	86	41.50		-41.50	
41.50							80	28	40		Strong to very strong, grey, slightly weathered thickly laminated MUDSTONE. Closely spacing, smooth planar, open and close discontilies calcite coated. Between 41.70-41.90m:Strong, grey, slightly weathered Sandstone band. Between 43.70-43.90m:Recovered as; fine to medium gravel sized angular fragments.		
42.00							75	54	72				
42.50							90	45	48				
43.25					37.50	8.00							
43.30					08.02.10	4.50	65	45	45				
43.70							85	28	50	44.10		-44.10	
44.30							80	0	0				
44.50							100	70	70				
45.00							40	22	22				
45.50							65	0	36				
46.00							90	71	71				
46.80							70	33	59				
47.00							100	48	96				
47.10	WPT2						60	20	33				
47.60							35	0	0		Strong to very strong, grey, slightly weathered fine to medium grained SANDSTONE.		
47.90							50	18	18		Closly to very closly spacing, rough stepped, open and close discontinuities calcite coated.		
48.50							90	67	67				
49.20					37.50	6.80					Joint set 1; Subvertical to vertical, rough stepped, open and close infilled with calcite.		
49.70					10.02.10	5.20	50	20	20				
50.20											Joint set 2; Subhorizontal to horizontal, rough stepped, open and close infilled with calcite.		
50.40							40	0	0				
50.70							55	0	0		Between 44.25-44.50m, 45.10-45.45m, 50.20-51.40m: Recovered as fine to course gravel sized angular fragments.		
51.40							35	0	0				
52.00							95	71	79		Between 47.60-47.90m: Highly weathered.		
52.10	WPT3				37.50	6.50							
52.30					12.02.10	5.50	90	0	0				
53.00							75	20	47		Between 46.90-47.10m, 53.00-53.50m, 56.90-57.65m, 58.15-58.30m;		
53.70							80	36	56				
54.00							100	90	90		Strong to very strong, grey, slightly weathered Mudstone.		
55.50							95	60	69				
56.50							100	86	86				
58.30							95	79	82				
										58.30	END OF BOREHOLE	-58.30	

REMARKS :

OPERATOR : A.ÜSTÜNDAĞ LOGGED BY : S.DEMİRBAS

Figure B.21. Borehole No.NTB-02 (Page 3/3)

temel investigation inc.

ISTANBUL STRAIT ROAD TUNNEL CROSSING PROJECT
GEOTECHNICAL INVESTIGATIONS

Sheet 1 of 4

LOCATION : NUMUNE HOSPITAL BRIDGE	**BOREHOLE NO :** NTB-03
EQUIPMENT : DIAMEC 262	**GROUND LEVEL :** 36.51 m. C.D.
BORING METHOD : Rotary Drilling from 0.00 to 3.13m. Rotary Core Drilling from 3.13 to 67.70m.	**COORDS. :** N : 417645.62 E : 4541691.037
BOREHOLE DIAMETER : from 0.00 to 25.50m - 114mm.	**STARTED ON :** 22.02.2010 **FINISHED ON :** 10.03.2010

SAMPLES AND IN SITU TESTS		S.P.T. blows in cm			Casing Depth (m) Date	Water Depth (m)	TCR %	RQD %	SCR %	Depth (m)	DESCRIPTION OF STRATA	C.D. (m)	LEGEND
DEPTH (M)	TYPE	15	15	15									
					22.02.20						MADE GROUND Brick pieces, cobbles, sand and gravel.		
1.50	D1	20	30	33						1.80		34.71	
1.95			N =	63							Weak to very weak, dark yellowish brown, highly weathered, fine grained SANDSTONE.		
3.10 3.00 3.13	D2	50/13	-	-			75	0	13	3.45	3.13-3.45m; Recovered as fine to coarse gravel sized angular fragments and sand.	33.06	
3.50							80	0	21				
4.00						G W L	95	47	63				
4.30						4.40	90	36	57				
5.10							95	47	57				
5.70							85	36	48				
6.50							90	20	25				
7.10							85	41	59				
7.90							100	82	98				
8.40							90	0	28				
8.80					7.50	1.80	85	0	13		Moderately strong, dark yellowish brown, moderately to slightly weathered fine to coarse grained SANDSTONE.		
9.30					23.02.10	1.20	80	0	11				
9.80							90	44	44		Subhoritontal,open, closely to moderately widely spaced, planar, rough discontinuitis ironoxide coated and reddish clay filled.		
10.30							95	61	76				
11.00							85	53	58		3.70-8.50m,9.75-14.20m: About 45 o inclined, medium widely spaced, open, planar, rough joints,ironoxide coated.		
12.00							90	24	38		6.00-21.50m: Subvertical, medium widely sapced,open, undulating, rough joints,ironoxide coated.		
12.50							100	73	73				
13.50							100	75	89		4.70-4.90m,5.65-5.80m,8.60-9.75m,16.50-16.80m, 17.50-17.80m,18.10-18.50m,20.00-21.00m: Recovered as fine to coarse gravel sized angular fragments, ironoxide coated.		
14.10							95	89	89				
14.40							100	78	94				
14.90							100	65	65				
15.30							70	40	54				
15.80					15.00	1.60	95	74	74				
16.30					24.02.10	1.00	90	25	53				
16.70							95	0	35				
17.10							85	20	20				
17.60							80	30	48				
18.10							75	0	38				
18.70							90	58	58				
19.30							100	69	69				

REMARKS :

OPERATOR : Y.YAZGU **LOGGED BY :** S.DEMIRBAS **REVIEWED BY :** M.BOL

Figure B.22. Borehole No.NTB-03 (Page 1/4)

temel investigation inc.

ISTANBUL STRAIT ROAD TUNNEL CROSSING PROJECT
GEOTECHNICAL INVESTIGATIONS

Sheet 2 of 4

LOCATION : NUMUNE HOSPITAL BRIDGE	BOREHOLE NO : NTB-03
EQUIPMENT : DIAMEC 262	GROUND LEVEL : 36.51 m. C.D.
BORING METHOD : Rotary Core Drilling from 3.13 to 67.70m.	COORDS. : N : 417645.62 E : 4541691.037
BOREHOLE DIAMETER : from 0.00 to 25.50m - 114mm. from 25.50 to 48.10m - 98mm.	STARTED ON : 22.02.2010 FINISHED ON : 10.03.2010

SAMPLES AND IN SITU TESTS		S.P.T. blows in cm			Casing Depth (m)	Water Depth	TCR	RQD	SCR	Depth	DESCRIPTION OF STRATA	C.D.	LEGEND
DEPTH (M)	TYPE	15	15	15	Date	(m)	%	%	%	(m)		(m)	
20.20					24.02.10		100	69	69				
20.50							100	29	71				
21.00							95	0	16				
21.40							95	58	58		See previous sheet (1)		
21.90					19.50	2.00	100	80	92				
					25.02.10	1.20	70	11	40	22.50		14.01	
22.90							100	81	87		Moderately strong to strong, grey and dark grey, slightly weathered, thickly vertical laminated MUDSTONE. 22.50-23.10m: Subhorizontal, closely sapced,open, planar, rough discontinuities, ironoxide and calcite coated. 23.10-25.50m: Subhorizontal, moderately widely spaced, open, planar, rough discontinuities, ironoxide and calicte coated.		
24.30							95	0	0				
24.60							80	62	62		24.30-25.30m: Subvertical, open, planar, smouth discontiniuties, irionoxide coated.		
25.50							90	68	64	25.50		11.01	
26.00							65	0	13	26.45	Moderately strong to strong, light grey and brown, moderately to slightly weathered DIABASE. Subhorizontal, closely spaced,open,stepped,smooth discontinuities, ironoxide coated.	10.06	
26.40											Between 26.00-26.40m: Recovered as fine to course gravel sized angular fragments.		
27.00					25.50	1.80							
27.60					26.02.10	1.20	75	40	48				
28.10							95	49	60				
28.30							90	0	60				
28.70							80	0	0				
29.10							85	25	37				
30.60							100	81	85				
31.70							100	89	89		Strong, grey and dark grey, slightly weathered, thickly vertical laminated MUDSTONE.		
32.20							100	94	94				
33.20							95	58	74		Joint set 1; Vertical, subvertical, closely, very closely spacing, open, planar rough and smooth, joints, infilled calcite.		
34.30							100	65	72		Joint set 2; Horizontal subhorizontal, closely, very closely spacing, open, planar rough and smooth, joints infilled calcite.		
34.90							95	25	40		Between 28.20-29.00m, 34.00-35.30m, 35.60-36.10m, 36.70-37.20m, 37.50-37.70m, 38.80-41.40m, 41.80-42.10m and 43.10-43.30m:Recovered as highly fructured and fine to coarse gravel sized angular fragments.		
35.30							90	40	50				
36.10					30.00	2.40	85	15	35		(crushed zone).		
36.70					01.03.10	2.60	90	67	80				
37.70							95	27	27				
38.70							95	32	43				
39.00							95	60	60				
39.70							80	0	21				
							75	0	20				

REMARKS : Pressuremeter Test (P.T.1) was carried out at 38.40m depth.
Water Pressure Test (WPT1) was carried out between 40.30-43.30m.

OPERATOR : Y.YAZGU LOGGED BY : S.DEMIRBAS REVIEWED BY : M.BOL

Figure B.23. Borehole No.NTB-03 (Page 2/4)

temel investigation inc.

ISTANBUL STRAIT ROAD TUNNEL CROSSING PROJECT
GEOTECHNICAL INVESTIGATIONS

LOCATION : NUMUNE HOSPITAL BRIDGE — **BOREHOLE NO :** NTB-03

EQUIPMENT : DIAMEC 262 — **GROUND LEVEL :** 36.51 m. C.D.

BORING METHOD : Rotary Core Drilling from 3.13 to 67.70m. — **COORDS. :** N : 417645.62 E : 4541691.037

BOREHOLE DIAMETER : from 25.50 to 48.10m - 98mm. from 48.10 to 67.70m - 86mm. — **STARTED ON :** 22.02.2010 **FINISHED ON :** 10.03.2010

SAMPLES AND IN SITU TESTS		S.P.T. blows in cm			Casing Depth (m)	Water Depth	TCR	RQD	SCR	Depth	DESCRIPTION OF STRATA	C.D.	LEGEND
DEPTH (M)	TYPE	15	15	15	Date	(m)	%	%	%	(m)		(m)	
40.10 40.30	WPT1				01.03.10		85	48	48				
40.60							70	0	16				
41.70													
42.40					37.50	3.30	95	26	36		See previous sheet (2)		
43.30					03.03.10	2.80	95	39	52				
43.80							95	44	44	44.00		-7.49	
44.40							80	25	40				
44.80							75	0	30		Strong to very strong, grey, slighly weathered, fine to course grained SANDSTONE.		
45.40					37.50	2.10	90	42	52				
46.20					04.03.10	2.70	100	81	81		Between 45.60-45.90m: Strong, light grey, slightly weathered Diabase.		
47.40							100	83	83		Between 46.70-49.70m: Thinly interbedded with Mudstone. About 45 o inclined, medium spaced, open, planar, rough joints, ironoxide and calicte coated.		
48.20					37.50	2.60	100	87	87		44.40-44.80m, 45.60-45.90m: Subvertical, open, planar, rough discontinuities, ironoxide coated.		
48.80					05.03.10	2.10	95	45	72				
50.00							100	69	76	49.70		-13.19	
51.10					37.50	2.70	100	55	61		Strong, grey and dark grey, slightly weathered, thickly laminated MUDSTONE. Joint set 1; Vertical, subvertical, closely spacing, open, planar, smooth, joints infilled calcite.		
51.90					06.02.10	2.20	100	80	85		Joint set 2; Horizontal, subhorizontal, closely spacing, open, planar, smooth, joints infilled calcite.		
53.00							90	52	52	52.90	Between 51.90-52.00m:Highly weathered.	-16.39	
53.40							80	0	20		Strong ,grey, slightly weathered, fine to coarse grained SANDSTONE. Between 55.50-55.90m thinly interbedded with mudstone. Joint set 1; Vertical, subvertical, closely, very closely spaced, open, stepped, rough and smooth,joints infilled calcite. Joint set 2; Horizontal, subhorizontal, closely, very closely spacing, open, stepped, rough and smooth, joints infilled calcite.		
54.70							95	68	78				
55.50							100	96	96				
56.10					37.50	3.00	100	33	45	56.00		-19.49	
57.40					07.02.10	2.20	100	55	67		Strong to very strong, grey, dark grey, slightly weathered, thickly laminated MUDSTONE. Generally vertical, subvertical, closely, very closely spacing, open, planar rough and smooth, joints infilled calcite.		
58.40							90	55	55	57.90		-21.39	
59.05					48.10	3.50	95	55	68		Strong to very strong, grey, slightly weathered fine to coarse grained SANDSTONE.		
59.10					08.03.10	3.30	90	48	48		Joint set 1; Vertical, subvertical, closely, very closely spaced, open, stepped, rough, joints infilled with calcite. See next sheet (4)		
59.90													

REMARKS :

OPERATOR : Y.YAZGU — **LOGGED BY :** S.DEMIRBAS — **REVIEWED BY :** M.BOL

Figure B.24. Borehole No.NTB-03 (Page 3/4)

temel investigation inc.

ISTANBUL STRAIT ROAD TUNNEL CROSSING PROJECT
GEOTECHNICAL INVESTIGATIONS

Sheet 4 of 4

LOCATION : NUMUNE HOSPITAL BRIDGE	**BOREHOLE NO :** NTB-03
EQUIPMENT : DIAMEC 262	**GROUND LEVEL :** 36.51 m. C.D.
BORING METHOD : Rotary Core Drilling from 3.13 to 67.70m.	**COORDS. : N :** 417645.62 **E :** 4541691.037
BOREHOLE DIAMETER : from 48.10 to 67.70m - 86mm.	**STARTED ON :** 22.02.2010 **FINISHED ON :** 10.03.2010

SAMPLES AND IN SITU TESTS		S.P.T. blows in cm			Casing Depth (m)	Water Depth	TCR	RQD	SCR	Depth	DESCRIPTION OF STRATA	C.D.	LEGEND
DEPTH (M)	TYPE	15	15	15	Date	(m)	%	%	%	(m)		(m)	
					08.03.10		80	13	34		Joint set 2; Horizontal, subhorizontal, closely, very closely, open, stepped,rough, joints infilled with calcite.		
61.00							95	30	30		Belween 60.00-60.20m, 61.50-61.90m, 62.00-62.50m: Recovered as highly fructured and fine to coarse gravel sized angular fragments.		
61.70							45	0	0				
61.90							80	35	35		See previous sheet (3)		
					48.10	3.50				62.70		-26.19	
62.50					09.03.10	3.40	75	22	22				
63.00							40	0	0				
63.30							55	0	11		Moderately weak, grey and dark grey, highly crushed, fine to coarse grained SANDSTONE. Generally highly fructured and fine to coarse gravel sized angular fragments and sand. (Crushed Zone)		
64.00							50	0	0				
										65.00		-28.49	
65.00							70	24	24				
65.50							80	0	0		Strong to very strong, grey, slightly weathered, fine to course grained SANDSTONE. 66.20-66.90m, 66.40-67.70m: About 60 o inclined, closely spaced, open, planar, rough joints, ironoxide coated. Between 65.00-66.30m and 66.90-67.70m:Recovered as highly fructured and fine to coarse gravel sized angular fragments.		
66.00							85	25	25				
66.40					48.10	10.30							
66.90					10.03.10	4.40	90	54	54				
67.30							85	0	0				
67.70							80	0	0	67.70	END OF BOREHOLE	-31.19	

REMARKS : PS Logging Test is carried out.

OPERATOR : Y.YAZGU **LOGGED BY :** S.DEMIRBAS **REVIEWED BY :** M.BOL

Figure B.25. Borehole No.NTB-03 (Page 4/4)

temel investigation inc.

ISTANBUL STRAIT ROAD TUNNEL CROSSING PROJECT
GEOTECHNICAL INVESTIGATIONS

Sheet 1 of 3

LOCATION : NUMUNE HOSPITAL	**BOREHOLE NO :** NTB-04
EQUIPMENT : ACER ACE	**GROUND LEVEL :** 0.00 m. C.D.
BORING METHOD : Rotary Coring Water Flus with Diamond Bit. from 0.00 to 59.00m.	**COORDS. : N :** **E :**
BOREHOLE DIAMETER : from 0.00 to 25.50m - 98mm.	**STARTED ON :** 04.02.2010 **FINISHED ON :** 21.02.2010

SAMPLES AND IN SITU TESTS		S.P.T. blows in cm			Casing Depth (m) Date	Water Depth (m)	TCR %	RQD %	SCR %	Depth (m)	DESCRIPTION OF STRATA	C.D. (m)	LEGEND
DEPTH (M)	TYPE	15	15	15									
0.50-1.00	BD1				04.02.20								
						G W L					MADE GROUND		
1.60	W1					1.60					Recovered as Asfalt,Cobbles, Gravel,Clay.		
										3.00		-3.00	
3.00	D1	50/7	-	-									
3.07							75	41	47		Moderately weak to weak, brown, slighlly weathered MUDSTONE. Closely spacing, smooth planar, open and close, generally subvertical and vertical discontinuities, ironoxide coated.		
4.50										4.50		-4.50	
							85	53	69				
5.50							90	27	60				
6.10							50	13	36				
					6.00	0.75							
7.10					05.02.10	0.50	90	80	80		Moderately weak to weak, brown, slighlly weathered fine grained SANDSTONE.		
7.50							60	24	39		Closely spacing, smooth and rough stepped, open and close discontinuities ironoxide coated.		
8.50							95	54	86		Generally vertical, subvertical, closely spacing, open and close joints, infilled with ironoxide.		
9.00							70	22	42				
9.50					9.00	1.30	80	74	74		Between 12.60-12.75m; Highly weathered; Recovered as; fine to medium sandstone fragments and sand.		
10.00					06.02.10	2.00	95	67	75				
11.00							90	45	60				
12.00							85	23	48	12.75		-12.75	
12.80							90	51	66		Moderately weak to weak,dark yellowish brown, moderately weathered MUDSTONE. Interbedded with dark yellowish brown Sandstone. Closely and very closely spacing, rough planar and smooth stepped, open and close discontinuities, coated with clay and ironoxide. Joint set 1; Vertical, subvertical, closely and very closely spacing, open and close joints, infilled with clay and ironoxide. Joint set 2; Horizontal, subhorizontal, closely and very closely spacing,open and close joints, infilled with clay and ironoxide. Belween 13.70-14.00 m and 14.50-14.90 m :Recovered as fine to coarse gravel sized mudstone and sandstone angular fragments, locally sand.		
14.00					12.00	0.50							
14.50					07.02.10	2.33	95	82	82				
15.00							60	20	34				
15.70							70	24	46				
16.20							95	86	86				
17.00							95	60	69	17.15		-17.15	
17.70					15.00	5.00	90	64	70		Moderately strong and strong, brown, moderately weathered fine to couse grained SANDSTONE.		
18.40					08.02.10	1.92	100	85	85		Vertical, subvertical, very closely,closely spacing, rough stepped, open and close discontinities, with coated ironoxide and calcite.		
19.00							90	49	57				
19.50							85	84	84		Generally irregular , very closely spacing, open and close joints infilled with ironoxide and calcite.		
20.00							85	22	50				

REMARKS :

OPERATOR : Y.KAPDAN LOGGED BY : S.DEMIRBAS

Figure B.26. Borehole No.NTB-04 (Page 1/3)

temel investigation inc.

ISTANBUL STRAIT ROAD TUNNEL CROSSING PROJECT
GEOTECHNICAL INVESTIGATIONS

Sheet 2 of 3

LOCATION : NUMUNE HOSPITAL	**BOREHOLE NO :** NTB-04
EQUIPMENT : ACER ACE	**GROUND LEVEL :** 0.00 m. C.D.
BORING METHOD : Rotary Coring Water Flus with Diamond Bit. from 0.00 to 59.00m.	**COORDS. : N :** **E :**
BOREHOLE DIAMETER : from 0.00 to 25.50m - 98mm. from 25.50 to 59.00m - 86mm.	**STARTED ON :** 04.02.2010 **FINISHED ON :** 21.02.2010

SAMPLES AND IN SITU TESTS		S.P.T. blows in cm			Casing Depth (m)	Water Depth	TCR	RQD	SCR	Depth	DESCRIPTION OF STRATA	C.D.	LEGEND
DEPTH (M)	TYPE	15	15	15	Date	(m)	%	%	%	(m)		(m)	
20.00					08.02.10		80	41	55		See previous sheet (1)		
										21.00		-21.00	
21.00							80	30	53		Moderately strong and strong, brown, moderately weathered thickly laminated MUDSTONE. Vertical, subvertical closely spacing, rough planar, open and close discontilies coated with ironoxide.		
22.00							60	10	20	22.40	Irregular closely spacing, open and close joints, infilled with ironoxide.	-22.40	
					19.50	1.50							
23.00					09.02.10	1.95	50	0	12		Moderately weak, brown, moderately and highly weathered fine to course grained SANDSTONE.		
23.50							70	20	56				
24.00							35	0	16		Vertical and subvertical, closely and very closely spacing, rough and smooth stepped, open and close discontities with coated calsit.		
24.50							45	0	0				
25.00							40	20	26		Between 22.40-23.00m, 23.25-23.60m and 24.30-25.00m ; Highly weathered;		
25.50							50	0	38				
26.00							55	0	32		Recovered as; fine to course gravel sized sandstone fragments and sand , locally lean clay.		
26.50											26.50-27.00m:Core loss, possible highly weathered zone.		
27.00					21.00	1.95	0	0	0	27.00		-27.00	
27.50					10.02.10	1.50	80	38	50				
							95	79	79		Strong to very strong, grey, slightly weathered fine to medium grained SANDSTONE.		
28.20							85	43	80				
28.80							70	33	33		Closely spacing, rough stepped, open and close discontinuitues with coated calcite. Joint set 1; Vertical, subvertical, closely spacing, open and close joints, infilled with calcite.		
29.20							90	53	53				
29.90											Joint set 2 ; Horizontal, subhorizontal, closely spacing, open and close joints, infilled with calcite.		
					25.50	2.00	60	20	52				
30.40					11.02.10	1.60	100	85	93		Between 27.00-29.00m; Generally very closely spacing, open and close irregular joints, infilled with calcite.		
31.00							100	98	98				
31.50											Between 27.00-27.50m; Interbedded with dark grey Mudstone.		
							100	87	87				
32.50										32.60		-32.60	
33.10							100	93	93				
							70	29	52		Strong to very strong, dark grey, slightly weathered MUDSTONE.		
					25.50	3.00							
34.00							95	50	50		Generally vertical and subvertical, closely spacing, smooth planar, close discontinuities, calcite coated.		
34.20					12.02.10	2.25							
34.75	WPT-1						85	16	49	35.00		-35.00	
35.00							95	72	83		Strong to very strong, dark grey, slightly weathered fine grained SANDSTONE. Closely to very closely, spacing, smooth stepped, open and close discontinuities calcite coated.		
35.80							100	67	85		Generally irregular joints, very closely spacing, close, infilled with calcite.		
36.80										37.00	Between 35.75-36.25m; Vertically interbeded with dark grey Mudstone.	-37.00	
37.25					25.50	3.75	95	62	78				
37.30					13.02.10	4.00					Strong to very strong, dark grey, slightly weathered MUDSTONE.		
					25.50	4.00	90	60	60		Vertical, subvertical, closely to medium closely, smooth planar, close discontinuities calcite coated.		
38.25										38.30		-38.30	
38.30					15.02.10	1.70	95	57	64		See next sheet (3)		
39.80							70	21	38				

REMARKS : P.T.1 was made at 33.10m.
P.T.2 was made at 42.00m.

OPERATOR : Y.KAPDAN **LOGGED BY :** S.DEMIRBAS

Figure B.27. Borehole No.NTB-04 (Page 2/3)

temel investigation inc.

ISTANBUL STRAIT ROAD TUNNEL CROSSING PROJECT
GEOTECHNICAL INVESTIGATIONS

Sheet 3 of 3

LOCATION : NUMUNE HOSPITAL	BOREHOLE NO : NTB-04
EQUIPMENT : ACER ACE	GROUND LEVEL : 0.00 m. C.D.
BORING METHOD : Rotary Coring Water Flus with Diamond Bit. from 0.00 to 59.00m.	COORDS. : N : E :
BOREHOLE DIAMETER : from 25.50 to 59.00m - 86mm.	STARTED ON : 04.02.2010 FINISHED ON : 21.02.2010

SAMPLES AND IN SITU TESTS		S.P.T. blows in cm			Casing Depth (m) Date	Water Depth (m)	TCR %	RQD %	SCR %	Depth (m)	DESCRIPTION OF STRATA	C.D. (m)	LEGEND
DEPTH (M)	TYPE	15	15	15									
					15.02.10		70	21	38				
40.80													
41.00					25.50	3.87	95	52	76		Strong to very strong,dark grey, slightly weathered, fine grained SANDSTONE.		
41.30					16.02.10	1.66							
							100	67	85		Closely spacing, rough and smooth stepped, open and close discontinuities calcite coated.		
42.30													
42.60							100	69	69		Joint set 1; Vertical, subvertical, closely spacing, open and close, infilled with calcite.		
43.00	WPT-2						100	69	78				
					25.50	5.00					Joint set 2; Horizontal, subhorizontal, closely spacing, open and close, infilled with calcite.		
43.50							100	0	90				
43.60					17.02.10	2.00	100	60	60				
44.00							90	0	45		Between 40.25-40.75m; fine to course gravel sized sandstone fragments.		
44.20							90	22	37				
44.80											Between 44.30-44.45m; Vertically interbedded with dark grey Mudstone.		
							80	33	57				
45.40													
45.90							85	84	84				
							65	25	32	46.50		-46.50	
46.50													
							100	83	83	47.35	Strong to very strong, dark grey, slightly weathered thinly laminated MUDSTONE.	-47.35	
47.50													
					25.50	3.75	95	98	98				
48.00					18.02.10	1.50	100	90	90				
48.50							65	24	24				
49.00													
49.50	WPT-3						45	13	21				
49.80													
							50	0	33				
50.50							80	0	22				
51.00											Strong to very strong, dark grey, slightly weathered, fine to medium grained SANDSTONE		
51.50							80	0	10				
							60	0	34		Thinly interbedded with dark grey Mudstone.		
52.00					25.50	4.40	90	60	70		Closely space, smooth stepped, open and close discontinuities, calcite coated.		
52.50					19.02.10	2.10	75	23	31		Joint set 1; Vertical, subvertical, close spacing, open and close, infilled with calcite.		
53.50													
54.00					25.50	6.00	80	22	34		Joint set 2; Horizontal, subhorizontal, close spacing, open and close, infilled with calcite.		
54.50					20.02.10	1.77	40	20	30				
55.00							80	28	56				
55.50							85	38	50		Between 49.25-49.50m, 50.50-50.70m, 57.10-57.50m, 58.75-59.00m: Recovered as: fine to course gravel sized sandstone fragments.		
56.00							85	80	80				
56.50					25.50	5.00	70	20	44				
					21.02.10	1.60	50	0	7				
57.50													
							70	15	22				
					25.50	4.00				59.00	END OF BOREHOLE	-59.00	
59.00					22.02.10	1.75							

REMARKS :

OPERATOR : Y.KAPDAN LOGGED BY : S.DEMIRBAS

Figure B.28. Borehole No.NTB-04 (Page 3/3)

APPENDIX C

CORE BOX PHOTOGRAPHS

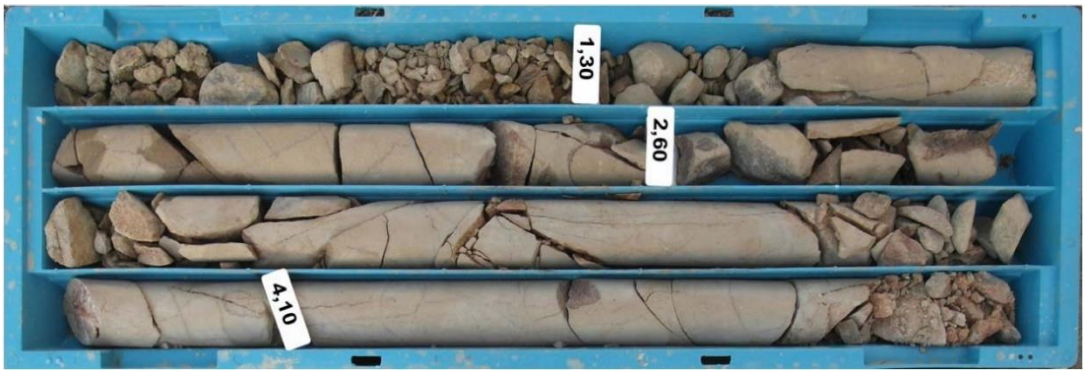

Figure C.1. S-AS-105, core box no: 1/13

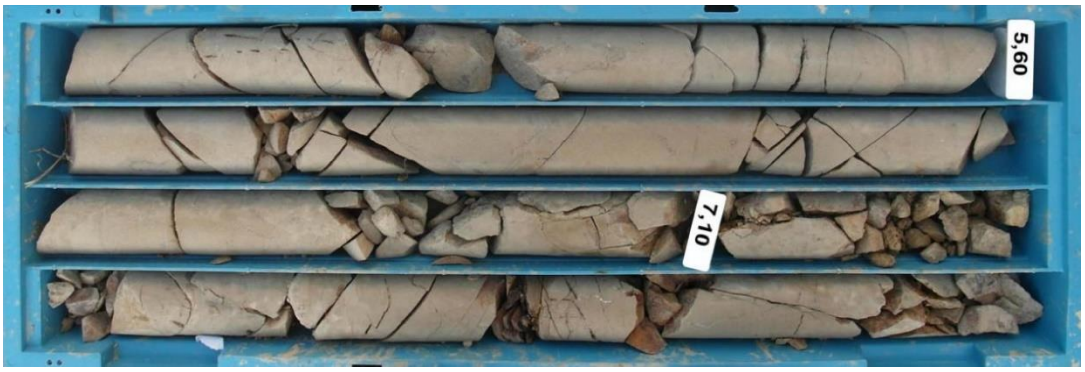

Figure C.2. S-AS-105, core box no: 2/13

Figure C.3. S-AS-105, core box no: 3/13

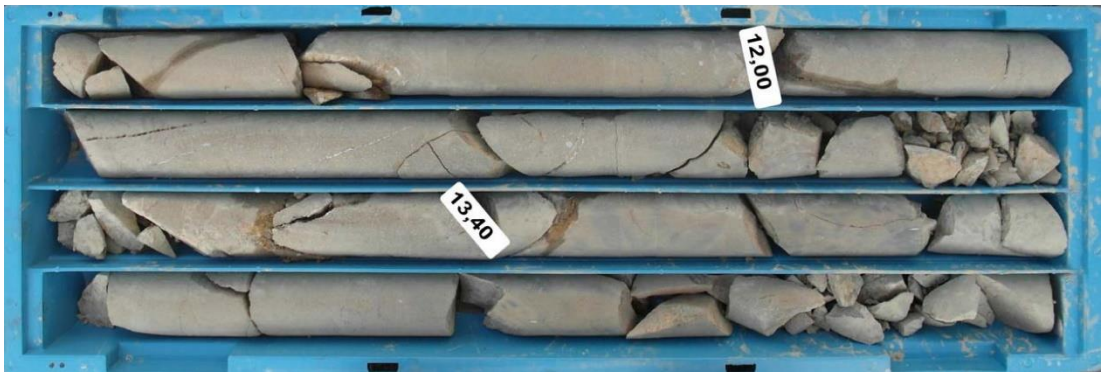

Figure C.4. S-AS-105, core box no: 4/13

Figure C.5. S-AS-105, core box no: 5/13

Figure C.6. S-AS-105, core box no: 6/13

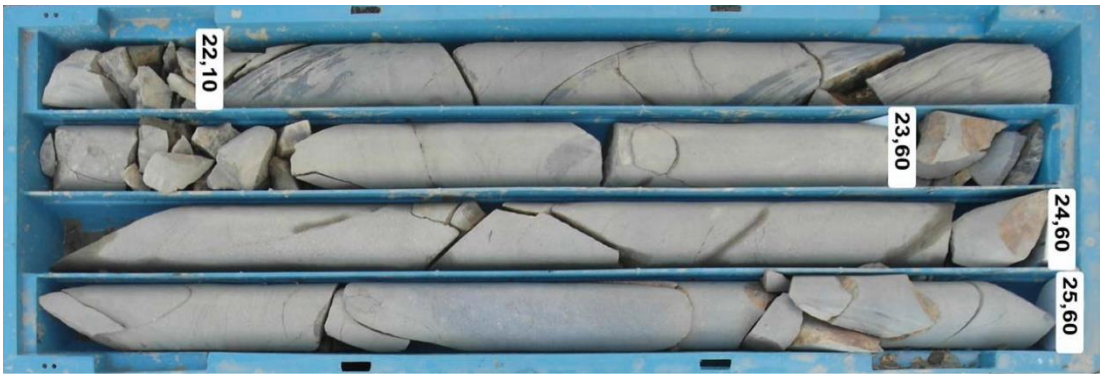

Figure C.7. S-AS-105, core box no: 7/13

Figure C.8. S-AS-105, core box no: 8/13

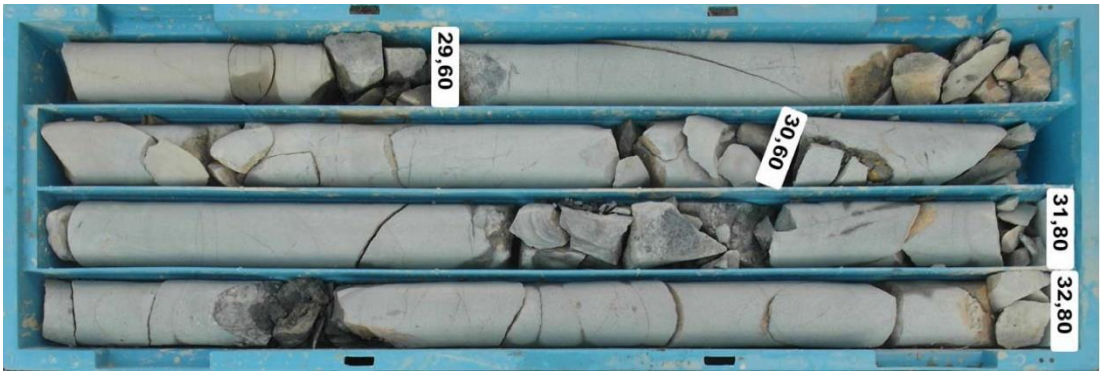

Figure C.9. S-AS-105, core box no: 9/13

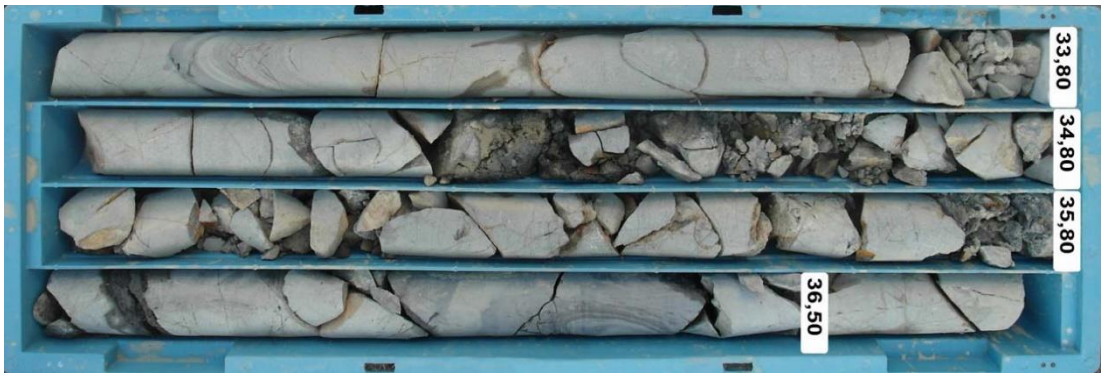

Figure C.10. S-AS-105, core box no: 10/13

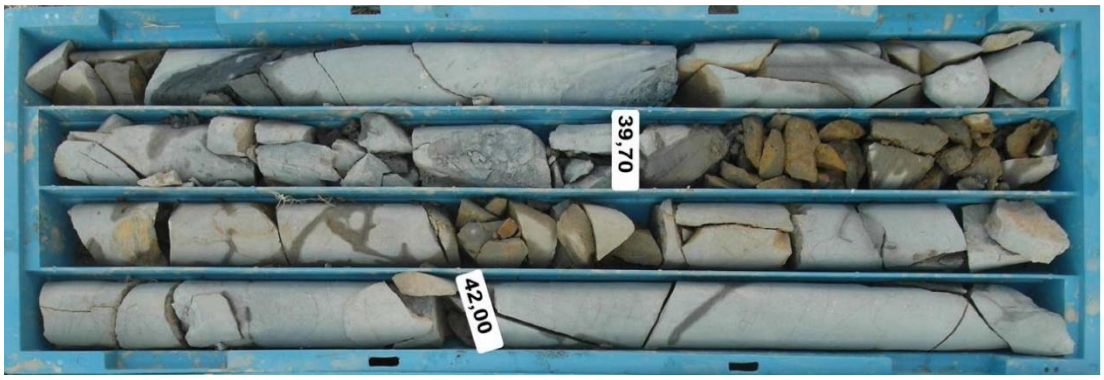

Figure C.11. S-AS-105, core box no: 11/13

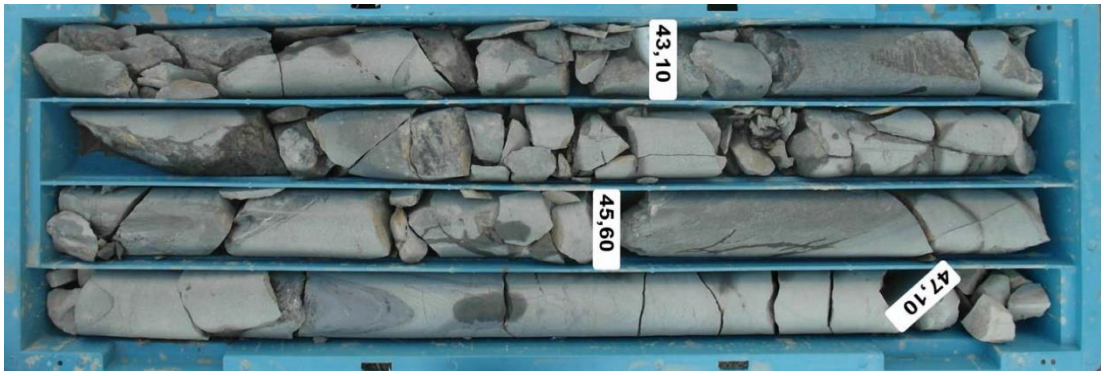

Figure C.12. S-AS-105, core box no: 12/13

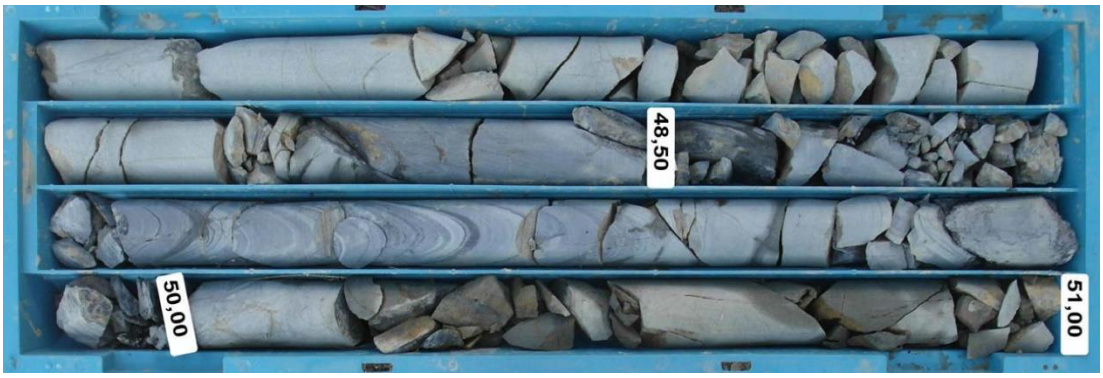

Figure C.13. S-AS-105, core box no: 13/13

Figure C.14. S-AS-106, core box no: 1/13

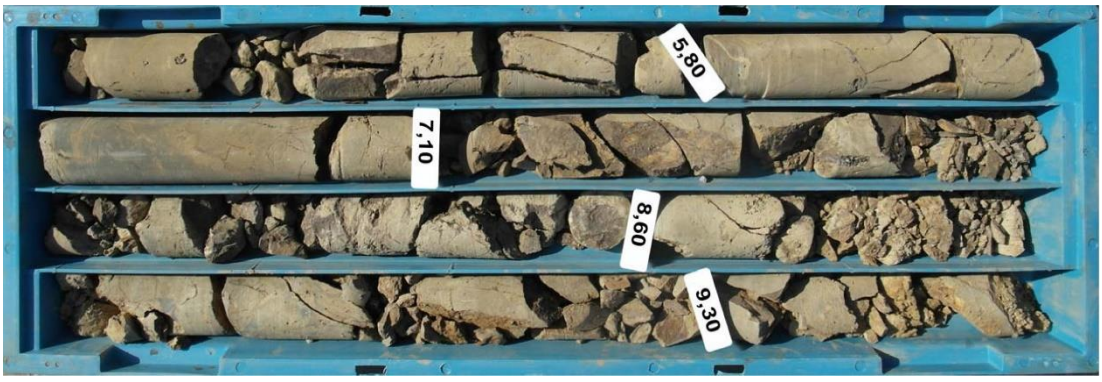

Figure C.15. S-AS-106, core box no: 2/13

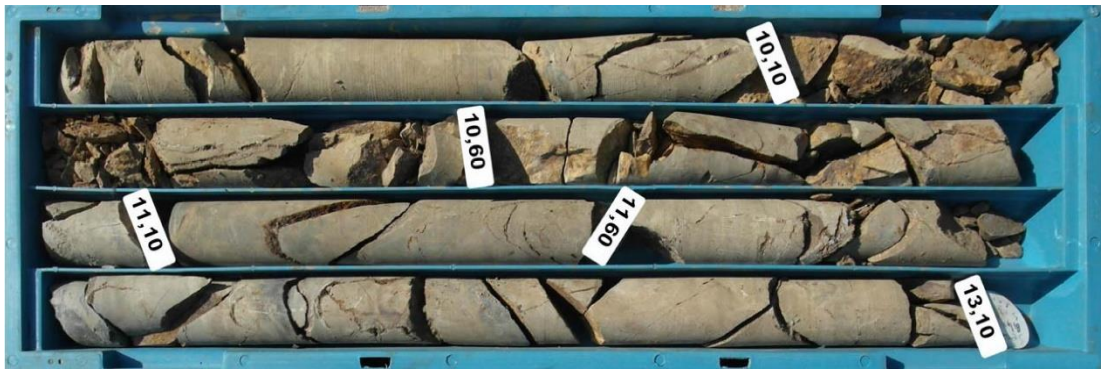

Figure C.16. S-AS-106, core box no: 3/13

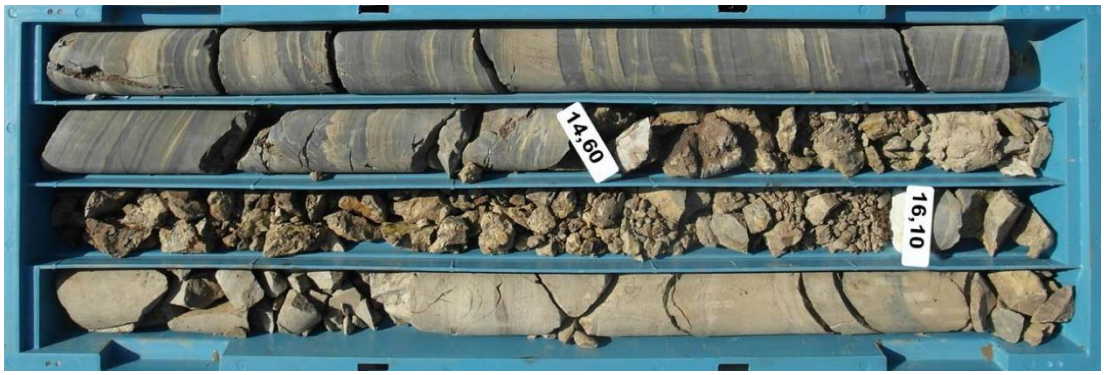

Figure C.17. S-AS-106, core box no: 4/13

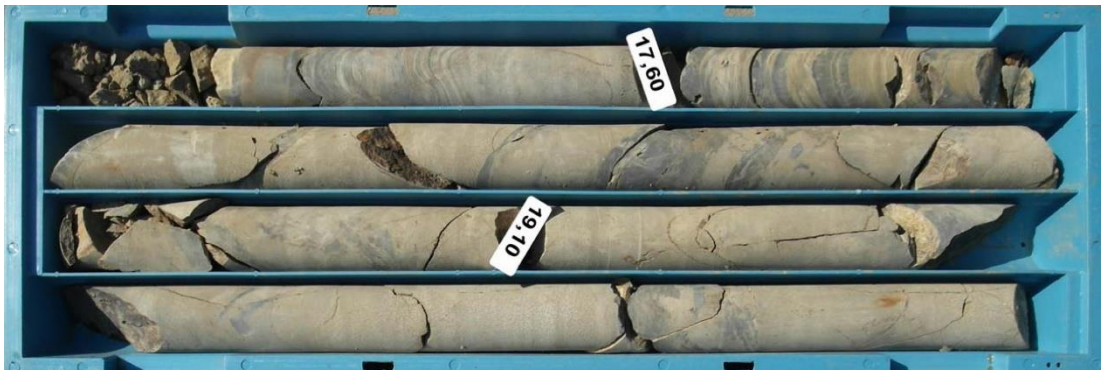

Figure C.18. S-AS-106, core box no: 5/13

Figure C.19. S-AS-106, core box no: 6/13

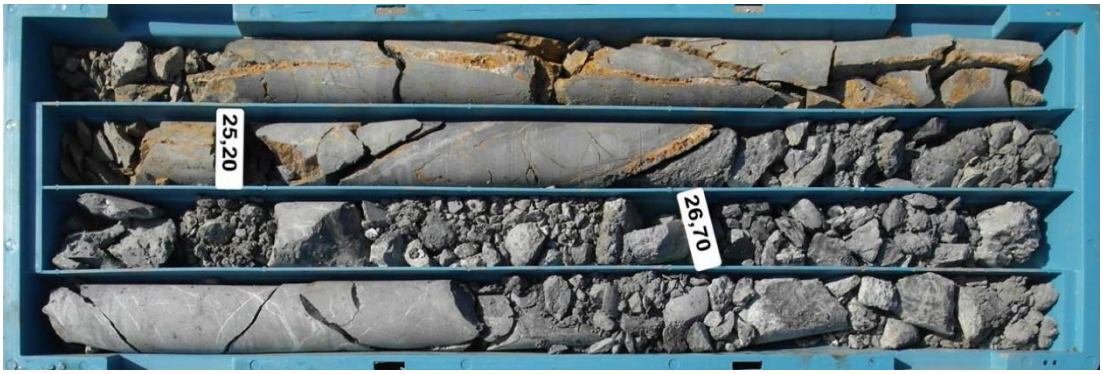

Figure C.20. S-AS-106, core box no: 7/13

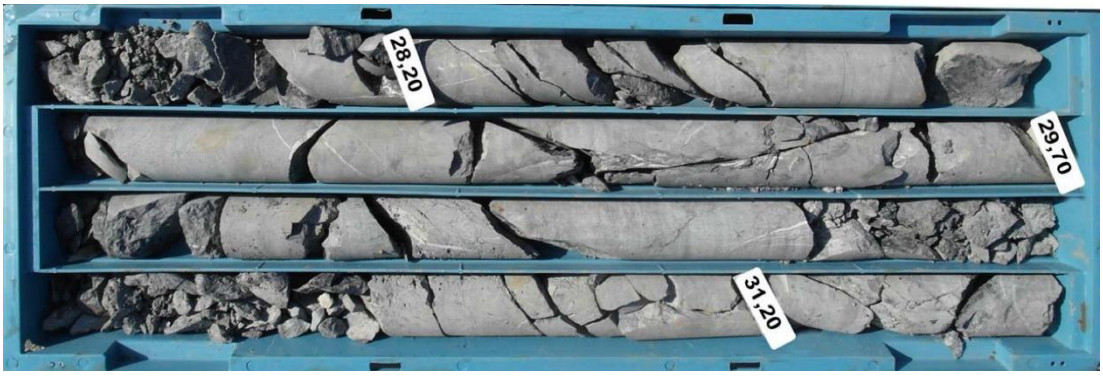

Figure C.21. S-AS-106, core box no: 8/13

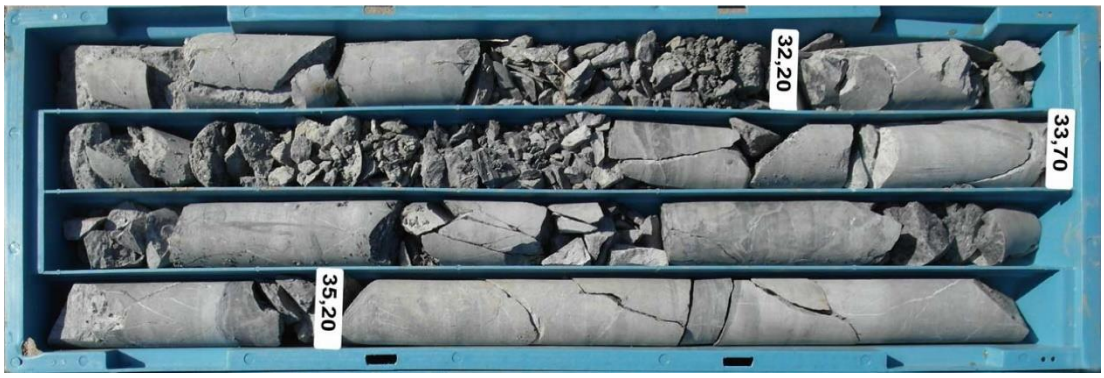

Figure C.22. S-AS-106, core box no: 9/13

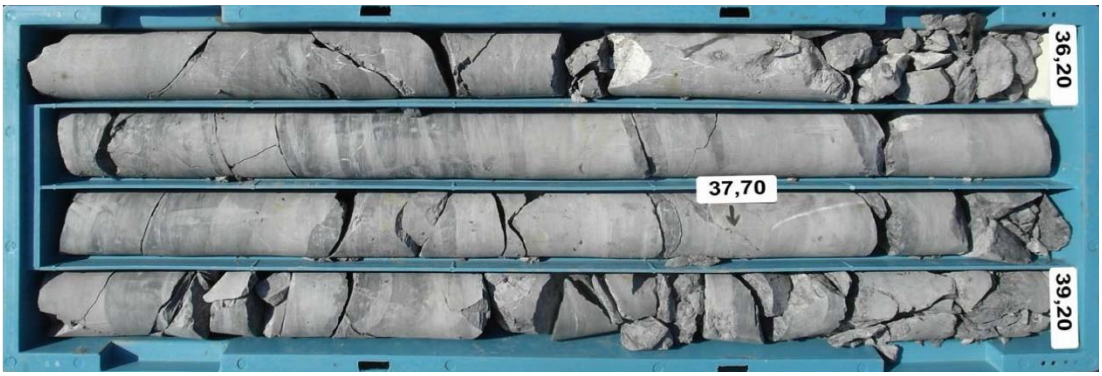

Figure C.23. S-AS-106, core box no: 10/13

Figure C.24. S-AS-106, core box no: 11/13

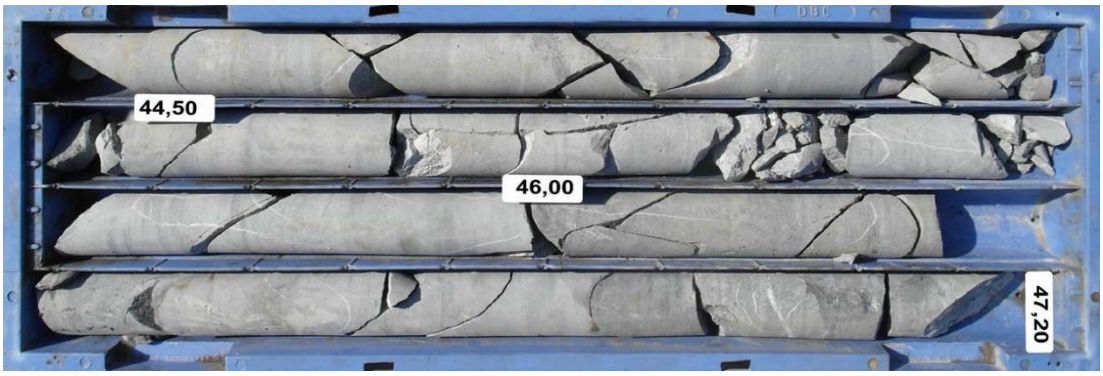

Figure C.25. S-AS-106, core box no: 12/13

Figure C.26. S-AS-106, core box no: 13/13

Figure C.27. S-AS-107, core box no: 1/7

Figure C.28. S-AS-107, core box no: 2/7

Figure C.29. S-AS-107, core box no: 3/7

Figure C.30. S-AS-107, core box no: 4/7

Figure C.31. S-AS-107, core box no: 5/7

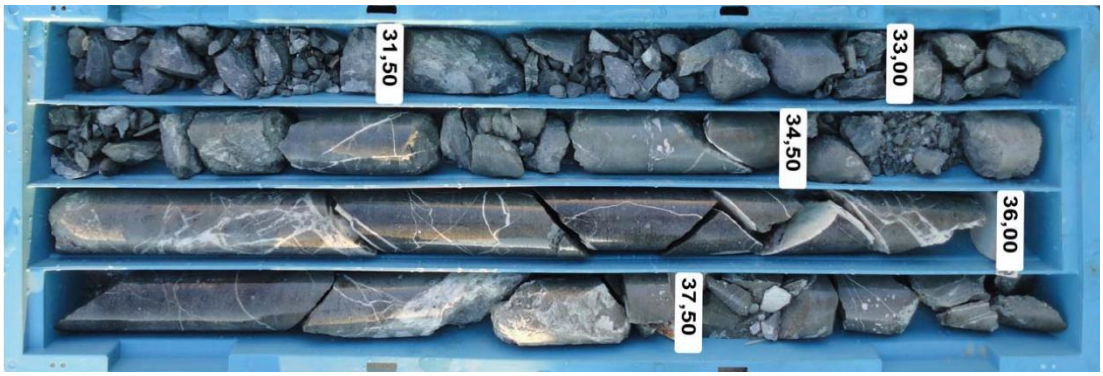

Figure C.32. S-AS-107, core box no: 6/7

Figure C.33. S-AS-107, core box no: 7/7

Figure C.34. S-AS-115, core box no: 1/3

Figure C.35. S-AS-115, core box no: 2/3

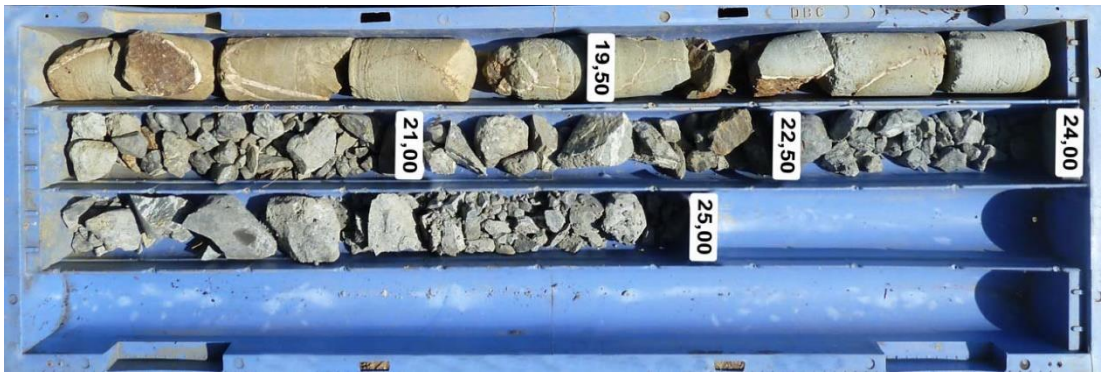

Figure C.36. S-AS-115, core box no: 3/3

Figure C.37. NTB-01, core box no: 1/13

Figure C.38. NTB-01, core box no: 2/13

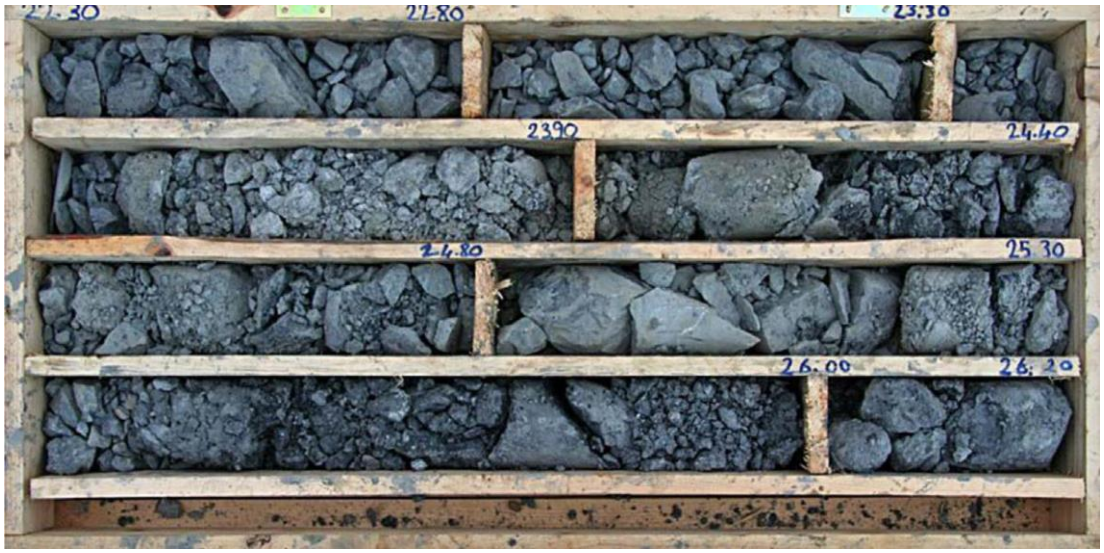

Figure C.39. NTB-01, core box no: 3/13

Figure C.40. NTB-01, core box no: 4/13

Figure C.41. NTB-01, core box no: 5/13

Figure C.42. NTB-01, core box no: 6/13

Figure C.43. NTB-01, core box no: 7/13

Figure C.44. NTB-01, core box no: 8/13

Figure C.45. NTB-01, core box no: 9/13

Figure C.46. NTB-01, core box no: 10/13

Figure C.47. NTB-01, core box no: 11/13

Figure C.48. NTB-01, core box no: 12/13

Figure C.49. NTB-01, core box no: 13/13

Figure C.50. NTB-02, core box no: 1/12

Figure C.51. NTB-02, core box no: 2/12

Figure C.52. NTB-02, core box no: 3/12

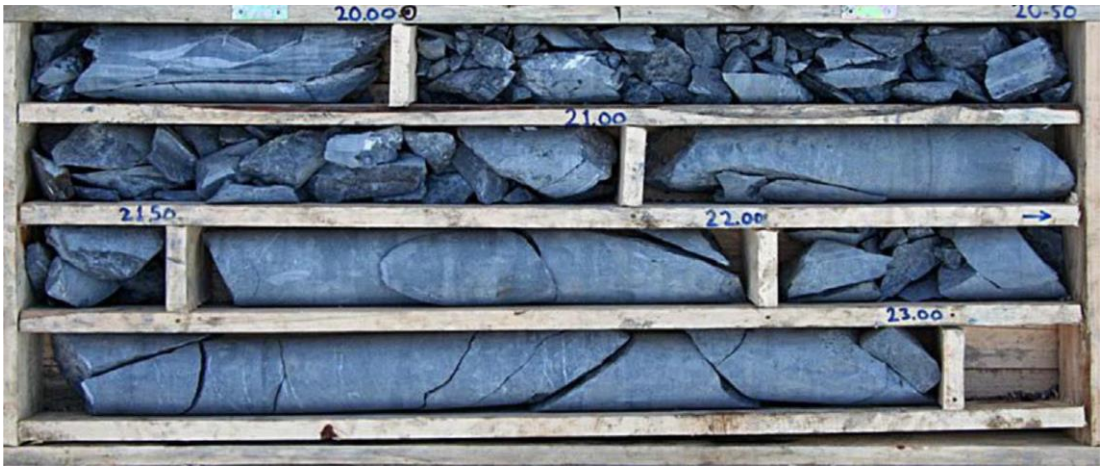

Figure C.53. NTB-02, core box no: 4/12

Figure C.54. NTB-02, core box no: 5/12

Figure C.55. NTB-02, core box no: 6/12

Figure C.56. NTB-02, core box no: 7/12

Figure C.57. NTB-02, core box no: 8/12

Figure C.58. NTB-02, core box no: 9/12

Figure C.59. NTB-02, core box no: 10/12

Figure C.60. NTB-02, core box no: 11/12

Figure C.61. NTB-02, core box no: 12/12

Figure C.62. NTB-03, core box no: 1/18

Figure C.63. NTB-03, core box no: 2/18

Figure C.64. NTB-03, core box no: 3/18

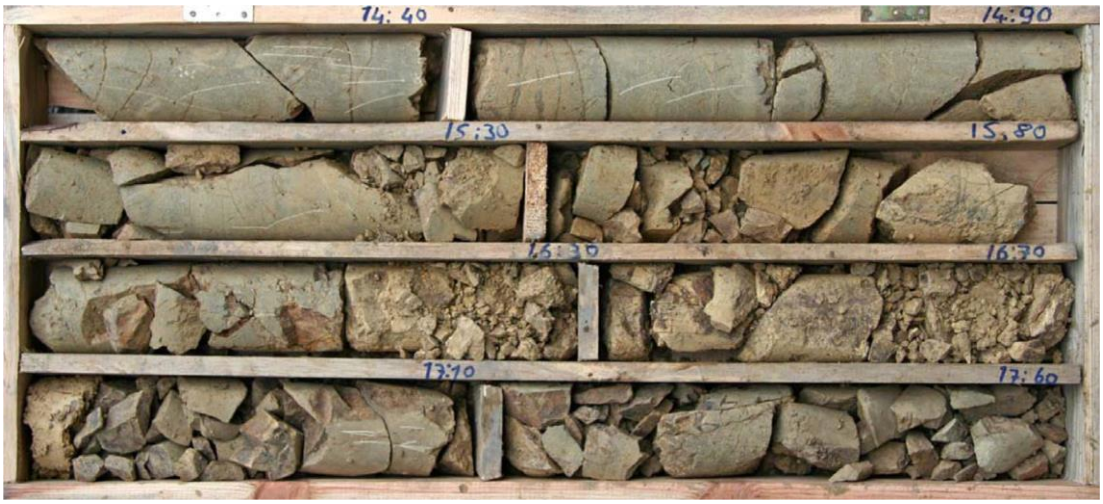

Figure C.65. NTB-03, core box no: 4/18

Figure C.66. NTB-03, core box no: 5/18

Figure C.67. NTB-03, core box no: 6/18

Figure C.68. NTB-03, core box no: 7/18

Figure C.69. NTB-03, core box no: 8/18

Figure C.70. NTB-03, core box no: 9/18

Figure C.71. NTB-03, core box no: 10/18

Figure C.72. NTB-03, core box no: 11/18

Figure C.73. NTB-03, core box no: 12/18

Figure C.74. NTB-03, core box no: 13/18

Figure C.75. NTB-03, core box no: 14/18

Figure C.76. NTB-03, core box no: 15/18

Figure C.77. NTB-03, core box no: 16/18

Figure C.78. NTB-03, core box no: 17/18

Figure C.79. NTB-03, core box no: 18/18

Figure C.80. NTB-04, core box no: 1/14

Figure C.81. NTB-04, core box no: 2/14

Figure C.82. NTB-04, core box no: 3/14

Figure C.83. NTB-04, core box no: 4/14

Figure C.84. NTB-04, core box no: 5/14

Figure C.85. NTB-04, core box no: 6/14

Figure C.86. NTB-04, core box no: 7/14

Figure C.87. NTB-04, core box no: 8/14

Figure C.88. NTB-04, core box no: 9/14

Figure C.89. NTB-04, core box no: 10/14

Figure C.90. NTB-04, core box no: 11/14

Figure C.91. NTB-04, core box no: 12/14

Figure C.92. NTB-04, core box no: 13/14

Figure C.93. NTB-04, core box no: 14/14

APPENDIX D

SOIL AND ROCK MECHANICS TEST RESULTS

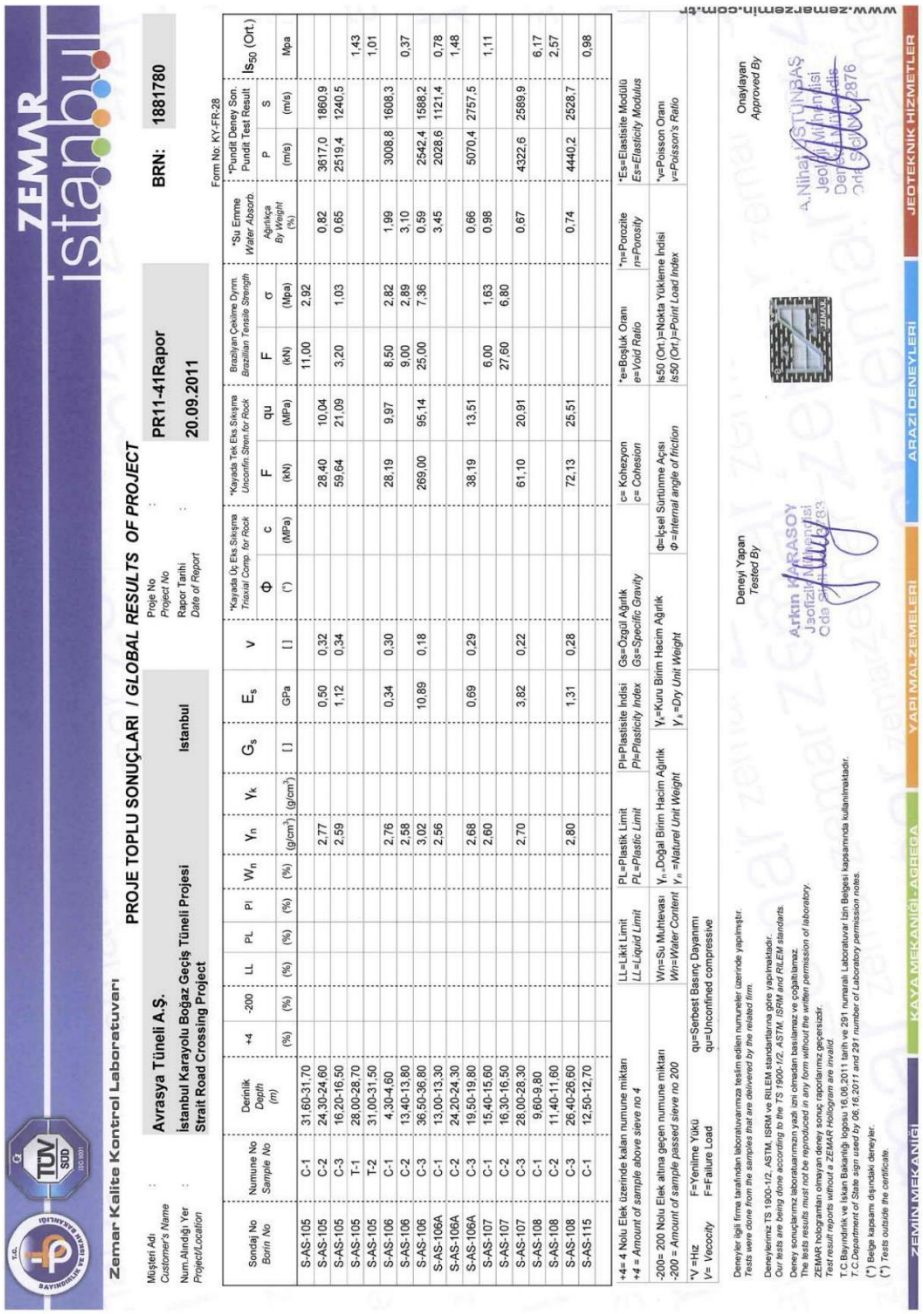

Zemar Kalite Kontrol Laboratuvarı

PROJE TOPLU SONUÇLARI / *GLOBAL RESULTS OF PROJECT*

Müşteri Adı / *Customer's Name*: Avrasya Tüneli A.Ş.

Num.Alındığı Yer / *Project/Location*: İstanbul Karayolu Boğaz Geçiş Tüneli Projesi / *Strait Road Crossing Project* — İstanbul

Proje No / *Project No*: PR11-41Rapor

Rapor Tarihi / *Date of Report*: 20.09.2011

BRN: 1881780

Form No: KY-FR.28

Sondaj No / *Boring No*	Numune No / *Sample No*	Derinlik / *Depth* (m)	+4 (%)	-200 (%)	LL (%)	PL (%)	PI (%)	W_n (%)	γ_n (g/cm³)	γ_k (g/cm³)	G_s [ ]	E_s GPa	v [ ]	*Kayada Üç Eks.Sıkışma / *Triaxial Comp. for Rock* Φ (°)	c (MPa)	*Kayada Tek Eks.Sıkışma / *Uniaxilh.Stren.for Rock* F (kN)	qu (MPa)	Brazilyan Çekme Dyn. / *Brazilian Tensile Strengh.* F (kN)	σ (Mpa)	*Su Emme / *Water Absorb.* Ağırlıkça / *By Weight* (%)	*Pundit Deney Son. / *Pundit Test Result* P (m/s)	S (m/s)	Is_{50} (Ort.) Mpa
S-AS-105	C-1	31,60-31,70							2,77			0,50	0,32			28,40	10,04	11,00	2,92				
S-AS-105	C-2	24,30-24,60																		0,82	3617,0	1860,9	
S-AS-105	C-3	16,20-16,50							2,59			1,12	0,34			59,64	21,09	3,20	1,03	0,65	2519,4	1240,5	
S-AS-105	T-1	28,00-28,70																					1,43
S-AS-105	T-2	31,00-31,50																					1,01
S-AS-106	C-1	4,30-4,60							2,76			0,34	0,30			28,19	9,97	8,50	2,82	1,99	3008,8	1608,3	
S-AS-106	C-2	13,40-13,80							2,58									9,00	2,89	3,10			0,37
S-AS-106	C-3	36,50-36,80							3,02			10,89	0,18			269,00	95,14	25,00	7,36	0,59	2542,4	1588,2	
S-AS-106A	C-1	13,00-13,30							2,56											3,45	2028,6	1121,4	0,78
S-AS-106A	C-2	24,20-24,30																					1,48
S-AS-106A	C-3	19,50-19,80							2,68			0,69	0,29			38,19	13,51			0,66	5070,4	2757,5	
S-AS-107	C-1	15,40-15,60							2,60									6,00	1,63	0,98			1,11
S-AS-107	C-2	16,30-16,50																27,60	6,80				
S-AS-107	C-3	28,00-28,30							2,70			3,82	0,22			61,10	20,91			0,67	4322,6	2589,9	
S-AS-108	C-1	9,60-9,80																					6,17
S-AS-108	C-2	11,40-11,60																					2,57
S-AS-108	C-3	26,40-26,60							2,80			1,31	0,28			72,13	25,51			0,74	4440,2	2528,7	
S-AS-115	C-1	12,50-12,70																					0,98

*+4= Nolu Elek üzerinde kalan numune miktarı / *+4 = Amount of sample above sieve no 4*

*-200= 200 Nolu Elek altına geçen numune miktarı / *-200 = Amount of sample passed sieve no 200*

*V =Hız / *v= Velocity*

F=Yenilme Yükü / *F=Failure Load*

qu=Serbest Basınç Dayanımı / *qu=Unconfined compressive*

LL=Likit Limit / *LL=Liquid Limit*

PL=Plastik Limit / *PL=Plastic Limit*

Pl=Plastisite İndisi / *Pl=Plasticity Index*

Gs=Özgül Ağırlık / *Gs=Specific Gravity*

c= Kohezyon / *c= Cohesion*

Φ=İçsel Sürtünme Açısı / *Φ=Internal angle of friction*

*Ts=Boşluk Oranı / *e=Void Ratio*

*n=Porozite / *n=Porosity*

*Es=Elastisite Modülü / *Es=Elasticity Modulus*

Win=Su Muhtevası / *Win=Water Content*

γ_n =Doğal Birim Hacim Ağırlık / γ_n =*Natural Unit Weight*

γ_k =Kuru Birim Hacim Ağırlık / γ_k =*Dry Unit Weight*

Is50 (Ort.)=Nokta Yükleme İndisi / *Is50 (Ort.)=Point Load Index*

*ν=Poisson Oranı / *ν=Poisson's Ratio*

Deneyler ilgi firma tarafından laboratuvarımıza teslim edilen numuneler üzerinde yapılmıştır.
Tests were done from the samples that are delivered by the related firm.

Deneylerimiz TS 1900-1/2, ASTM, ISRM ve RILEM standartlarına göre yapılmaktadır.
Our tests are being done according to the TS 1900-1/2, ASTM, ISRM and RILEM standards.

Deney sonuçlarımız laboratuarımızın yazılı izni olmadan basılamaz ve çoğaltılamaz.
The test results must not be reproduced in any form without the written permission of laboratory.

ZEMAR'a ait olmayan numune deney sonuçlarını kapsamaz.
Test result reports without a ZEMAR hologram are invalid.

T.C Bayındırlık ve İskan Bakanlığı logosu 16.06.2011 tarih ve 291 numaralı Laboratuvar İzin Belgesi kapsamında kullanılmaktadır.
T.C.Department of State sign used by 06.16.2011 and 291 number of Laboratory permission notes.

(*) Belge kapsamı dışındaki deneyler.
(*) *Tests outside the certificate.*

Deneyi Yapan / *Tested By*

Onaylayan / *Approved By*

ZEMİNMEKANİĞİ | KAYA MEKANİĞİ-AGREGA | YAPI MALZEMELERİ | ARAZİ DENEYLERİ | JEOTEKNİK HİZMETLER

www.zemarzemin.com.tr

Figure D.1. Global results of rock mechanic laboratory tests

İSTANBUL KÜLTÜR ÜNİVERSİTESİ * GEOTEKNİK LABORATUVARI

SHEARBOX TEST (CD)

PROJECT	EURASIAN TUNNEL		
LOCATION	ISTANBUL		
DESCRIPTION OF SAMPLE	gray, gravelly		
BOREHOLE NO.	NTB - 1	*RATE OF SHEAR*	0,3 mm/dak
DEPTH	9.0-12.00 m	*PROV.RING.CONSTANT*	1,503
DATE	26.03.2010	*OPERATOR*	...UAT YAKUT TEKNİSYEN

TEST NO.		1	2
SAMPLE SIZE (cm)		6,33	6,33
SAMPLE HEIGHT (cm)		2,00	2,00
CROSS SECTION (cm²)		31,47	31,47
VOLUME (cm³)		62,94	62,94
RING+SAMPLE (g)		267,64	262,24
MASS OF RING (g)		131,30	131,25
MASS OF SAMPLE BEFORE TEST (g)		136,34	130,99
MASS OF SAMPLE AFTER TEST (g)		132,66	126,00
DRY SAMPLE (g)		119,56	114,63
MASS OF WATER (g)		16,78	16,36
MOISTURE CONTENT (%)		14	14
UNIT WEIGHT BEFORE TEST (kN/m³)		21,25	20,42
UNIT WEIGHT AFTER TEST (kN/m³)		13,92	12,82
VERTICAL LOAD (kg)		63	126
σ_n *(kPa)*		200	400
INITIAL DIAL GAUGE READING		2500	2500
DIAL GAUGE AFTER CONSOLIDATION		2358	2216
COMPRESSION (mm)		0,284	0,568
VOID RATIO		0,40	0,46
DEGREE OF SATURATION (%)		94	83
SPECIFIC GRAVITY OF SOIL		2,65	

30 Mart 2010
Prof.Dr. Ahmet ONAT
Laboratuvar Teknik Yöneticisi
Denetçi NO: 13183

Figure D.2. Summary table of shear box test results of borehole NTB-1 (9.0-12.0 m sample depth)

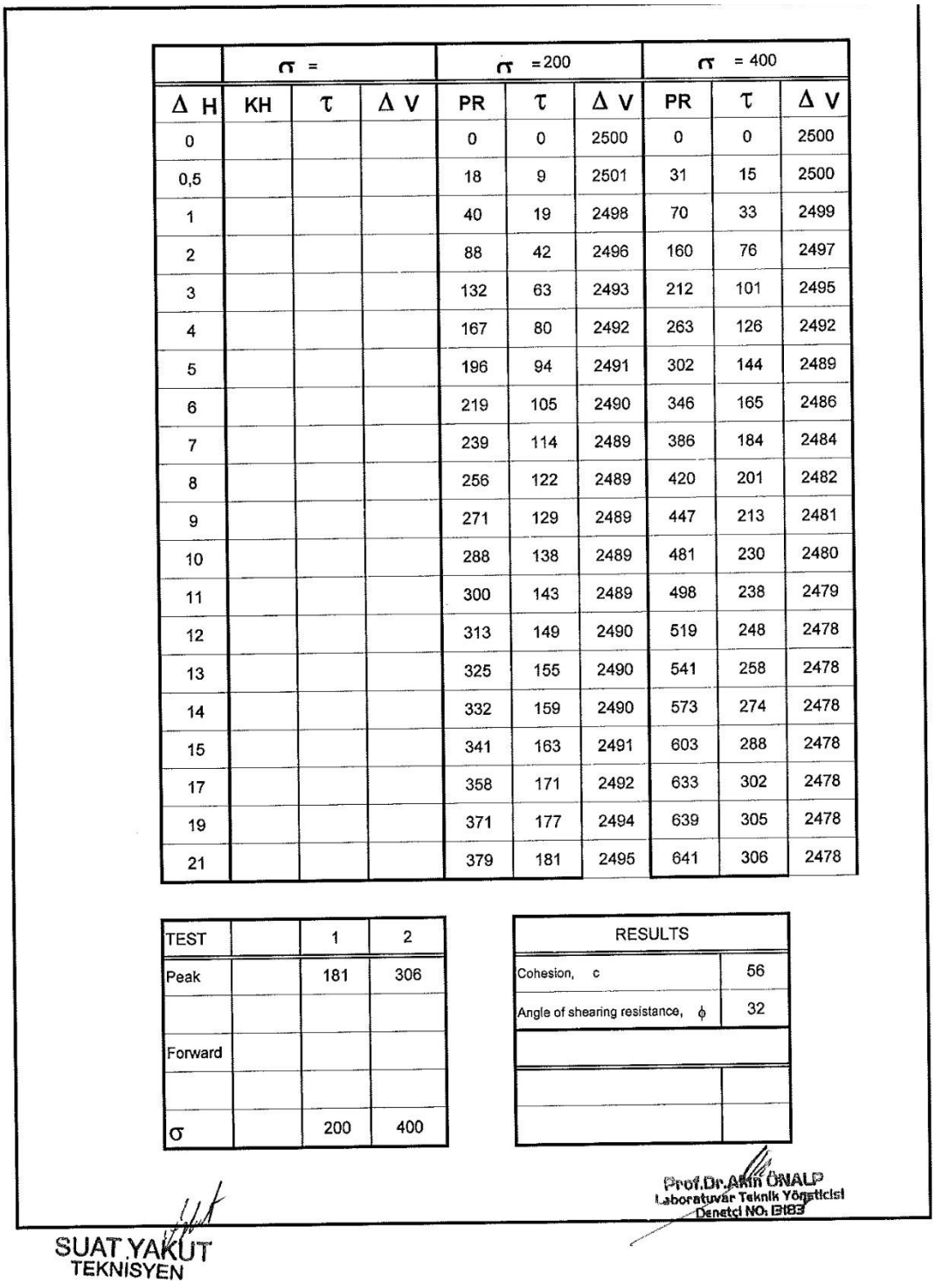

	σ =			σ = 200			σ = 400		
Δ H	KH	τ	Δ V	PR	τ	Δ V	PR	τ	Δ V
0				0	0	2500	0	0	2500
0,5				18	9	2501	31	15	2500
1				40	19	2498	70	33	2499
2				88	42	2496	160	76	2497
3				132	63	2493	212	101	2495
4				167	80	2492	263	126	2492
5				196	94	2491	302	144	2489
6				219	105	2490	346	165	2486
7				239	114	2489	386	184	2484
8				256	122	2489	420	201	2482
9				271	129	2489	447	213	2481
10				288	138	2489	481	230	2480
11				300	143	2489	498	238	2479
12				313	149	2490	519	248	2478
13				325	155	2490	541	258	2478
14				332	159	2490	573	274	2478
15				341	163	2491	603	288	2478
17				358	171	2492	633	302	2478
19				371	177	2494	639	305	2478
21				379	181	2495	641	306	2478

TEST		1	2
Peak		181	306
Forward			
σ		200	400

RESULTS	
Cohesion, c	56
Angle of shearing resistance, ϕ	32

Figure D.3. First detailed result page of shear box test of borehole NTB-1 (9.0-12.0 m sample depth)

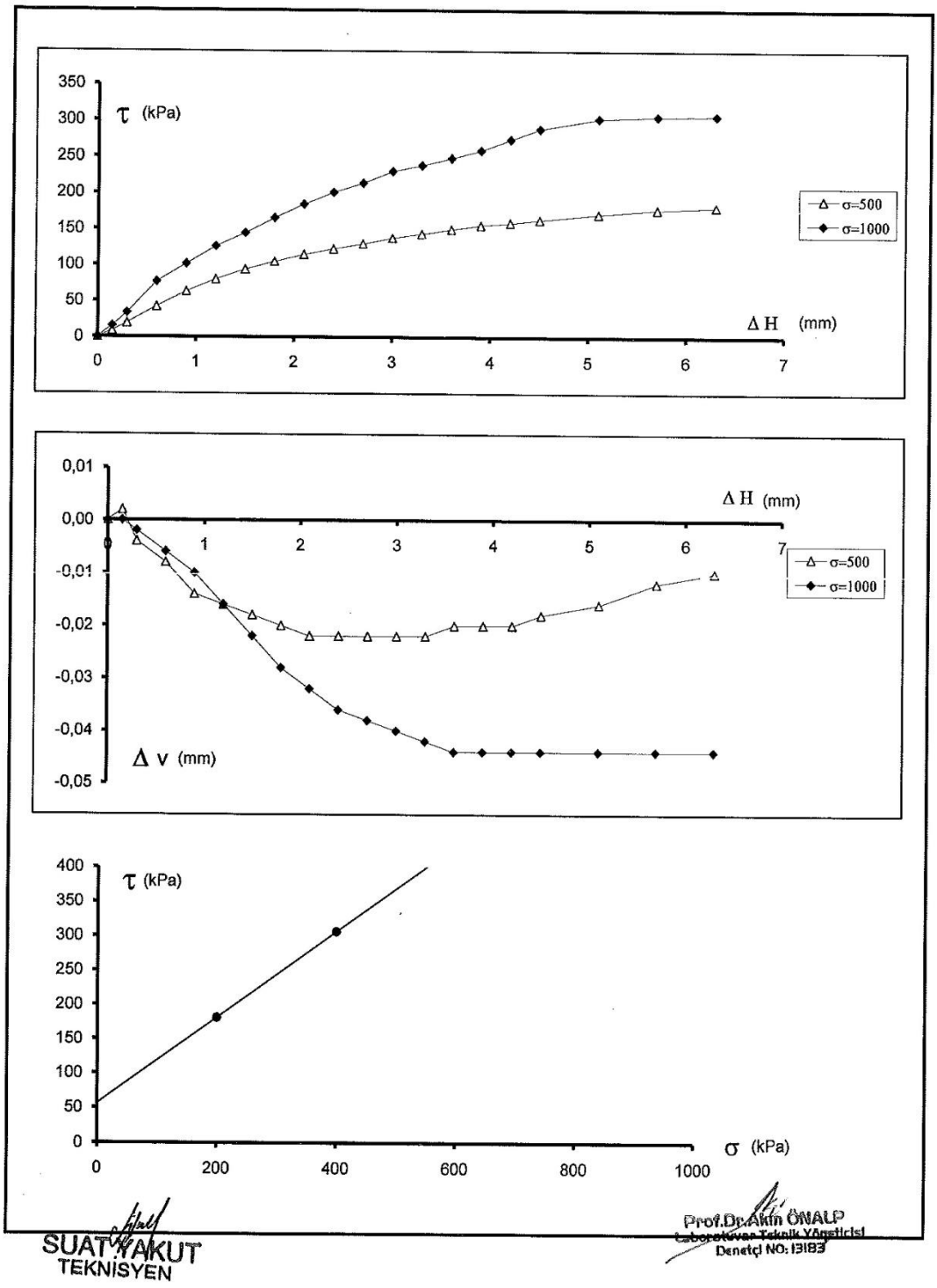

Figure D.4. Second detailed result page of shear box test of borehole NTB-1 (9.0-12.0 m sample depth)

İSTANBUL KÜLTÜR ÜNİVERSİTESİ ** GEOTEKNİK LABORATUVARI

DETERMINATION OF SPECIFIC GRAVITY/ÖZGÜL AĞIRLIK TAYİNİ

Reference
ASTM D854

Project No.:		**Client:**	AVRASYA TÜNEL AŞ
Project:	EURASIAN TUNNEL	**Lab ID No:**	PR001/8
Location:	ISTANBUL	**Date:**	23.03.2010

BOREHOLE	SAMPLE NUMBER	Depth (m):	PİKNOMETRE NO.	PİKNOMETRE AĞ. (g)	PİKNOMETRE+NUMUNE (g)	PİKNOMETRE+SU (g)	PİKNOMETRE+NUMUNE+SU (g)	SICAKLIK (°C)	ÖZGÜL AĞIRLIK	ORTALAMA
NTB2	SPT		41	36,479	57,58	86,9	99,98	25	2,631	2,62
			19	28,089	45,18	78,45	88,99	25	2,609	
NTB-1	SPT	9.00	41	35,11	56,91	84,50	98,25	25	2,708	2,72
			10	36,28	58,32	86,01	100,00	25	2,738	

SUAT YAKUT
TEKNİSYEN

Prof.Dr.Aşkın ÖNALP
Laboratuvar Teknik Yöneticisi
Denetçi NO: İNŞ

Figure D.5. Determination of specific gravity of SPT sample from borehole NTB-1 and NTB-2 (9.0-12.0 m sample depth)

BELGE NO:44

İSTANBUL KÜLTÜR ÜNİVERSİTESİ * GEOTEKNİK LABORATUVARI

SHEARBOX TEST (CU)

PROJECT	EURASIAN TUNNEL		
LOCATION	ISTANBUL		
DESCRIPTION OF SAMPLE	dark brown,contains claystone fragments		
BOREHOLE NO.	NTB - 2	RATE OF SHEAR	0,5 mm/dak
DEPTH	3.0-7.5 m	PROV.RING.CONSTANT	1,503
DATE	23.03.2010	OPERATOR	SUAT YAKUT TEKNİSYEN

TEST NO.		1	2
SAMPLE SIZE (cm)		6,33	6,33
SAMPLE HEIGHT (cm)		2,85	2,73
CROSS SECTION (cm^2)		31,47	31,47
VOLUME (cm^3)		89,69	85,91
RING+SAMPLE (g)		254,88	254,99
MASS OF RING (g)		131,28	133,03
MASS OF SAMPLE BEFORE TEST (g)		123,60	121,96
MASS OF SAMPLE AFTER TEST (g)		121,88	118,19
DRY SAMPLE (g)		101,46	99,68
MASS OF WATER (g)		22,14	22,28
MOISTURE CONTENT (%)		22	22
UNIT WEIGHT BEFORE TEST (kN/m^3)		13,52	13,93
UNIT WEIGHT AFTER TEST (kN/m^3)		12,78	11,98
VERTICAL LOAD (kg)		47	95
σ_n (kPa)		149	302
INITIAL DIAL GAUGE READING		2500	2500
DIAL GAUGE AFTER CONSOLIDATION		2361	2281
COMPRESSION (mm)		0,278	0,438
VOID RATIO		1,38	1,32
DEGREE OF SATURATION (%)		43	46
SPECIFIC GRAVITY OF SOIL		2,69	

22 Mart 2010
Prof.Dr.Atilla ÜNAL
Laboratuvar Teknik Yöneticisi
Denetçi NO: 8183

Figure D.6. Summary table of shear box test results of borehole NTB-2 (3.0-7.5 m sample depth)

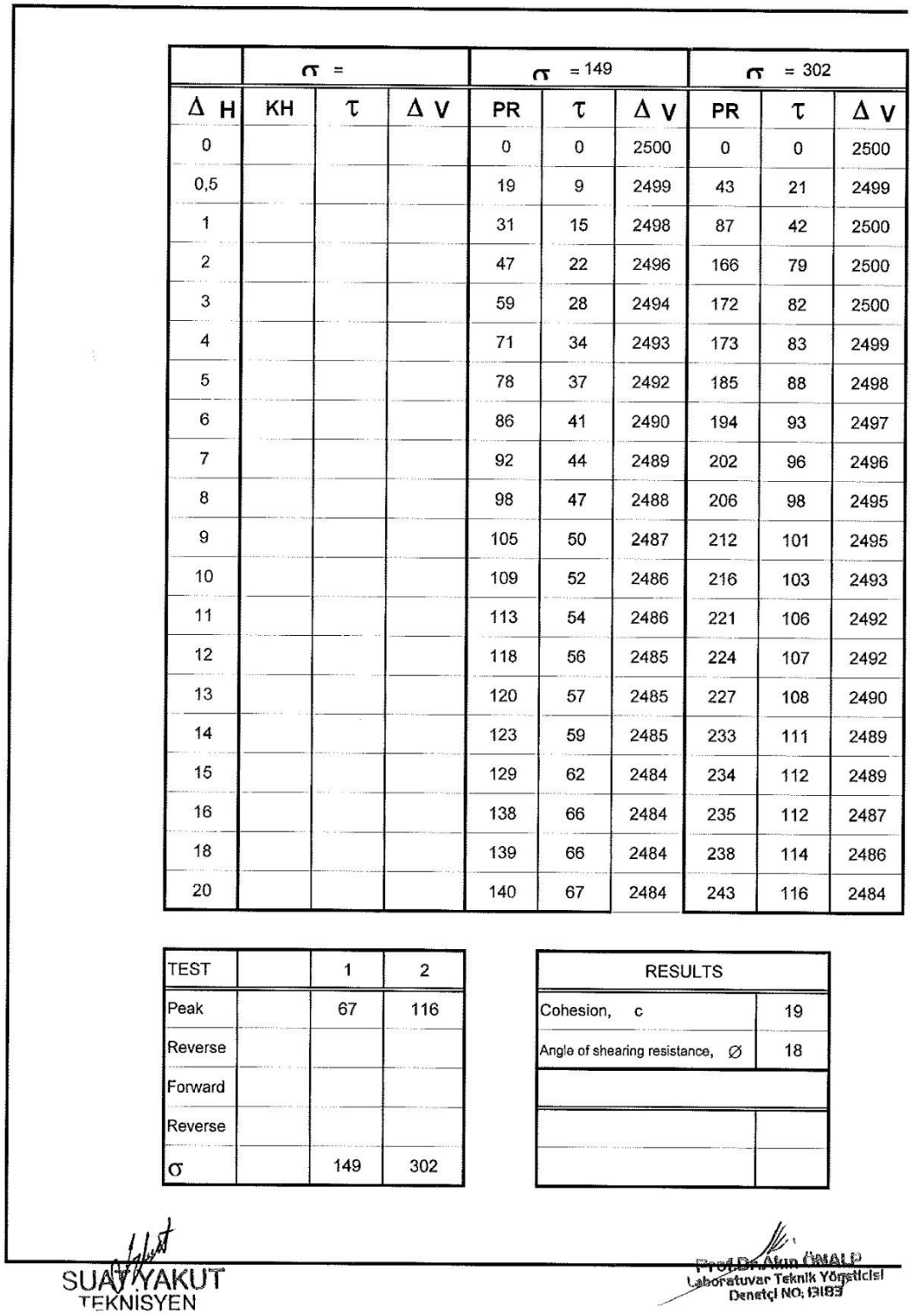

	σ =			σ = 149			σ = 302		
Δ H	KH	τ	Δ V	PR	τ	Δ V	PR	τ	Δ V
0				0	0	2500	0	0	2500
0,5				19	9	2499	43	21	2499
1				31	15	2498	87	42	2500
2				47	22	2496	166	79	2500
3				59	28	2494	172	82	2500
4				71	34	2493	173	83	2499
5				78	37	2492	185	88	2498
6				86	41	2490	194	93	2497
7				92	44	2489	202	96	2496
8				98	47	2488	206	98	2495
9				105	50	2487	212	101	2495
10				109	52	2486	216	103	2493
11				113	54	2486	221	106	2492
12				118	56	2485	224	107	2492
13				120	57	2485	227	108	2490
14				123	59	2485	233	111	2489
15				129	62	2484	234	112	2489
16				138	66	2484	235	112	2487
18				139	66	2484	238	114	2486
20				140	67	2484	243	116	2484

TEST		1	2
Peak		67	116
Reverse			
Forward			
Reverse			
σ		149	302

RESULTS	
Cohesion, c	19
Angle of shearing resistance, Ø	18

SUAT YAKUT
TEKNISYEN

Prof.Dr. Akın ÖNALP
Laboratuvar Teknik Yöneticisi
Denetçi NO: 13183

Figure D.7. First detailed result page of shear box test of borehole NTB-2 (3.0-7.5 m sample depth)

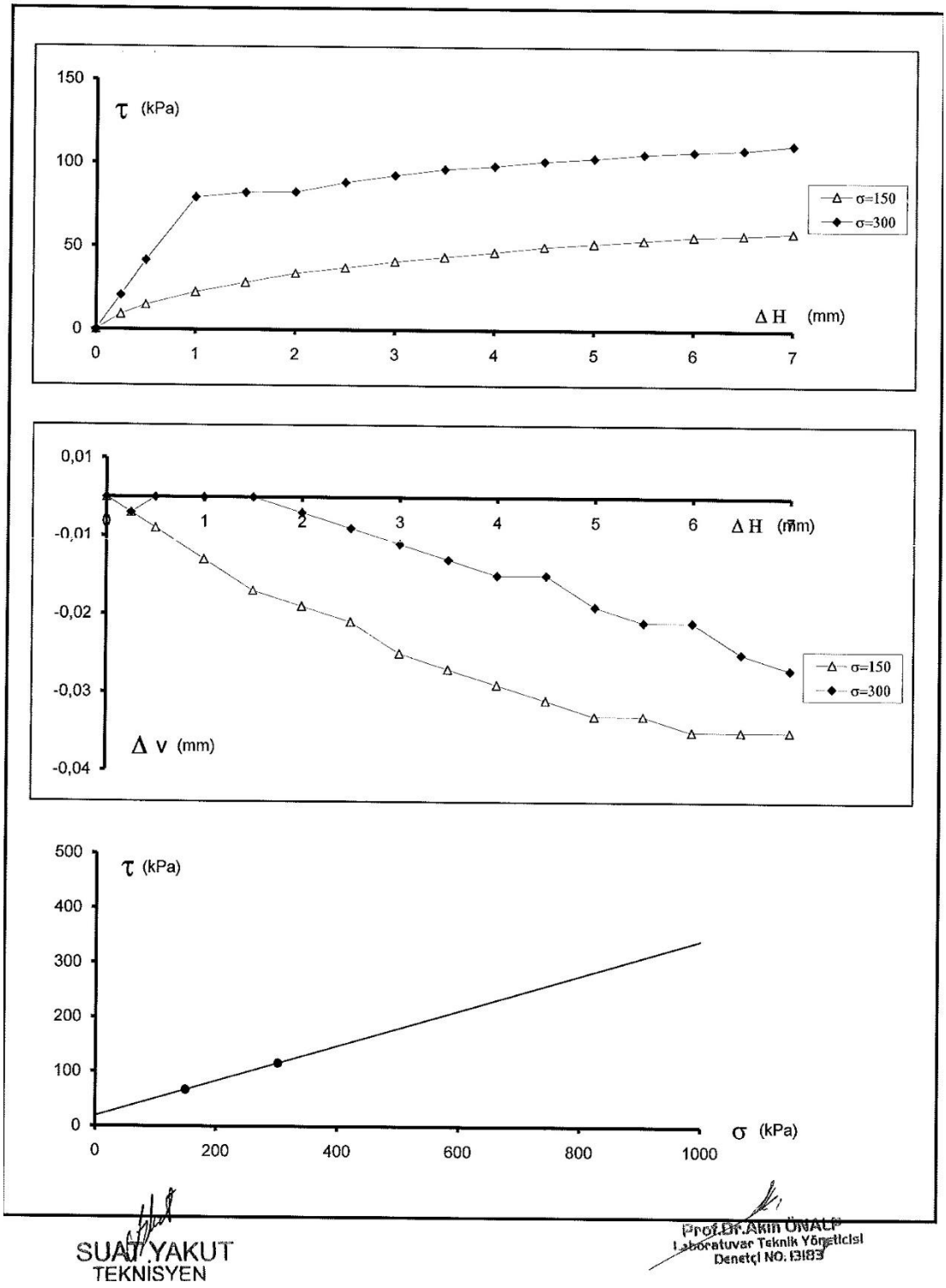

Figure D.8. Second detailed result page of shear box test of borehole NTB-2 (3.0-7.5 m sample depth)

APPENDIX E

WATER PRESSURE TEST RESULTS

ZEMAR İSTANBUL ZEMAR Zemin Araştırma ve Mühendislik

Istanbul Strait Road Crossing Project
İstanbul Karayolu Boğaz Geçiş Projesi

Avrasya TÜNELİ

Water Pressure Test (Lugeon Test) / *Basınçlı Su Testi (Lugeon Deneyi)*

Borehole No: *Sondaj No*	**S-AS-105**	**Location:** *Lokasyon*	**KM9+890**	**Date** / *Tarih:*	**07.09.2011**
Ground Water Level *Yeraltısuyu Seviyesi*	5,00 m			***Test Hole Diameter*** *Kuyu Çapı*	96 mm
Stage (m) *Kademe*	3,00 - 4,00			**Stage Length** *Kademe Uzunluğu*	1,00 m
Hole Inclination (from vertical) *Kuyu Eğimi*	0 (°)			**Total Pipe Lenght** *Toplam Boru Uzunluğu*	3,00 m
Rod Diameter *Tij İç Çapı*	77,80 mm			**Rod+Coupling Lenght** *Tij+Manşon Uzunluğu*	3,00 m
Coupling Diameter *Manşon İç Çapı*	77,80 mm			**Coupling Lenght** *Manşon Uzunluğu*	0,00 m
Packer Inner Diameter *Tıkaç İç Çapı*	22,00 mm			**Packer Lenght** *Tıkaç Uzunluğu*	1,34 m
Hose Diameter *Hortum İç Çapı*	22,00 mm			**Hose Lenght** *Hortum Uzunluğu*	5,00 m

PM	T	TOTAL Q	H	PC	PE	AQ	LUGEON
					0,00	0,00	
3,0	5	**15**	0,40	0,000	3,40	3,00	8,72
6,0	5	**28**	0,40	0,001	6,40	5,60	6,08
9,0	5	**30**	0,40	0,001	9,40	6,00	6,36
6,0	5	**21**	0,40	0,000	6,40	4,20	6,84
3,0	5	**10**	0,40	0,000	3,40	2,00	5,88

LUGEON VALUE = **6,78** **Laminar** **PERMEABILITY (m/sec.) =** **3,14E-05**

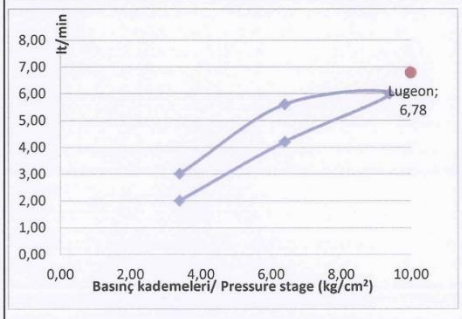

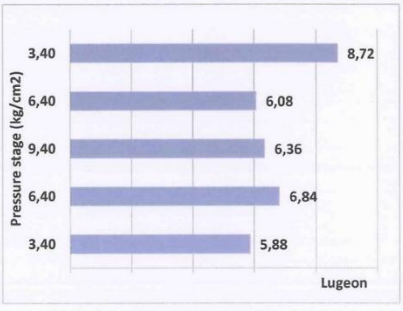

H : Hydrostatic head pressure (kg / cm^2)
PC : Friction losses (kg / cm^2)
PE : Effective pressure (kg / cm^2)
AQ : Coef. of absorption (l / m / min.)

PM : Mano pressure (kg/cm^2)
T : Time (min.)
T.Q : Total take (l)

Tested By
Deneyi Yapan

Approved By
Onaylayan

Figure E.1. Water pressure test result of borehole S-AS-105 at depth 3.00-4.0 m

ZEMAR İstanbul
ZEMAR Zemin Araştırma ve Mühendislik

Istanbul Strait Road Crossing Project
İstanbul Karayolu Boğaz Geçiş Projesi

Avrasya TÜNELİ

Water Pressure Test (Lugeon Test) / *Basınçlı Su Testi (Lugeon Deneyi)*

Borehole No: *Sondaj No*	**S-AS-105**	**Location:** *Lokasyon*	**KM9+890**	**Date / *Tarih:***	**07.09.2011**
Ground Water Level *Yeraltısuyu Seviyesi*	2,50 m			***Test Hole Diameter*** *Kuyu Çapı*	96 mm
Stage (m) *Kademe*	6,00 - 7,00			**Stage Length** *Kademe Uzunluğu*	1,00 m
Hole Inclination (from vertical) *Kuyu Eğimi*	0 (°)			**Total Pipe Lenght** *Toplam Boru Uzunluğu*	6,00 m
Rod Diameter *Tij İç Çapı*	77,80 mm			**Rod+Coupling Lenght** *Tij+Manşon Uzunluğu*	3,00 m
Coupling Diameter *Manşon İç Çapı*	77,80 mm			**Coupling Lenght** *Manşon Uzunluğu*	0,00 m
Packer Inner Diameter *Tıkaç İç Çapı*	22,00 mm			**Packer Lenght** *Tıkaç Uzunluğu*	1,34 m
Hose Diameter *Hortum İç Çapı*	22,00 mm			**Hose Lenght** *Hortum Uzunluğu*	5,00 m

PM	T	TOTAL Q	H	PC	PE	AQ	LUGEON
					0,00	0,00	
3,0	5	**10**	0,30	0,000	3,30	2,00	2,89
6,0	5	**12**	0,30	0,000	6,30	2,40	5,85
9,0	5	**26**	0,30	0,000	9,30	5,20	5,29
6,0	5	**24**	0,30	0,000	6,30	4,80	8,99
3,0	5	**7**	0,30	0,000	3,30	1,40	4,24

LUGEON VALUE = 5,46 **Laminar** **PERMEABILITY (m/sec.) = 2,43E-05**

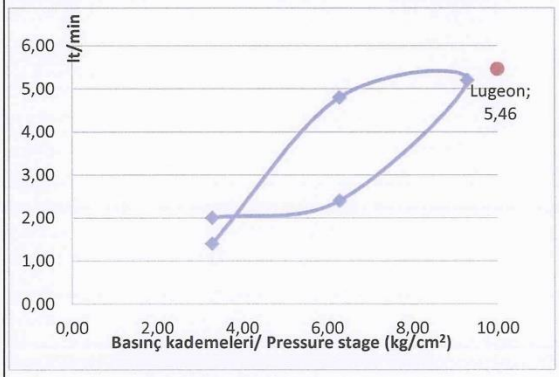

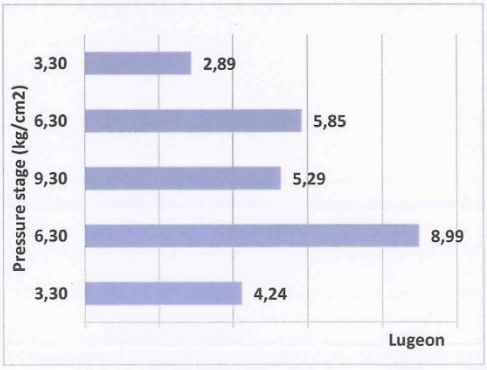

H : Hydrostatic head pressure (kg / cm^2)
PC : Friction losses (kg / cm^2)
PE : Effective pressure (kg / cm^2)
AQ : Coef. of absorption (l / m / min.)

PM : Mano pressure (kg/cm^2)
T : Time (min.)
T.Q : Total take (l)

Tested By
Deneyi Yapan

Approved By
Onaylayan

Figure E.2. Water pressure test result of borehole S-AS-105 at depth 6.00-7.0 m

ZEMAR İSTANBUL ZEMAR Zemin Araştırma ve Mühendislik

Istanbul Strait Road Crossing Project
İstanbul Karayolu Boğaz Geçiş Projesi

Avrasya TÜNELİ

Water Pressure Test (Lugeon Test) / *Basınçlı Su Testi (Lugeon Deneyi)*

Borehole No: *Sondaj No*	**S-AS-105**	**Location:** *Lokasyon*	**KM9+890**	**Date** / *Tarih:*	**08.09.2011**
Ground Water Level *Yeraltısuyu Seviyesi*	2,50 m			***Test Hole Diameter*** *Kuyu Çapı*	96 mm
Stage (m) *Kademe*	9,00 - 10,00			**Stage Length** *Kademe Uzunluğu*	1,00 m
Hole Inclination (from vertical) *Kuyu Eğimi*	0 (°)			**Total Pipe Lenght** *Toplam Boru Uzunluğu*	9,00 m
Rod Diameter *Tij İç Çapı*	77,80 mm			**Rod+Coupling Lenght** *Tij+Manşon Uzunluğu*	3,00 m
Coupling Diameter *Manşon İç Çapı*	77,80 mm			**Coupling Lenght** *Manşon Uzunluğu*	0,00 m
Packer Inner Diameter *Tıkaç İç Çapı*	22,00 mm			**Packer Lenght** *Tıkaç Uzunluğu*	1,34 m
Hose Diameter *Hortum İç Çapı*	22,00 mm			**Hose Lenght** *Hortum Uzunluğu*	5,00 m

PM	T	TOTAL Q	H	PC	PE	AQ	LUGEON
					0,00	0,00	
3,0	5	**12**	0,30	0,000	3,30	2,40	3,74
6,0	5	**15**	0,30	0,000	6,30	3,00	10,90
9,0	5	**47**	0,30	0,002	9,30	9,40	9,91
6,0	5	**36**	0,30	0,001	6,30	7,20	10,16
3,0	5	**24**	0,30	0,000	3,30	4,80	14,55

LUGEON VALUE = 9,85 **Laminar** **PERMEABILITY (m/sec.) = 4,11E-05**

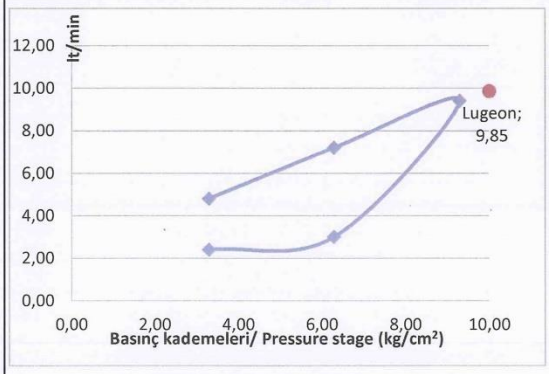

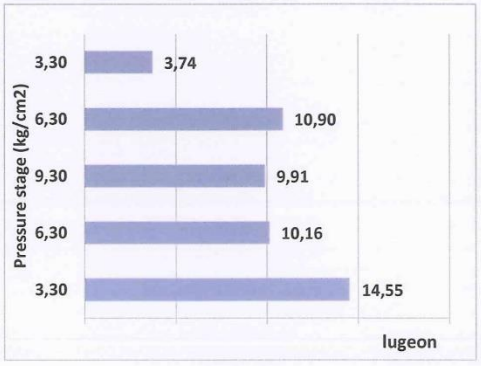

H : Hydrostatic head pressure (kg / cm^2)
PC : Friction losses (kg / cm^2)
PE : Effective pressure (kg / cm^2)
AQ : Coef. of absorption (l / m / min.)

PM : Mano pressure (kg/cm^2)
T : Time (min.)
T.Q : Total take (l)

Tested By
Deneyi Yapan

Approved By
Onaylayan

Figure E.3. Water pressure test result of borehole S-AS-105 at depth 9.00-10.0 m

ZEMAR İstanbul ZEMAR Zemin Araştırma ve Mühendislik

Istanbul Strait Road Crossing Project
İstanbul Karayolu Boğaz Geçiş Projesi

Avrasya TÜNELİ

Water Pressure Test (Lugeon Test) / *Basınçlı Su Testi (Lugeon Deneyi)*

Borehole No: *Sondaj No*	**S-AS-105**	**Location:** *Lokasyon*	**KM9+890**	**Date** / *Tarih:*	**08.09.2011**
Ground Water Level *Yeraltısuyu Seviyesi*	2,50 m			***Test Hole Diameter*** *Kuyu Çapı*	96 mm
Stage (m) *Kademe*	12,00 - 13,00			**Stage Length** *Kademe Uzunluğu*	1,00 m
Hole Inclination (from vertical) *Kuyu Eğimi*	0 (°)			**Total Pipe Lenght** *Toplam Boru Uzunluğu*	12,00 m
Rod Diameter *Tij İç Çapı*	77,80 mm			**Rod+Coupling Lenght** *Tij+Manşon Uzunluğu*	3,00 m
Coupling Diameter *Manşon İç Çapı*	77,80 mm			**Coupling Lenght** *Manşon Uzunluğu*	0,00 m
Packer Inner Diameter *Tıkaç İç Çapı*	22,00 mm			**Packer Lenght** *Tıkaç Uzunluğu*	1,34 m
Hose Diameter *Hortum İç Çapı*	22,00 mm			**Hose Lenght** *Hortum Uzunluğu*	5,00 m

PM	T	TOTAL Q	H	PC	PE	AQ	LUGEON
					0,00	0,00	
3,0	5	**2**	0,30	0,000	3,30	0,40	1,74
6,0	5	**5**	0,30	0,000	6,30	1,00	1,12
9,0	5	**6**	0,30	0,000	9,30	1,10	1,19
6,0	5	**4**	0,30	0,000	6,30	0,70	1,32
3,0	5	**1**	0,30	0,000	3,30	0,20	0,61

LUGEON VALUE = 1,20 **Laminar** **PERMEABILITY (m/sec.) = 4,57E-06**

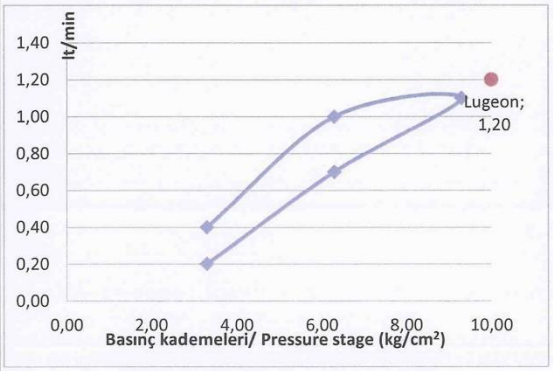

H : Hydrostatic head pressure (kg / cm^2)
PC : Friction losses (kg / cm^2)
PE : Effective pressure (kg / cm^2)
AQ : Coef. of absorption (l / m / min.)

PM : Mano pressure (kg/cm^2)
T : Time (min.)
T.Q : Total take (l)

Tested By
Deneyi Yapan

Approved By
Onaylayan

Figure E.4. Water pressure test result of borehole S-AS-105 at depth 12.00-13.0 m

ZEMAR İSTANBUL ZEMAR Zemin Araştırma ve Mühendislik

Istanbul Strait Road Crossing Project
İstanbul Karayolu Boğaz Geçiş Projesi

Avrasya TÜNELİ

Water Pressure Test (Lugeon Test) / *Basınçlı Su Testi (Lugeon Deneyi)*

Borehole No: *Sondaj No*	**S-AS-105**	**Location:** *Lokasyon*	**KM9+890**	**Date /** *Tarih:*	**08.09.2011**
Ground Water Level *Yeraltısuyu Seviyesi*	2,50 m			***Test Hole Diameter*** *Kuyu Çapı*	96 mm
Stage (m) *Kademe*	15,00 - 16,00			**Stage Length** *Kademe Uzunluğu*	1,00 m
Hole Inclination (from vertical) *Kuyu Eğimi*	0 (°)			**Total Pipe Lenght** *Toplam Boru Uzunluğu*	15,00 m
Rod Diameter *Tij İç Çapı*	77,80 mm			**Rod+Coupling Lenght** *Tij+Manşon Uzunluğu*	3,00 m
Coupling Diameter *Manşon İç Çapı*	77,80 mm			**Coupling Lenght** *Manşon Uzunluğu*	0,00 m
Packer Inner Diameter *Tıkaç İç Çapı*	22,00 mm			**Packer Lenght** *Tıkaç Uzunluğu*	1,34 m
Hose Diameter *Hortum İç Çapı*	22,00 mm			**Hose Lenght** *Hortum Uzunluğu*	5,00 m

PM	T	TOTAL Q	H	PC	PE	AQ	LUGEON
					0,00	0,00	
3,0	5	**18**	0,30	0,000	3,30	3,60	11,20
6,0	5	**35**	0,30	0,001	6,30	7,00	14,90
9,0	5	**67**	0,30	0,003	9,30	13,40	14,01
6,0	5	**54**	0,30	0,002	6,30	10,80	15,24
3,0	5	**36**	0,30	0,001	3,30	7,20	21,82

LUGEON VALUE = 21,82 **Wash-out** **PERMEABILITY (m/sec.) = 9,47E-05**

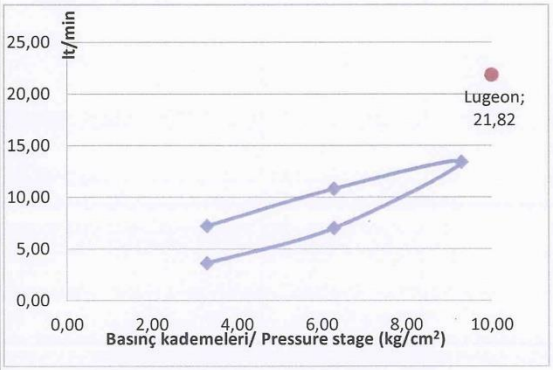

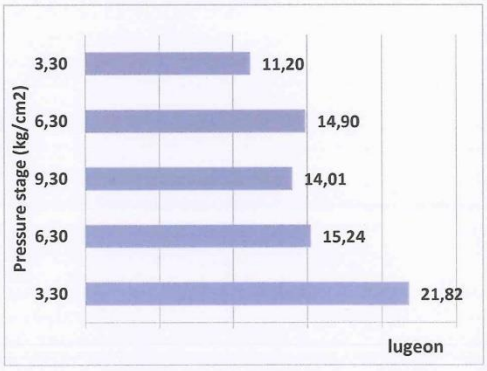

H : Hydrostatic head pressure (kg / cm^2)
PC : Friction losses (kg / cm^2)
PE : Effective pressure (kg / cm^2)
AQ : Coef. of absorption (l / m / min.)

PM : Mano pressure (kg/cm^2)
T : Time (min.)
T.Q : Total take (l)

Tested By
Deneyi Yapan

Approved By
Onaylayan

Figure E.5. Water pressure test result of borehole S-AS-105 at depth 15.00-16.0 m

ZEMAR istanbul
ZEMAR Zemin Araştırma ve Mühendislik

Istanbul Strait Road Crossing Project
İstanbul Karayolu Boğaz Geçiş Projesi

Avrasya TÜNELİ

Water Pressure Test (Lugeon Test) / *Basınçlı Su Testi (Lugeon Deneyi)*

Borehole No: *Sondaj No*	**S-AS-105**	**Location:** *Lokasyon*	**KM9+890**	**Date** / *Tarih:*	**08.09.2011**
Ground Water Level *Yeraltısuyu Seviyesi*	2,50 m			***Test Hole Diameter*** *Kuyu Çapı*	96 mm
Stage (m) *Kademe*	18,00 - 19,00			**Stage Length** *Kademe Uzunluğu*	1,00 m
Hole Inclination (from vertical) *Kuyu Eğimi*	0 (°)			**Total Pipe Lenght** *Toplam Boru Uzunluğu*	18,00 m
Rod Diameter *Tij İç Çapı*	77,80 mm			**Rod+Coupling Lenght** *Tij+Manşon Uzunluğu*	3,00 m
Coupling Diameter *Manşon İç Çapı*	77,80 mm			**Coupling Lenght** *Manşon Uzunluğu*	0,00 m
Packer Inner Diameter *Tıkaç İç Çapı*	22,00 mm			**Packer Lenght** *Tıkaç Uzunluğu*	1,34 m
Hose Diameter *Hortum İç Çapı*	22,00 mm			**Hose Lenght** *Hortum Uzunluğu*	5,00 m

PM	T	TOTAL Q	H	PC	PE	AQ	LUGEON
					0,00	0,00	
3,0	5	**15**	0,30	0,000	3,30	3,00	7,47
6,0	5	**25**	0,30	0,000	6,30	5,00	14,88
9,0	5	**65**	0,30	0,003	9,30	13,00	13,80
6,0	5	**48**	0,30	0,002	6,30	9,60	14,78
3,0	5	**27**	0,30	0,000	3,30	5,40	16,37

LUGEON VALUE = 13,46 **Laminar** **PERMEABILITY (m/sec.) = 5,48E-05**

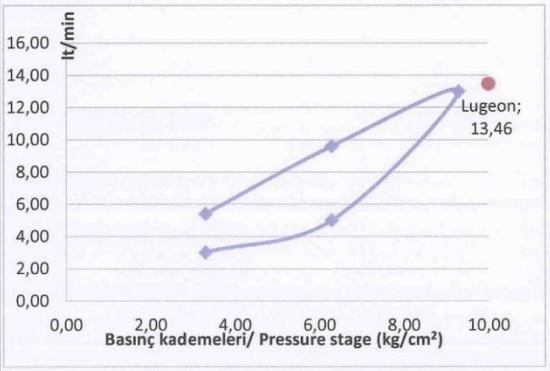

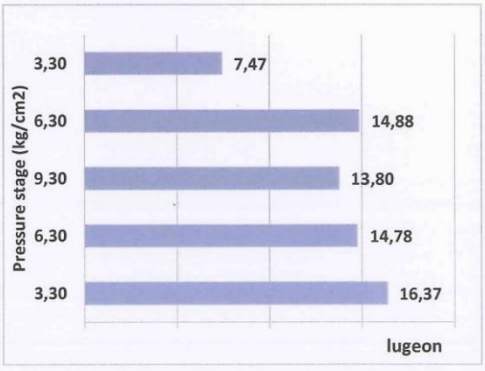

H : Hydrostatic head pressure (kg / cm^2)
PC : Friction losses (kg / cm^2)
PE : Effective pressure (kg / cm^2)
AQ : Coef. of absorption (l / m / min.)

PM : Mano pressure (kg/cm^2)
T : Time (min.)
T.Q : Total take (l)

Tested By
Deneyi Yapan

Approved By
Onaylayan

Figure E.6. Water pressure test result of borehole S-AS-105 at depth 18.00-19.0 m

ZEMAR İstanbul
ZEMAR Zemin Araştırma ve Mühendislik

Istanbul Strait Road Crossing Project
İstanbul Karayolu Boğaz Geçiş Projesi

Avrasya TÜNELİ

Water Pressure Test (Lugeon Test) / *Basınçlı Su Testi (Lugeon Deneyi)*

Borehole No: *Sondaj No*	**S-AS-105**	**Location:** *Lokasyon*	**KM9+890**	**Date** / *Tarih:*	**08.09.2011**
Ground Water Level *Yeraltısuyu Seviyesi*	2,50 m			***Test Hole Diameter*** *Kuyu Çapı*	96 mm
Stage (m) *Kademe*	21,00 - 22,00			**Stage Length** *Kademe Uzunluğu*	1,00 m
Hole Inclination (from vertical) *Kuyu Eğimi*	0 (°)			**Total Pipe Lenght** *Toplam Boru Uzunluğu*	21,00 m
Rod Diameter *Tij İç Çapı*	77,80 mm			**Rod+Coupling Lenght** *Tij+Manşon Uzunluğu*	3,00 m
Coupling Diameter *Manşon İç Çapı*	77,80 mm			**Coupling Lenght** *Manşon Uzunluğu*	0,00 m
Packer Inner Diameter *Tıkaç İç Çapı*	22,00 mm			**Packer Lenght** *Tıkaç Uzunluğu*	1,34 m
Hose Diameter *Hortum İç Çapı*	22,00 mm			**Hose Lenght** *Hortum Uzunluğu*	5,00 m

PM	T	TOTAL Q	H	PC	PE	AQ	LUGEON
					0,00	0,00	
3,0	5	**2**	0,30	0,000	3,30	0,40	2,19
6,0	5	**6**	0,30	0,000	6,30	1,20	1,45
9,0	5	**7**	0,30	0,000	9,30	1,40	1,54
6,0	5	**4**	0,30	0,000	6,30	0,80	1,54
3,0	5	**1**	0,30	0,000	3,30	0,20	0,61

LUGEON VALUE = 0,61 **Void Filling** **PERMEABILITY (m/sec.) = 2,63E-06**

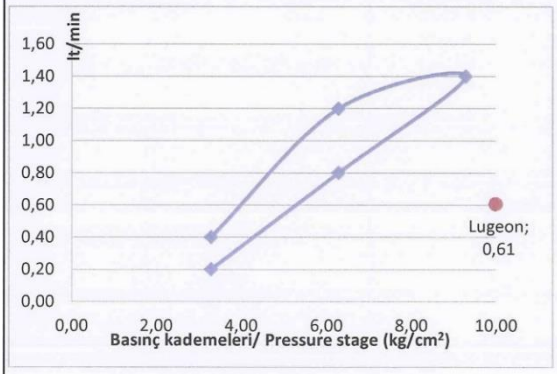

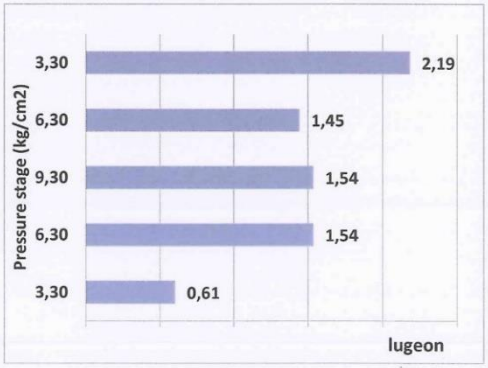

H : Hydrostatic head pressure (kg / cm^2)
PC : Friction losses (kg / cm^2)
PE : Effective pressure (kg / cm^2)
AQ : Coef. of absorption (l / m / min.)

PM : Mano pressure (kg/cm^2)
T : Time (min.)
T.Q : Total take (l)

Tested By
Deneyi Yapan

Approved By
Onaylayan

Figure E.7. Water pressure test result of borehole S-AS-105 at depth 21.00-22.0 m

ZEMAR İstanbul ZEMAR Zemin Araştırma ve Mühendislik

Istanbul Strait Road Crossing Project
İstanbul Karayolu Boğaz Geçiş Projesi

Avrasya TÜNELİ

Water Pressure Test (Lugeon Test) / *Basınçlı Su Testi (Lugeon Deneyi)*

Borehole No: *Sondaj No*	**S-AS-105**	**Location:** *Lokasyon*	**KM9+890**	**Date** / *Tarih:*	**10.09.2011**
Ground Water Level *Yeraltısuyu Seviyesi*	2,50 m			***Test Hole Diameter*** *Kuyu Çapı*	96 mm
Stage (m) *Kademe*	24,00 - 25,00			**Stage Length** *Kademe Uzunluğu*	1,00 m
Hole Inclination (from vertical) *Kuyu Eğimi*	0 (°)			**Total Pipe Lenght** *Toplam Boru Uzunluğu*	24,00 m
Rod Diameter *Tij İç Çapı*	77,80 mm			**Rod+Coupling Lenght** *Tij+Manşon Uzunluğu*	3,00 m
Coupling Diameter *Manşon İç Çapı*	77,80 mm			**Coupling Lenght** *Manşon Uzunluğu*	0,00 m
Packer Inner Diameter *Tıkaç İç Çapı*	22,00 mm			**Packer Lenght** *Tıkaç Uzunluğu*	1,34 m
Hose Diameter *Hortum İç Çapı*	22,00 mm			**Hose Lenght** *Hortum Uzunluğu*	5,00 m

PM	T	TOTAL Q	H	PC	PE	AQ	LUGEON
					0,00	0,00	
3,0	5	**2**	0,30	0,000	3,30	0,40	1,52
6,0	5	**5**	0,30	0,000	6,30	0,90	1,02
9,0	5	**5**	0,30	0,000	9,30	1,00	1,09
6,0	5	**3**	0,30	0,000	6,30	0,60	1,09
3,0	5	**1**	0,30	0,000	3,30	0,20	0,61

LUGEON VALUE = **0,61** **Void Filling** **PERMEABILITY (m/sec.) =** **2,63E-06**

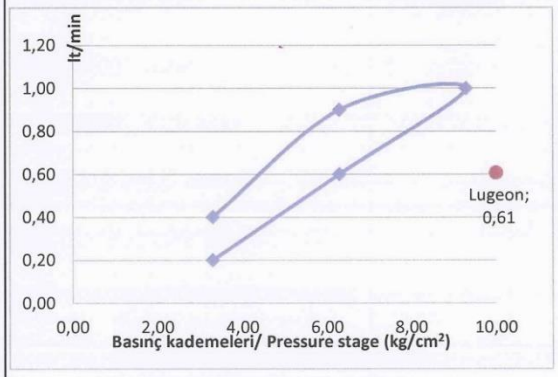

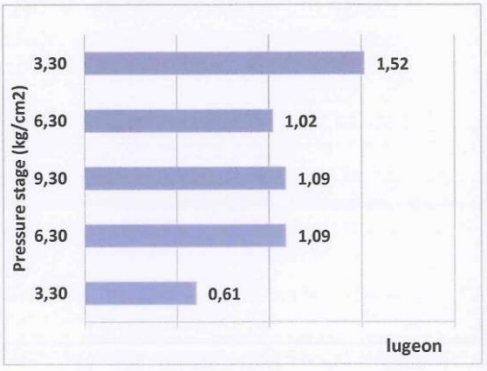

H : Hydrostatic head pressure (kg / cm²)
PC : Friction losses (kg / cm²)
PE : Effective pressure (kg / cm²)
AQ : Coef. of absorption (l / m / min.)

PM : Mano pressure (kg/cm²)
T : Time (min.)
T.Q : Total take (l)

Tested By
Deneyi Yapan

Approved By
Onaylayan

Figure E.8. Water pressure test result of borehole S-AS-105 at depth 24.00-25.0 m

ZEMAR İSTANBUL ZEMAR Zemin Araştırma ve Mühendislik

Istanbul Strait Road Crossing Project
İstanbul Karayolu Boğaz Geçiş Projesi

Avrasya TÜNELİ

Water Pressure Test (Lugeon Test) / *Basınçlı Su Testi (Lugeon Deneyi)*

Borehole No: *Sondaj No*	**S-AS-105**	**Location:** *Lokasyon*	**KM9+890**	**Date** / *Tarih:*	**10.09.2011**
Ground Water Level *Yeraltısuyu Seviyesi*	2,50 m			***Test Hole Diameter*** *Kuyu Çapı*	96 mm
Stage (m) *Kademe*	27,00 - 28,00			**Stage Length** *Kademe Uzunluğu*	1,00 m
Hole Inclination (from vertical) *Kuyu Eğimi*	0 (°)			**Total Pipe Lenght** *Toplam Boru Uzunluğu*	27,00 m
Rod Diameter *Tij İç Çapı*	77,80 mm			**Rod+Coupling Lenght** *Tij+Manşon Uzunluğu*	3,00 m
Coupling Diameter *Manşon İç Çapı*	77,80 mm			**Coupling Lenght** *Manşon Uzunluğu*	0,00 m
Packer Inner Diameter *Tıkaç İç Çapı*	22,00 mm			**Packer Lenght** *Tıkaç Uzunluğu*	1,34 m
Hose Diameter *Hortum İç Çapı*	22,00 mm			**Hose Lenght** *Hortum Uzunluğu*	5,00 m

PM	T	TOTAL Q	H	PC	PE	AQ	LUGEON
					0,00	0,00	
3,0	5	**10**	0,30	0,000	3,30	2,00	4,23
6,0	5	**15**	0,30	0,000	6,30	3,00	15,84
9,0	5	**67**	0,30	0,003	9,30	13,40	14,53
6,0	5	**43**	0,30	0,001	6,30	8,60	16,25
3,0	5	**12**	0,30	0,000	3,30	2,40	7,27

LUGEON VALUE = 11,62 **Laminar** **PERMEABILITY (m/sec.) = 4,41E-05**

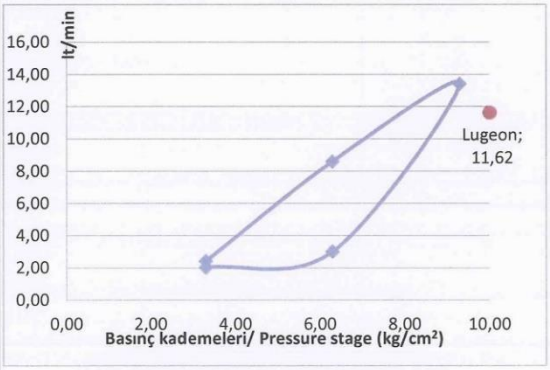

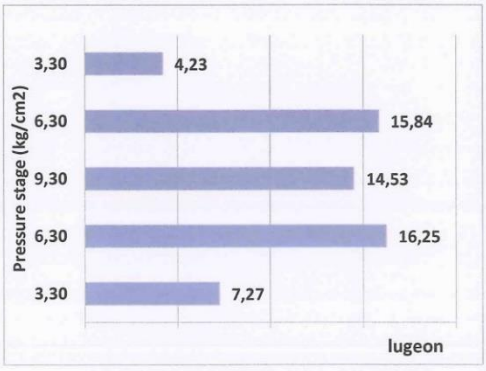

H : Hydrostatic head pressure (kg / cm^2)
PC : Friction losses (kg / cm^2)
PE : Effective pressure (kg / cm^2)
AQ : Coef. of absorption (l / m / min.)

PM : Mano pressure (kg/cm^2)
T : Time (min.)
T.Q : Total take (l)

Tested By
Deneyi Yapan

Approved By
Onaylayan

Figure E.9. Water pressure test result of borehole S-AS-105 at depth 27.00-28.0 m

ZEMAR istanbul
ZEMAR Zemin Araştırma ve Mühendislik

Istanbul Strait Road Crossing Project
İstanbul Karayolu Boğaz Geçiş Projesi

Avrasya TÜNELİ

Water Pressure Test (Lugeon Test) / *Basınçlı Su Testi (Lugeon Deneyi)*

Borehole No: *Sondaj No*	**S-AS-105**	**Location:** *Lokasyon*	**KM9+890**	**Date** / *Tarih:*	**10.09.2011**
Ground Water Level *Yeraltısuyu Seviyesi*	2,50 m			***Test Hole Diameter*** *Kuyu Çapı*	96 mm
Stage (m) *Kademe*	30,00 - 31,00			**Stage Length** *Kademe Uzunluğu*	1,00 m
Hole Inclination (from vertical) *Kuyu Eğimi*	0 (°)			**Total Pipe Lenght** *Toplam Boru Uzunluğu*	30,00 m
Rod Diameter *Tij İç Çapı*	77,80 mm			**Rod+Coupling Lenght** *Tij+Manşon Uzunluğu*	3,00 m
Coupling Diameter *Manşon İç Çapı*	77,80 mm			**Coupling Lenght** *Manşon Uzunluğu*	0,00 m
Packer Inner Diameter *Tıkaç İç Çapı*	22,00 mm			**Packer Lenght** *Tıkaç Uzunluğu*	1,34 m
Hose Diameter *Hortum İç Çapı*	22,00 mm			**Hose Lenght** *Hortum Uzunluğu*	5,00 m

PM	T	TOTAL Q	H	PC	PE	AQ	LUGEON
					0,00	0,00	
3,0	5	**8**	0,30	0,000	3,30	1,60	3,39
6,0	5	**12**	0,30	0,000	6,30	2,40	8,82
9,0	5	**38**	0,30	0,001	9,30	7,60	8,07
6,0	5	**28**	0,30	0,001	6,30	5,60	8,07
3,0	5	**18**	0,30	0,000	3,30	3,60	10,91

LUGEON VALUE = 10,91 **Wash-out** **PERMEABILITY (m/sec.) = 4,73E-05**

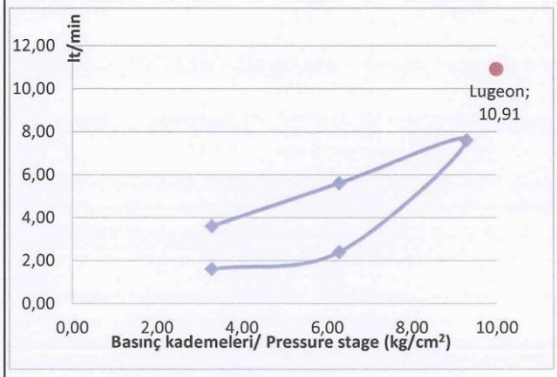

H : Hydrostatic head pressure (kg / cm^2)
PC : Friction losses (kg / cm^2)
PE : Effective pressure (kg / cm^2)
AQ : Coef. of absorption (l / m / min.)

PM : Mano pressure (kg/cm^2)
T : Time (min.)
T.Q : Total take (l)

Tested By
Deneyi Yapan

Approved By
Onaylayan

Figure E.10. Water pressure test result of borehole S-AS-105 at depth 30.00-31.0 m

ZEMAR İstanbul — ZEMAR Zemin Araştırma ve Mühendislik

Istanbul Strait Road Crossing Project
İstanbul Karayolu Boğaz Geçiş Projesi

Avrasya Tüneli

Water Pressure Test (Lugeon Test) / *Basınçlı Su Testi (Lugeon Deneyi)*

Borehole No: *Sondaj No*	**S-AS-105**	**Location:** *Lokasyon*	**KM9+890**	**Date** / *Tarih:*	**11.09.2011**
Ground Water Level *Yeraltısuyu Seviyesi*	2,50 m			***Test Hole Diameter*** *Kuyu Çapı*	96 mm
Stage (m) *Kademe*	35,00 - 36,00			**Stage Length** *Kademe Uzunluğu*	1,00 m
Hole Inclination (from vertical) *Kuyu Eğimi*	0 (°)			**Total Pipe Lenght** *Toplam Boru Uzunluğu*	35,00 m
Rod Diameter *Tij İç Çapı*	77,80 mm			**Rod+Coupling Lenght** *Tij+Manşon Uzunluğu*	3,00 m
Coupling Diameter *Manşon İç Çapı*	77,80 mm			**Coupling Lenght** *Manşon Uzunluğu*	0,00 m
Packer Inner Diameter *Tıkaç İç Çapı*	22,00 mm			**Packer Lenght** *Tıkaç Uzunluğu*	1,34 m
Hose Diameter *Hortum İç Çapı*	22,00 mm			**Hose Lenght** *Hortum Uzunluğu*	5,00 m

PM	T	TOTAL Q	H	PC	PE	AQ	LUGEON
					0,00	0,00	
3,0	5	**25**	0,30	0,000	3,30	5,00	25,12
6,0	5	**70**	0,30	0,003	6,30	14,00	15,98
9,0	5	**78**	0,30	0,004	9,30	15,60	16,92
6,0	5	**50**	0,30	0,002	6,30	10,00	17,90
3,0	5	**18**	0,30	0,000	3,30	3,60	10,91

LUGEON VALUE = 10,91 **Void filling** **PERMEABILITY (m/sec.) = 4,73E-05**

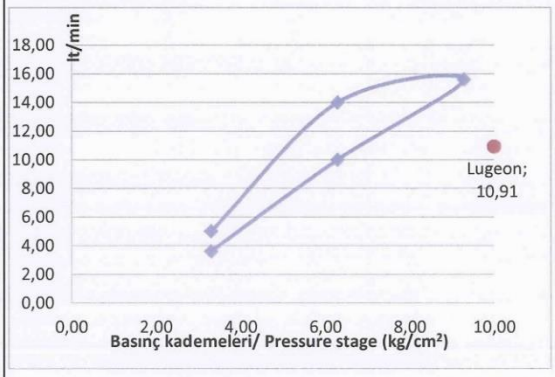

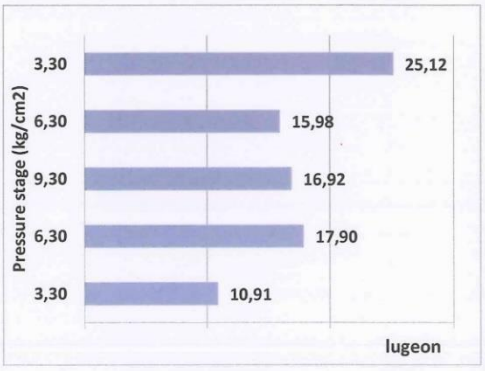

H : Hydrostatic head pressure (kg / cm^2)
PC : Friction losses (kg / cm^2)
PE : Effective pressure (kg / cm^2)
AQ : Coef. of absorption (l / m / min.)

PM : Mano pressure (kg/cm^2)
T : Time (min.)
T.Q : Total take (l)

Tested By
Deneyi Yapan

Approved By
Onaylayan

Figure E.11. Water pressure test result of borehole S-AS-105 at depth 35.00-36.0 m

ZEMAR İSTANBUL ZEMAR Zemin Araştırma ve Mühendislik

Istanbul Strait Road Crossing Project
İstanbul Karayolu Boğaz Geçiş Projesi

Avrasya TÜNELİ

Water Pressure Test (Lugeon Test) / *Basınçlı Su Testi (Lugeon Deneyi)*

Borehole No: *Sondaj No*	**S-AS-105**	**Location:** *Lokasyon*	**KM9+890**	**Date** / *Tarih:*	**11.09.2011**
Ground Water Level *Yeraltısuyu Seviyesi*		2,50 m		***Test Hole Diameter*** *Kuyu Çapı*	96 mm
Stage (m) *Kademe*		39,00 - 40,00		**Stage Length** *Kademe Uzunluğu*	1,00 m
Hole Inclination (from vertical) *Kuyu Eğimi*		0 (°)		**Total Pipe Lenght** *Toplam Boru Uzunluğu*	39,00 m
Rod Diameter *Tij İç Çapı*		77,80 mm		**Rod+Coupling Lenght** *Tij+Manşon Uzunluğu*	3,00 m
Coupling Diameter *Manşon İç Çapı*		77,80 mm		**Coupling Lenght** *Manşon Uzunluğu*	0,00 m
Packer Inner Diameter *Tıkaç İç Çapı*		22,00 mm		**Packer Lenght** *Tıkaç Uzunluğu*	1,34 m
Hose Diameter *Hortum İç Çapı*		22,00 mm		**Hose Lenght** *Hortum Uzunluğu*	5,00 m

PM	T	TOTAL Q	H	PC	PE	AQ	LUGEON
					0,00	0,00	
3,0	5	**36**	0,30	0,001	3,30	7,20	28,22
6,0	5	**83**	0,30	0,005	6,30	16,60	18,82
9,0	5	**92**	0,30	0,006	9,29	18,40	20,33
6,0	5	**51**	0,30	0,002	6,30	10,20	16,87
3,0	5	**24**	0,30	0,000	3,30	4,80	14,55

LUGEON VALUE = 14,55 **Void Filling** **PERMEABILITY (m/sec.) = 6,31E-05**

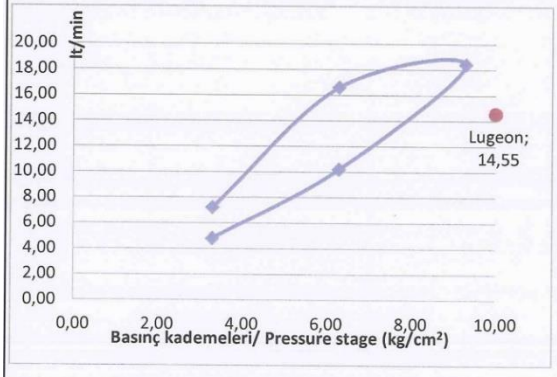

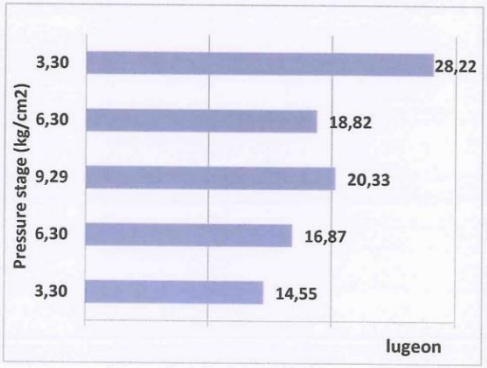

H : Hydrostatic head pressure (kg / cm^2)
PC : Friction losses (kg / cm^2)
PE : Effective pressure (kg / cm^2)
AQ : Coef. of absorption (l / m / min.)

PM : Mano pressure (kg/cm^2)
T : Time (min.)
T.Q : Total take (l)

Tested By
Deneyi Yapan

Approved By
Onaylayan

Figure E.12. Water pressure test result of borehole S-AS-105 at depth 39.00-40.0 m

ZEMAR İSTANBUL ZEMAR Zemin Araştırma ve Mühendislik

Istanbul Strait Road Crossing Project
İstanbul Karayolu Boğaz Geçiş Projesi

Avrasya TÜNELİ

Water Pressure Test (Lugeon Test) / *Basınçlı Su Testi (Lugeon Deneyi)*

Borehole No: *Sondaj No*	**S-AS-105**	**Location:** *Lokasyon*	**KM9+890**	**Date** / *Tarih:*	**11.09.2011**
Ground Water Level *Yeraltısuyu Seviyesi*	2,50 m			***Test Hole Diameter*** *Kuyu Çapı*	96 mm
Stage (m) *Kademe*	43,00 - 44,00			**Stage Length** *Kademe Uzunluğu*	1,00 m
Hole Inclination (from vertical) *Kuyu Eğimi*	0 (°)			**Total Pipe Lenght** *Toplam Boru Uzunluğu*	43,00 m
Rod Diameter *Tij İç Çapı*	77,80 mm			**Rod+Coupling Lenght** *Tij+Manşon Uzunluğu*	3,00 m
Coupling Diameter *Manşon İç Çapı*	77,80 mm			**Coupling Lenght** *Manşon Uzunluğu*	0,00 m
Packer Inner Diameter *Tıkaç İç Çapı*	22,00 mm			**Packer Lenght** *Tıkaç Uzunluğu*	1,34 m
Hose Diameter *Hortum İç Çapı*	22,00 mm			**Hose Lenght** *Hortum Uzunluğu*	5,00 m

PM	T	TOTAL Q	H	PC	PE	AQ	LUGEON
					0,00	0,00	
3,0	5	**30**	0,30	0,001	3,30	6,00	16,73
6,0	5	**54**	0,30	0,002	6,30	10,80	12,28
9,0	5	**60**	0,30	0,002	9,30	12,00	13,31
6,0	5	**32**	0,30	0,001	6,30	6,40	9,36
3,0	5	**20**	0,30	0,000	3,30	4,00	12,12

LUGEON VALUE = 12,12 Laminar PERMEABILITY (m/sec.) = 5,26E-05

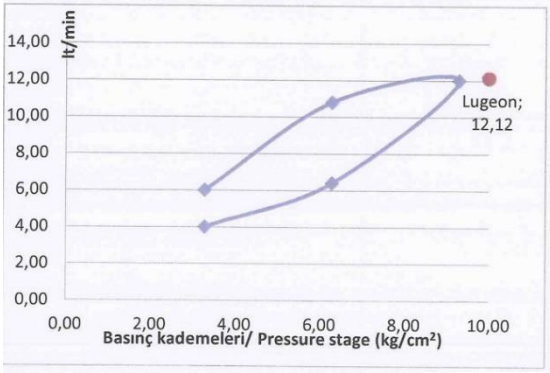

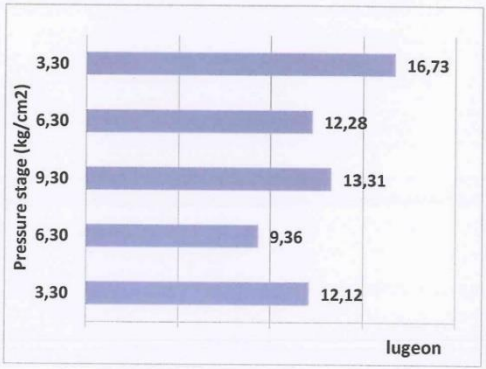

H : Hydrostatic head pressure (kg / cm^2)
PC : Friction losses (kg / cm^2)
PE : Effective pressure (kg / cm^2)
AQ : Coef. of absorption (l / m / min.)

PM : Mano pressure (kg/cm^2)
T : Time (min.)
T.Q : Total take (l)

Tested By
Deneyi Yapan

Approved By
Onaylayan

Figure E.13. Water pressure test result of borehole S-AS-105 at depth 43.00-44.0 m

ZEMAR istanbul ZEMAR Zemin Araştırma ve Mühendislik

Istanbul Strait Road Crossing Project
İstanbul Karayolu Boğaz Geçiş Projesi

Avrasya TÜNELİ

Water Pressure Test (Lugeon Test) / *Basınçlı Su Testi (Lugeon Deneyi)*

Borehole No: *Sondaj No*	**S-AS-105**	**Location:** *Lokasyon*	**KM9+890**	**Date** / *Tarih:*	**11.09.2011**
Ground Water Level *Yeraltısuyu Seviyesi*	2,50 m			***Test Hole Diameter*** *Kuyu Çapı*	96 mm
Stage (m) *Kademe*	46,00 - 47,00			**Stage Length** *Kademe Uzunluğu*	1,00 m
Hole Inclination (from vertical) *Kuyu Eğimi*	0 (°)			**Total Pipe Lenght** *Toplam Boru Uzunluğu*	46,00 m
Rod Diameter *Tij İç Çapı*	77,80 mm			**Rod+Coupling Lenght** *Tij+Manşon Uzunluğu*	3,00 m
Coupling Diameter *Manşon İç Çapı*	77,80 mm			**Coupling Lenght** *Manşon Uzunluğu*	0,00 m
Packer Inner Diameter *Tıkaç İç Çapı*	22,00 mm			**Packer Lenght** *Tıkaç Uzunluğu*	1,34 m
Hose Diameter *Hortum İç Çapı*	22,00 mm			**Hose Lenght** *Hortum Uzunluğu*	5,00 m

PM	T	TOTAL Q	H	PC	PE	AQ	LUGEON
					0,00	0,00	
3,0	5	**5**	0,30	0,000	3,30	1,00	1,89
6,0	5	**7**	0,30	0,000	6,30	1,40	2,14
9,0	5	**10**	0,30	0,000	9,30	2,00	2,05
6,0	5	**9**	0,30	0,000	6,30	1,80	2,54
3,0	5	**6**	0,30	0,000	3,30	1,20	3,64

LUGEON VALUE = 3,64 **Laminar** **PERMEABILITY (m/sec.) = 1,58E-05**

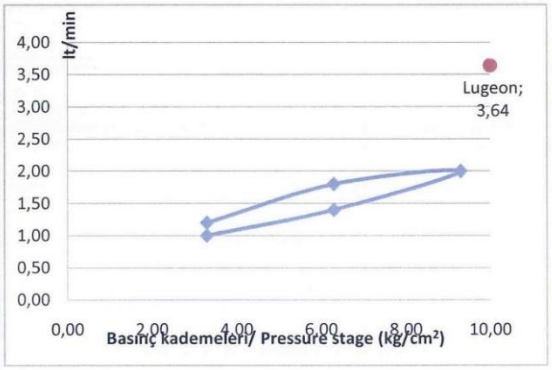

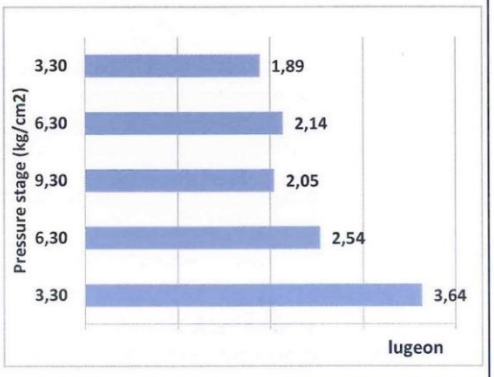

H : Hydrostatic head pressure (kg / cm^2)
PC : Friction losses (kg / cm^2)
PE : Effective pressure (kg / cm^2)
AQ : Coef. of absorption (l / m / min.)

PM : Mano pressure (kg/cm^2)
T : Time (min.)
T.Q : Total take (l)

Tested By
Deneyi Yapan

Approved By
Onaylayan

Figure E.14. Water pressure test result of borehole S-AS-105 at depth 46.00-47.0 m

ZEMAR İstanbul
ZEMAR Zemin Araştırma ve Müh.

Istanbul Strait Road Crossing Project
İstanbul Karayolu Boğaz Geçiş Projesi

Avrasya Tüneli

Water Pressure Test (Lugeon Test) / *Basınçlı Su Testi (Lugeon Deneyi)*

Borehole No: *Sondaj No*	**S-AS-106**	**Location:** *Lokasyon*	**Haydarpaşa**	**Date** / *Tarih:*	**22.08.2011**
Ground Water Level *Yeraltısuyu Seviyesi*	4,30 m			***Test Hole Diameter*** *Kuyu Çapı*	96 mm
Stage (m) *Kademe*	7,00 - 8,00			**Stage Length** *Kademe Uzunluğu*	1,00 m
Hole Inclination (from vertical) *Kuyu Eğimi*	0 (°)			**Total Pipe Lenght** *Toplam Boru Uzunluğu*	7,00 m
Rod Diameter *Tij İç Çapı*	60,30 mm			**Rod+Coupling Lenght** *Tij+Manşon Uzunluğu*	3,00 m
Coupling Diameter *Manşon İç Çapı*	60,30 mm			**Coupling Lenght** *Manşon Uzunluğu*	0,00 m
Packer Inner Diameter *Tıkaç İç Çapı*	15,00 mm			**Packer Lenght** *Tıkaç Uzunluğu*	1,34 m
Hose Diameter *Hortum İç Çapı*	22,00 mm			**Hose Lenght** *Hortum Uzunluğu*	5,00 m

PM	T	TOTAL Q	H	PC	PE	AQ	LUGEON
					0,00	0,00	
3,0	5	**38**	0,48	0,002	3,48	7,60	12,39
6,0	5	**49**	0,48	0,004	6,48	9,80	15,45
9,0	5	**73**	0,48	0,009	9,47	14,60	15,34
6,0	5	**52**	0,48	0,004	6,48	10,40	13,22
3,0	5	**40**	0,48	0,003	3,48	8,00	23,01

LUGEON VALUE = 15,88 **Wash out** **PERMEABILITY (m/sec.) = 7,38E-05**

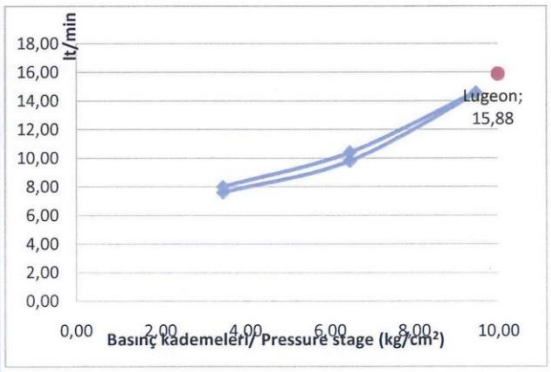

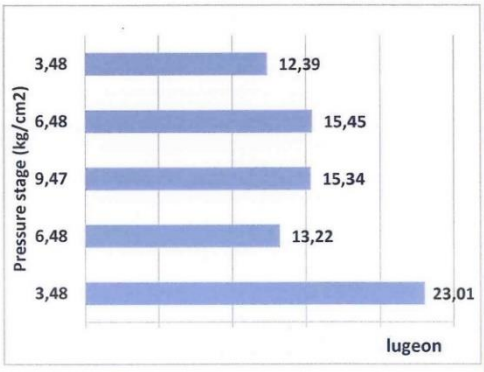

H : Hydrostatic head pressure (kg / cm^2)
PC : Friction losses (kg / cm^2)
PE : Effective pressure (kg / cm^2)
AQ : Coef. of absorption (l / m / min.)

PM : Mano pressure (kg/cm^2)
T : Time (min.)
T.Q : Total take (l)

Tested By
Deneyi Yapan

Approved By
Onaylayan

Figure E.15. Water pressure test result of borehole S-AS-106 at depth 7.00-8.0 m

ZEMAR İstanbul ZEMAR Zemin Araştırma ve Mühendislik

Istanbul Strait Road Crossing Project
İstanbul Karayolu Boğaz Geçiş Projesi

Avrasya TÜNELİ

Water Pressure Test (Lugeon Test) / *Basınçlı Su Testi (Lugeon Deneyi)*

Borehole No: *Sondaj No*	**S-AS-106**	**Location:** *Lokasyon*	**Haydarpaşa**	**Date / *Tarih:***	**23.08.2011**
Ground Water Level *Yeraltısuyu Seviyesi*	2,70 m			***Test Hole Diameter*** *Kuyu Çapı*	96 mm
Stage (m) *Kademe*	15,00 - 16,00			**Stage Length** *Kademe Uzunluğu*	1,00 m
Hole Inclination (from vertical) *Kuyu Eğimi*	0 (°)			**Total Pipe Lenght** *Toplam Boru Uzunluğu*	15,00 m
Rod Diameter *Tij İç Çapı*	77,80 mm			**Rod+Coupling Lenght** *Tij+Manşon Uzunluğu*	3,00 m
Coupling Diameter *Manşon İç Çapı*	77,80 mm			**Coupling Lenght** *Manşon Uzunluğu*	0,00 m
Packer Inner Diameter *Tıkaç İç Çapı*	22,00 mm			**Packer Lenght** *Tıkaç Uzunluğu*	1,34 m
Hose Diameter *Hortum İç Çapı*	22,00 mm			**Hose Lenght** *Hortum Uzunluğu*	5,00 m

PM	T	TOTAL Q	H	PC	PE	AQ	LUGEON
					0,00	0,00	
3,0	5	**34**	0,32	0,001	3,32	6,80	19,28
6,0	5	**62**	0,32	0,003	6,32	12,40	18,79
9,0	5	**88**	0,32	0,005	9,31	17,60	18,15
6,0	5	**76**	0,32	0,004	6,32	15,20	20,61
3,0	5	**54**	0,32	0,002	3,32	10,80	32,55

LUGEON VALUE = 32,55 **Wash-out** **PERMEABILITY (m/sec.) = 1,41E-04**

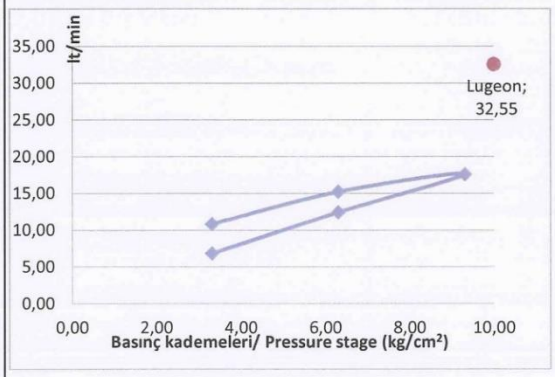

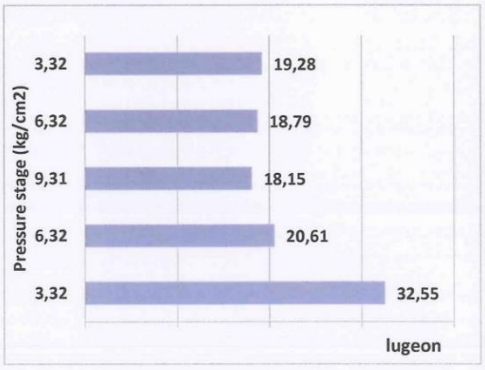

H : Hydrostatic head pressure (kg / cm^2)
PC : Friction losses (kg / cm^2)
PE : Effective pressure (kg / cm^2)
AQ : Coef. of absorption (l / m / min.)

PM : Mano pressure (kg/cm^2)
T : Time (min.)
T.Q : Total take (l)

Tested By
Deneyi Yapan

Approved By
Onaylayan

Figure E.16. Water pressure test result of borehole S-AS-106 at depth 15.00-16.0 m

ZEMAR İstanbul
ZEMAR Zemin Araştırma ve Mühendislik

Istanbul Strait Road Crossing Project
İstanbul Karayolu Boğaz Geçiş Projesi

Avrasya TÜNELİ

Water Pressure Test (Lugeon Test) / *Basınçlı Su Testi (Lugeon Deneyi)*

Borehole No: *Sondaj No*	**S-AS-106**	**Location:** *Lokasyon*	**Haydarpaşa**	**Date** / *Tarih:*	**25.08.2011**
Ground Water Level *Yeraltısuyu Seviyesi*	7,50 m			***Test Hole Diameter*** *Kuyu Çapı*	96 mm
Stage (m) *Kademe*	17,00 - 18,00			**Stage Length** *Kademe Uzunluğu*	1,00 m
Hole Inclination (from vertical) *Kuyu Eğimi*	0 (°)			**Total Pipe Lenght** *Toplam Boru Uzunluğu*	17,00 m
Rod Diameter *Tij İç Çapı*	77,80 mm			**Rod+Coupling Lenght** *Tij+Manşon Uzunluğu*	3,00 m
Coupling Diameter *Manşon İç Çapı*	77,80 mm			**Coupling Lenght** *Manşon Uzunluğu*	0,00 m
Packer Inner Diameter *Tıkaç İç Çapı*	22,00 mm			**Packer Lenght** *Tıkaç Uzunluğu*	1,34 m
Hose Diameter *Hortum İç Çapı*	22,00 mm			**Hose Lenght** *Hortum Uzunluğu*	5,00 m

PM	T	TOTAL Q	H	PC	PE	AQ	LUGEON
					0,00	0,00	
3,0	5	**22**	0,80	0,000	3,80	4,40	11,84
6,0	5	**40**	0,80	0,001	6,80	8,00	7,36
9,0	5	**37**	0,80	0,001	9,80	7,40	7,63
6,0	5	**20**	0,80	0,000	6,80	4,00	5,92
3,0	5	**11**	0,80	0,000	3,80	2,20	5,79

LUGEON VALUE = 5,79 **Void Filling** **PERMEABILITY (m/sec.) = 2,51E-05**

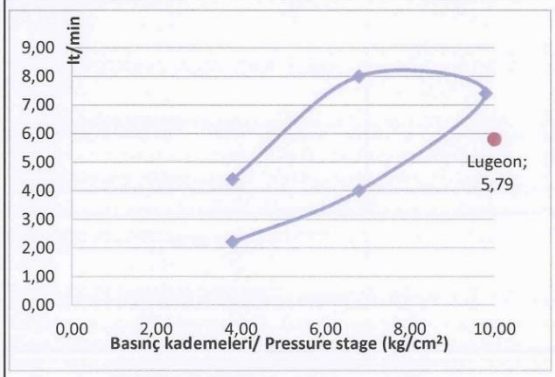

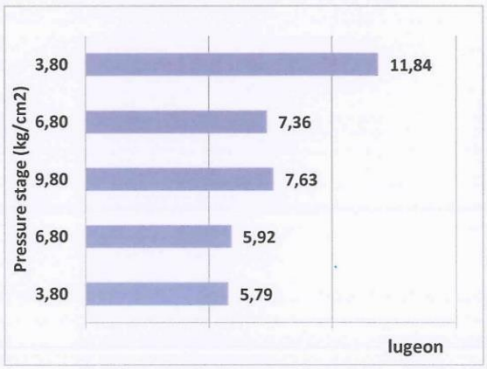

H : Hydrostatic head pressure (kg / cm^2)
PC : Friction losses (kg / cm^2)
PE : Effective pressure (kg / cm^2)
AQ : Coef. of absorption (l / m / min.)

PM : Mano pressure (kg/cm^2)
T : Time (min.)
T.Q : Total take (l)

Tested By
Deneyi Yapan

Approved By
Onaylayan

Figure E.17. Water pressure test result of borehole S-AS-106 at depth 17.00-18.0 m

ZEMAR İstanbul
ZEMAR Zemin Araştırma ve Mühendislik

Istanbul Strait Road Crossing Project
İstanbul Karayolu Boğaz Geçiş Projesi

Avrasya TÜNELİ

Water Pressure Test (Lugeon Test) / *Basınçlı Su Testi (Lugeon Deneyi)*

Borehole No: *Sondaj No*	**S-AS-106**	**Location:** *Lokasyon*	**Haydarpaşa**	**Date** / *Tarih:*	**25.08.2011**
Ground Water Level *Yeraltısuyu Seviyesi*	7,50 m			***Test Hole Diameter*** *Kuyu Çapı*	96 mm
Stage (m) *Kademe*	21,50 - 22,50			**Stage Length** *Kademe Uzunluğu*	1,00 m
Hole Inclination (from vertical) *Kuyu Eğimi*	0 (°)			**Total Pipe Lenght** *Toplam Boru Uzunluğu*	21,50 m
Rod Diameter *Tij İç Çapı*	77,80 mm			**Rod+Coupling Lenght** *Tij+Manşon Uzunluğu*	3,00 m
Coupling Diameter *Manşon İç Çapı*	77,80 mm			**Coupling Lenght** *Manşon Uzunluğu*	0,00 m
Packer Inner Diameter *Tıkaç İç Çapı*	22,00 mm			**Packer Lenght** *Tıkaç Uzunluğu*	1,34 m
Hose Diameter *Hortum İç Çapı*	22,00 mm			**Hose Lenght** *Hortum Uzunluğu*	5,00 m

PM	T	TOTAL Q	H	PC	PE	AQ	LUGEON
					0,00	0,00	
3,0	5	**9**	0,80	0,000	3,80	1,80	3,87
6,0	5	**14**	0,80	0,000	6,80	2,80	5,57
9,0	5	**27**	0,80	0,000	9,80	5,40	5,47
6,0	5	**22**	0,80	0,000	6,80	4,40	6,32
3,0	5	**13**	0,80	0,000	3,80	2,60	6,84

LUGEON VALUE = 6,84 **Laminar** **PERMEABILITY (m/sec.) = 2,97E-05**

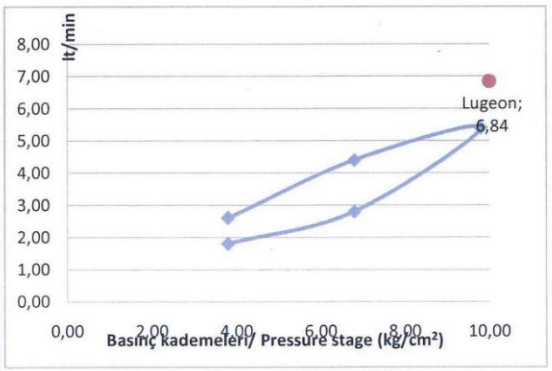

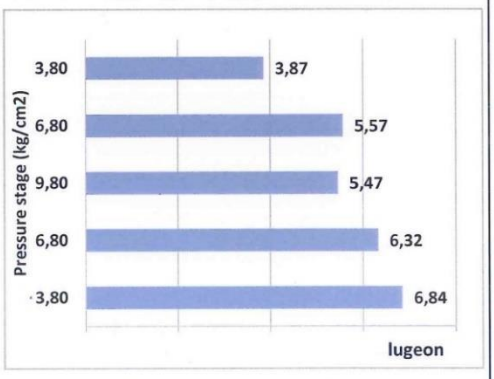

H : Hydrostatic head pressure (kg / cm^2)
PC : Friction losses (kg / cm^2)
PE : Effective pressure (kg / cm^2)
AQ : Coef. of absorption (l / m / min.)

PM : Mano pressure (kg/cm^2)
T : Time (min.)
T.Q : Total take (l)

Tested By
Deneyi Yapan

Approved By
Onaylayan

Figure E.18. Water pressure test result of borehole S-AS-106 at depth 21.50-22.5 m

ZEMAR İSTANBUL ZEMAR Zemin Araştırma ve Mühendislik

Istanbul Strait Road Crossing Project
İstanbul Karayolu Boğaz Geçiş Projesi

Avrasya TÜNELİ

Water Pressure Test (Lugeon Test) / *Basınçlı Su Testi (Lugeon Deneyi)*

Borehole No: *Sondaj No*	**S-AS-106**	**Location:** *Lokasyon*	**Haydarpaşa**	**Date / *Tarih:***	**06.09.2011**
Ground Water Level *Yeraltısuyu Seviyesi*	7,50 m			***Test Hole Diameter*** *Kuyu Çapı*	96 mm
Stage (m) *Kademe*	41,00 - 42,00			**Stage Length** *Kademe Uzunluğu*	1,00 m
Hole Inclination (from vertical) *Kuyu Eğimi*	0 (°)			**Total Pipe Lenght** *Toplam Boru Uzunluğu*	41,00 m
Rod Diameter *Tij İç Çapı*	77,80 mm			**Rod+Coupling Lenght** *Tij+Manşon Uzunluğu*	3,00 m
Coupling Diameter *Manşon İç Çapı*	77,80 mm			**Coupling Lenght** *Manşon Uzunluğu*	0,00 m
Packer Inner Diameter *Tıkaç İç Çapı*	22,00 mm			**Packer Lenght** *Tıkaç Uzunluğu*	1,34 m
Hose Diameter *Hortum İç Çapı*	22,00 mm			**Hose Lenght** *Hortum Uzunluğu*	5,00 m

PM	T	TOTAL Q	H	PC	PE	AQ	LUGEON
					0,00	0,00	
3,0	5	**16**	0,80	0,000	3,80	3,20	3,61
6,0	5	**17**	0,80	0,000	6,80	3,40	5,32
9,0	5	**26**	0,80	0,000	9,80	5,20	5,37
6,0	5	**13**	0,80	0,000	6,80	2,60	2,81
3,0	5	**12**	0,80	0,000	3,80	2,40	6,32

LUGEON VALUE = **4,69** **Laminar** **PERMEABILITY (m/sec.) =** **2,38E-05**

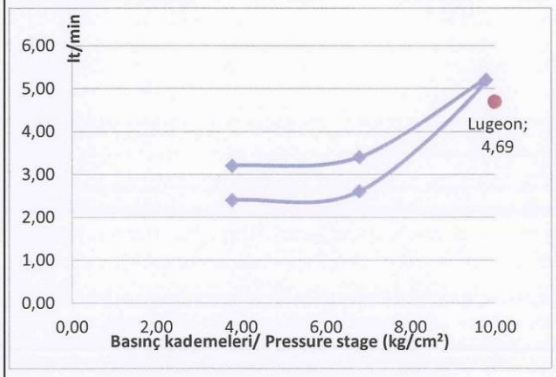

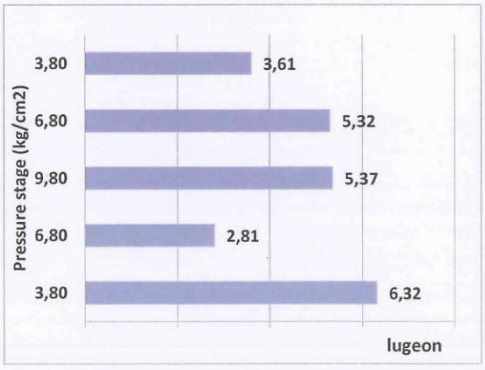

H : Hydrostatic head pressure (kg / cm^2)
PC : Friction losses (kg / cm^2)
PE : Effective pressure (kg / cm^2)
AQ : Coef. of absorption (l / m / min.)

PM : Mano pressure (kg/cm^2)
T : Time (min.)
T.Q : Total take (l)

Tested By
Deneyi Yapan

Approved By
Onaylayan

Figure E.19. Water pressure test result of borehole S-AS-106 at depth 41.00-42.0 m

ZEMAR istanbul
ZEMAR Zemin Araştırma ve Mühendislik

Istanbul Strait Road Crossing Project
İstanbul Karayolu Boğaz Geçiş Projesi

Avrasya TÜNELİ

Water Pressure Test (Lugeon Test) / *Basınçlı Su Testi (Lugeon Deneyi)*

Borehole No: *Sondaj No*	**S-AS-106**	**Location:** *Lokasyon*	**Haydarpaşa**	**Date / *Tarih:***	**06.09.2011**
Ground Water Level *Yeraltısuyu Seviyesi*	7,50 m			***Test Hole Diameter*** *Kuyu Çapı*	96 mm
Stage (m) *Kademe*	43,00 - 44,00			**Stage Length** *Kademe Uzunluğu*	1,00 m
Hole Inclination (from vertical) *Kuyu Eğimi*	0 (°)			**Total Pipe Lenght** *Toplam Boru Uzunluğu*	43,00 m
Rod Diameter *Tij İç Çapı*	77,80 mm			**Rod+Coupling Lenght** *Tij+Manşon Uzunluğu*	3,00 m
Coupling Diameter *Manşon İç Çapı*	77,80 mm			**Coupling Lenght** *Manşon Uzunluğu*	0,00 m
Packer Inner Diameter *Tıkaç İç Çapı*	22,00 mm			**Packer Lenght** *Tıkaç Uzunluğu*	1,34 m
Hose Diameter *Hortum İç Çapı*	22,00 mm			**Hose Lenght** *Hortum Uzunluğu*	5,00 m

PM	T	TOTAL Q	H	PC	PE	AQ	LUGEON
					0,00	0,00	
3,0	5	**7**	0,80	0,000	3,80	1,40	2,23
6,0	5	**9**	0,80	0,000	6,80	1,80	2,23
9,0	5	**11**	0,80	0,000	9,80	2,20	2,28
6,0	5	**5**	0,80	0,000	6,80	1,00	1,21
3,0	5	**4**	0,80	0,000	3,80	0,80	2,11

LUGEON VALUE = 2,01 laminar PERMEABILITY (m/sec.) = 9,79E-06

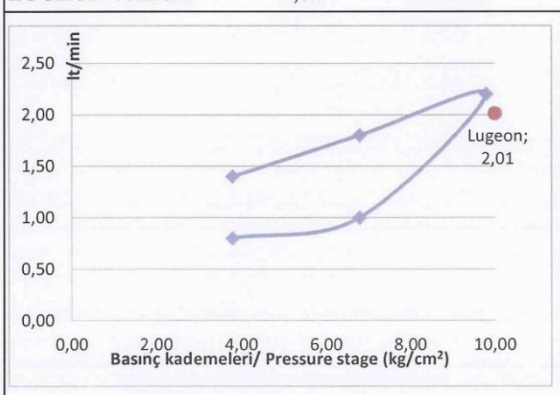

H : Hydrostatic head pressure (kg / cm^2)
PC : Friction losses (kg / cm^2)
PE : Effective pressure (kg / cm^2)
AQ : Coef. of absorption (l / m / min.)

PM : Mano pressure (kg/cm^2)
T : Time (min.)
T.Q : Total take (l)

Tested By
Deneyi Yapan

Approved By
Onaylayan

Figure E.20. Water pressure test result of borehole S-AS-106 at depth 43.00-44.0 m

ZEMAR İSTANBUL ZEMAR Zemin Araştırma ve Mühendislik

Istanbul Strait Road Crossing Project
İstanbul Karayolu Boğaz Geçiş Projesi

Avrasya TÜNELİ

Water Pressure Test (Lugeon Test) / *Basınçlı Su Testi (Lugeon Deneyi)*

Borehole No: *Sondaj No*	**S-AS-107**	**Location:** *Lokasyon*	**Haydarpaşa**	**Date / *Tarih:***	**00.01.1900**
Ground Water Level *Yeraltısuyu Seviyesi*	5,70 m			***Test Hole Diameter*** *Kuyu Çapı*	76,30 mm
Stage (m) *Kademe*	15,00 - 16,00			**Stage Length** *Kademe Uzunluğu*	1,00 m
Hole Inclination (from vertical) *Kuyu Eğimi*	0,00 (°)			**Total Pipe Lenght** *Toplam Boru Uzunluğu*	15,00 m
Rod Diameter *Tij İç Çapı*	76,30 mm			**Rod+Coupling Lenght** *Tij+Manşon Uzunluğu*	1,51 m
Coupling Diameter *Manşon İç Çapı*	76,30 mm			**Coupling Lenght** *Manşon Uzunluğu*	0,31 m
Packer Inner Diameter *Tıkaç İç Çapı*	25,40 mm			**Packer Lenght** *Tıkaç Uzunluğu*	1,50 m
Hose Diameter *Hortum İç Çapı*	20,00 mm			**Hose Lenght** *Hortum Uzunluğu*	4,50 m

PM	T	TOTAL Q	H	PC	PE	AQ	LUGEON
					0,00	0,00	
3,0	5	**46**	0,62	0,002	3,62	9,20	18,14
6,0	5	**67**	0,62	0,004	6,62	13,40	16,79
9,0	5	**82**	0,62	0,006	9,61	16,40	17,07
6,0	5	**56**	0,62	0,003	6,62	11,20	14,81
3,0	5	**40**	0,62	0,001	3,62	8,00	22,11

LUGEON VALUE = 17,79 Laminar PERMEABILITY (m/sec.) = 8,37E-05

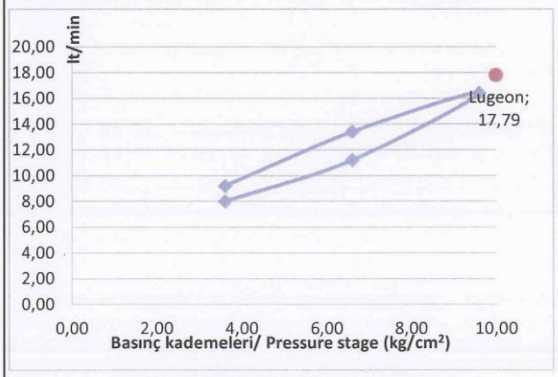

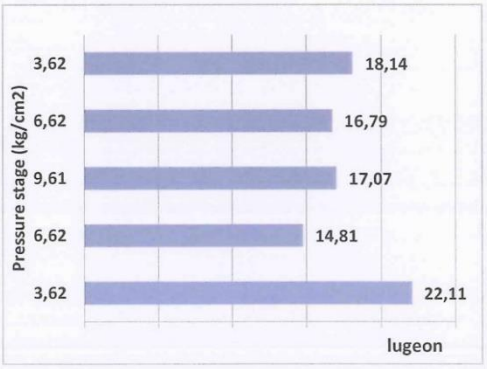

H : Hydrostatic head pressure (kg / cm^2)
PC : Friction losses (kg / cm^2)
PE : Effective pressure (kg / cm^2)
AQ : Coef. of absorption (l / m / min.)

PM : Mano pressure (kg/cm^2)
T : Time (min.)
T.Q : Total take (l)

Tested By
Deneyi Yapan

Approved By
Onaylayan

Figure E.21. Water pressure test result of borehole S-AS-107 at depth 15.00-16.00 m

ZEMAR İstanbul — ZEMAR Zemin Araştırma ve Mühendislik

Istanbul Strait Road Crossing Project
İstanbul Karayolu Boğaz Geçiş Projesi

Avrasya Tüneli

Water Pressure Test (Lugeon Test) / *Basınçlı Su Testi (Lugeon Deneyi)*

Borehole No: *Sondaj No*	**S-AS-107**	**Location:** *Lokasyon*	**Haydarpaşa**	**Date** / *Tarih:*	**00.01.1900**
Ground Water Level *Yeraltısuyu Seviyesi*	5,70 m			***Test Hole Diameter*** *Kuyu Çapı*	76,30 mm
Stage (m) *Kademe*	18,00 - 19,00			**Stage Length** *Kademe Uzunluğu*	1,00 m
Hole Inclination (from vertical) *Kuyu Eğimi*	0,00 (°)			**Total Pipe Lenght** *Toplam Boru Uzunluğu*	18,00 m
Rod Diameter *Tij İç Çapı*	76,30 mm			**Rod+Coupling Lenght** *Tij+Manşon Uzunluğu*	1,51 m
Coupling Diameter *Manşon İç Çapı*	76,30 mm			**Coupling Lenght** *Manşon Uzunluğu*	0,31 m
Packer Inner Diameter *Tıkaç İç Çapı*	25,40 mm			**Packer Lenght** *Tıkaç Uzunluğu*	1,50 m
Hose Diameter *Hortum İç Çapı*	20,00 mm			**Hose Lenght** *Hortum Uzunluğu*	4,50 m

PM	T	TOTAL Q	H	PC	PE	AQ	LUGEON
					0,00	0,00	
3,0	5	**26**	0,62	0,001	3,62	5,20	9,88
6,0	5	**37**	0,62	0,001	6,62	7,40	12,14
9,0	5	**58**	0,62	0,003	9,62	11,60	11,88
6,0	5	**47**	0,62	0,002	6,62	9,40	11,43
3,0	5	**38**	0,62	0,001	3,62	7,60	21,00

LUGEON VALUE = 21,00 **Wash-out** **PERMEABILITY (m/sec.) = 9,11E-05**

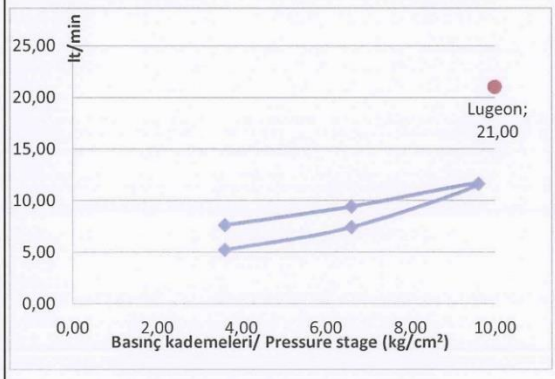

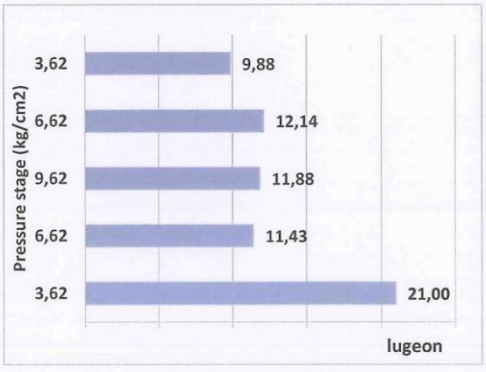

H : Hydrostatic head pressure (kg / cm^2)
PC : Friction losses (kg / cm^2)
PE : Effective pressure (kg / cm^2)
AQ : Coef. of absorption (l / m / min.)

PM : Mano pressure (kg/cm^2)
T : Time (min.)
T.Q : Total take (l)

Tested By
Deneyi Yapan

Approved By
Onaylayan

Figure E.22. Water pressure test result of borehole S-AS-107 at depth 18.00-19.00 m

ZEMAR İSTANBUL ZEMAR Zemin Araştırma ve Mühendislik

Istanbul Strait Road Crossing Project
İstanbul Karayolu Boğaz Geçiş Projesi

Avrasya TÜNELİ

Water Pressure Test (Lugeon Test) / *Basınçlı Su Testi (Lugeon Deneyi)*

Borehole No: *Sondaj No*	**S-AS-107**	**Location:** *Lokasyon*	**Haydarpaşa**	**Date / *Tarih:***	**00.01.1900**
Ground Water Level *Yeraltısuyu Seviyesi*	5,70 m			***Test Hole Diameter*** *Kuyu Çapı*	76,30 mm
Stage (m) *Kademe*	22,50 - 23,50			**Stage Length** *Kademe Uzunluğu*	1,00 m
Hole Inclination (from vertical) *Kuyu Eğimi*	0,00 (°)			**Total Pipe Lenght** *Toplam Boru Uzunluğu*	22,50 m
Rod Diameter *Tij İç Çapı*	76,30 mm			**Rod+Coupling Lenght** *Tij+Manşon Uzunluğu*	1,51 m
Coupling Diameter *Manşon İç Çapı*	76,30 mm			**Coupling Lenght** *Manşon Uzunluğu*	0,31 m
Packer Inner Diameter *Tıkaç İç Çapı*	25,40 mm			**Packer Lenght** *Tıkaç Uzunluğu*	1,50 m
Hose Diameter *Hortum İç Çapı*	20,00 mm			**Hose Lenght** *Hortum Uzunluğu*	4,50 m

PM	T	TOTAL Q	H	PC	PE	AQ	LUGEON
					0,00	0,00	
3,0	5	**21**	0,62	0,000	3,62	4,20	10,16
6,0	5	**35**	0,62	0,001	6,62	7,00	9,03
9,0	5	**44**	0,62	0,002	9,62	8,80	9,16
6,0	5	**30**	0,62	0,001	6,62	6,00	6,68
3,0	5	**27**	0,62	0,001	3,62	5,40	14,92

LUGEON VALUE = 9,99 Laminar PERMEABILITY (m/sec.) = 4,47E-05

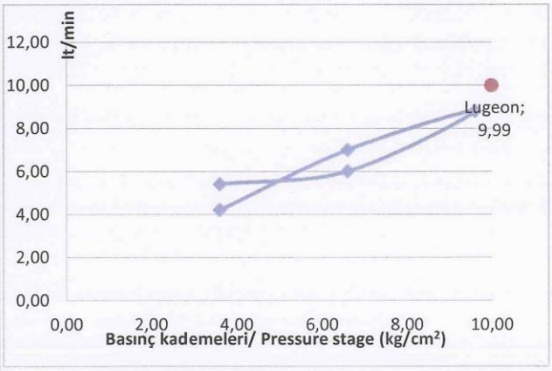

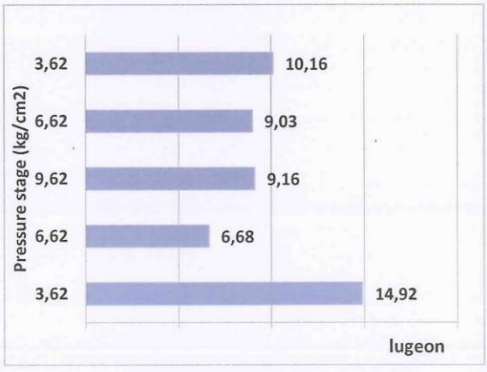

H : Hydrostatic head pressure (kg / cm^2)
PC : Friction losses (kg / cm^2)
PE : Effective pressure (kg / cm^2)
AQ : Coef. of absorption (l / m / min.)

PM : Mano pressure (kg/cm^2)
T : Time (min.)
T.Q : Total take (l)

Tested By
Deneyi Yapan

Approved By
Onaylayan

Figure E.23. Water pressure test result of borehole S-AS-107 at depth 22.50-23.50 m

ZEMAR İSTANBUL ZEMAR Zemin Araştırma ve Mühendislik

Istanbul Strait Road Crossing Project
İstanbul Karayolu Boğaz Geçiş Projesi

Avrasya TÜNELİ

Water Pressure Test (Lugeon Test) / *Basınçlı Su Testi (Lugeon Deneyi)*

Borehole No: *Sondaj No*	**S-AS-107**	**Location:** *Lokasyon*	**Haydarpaşa**	**Date** / *Tarih:*	**00.01.1900**
Ground Water Level *Yeraltısuyu Seviyesi*	5,70 m			***Test Hole Diameter*** *Kuyu Çapı*	76,30 mm
Stage (m) *Kademe*	28,50 - 29,50			**Stage Length** *Kademe Uzunluğu*	1,00 m
Hole Inclination (from vertical) *Kuyu Eğimi*	0,00 (°)			**Total Pipe Lenght** *Toplam Boru Uzunluğu*	28,50 m
Rod Diameter *Tij İç Çapı*	76,30 mm			**Rod+Coupling Lenght** *Tij+Manşon Uzunluğu*	1,51 m
Coupling Diameter *Manşon İç Çapı*	76,30 mm			**Coupling Lenght** *Manşon Uzunluğu*	0,31 m
Packer Inner Diameter *Tıkaç İç Çapı*	25,40 mm			**Packer Lenght** *Tıkaç Uzunluğu*	1,50 m
Hose Diameter *Hortum İç Çapı*	20,00 mm			**Hose Lenght** *Hortum Uzunluğu*	4,50 m

PM	T	TOTAL Q	H	PC	PE	AQ	LUGEON
					0,00	0,00	
3,0	5	**18**	0,62	0,000	3,62	3,60	8,28
6,0	5	**29**	0,62	0,001	6,62	5,80	7,38
9,0	5	**36**	0,62	0,001	9,62	7,20	7,58
6,0	5	**21**	0,62	0,000	6,62	4,20	5,78
3,0	5	**14**	0,62	0,000	3,62	2,80	7,74

LUGEON VALUE = 7,35 laminar PERMEABILITY (m/sec.) = 3,46E-05

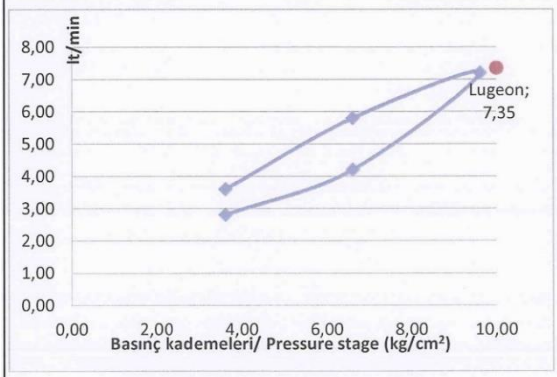

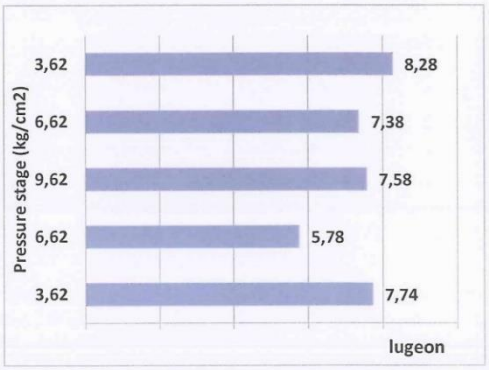

H : Hydrostatic head pressure (kg / cm^2)
PC : Friction losses (kg / cm^2)
PE : Effective pressure (kg / cm^2)
AQ : Coef. of absorption (l / m / min.)

PM : Mano pressure (kg/cm^2)
T : Time (min.)
T.Q : Total take (l)

Tested By
Deneyi Yapan

Approved By
Onaylayan

Figure E.24. Water pressure test result of borehole S-AS-107 at depth 28.50-29.50 m

ZEMAR istanbul — ZEMAR Zemin Araştırma ve Mühendislik

Istanbul Strait Road Crossing Project
İstanbul Karayolu Boğaz Geçiş Projesi

Avrasya TÜNELİ

Water Pressure Test (Lugeon Test) / *Basınçlı Su Testi (Lugeon Deneyi)*

Borehole No: *Sondaj No*	**S-AS-107**	**Location:** *Lokasyon*	**Haydarpaşa**	**Date / *Tarih:***	**00.01.1900**
Ground Water Level *Yeraltısuyu Seviyesi*	5,70 m			***Test Hole Diameter*** *Kuyu Çapı*	76,30 mm
Stage (m) *Kademe*	34,50 - 35,50			**Stage Length** *Kademe Uzunluğu*	1,00 m
Hole Inclination (from vertical) *Kuyu Eğimi*	0,00 (°)			**Total Pipe Lenght** *Toplam Boru Uzunluğu*	34,50 m
Rod Diameter *Tij İç Çapı*	76,30 mm			**Rod+Coupling Lenght** *Tij+Manşon Uzunluğu*	1,51 m
Coupling Diameter *Manşon İç Çapı*	76,30 mm			**Coupling Lenght** *Manşon Uzunluğu*	0,31 m
Packer Inner Diameter *Tıkaç İç Çapı*	25,40 mm			**Packer Lenght** *Tıkaç Uzunluğu*	1,50 m
Hose Diameter *Hortum İç Çapı*	20,00 mm			**Hose Lenght** *Hortum Uzunluğu*	4,50 m

PM	T	TOTAL Q	H	PC	PE	AQ	LUGEON
					0,00	0,00	
3,0	5	**26**	0,62	0,001	3,62	5,20	8,18
6,0	5	**33**	0,62	0,001	6,62	6,60	6,83
9,0	5	**34**	0,62	0,001	9,62	6,80	6,88
6,0	5	**31**	0,62	0,001	6,62	6,20	6,88
3,0	5	**28**	0,62	0,001	3,62	5,60	15,47

LUGEON VALUE = 15,47 **Wash-out** **PERMEABILITY (m/sec.) = 6,71E-05**

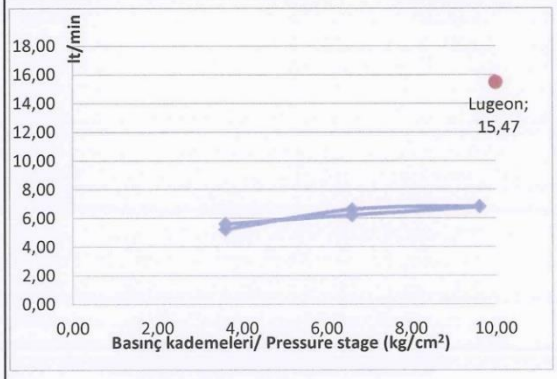

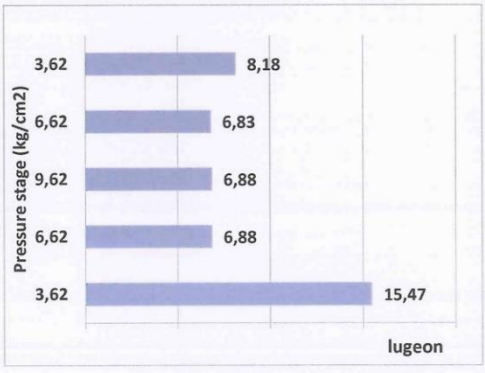

H : Hydrostatic head pressure (kg / cm^2)
PC : Friction losses (kg / cm^2)
PE : Effective pressure (kg / cm^2)
AQ : Coef. of absorption (l / m / min.)

PM : Mano pressure (kg/cm^2)
T : Time (min.)
T.Q : Total take (l)

Tested By
Deneyi Yapan

Approved By
Onaylayan

Figure E.25. Water pressure test result of borehole S-AS-107 at depth 34.50-35.50 m

ZEMAR İSTANBUL ZEMAR Zemin Araştırma ve Mühendislik

Istanbul Strait Road Crossing Project
İstanbul Karayolu Boğaz Geçiş Projesi

Avrasya TÜNELİ

Water Pressure Test (Lugeon Test) / *Basınçlı Su Testi (Lugeon Deneyi)*

Borehole No: *Sondaj No*	**S-AS-107**	**Location:** *Lokasyon*	**Haydarpaşa**	**Date** / *Tarih:*	**25.08.2011**
Ground Water Level *Yeraltısuyu Seviyesi*	5,70 m			***Test Hole Diameter*** *Kuyu Çapı*	76,30 mm
Stage (m) *Kademe*	39,00 - 40,00			**Stage Length** *Kademe Uzunluğu*	1,00 m
Hole Inclination (from vertical) *Kuyu Eğimi*	0,00 (°)			**Total Pipe Lenght** *Toplam Boru Uzunluğu*	39,00 m
Rod Diameter *Tij İç Çapı*	76,30 mm			**Rod+Coupling Lenght** *Tij+Manşon Uzunluğu*	1,51 m
Coupling Diameter *Manşon İç Çapı*	76,30 mm			**Coupling Lenght** *Manşon Uzunluğu*	0,31 m
Packer Inner Diameter *Tıkaç İç Çapı*	25,40 mm			**Packer Lenght** *Tıkaç Uzunluğu*	1,50 m
Hose Diameter *Hortum İç Çapı*	20,00 mm			**Hose Lenght** *Hortum Uzunluğu*	4,50 m

PM	T	TOTAL Q	H	PC	PE	AQ	LUGEON
					0,00	0,00	
3,0	5	**20**	0,62	0,000	3,62	4,00	11,66
6,0	5	**38**	0,62	0,001	6,62	7,60	9,85
9,0	5	**48**	0,62	0,002	9,62	9,60	9,88
6,0	5	**37**	0,62	0,001	6,62	7,40	10,78
3,0	5	**22**	0,62	0,000	3,62	4,40	12,16

LUGEON VALUE = 9,88 **Turbulent** **PERMEABILITY (m/sec.) = 4,33E-05**

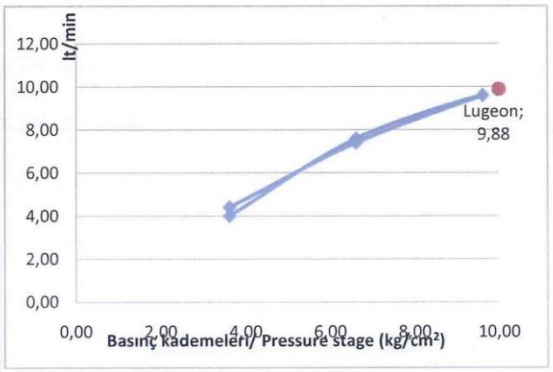

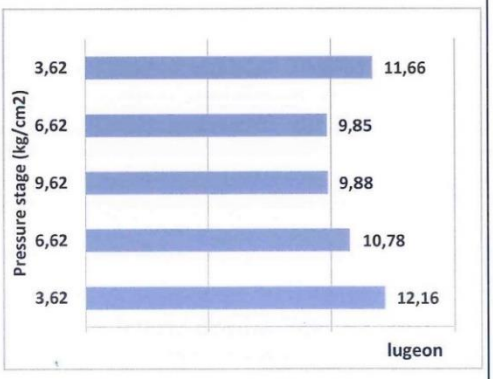

H : Hydrostatic head pressure (kg / cm^2)
PC : Friction losses (kg / cm^2)
PE : Effective pressure (kg / cm^2)
AQ : Coef. of absorption (l / m / min.)

PM : Mano pressure (kg/cm^2)
T : Time (min.)
T.Q : Total take (l)

Tested By
Deneyi Yapan

Approved By
Onaylayan

Figure E.26. Water pressure test result of borehole S-AS-107 at depth 39.00-40.00 m

APPENDIX F

PRESSUREMETER TEST RESULTS

STFA

STFA TEMEL ARAŞTIRMA ve SONDAJ A.Ş.
Zemin ve Kaya Mekaniği Laboratuarı

PRESSİYOMETRE DENEYİ B FORMU / THE MENARD PRESSUREMETER TEST B FORM

ASTM D4719

Proje:		**Deney No:**	
Project:	ISTANBUL STRAIT ROAD TUNNEL CROSSING PROJECT	**Test No:**	**P.T. 1**
Bölge:		**Deney Derinliği:**	
Site / Location:	HAYDARPASA PARK SITE	**Depth of Test:**	38.50m
Lab Kod No/Lab Code No:	8	**Tarih/Date:**	12.02.2010
Sondaj No:		**Kaya Tanımı:**	
Borehole No:	**NTB 1**	**Rock Type:**	SANDSTONE

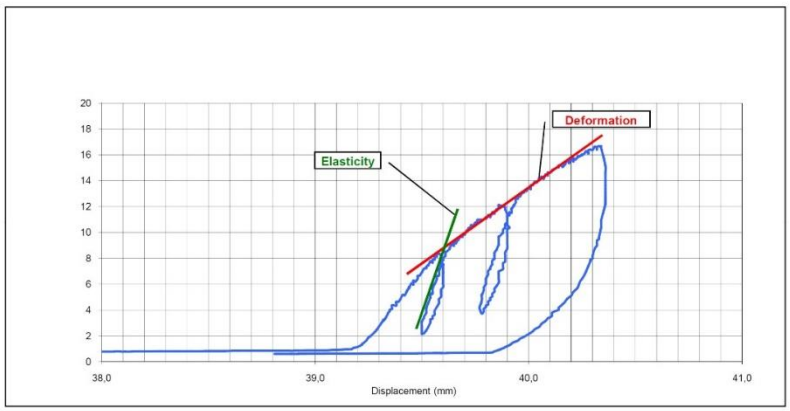

Deformation Constant (Dc)
Elasticity Constant (Ec)

Deformation Constant (Dc)	
V Poisson's ratio of ground	0,3
R1 (Displacement 1) (mm)	39,58
R2 (Displacement 2) (mm)	40,20
Rm=(R1+R2)/2 (mm)	39,89
P1 (Pressure 1) (Mpa)	8,35
P2 (Pressure 2) (Mpa)	15,67
Db= (1+V)*Rm*(P2-P1)/(R2-R1) (Mpa)	612,25
Db (Deformation in "kgf/cm²" unit)	6.244,92

Elasticity Constant (Ec)	
V Poisson's ratio of ground	0,3
R1 (Displacement 1) (mm)	39,5
R2 (Displacement 2) (mm)	39,61
Rm=(R1+R2)/2 (mm)	39,555
P1 (Pressure 1) (Mpa)	3,09
P2 (Pressure 2) (Mpa)	8,29
E=(1+V)*Rm*(P2-P1)/(R2-R1) (Mpa)	2.430,83
E (Elasticity in "kgf/cm²" unit)	24.794,51

Yapan / Performed by:

Mehmet AKDENİZ

Kontrol / Checked by:

Mehmet BOL

Figure F.1. Pressuremeter test result of borehole NTB-1 at depth 38.5 m

STFA

STFA TEMEL ARAŞTIRMA ve SONDAJ A.Ş.
Zemin ve Kaya Mekaniği Laboratuarı

PRESSİYOMETRE DENEYİ B FORMU / THE MENARD PRESSUREMETER TEST B FORM

ASTM D4719

Proje:		**Deney No:**	
Project:	ISTANBUL STRAIT ROAD TUNNEL CROSSING PROJECT	**Test No:**	**P.T. 2**
Bölge:		**Deney Derinliği:**	
Site / Location:	HAYDARPASA PARK SITE	**Depth of Test:**	44.50m
Lab Kod No/Lab Code No:	8	**Tarih/Date:**	15.02.2010
Sondaj No:		**Kaya Tanımı:**	
Borehole No:	**NTB 1**	**Rock Type:**	SANDSTONE

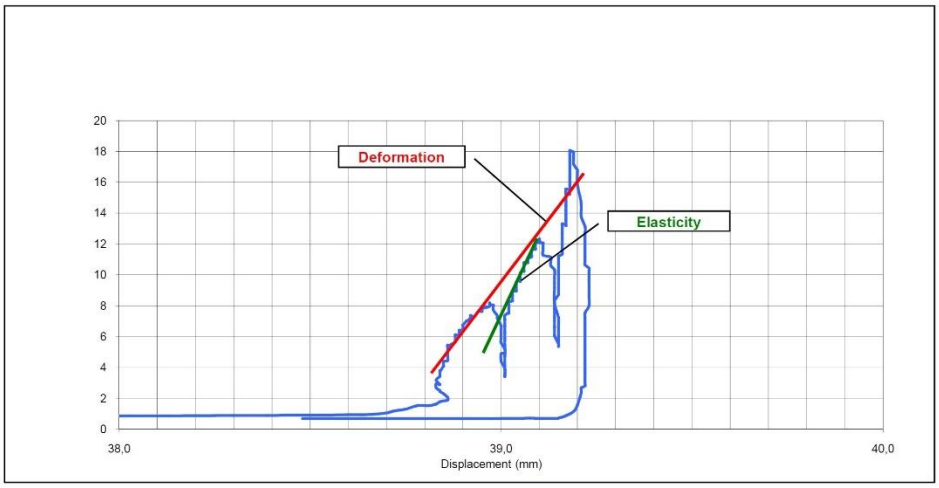

Deformation Constant (Dc)
Elasticity Constant (Ec)

Deformation Constant (Dc)	
V Poisson's ratio of ground	0,3
R1 (Displacement 1) (mm)	38,97
R2 (Displacement 2) (mm)	39,09
Rm=(R1+R2)/2 (mm)	39,03
P1 (Pressure 1) (Mpa)	8,19
P2 (Pressure 2) (Mpa)	12,03
Db= (1+V)*Rm*(P2-P1)/(R2-R1) (Mpa)	1.623,65
Db (Deformation in "kgf/cm^2" unit)	16.561,21

Elasticity Constant (Ec)	
V Poisson's ratio of ground	0,3
R1 (Displacement 1) (mm)	39,02
R2 (Displacement 2) (mm)	39,09
Rm=(R1+R2)/2 (mm)	39,055
P1 (Pressure 1) (Mpa)	8,06
P2 (Pressure 2) (Mpa)	12,03
E=(1+V)*Rm*(P2-P1)/(R2-R1) (Mpa)	2.879,47
E (Elasticity in "kgf/cm^2" unit)	29.370,59

Yapan / Performed by: Mehmet AKDENİZ

Kontrol / Checked by: Mehmet BOL

Figure F.2. Pressuremeter test result of borehole NTB-1 at depth 44.5 m

STFA

STFA TEMEL ARAŞTIRMA ve SONDAJ A.Ş.
Zemin ve Kaya Mekaniği Laboratuarı

PRESSİYOMETRE DENEYİ B FORMU / THE MENARD PRESSUREMETER TEST B FORM

ASTM D4719

Proje:		**Deney No:**	
Project:	ISTANBUL STRAIT ROAD TUNNEL CROSSING PROJECT	**Test No:**	**P.T. 3**
Bölge:		**Deney Derinliği:**	
Site / Location:	HAYDARPASA PARK SITE	**Depth of Test:**	52.60m
Lab Kod No/Lab Code No:	8	**Tarih/Date:**	17.02.2010
Sondaj No:		**Kaya Tanımı:**	
Borehole No:	**NTB 1**	**Rock Type:**	SANDSTONE

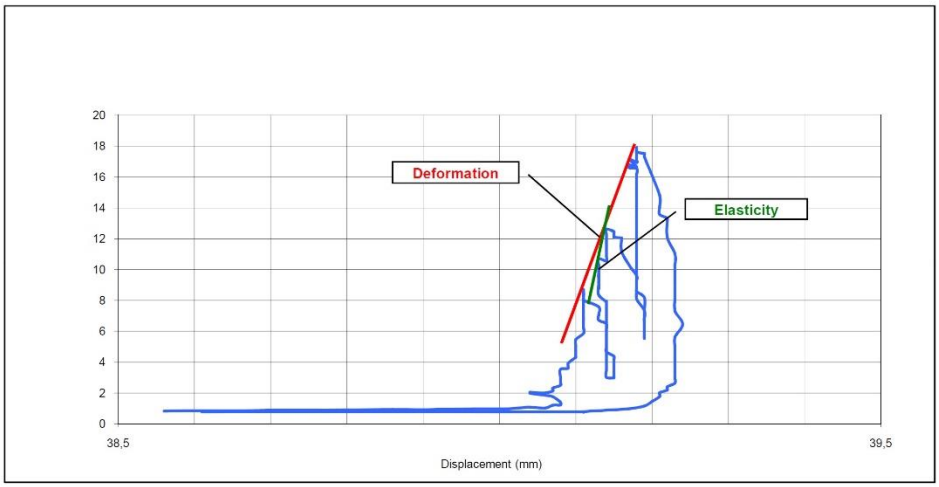

Deformation Constant (Dc)
Elasticity Constant (Ec)

Deformation Constant (Dc)	
V Poisson's ratio of ground	0,3
R1 (Displacement 1) (mm)	39,11
R2 (Displacement 2) (mm)	39,14
Rm=(R1+R2)/2 (mm)	39,13
P1 (Pressure 1) (Mpa)	8,40
P2 (Pressure 2) (Mpa)	12,25
Db= (1+V)*Rm*(P2-P1)/(R2-R1) (Mpa)	6.527,35
Db (Deformation in "kgf/cm²" unit)	66.579,01

Elasticity Constant (Ec)	
V Poisson's ratio of ground	0,3
R1 (Displacement 1) (mm)	39,13
R2 (Displacement 2) (mm)	39,14
Rm=(R1+R2)/2 (mm)	39,135
P1 (Pressure 1) (Mpa)	10,71
P2 (Pressure 2) (Mpa)	12,62
E=(1+V)*Rm*(P2-P1)/(R2-R1) (Mpa)	9.717,22
E (Elasticity in "kgf/cm²" unit)	99.115,65

Yapan / Performed by: Mehmet AKDENİZ

Kontrol / Checked by: Mehmet BOL

Figure F.3. Pressuremeter test result of borehole NTB-1 at depth 52.6 m

STFA

STFA TEMEL ARAŞTIRMA ve SONDAJ A.Ş.
Zemin ve Kaya Mekaniği Laboratuarı

PRESSİYOMETRE DENEYİ B FORMU / THE MENARD PRESSUREMETER TEST B FORM

ASTM D4719

Proje:		**Deney No:**	
Project:	ISTANBUL STRAIT ROAD TUNNEL CROSSING PROJECT	**Test No:**	**P.T. 1**
Bölge:		**Deney Derinliği:**	
Site / Location:	HAYDARPAŞA DLH OFICE GARDEN	**Depth of Test:**	37.80m
Lab Kod No/Lab Code No:	8	**Tarih/Date:**	05.02.2010
Sondaj No:		**Kaya Tanımı:**	
Borehole No:	**NTB 2**	**Rock Type:**	SANDSTONE

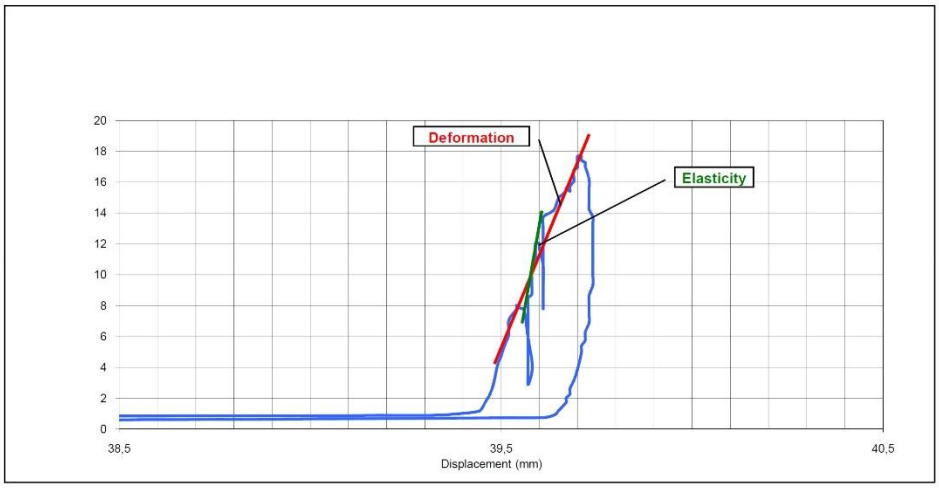

Deformation Constant (Dc)
Elasticity Constant (Ec)

Deformation Constant (Dc)	
V Poisson's ratio of ground	0,3
R1 (Displacement 1) (mm)	39,54
R2 (Displacement 2) (mm)	39,69
Rm=(R1+R2)/2 (mm)	39,62
P1 (Pressure 1) (Mpa)	8,01
P2 (Pressure 2) (Mpa)	16,05
Db= (1+V)*Rm*(P2-P1)/(R2-R1) (Mpa)	2.760,37
Db (Deformation in "kgf/cm²" unit)	28.155,81

Elasticity Constant (Ec)	
V Poisson's ratio of ground	0,3
R1 (Displacement 1) (mm)	39,57
R2 (Displacement 2) (mm)	39,6
Rm=(R1+R2)/2 (mm)	39,585
P1 (Pressure 1) (Mpa)	8,48
P2 (Pressure 2) (Mpa)	11,85
E=(1+V)*Rm*(P2-P1)/(R2-R1) (Mpa)	5.780,73
E (Elasticity in "kgf/cm²" unit)	58.963,44

Yapan / Performed by: Mehmet AKDENİZ

Kontrol / Checked by: Mehmet BOL

Figure F.4. Pressuremeter test result of borehole NTB-2 at depth 37.8 m

STFA

STFA TEMEL ARAŞTIRMA ve SONDAJ A.Ş.
Zemin ve Kaya Mekaniği Laboratuarı

PRESSİYOMETRE DENEYİ B FORMU / THE MENARD PRESSUREMETER TEST B FORM

ASTM D4719

Proje:		**Deney No:**	
Project:	ISTANBUL STRAIT ROAD TUNNEL CROSSING PROJECT	**Test No:**	**P.T. 1**
Bölge:		**Deney Derinliği:**	
Site / Location:	HAYDARPASA HARBOUR	**Depth of Test:**	38.40M
Lab Kod No/Lab Code No:	8	**Tarih/Date:**	01.03.2010
Sondaj No:		**Kaya Tanımı:**	
Borehole No:	**NTB 3**	**Rock Type:**	CLAYSTONE

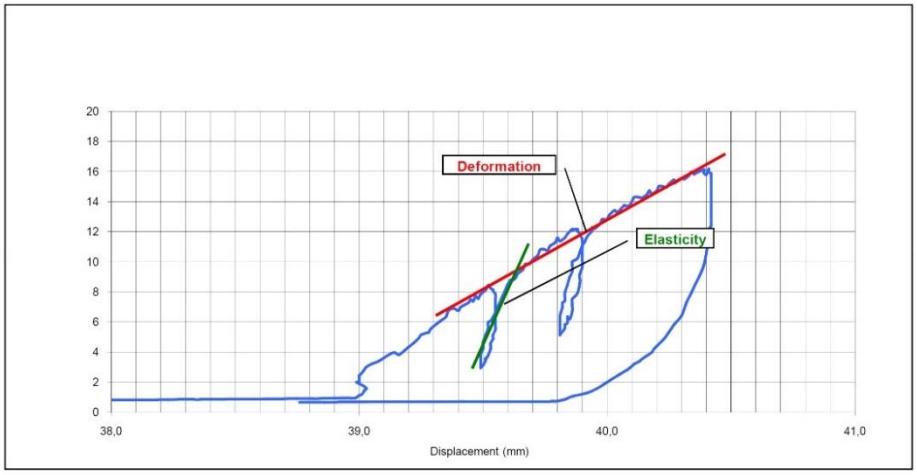

Deformation Constant (Dc)
Elasticity Constant (Ec)

Deformation Constant (Dc)	
V Poisson's ratio of ground	0,3
R1 (Displacement 1) (mm)	39,53
R2 (Displacement 2) (mm)	40,39
Rm=(R1+R2)/2 (mm)	39,96
P1 (Pressure 1) (Mpa)	8,24
P2 (Pressure 2) (Mpa)	16,13
Db= (1+V)*Rm*(P2-P1)/(R2-R1) (Mpa)	476,59
Db (Deformation in "kgf/cm²" unit)	4.861,25

Elasticity Constant (Ec)	
V Poisson's ratio of ground	0,3
R1 (Displacement 1) (mm)	39,53
R2 (Displacement 2) (mm)	39,61
Rm=(R1+R2)/2 (mm)	39,57
P1 (Pressure 1) (Mpa)	6,07
P2 (Pressure 2) (Mpa)	8,69
E=(1+V)*Rm*(P2-P1)/(R2-R1) (Mpa)	1.684,69
E (Elasticity in "kgf/cm²" unit)	17.183,87

Yapan / Performed by:

Servet DEMİRBAŞ

Kontrol / Checked by:

Mehmet BOL

Figure F.5. Pressuremeter test result of borehole NTB-3 at depth 38.4 m

STFA

STFA TEMEL ARAŞTIRMA ve SONDAJ A.Ş.
Zemin ve Kaya Mekaniği Laboratuarı

PRESSİYOMETRE DENEYİ B FORMU / THE MENARD PRESSUREMETER TEST B FORM

ASTM D4719

Proje:		**Deney No:**	
Project:	ISTANBUL STRAIT ROAD TUNNEL CROSSING PROJECT	**Test No:**	**P.T. 1**
Bölge:		**Deney Derinliği:**	
Site / Location:	HAYDARPASA NUMUNE HOSPITAL SITE	**Depth of Test:**	33.10m
Lab Kod No/Lab Code No:	8	**Tarih/Date:**	11.02.2010
Sondaj No:		**Kaya Tanımı:**	
Borehole No:	**NTB 4**	**Rock Type:**	SANDSTONE

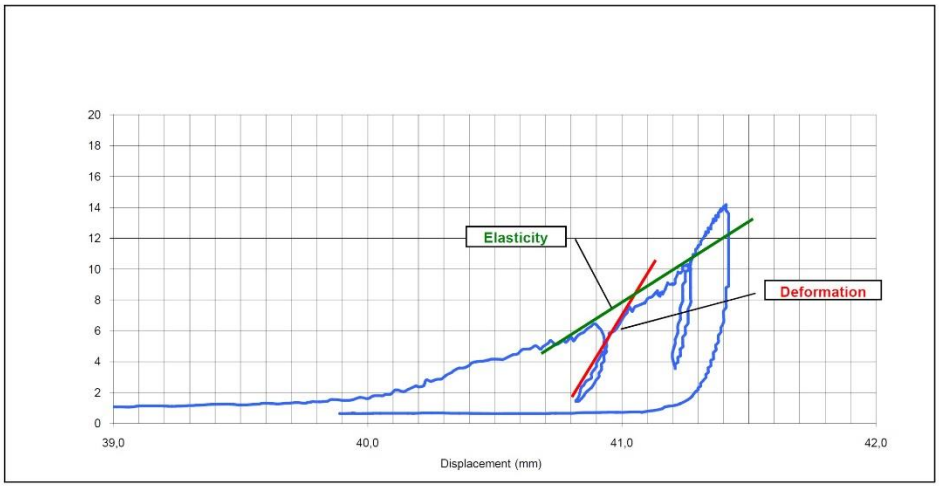

Deformation Constant (Dc)
Elasticity Constant (Ec)

Deformation Constant (Dc)	
V Poisson's ratio of ground	0,3
R1 (Displacement 1) (mm)	40,90
R2 (Displacement 2) (mm)	41,26
Rm=(R1+R2)/2 (mm)	41,08
P1 (Pressure 1) (Mpa)	6,39
P2 (Pressure 2) (Mpa)	10,14
Db= (1+V)*Rm*(P2-P1)/(R2-R1) (Mpa)	556,29
Db (Deformation in "kgf/cm²" unit)	5.674,18

Elasticity Constant (Ec)	
V Poisson's ratio of ground	0,3
R1 (Displacement 1) (mm)	40,85
R2 (Displacement 2) (mm)	40,97
Rm=(R1+R2)/2 (mm)	40,91
P1 (Pressure 1) (Mpa)	2,47
P2 (Pressure 2) (Mpa)	5,98
E=(1+V)*Rm*(P2-P1)/(R2-R1) (Mpa)	1.555,60
E (Elasticity in "kgf/cm²" unit)	15.867,15

Yapan / Performed by: Mehmet AKDENİZ

Kontrol / Checked by: Mehmet BOL

Figure F.6. Pressuremeter test result of borehole NTB-4 at depth 33.1 m

STFA

STFA TEMEL ARAŞTIRMA ve SONDAJ A.Ş.
Zemin ve Kaya Mekaniği Laboratuarı

PRESSİYOMETRE DENEYİ B FORMU / THE MENARD PRESSUREMETER TEST B FORM

ASTM D4719

Proje:		**Deney No:**	
Project:	ISTANBUL STRAIT ROAD TUNNEL CROSSING PROJECT	**Test No:**	**P.T. 2**
Bölge:		**Deney Derinliği:**	
Site / Location:	HAYDARPASA NUMUNE HOSPITAL SITE	**Depth of Test:**	42.00M
Lab Kod No/Lab Code No:	8	**Tarih/Date:**	16.02.2010
Sondaj No:		**Kaya Tanımı:**	
Borehole No:	**NTB 4**	**Rock Type:**	SANDSTONE

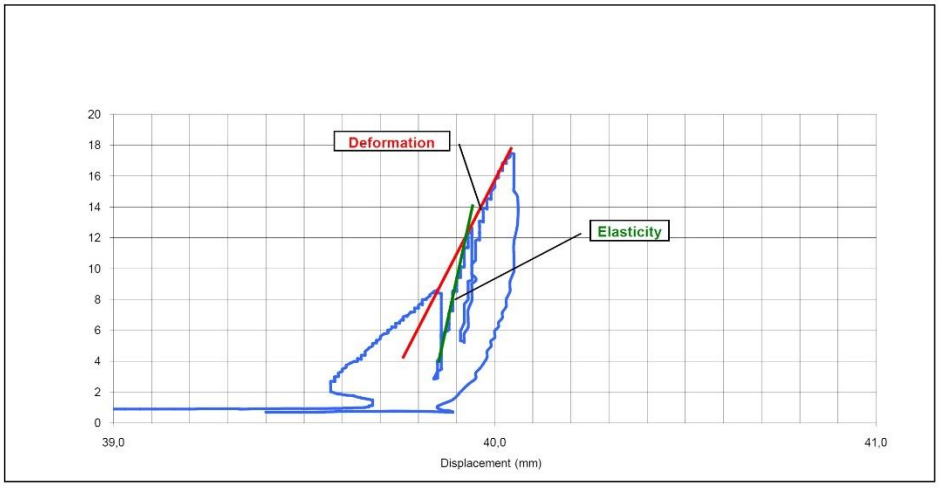

Deformation Constant (Dc)
Elasticity Constant (Ec)

Deformation Constant (Dc)	
V Poisson's ratio of ground	0,3
R1 (Displacement 1) (mm)	39,85
R2 (Displacement 2) (mm)	40,01
Rm=(R1+R2)/2 (mm)	39,93
P1 (Pressure 1) (Mpa)	8,62
P2 (Pressure 2) (Mpa)	16,19
Db= (1+V)*Rm*(P2-P1)/(R2-R1) (Mpa)	2.455,94
Db (Deformation in "kgf/cm²" unit)	25.050,63

Elasticity Constant (Ec)	
V Poisson's ratio of ground	0,3
R1 (Displacement 1) (mm)	39,89
R2 (Displacement 2) (mm)	39,94
Rm=(R1+R2)/2 (mm)	39,915
P1 (Pressure 1) (Mpa)	7,26
P2 (Pressure 2) (Mpa)	12,33
E=(1+V)*Rm*(P2-P1)/(R2-R1) (Mpa)	5.261,60
E (Elasticity in "kgf/cm²" unit)	53.668,27

Yapan / Performed by: Mehmet AKDENİZ

Kontrol / Checked by: Mehmet BOL

Figure F.7. Pressuremeter test result of borehole NTB-4 at depth 42.0 m

APPENDIX G

ROCLAB RESULTS

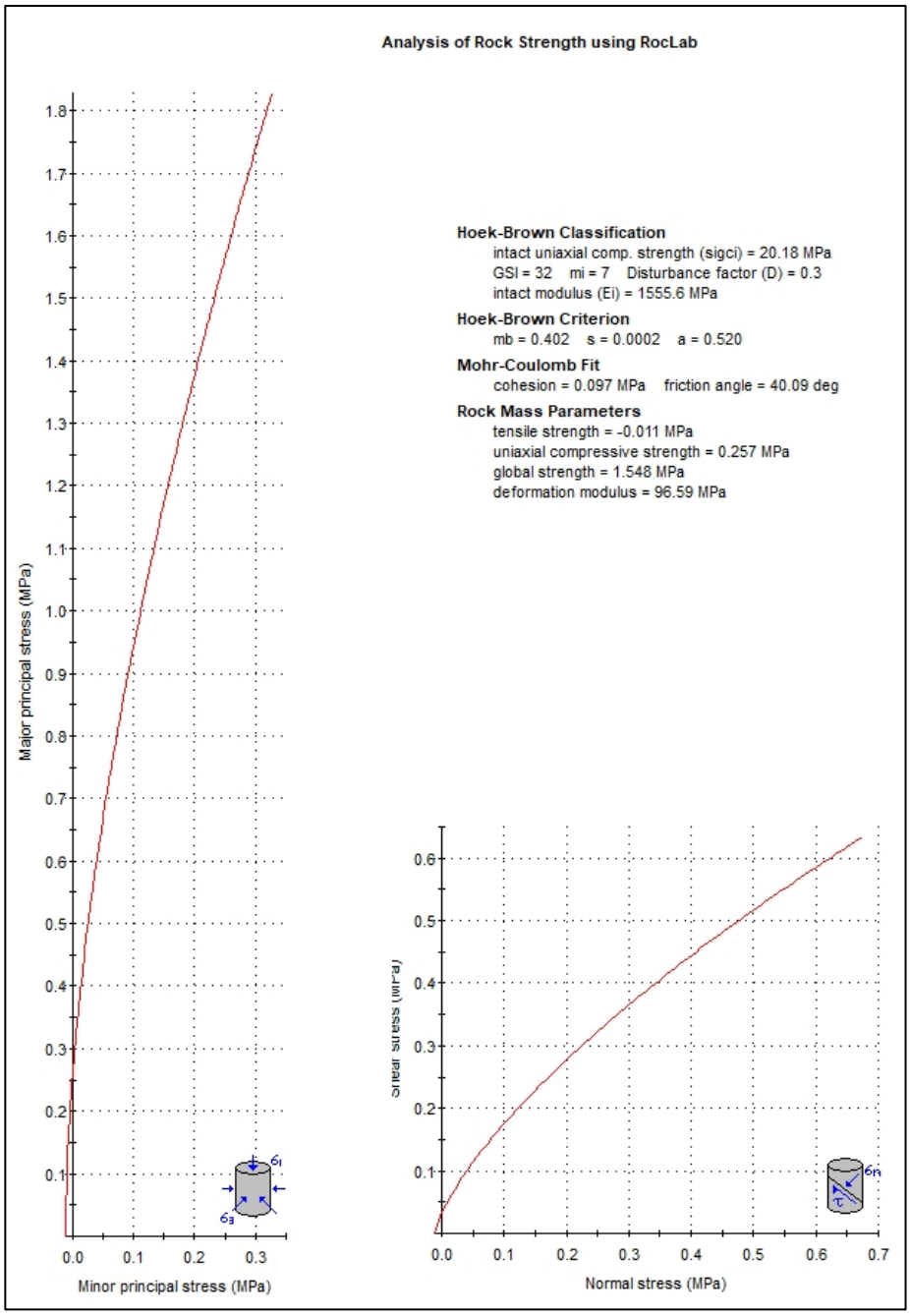

Figure G.1. RocLab results of Mudstone-0

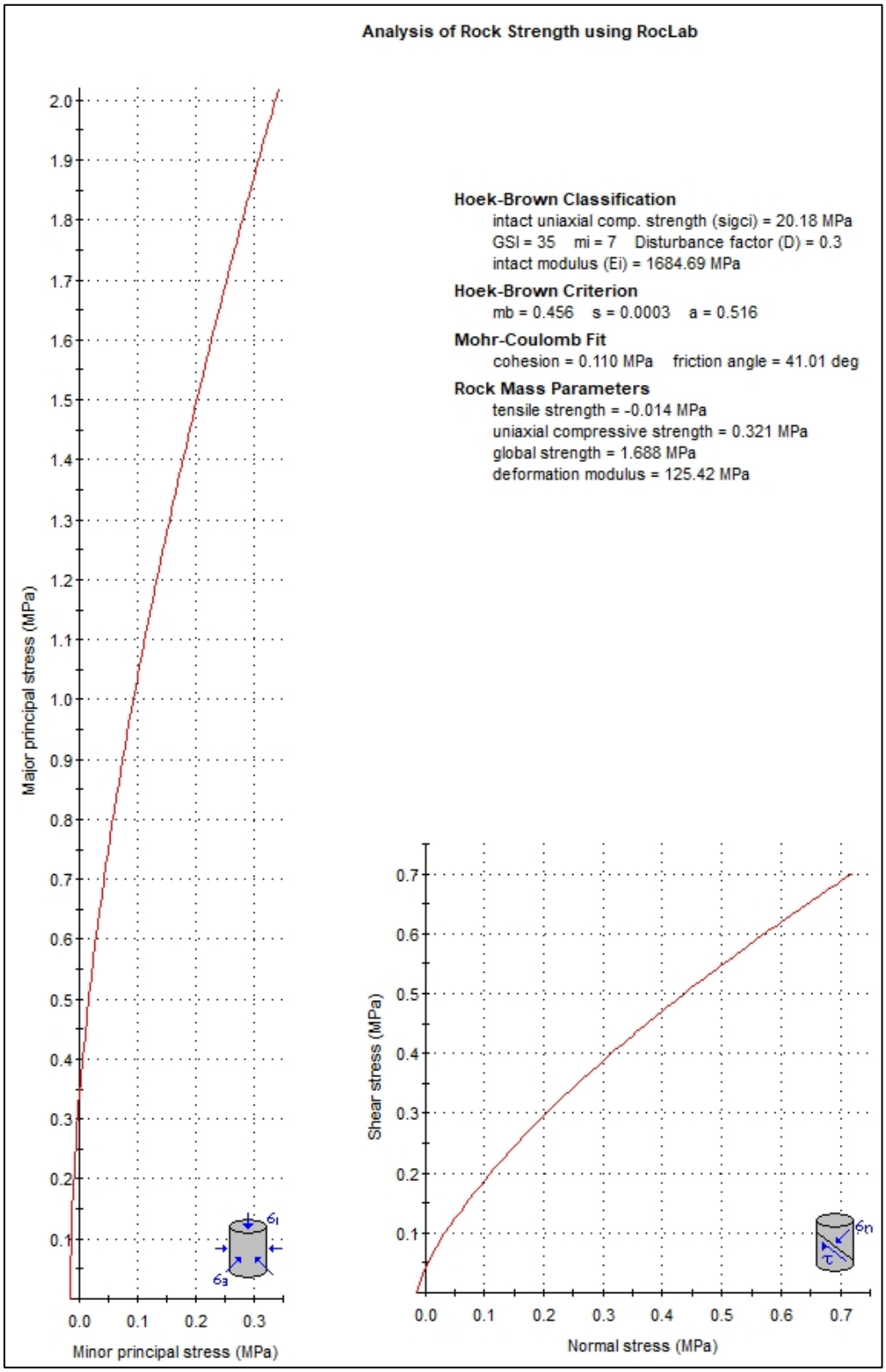

Figure G.2. RocLab results of Mudstone-1

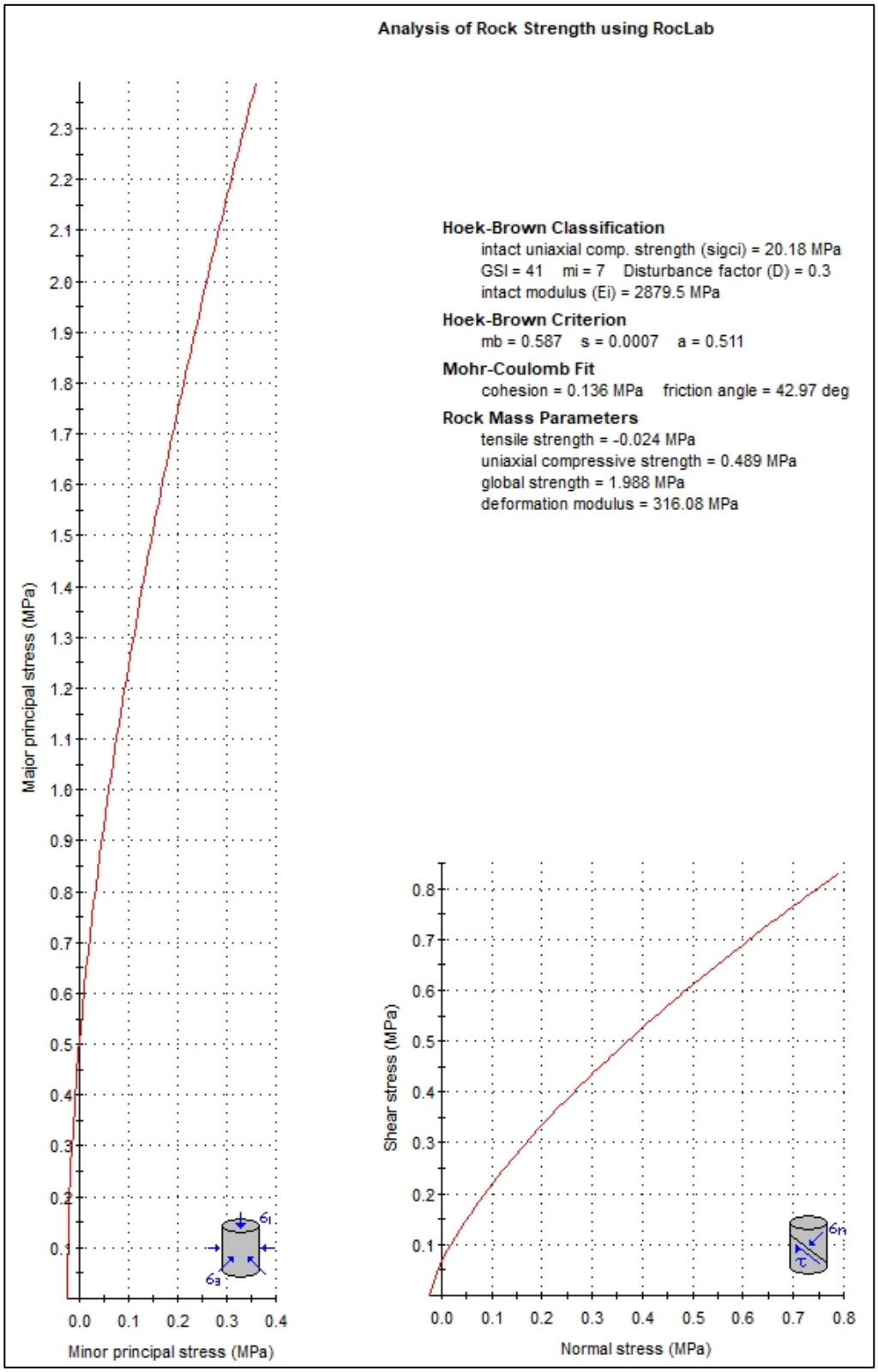

Figure G.3. RocLab results of Mudstone-2

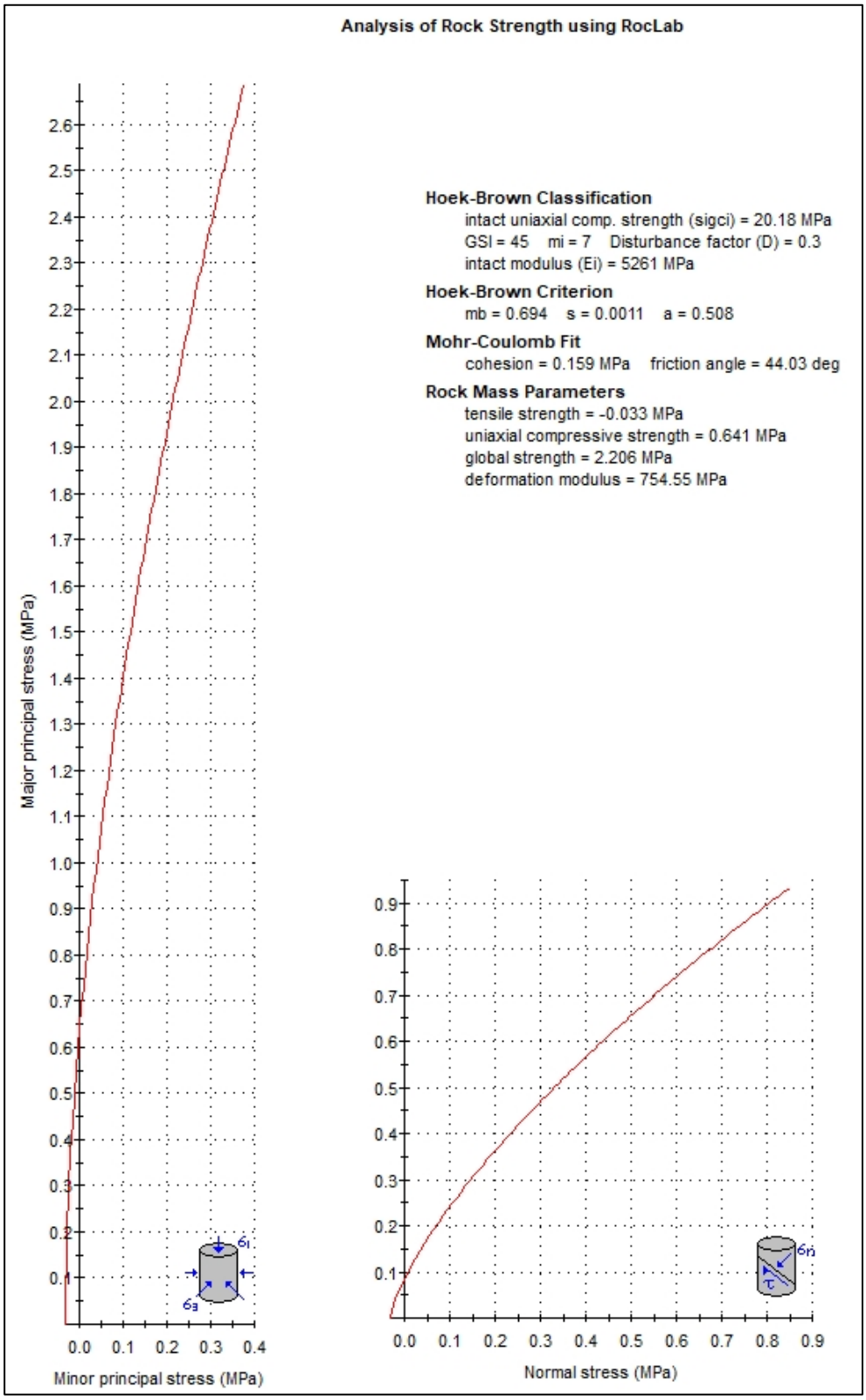

Figure G.4. RocLab results of Mudstone-3

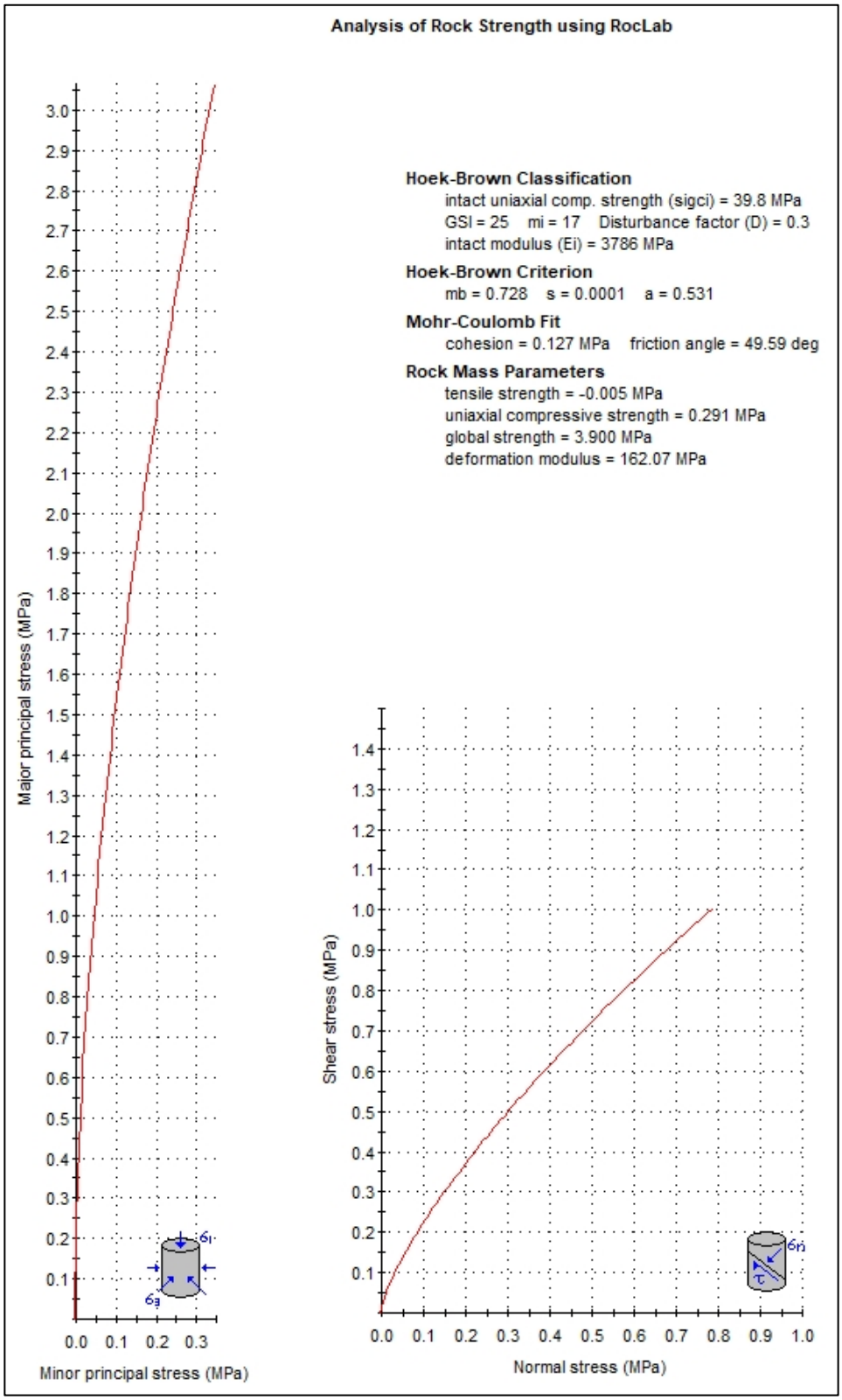

Figure G.5. RocLab results of Sandstone-0

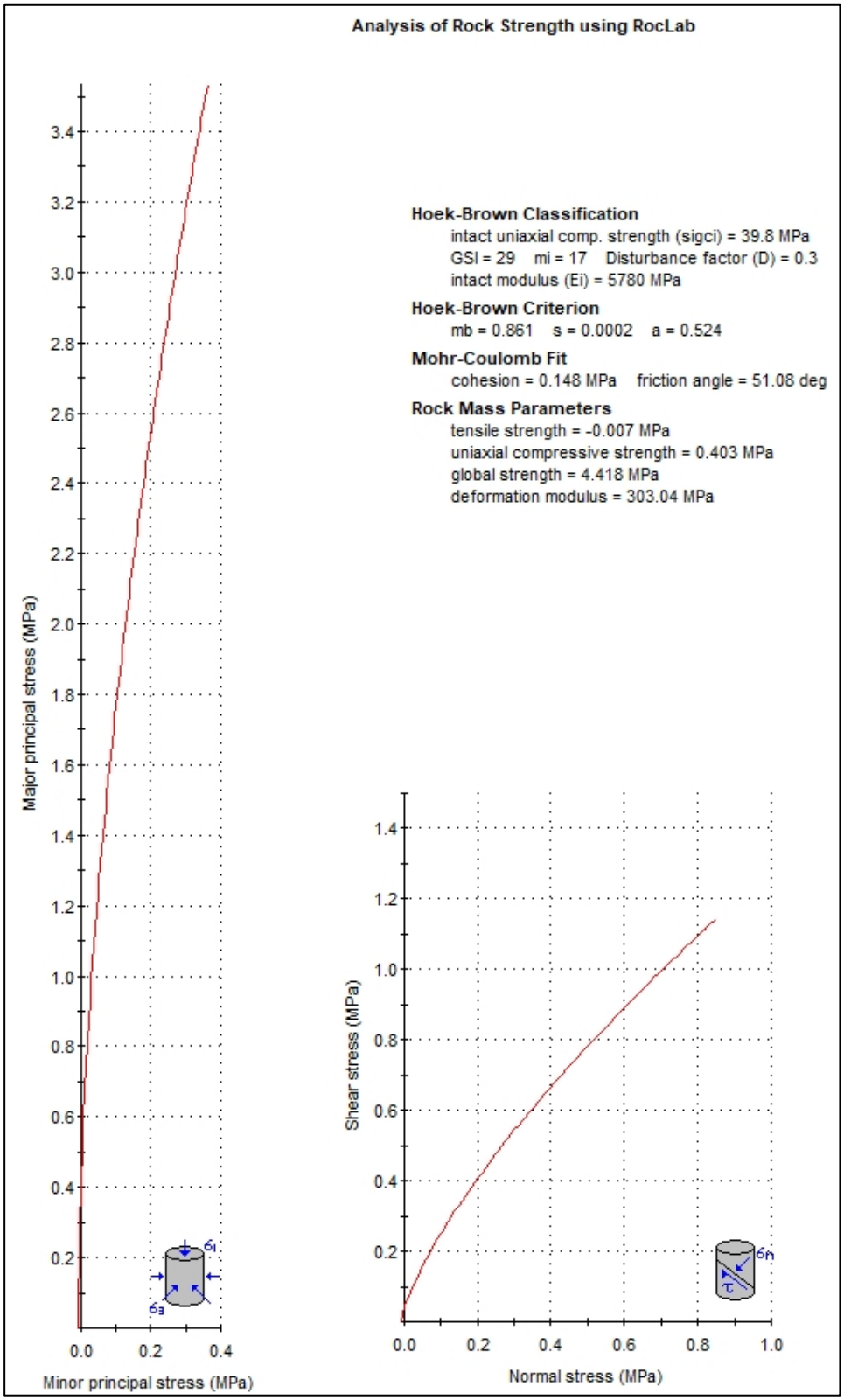

Figure G.6. RocLab results of Sandstone-1

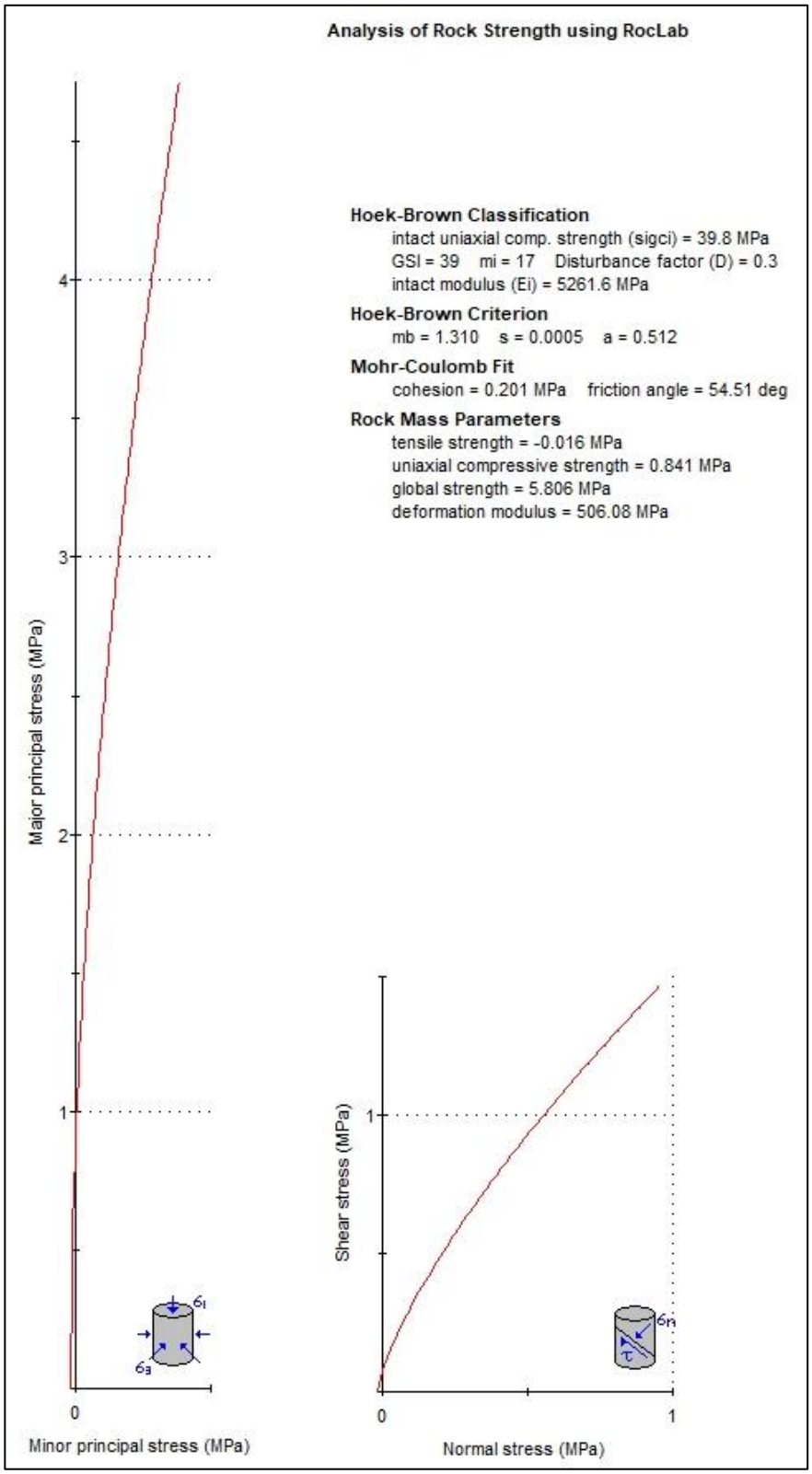

Figure G.7. RocLab results of Sandstone-2

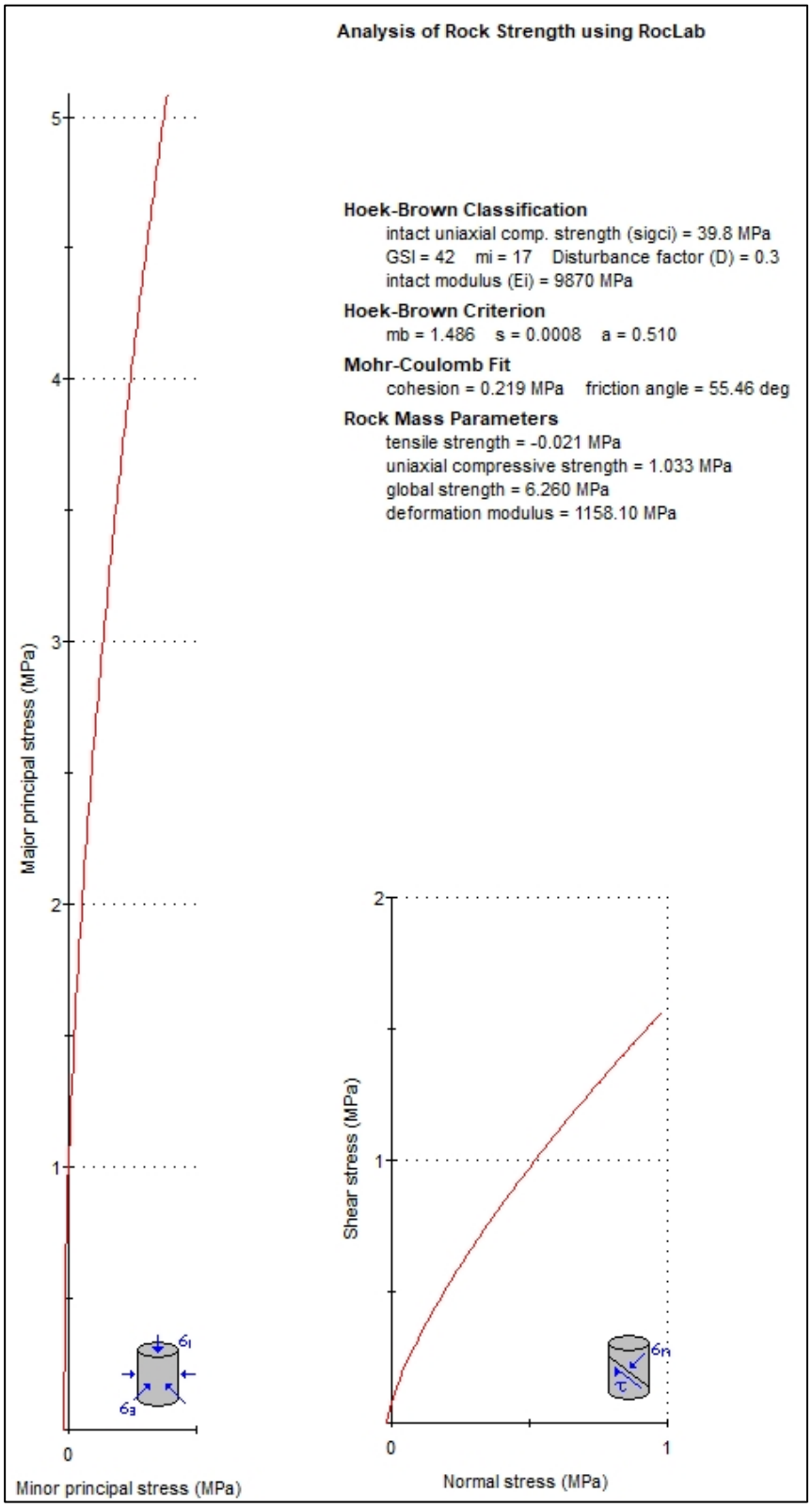

Figure G.8. RocLab results of Sandstone-3

APPENDIX H

CLOSER VIEW OF THE YIELDED ELEMENTS AND STRESS-STRAIN GRAPHS

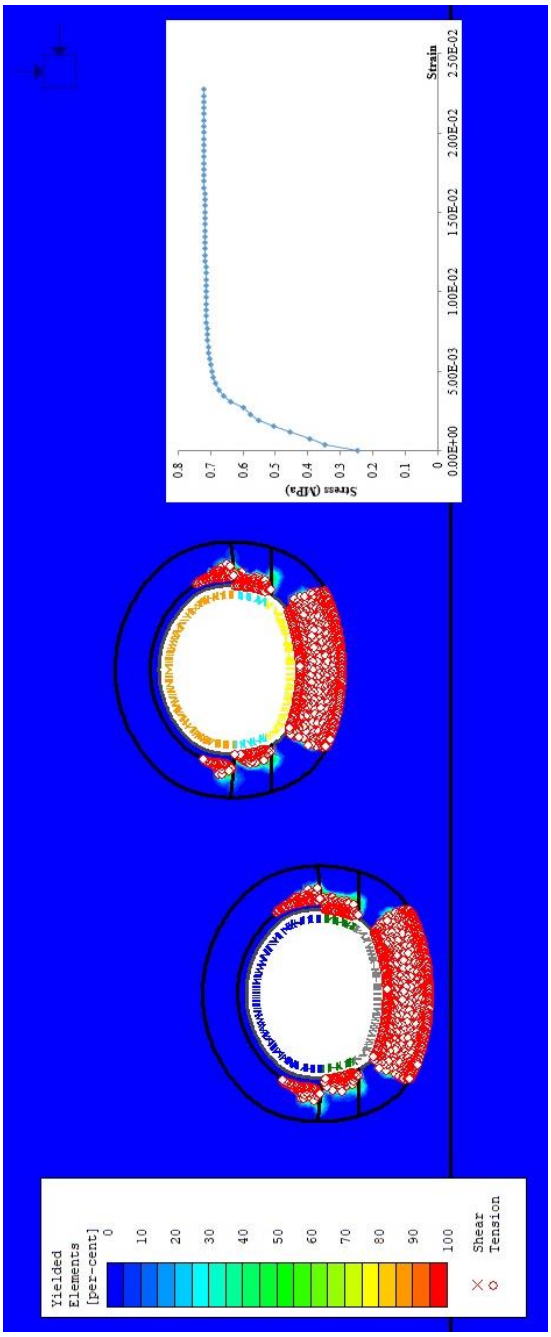

Figure H.1. Closer view of the yielded elements and stress-strain graph of the cross-section at Km 9+585

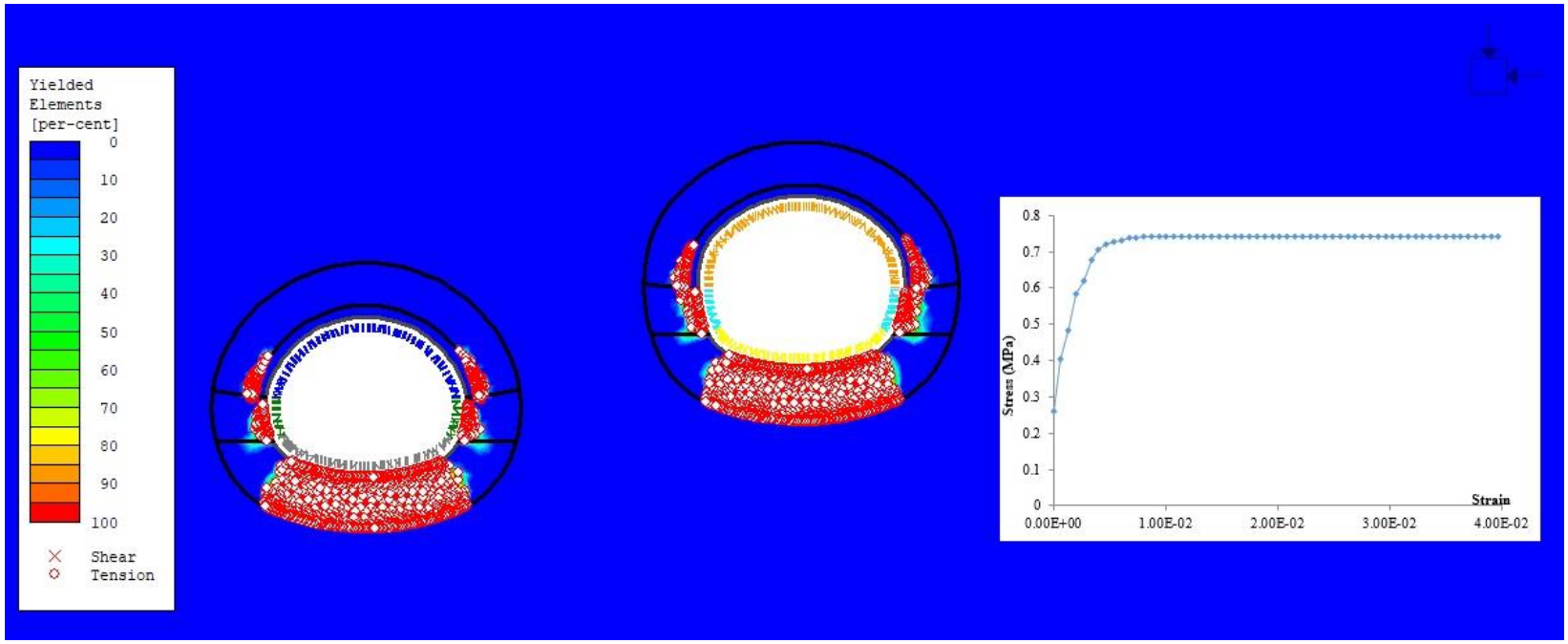

Figure H.2. Closer view of the yielded elements and stress-strain graph of the cross-section at Km 9+615

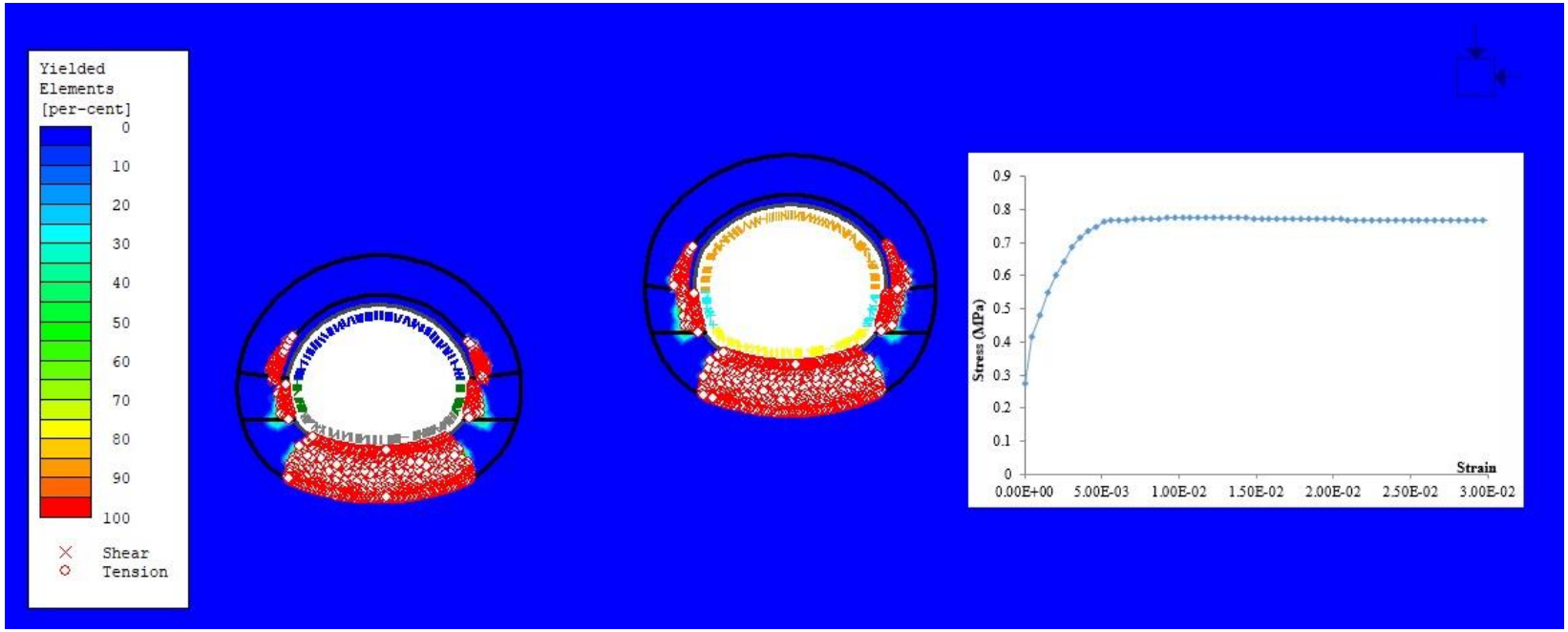

Figure H.3. Closer view of the yielded elements and stress-strain graph of the cross-section at Km 9+630

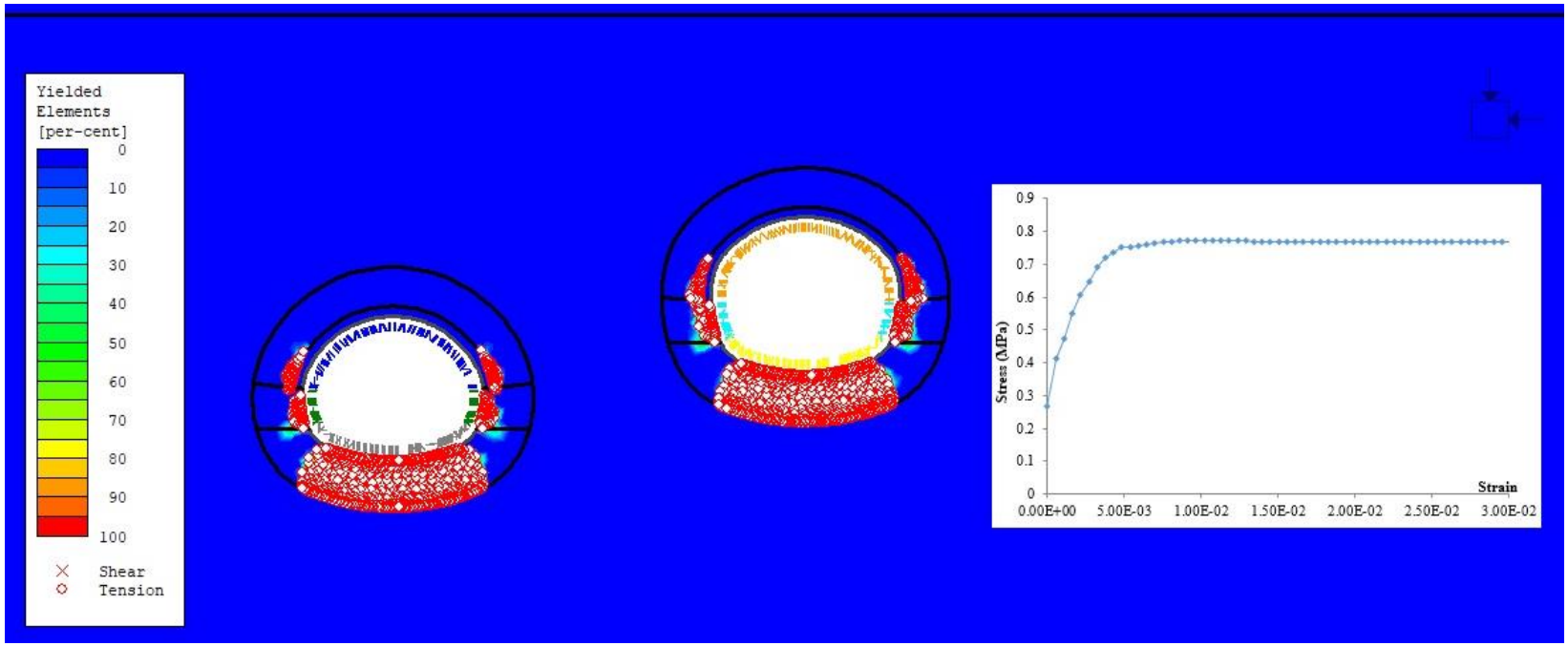

Figure H.4. Closer view of the yielded elements and stress-strain graph of the cross-section at Km 9+645

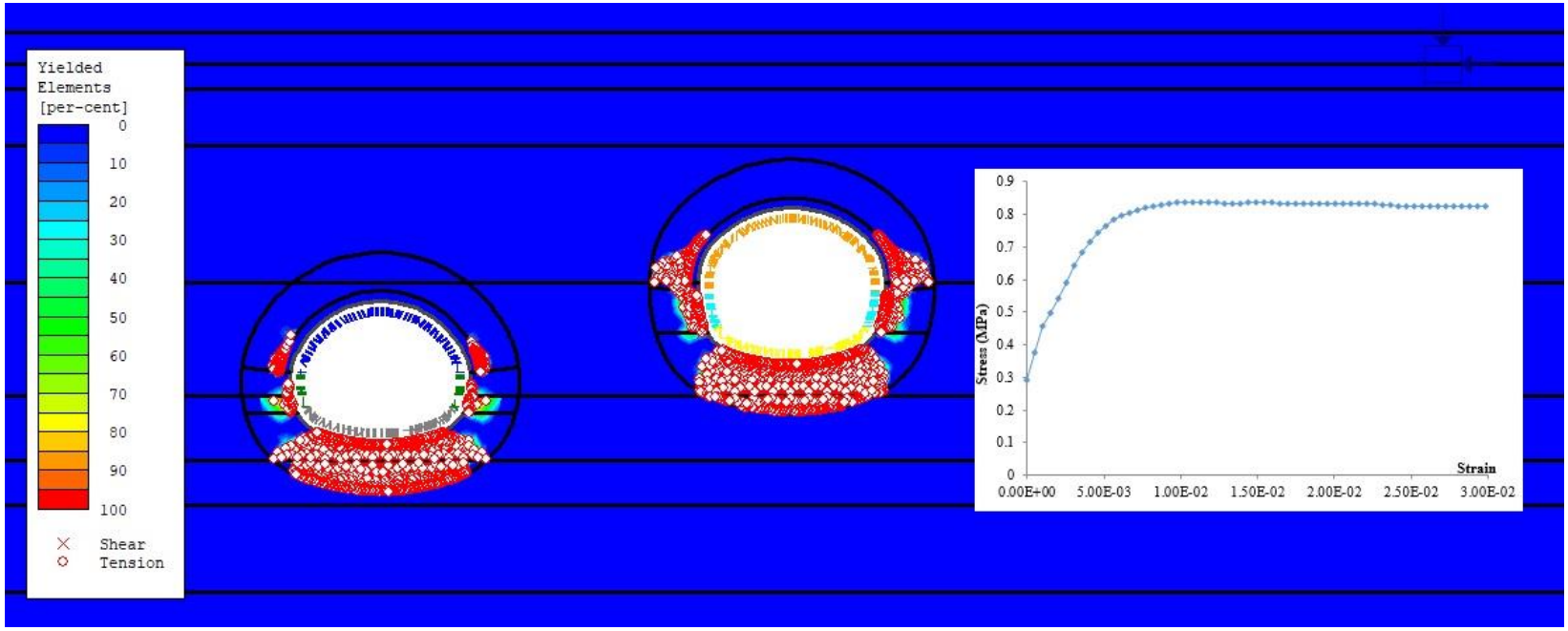

Figure H.5. Closer view of the yielded elements and stress-strain graph of the cross-section at Km 9+660

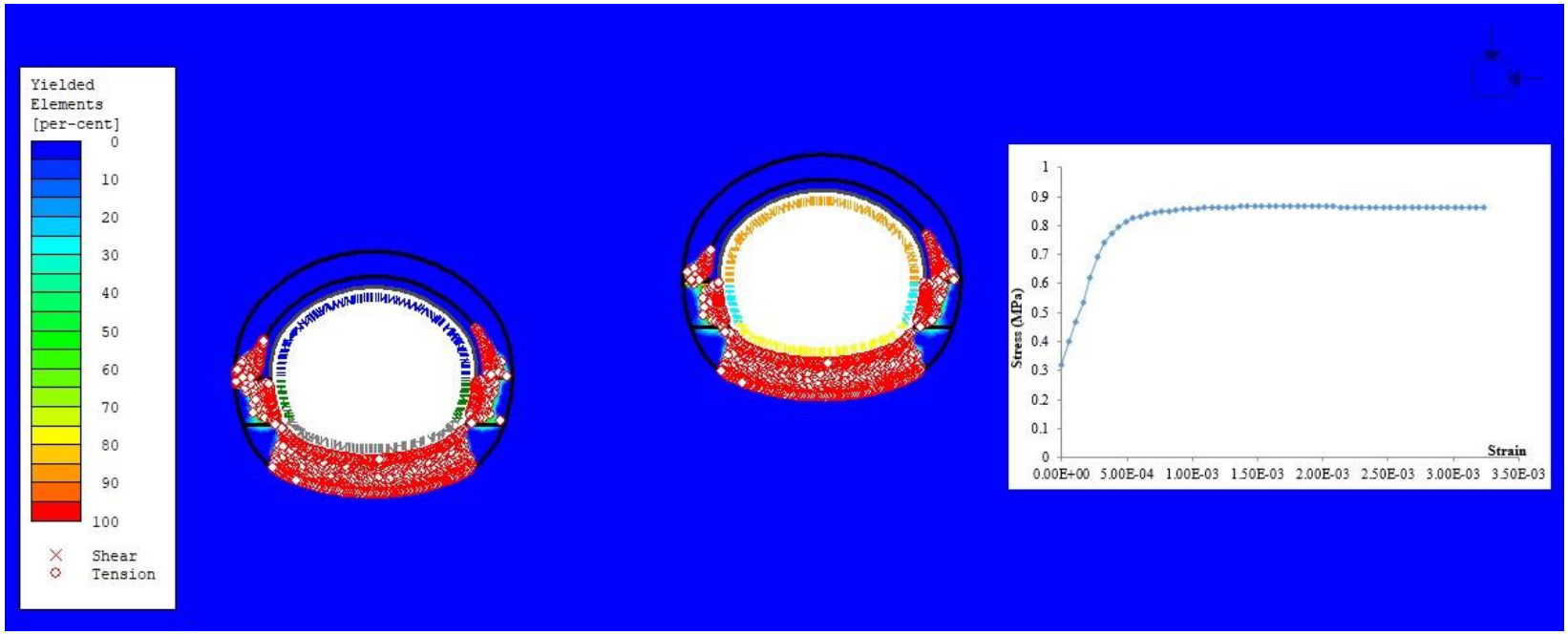

Figure H.6. Closer view of the yielded elements and stress-strain graph of the cross-section at Km 9+681

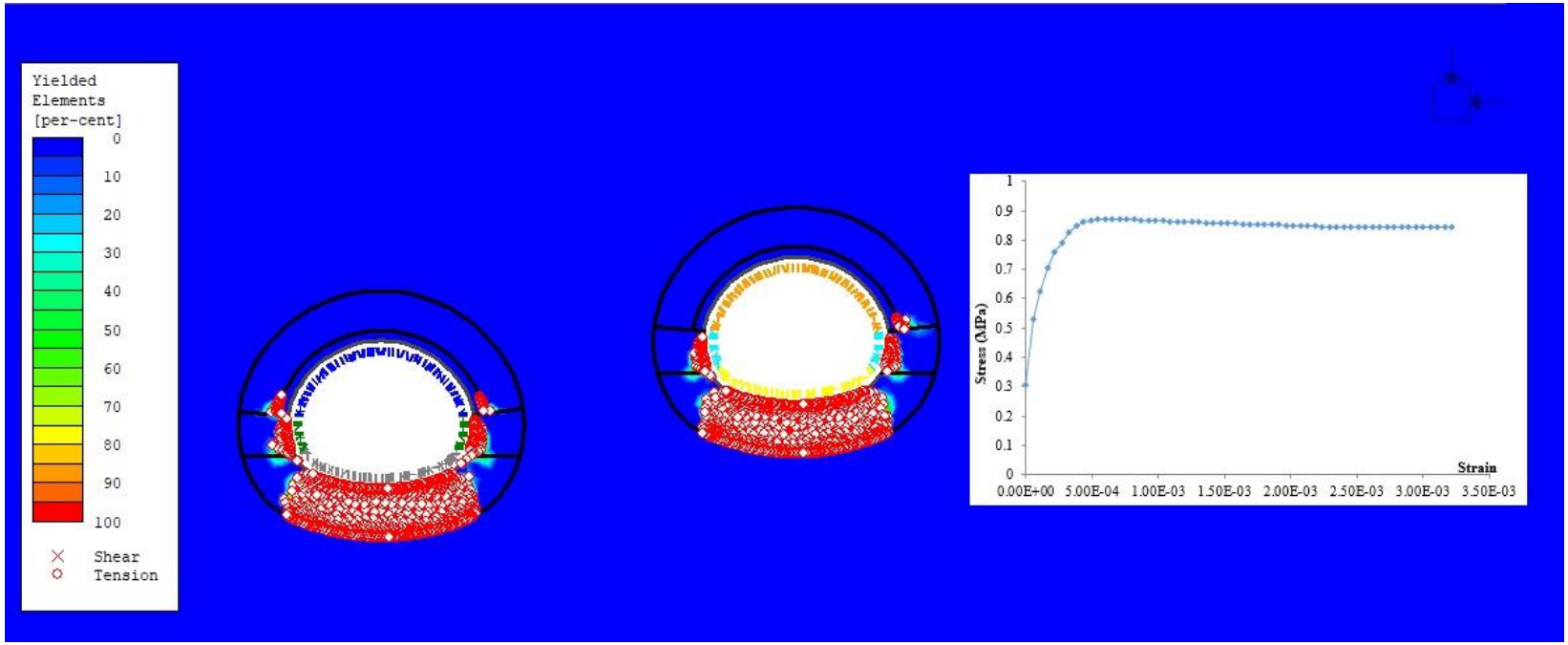

Figure H.7. Closer view of the yielded elements and stress-strain graph of the cross-section at Km 9+695

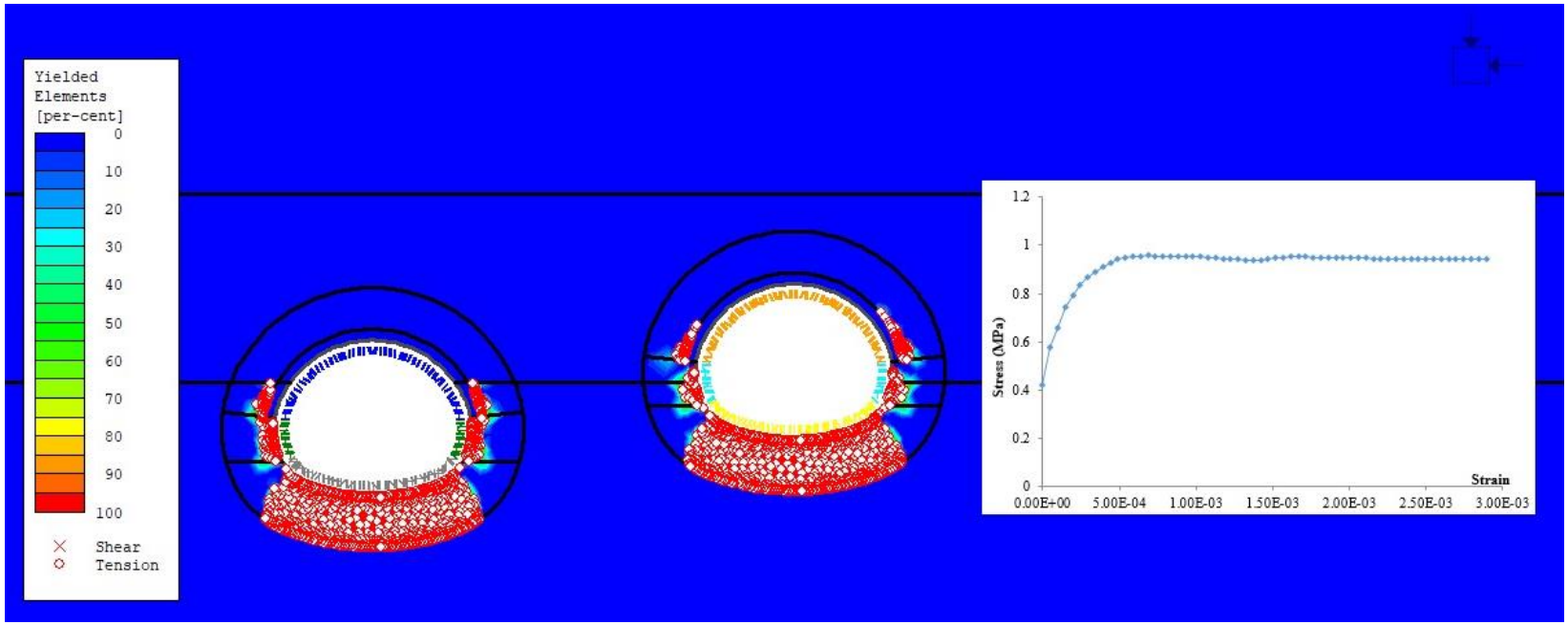

Figure H.8. Closer view of the yielded elements and stress-strain graph of the cross-section at Km 9+758

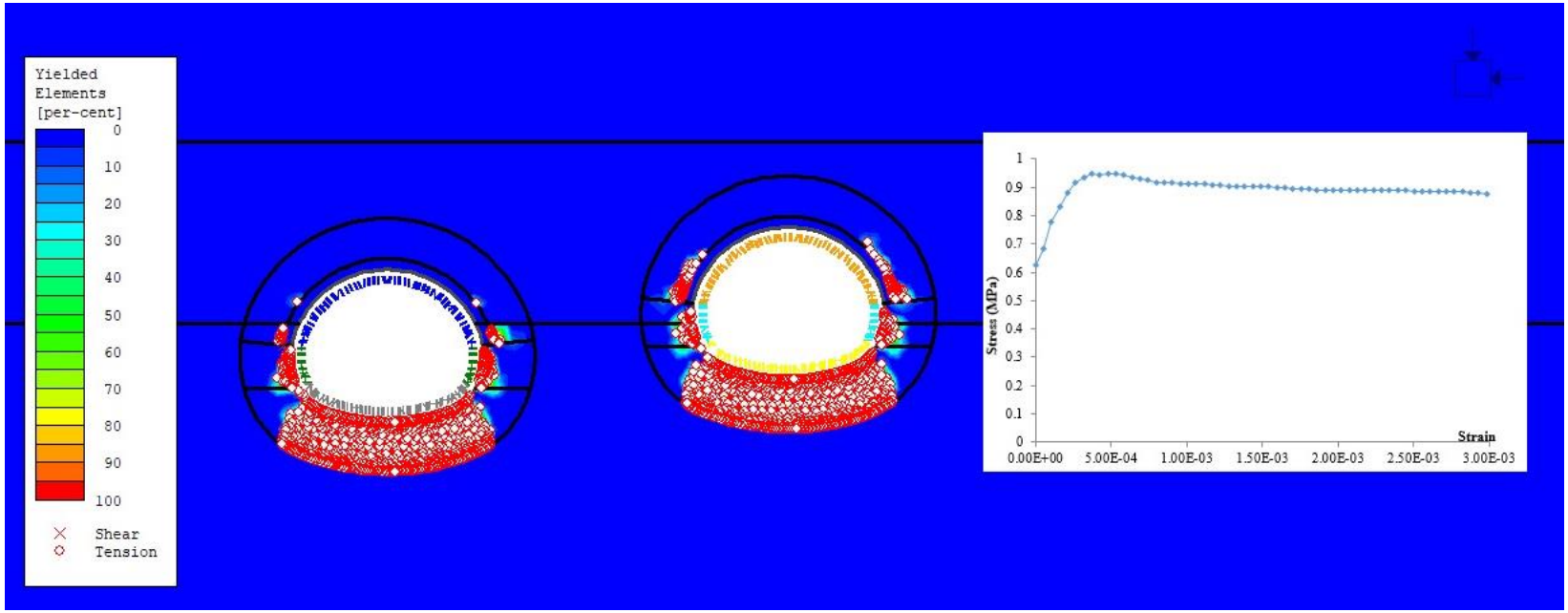

Figure H.9. Closer view of the yielded elements and stress-strain graph of the cross-section at Km 9+789

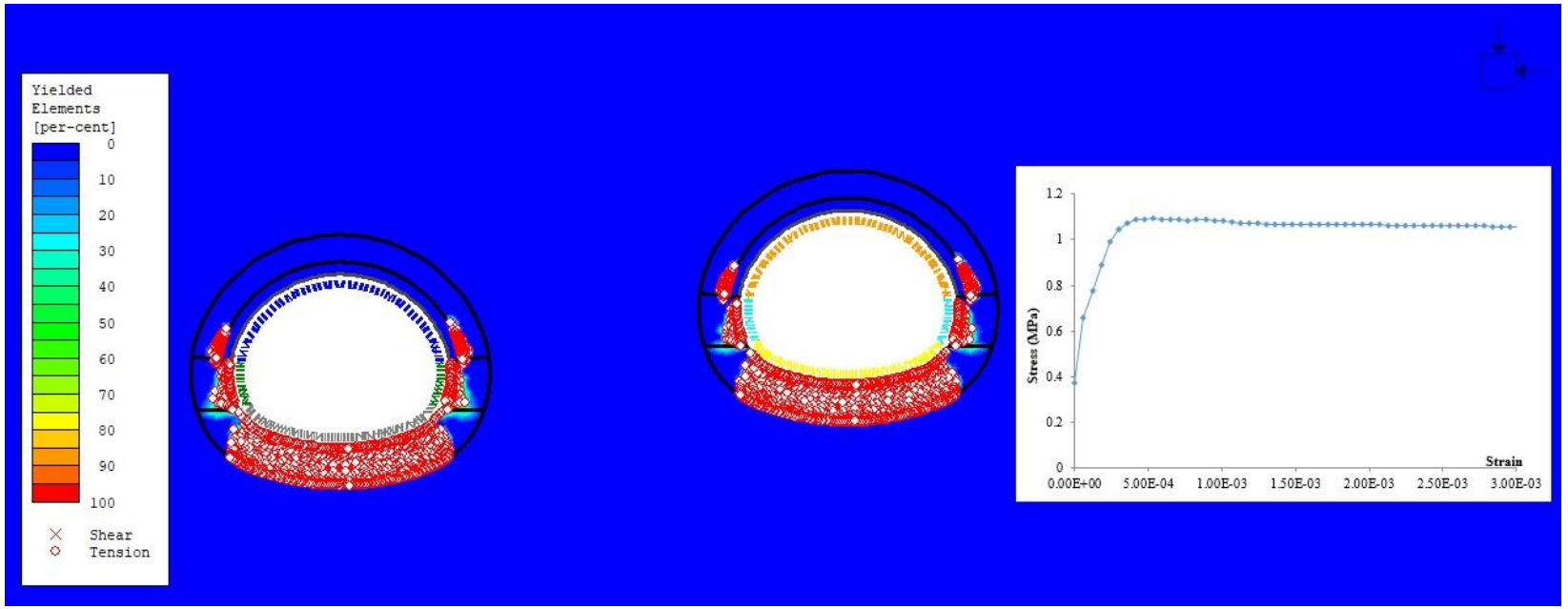

Figure H.10. Closer view of the yielded elements and stress-strain graph of the cross-section at Km 9+996

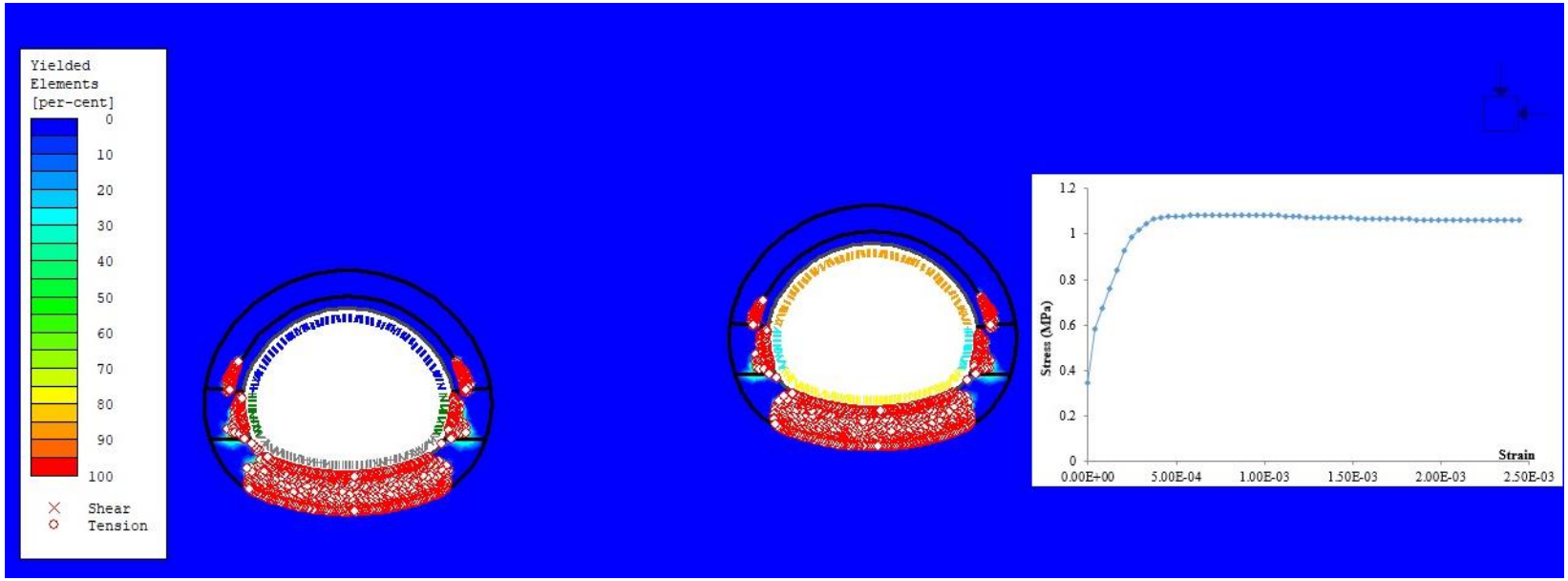

Figure H.11. Closer view of the yielded elements and stress-strain graph of the cross-section at Km 10+016

CURRICULUM VITAE

PERSONAL INFORMATION

Surname, Name: Ağbay, Ebru
Nationality: Turkish (TC)
Date and Place of Birth: 1 January 1988, Ankara
Phone: +90 554 877 15 32
E-mail: ebru.topsakal@metu.edu.tr

EDUCATION

Degree	Institution	Year of Graduation
MS	METU Geological Engineering	2012
BS	METU Geological Engineering	2010
High School	Bahçelievler Deneme High School	2004

WORK EXPERIENCE

Year	Place	Enrollment
2018-Present	TÜBİTAK BİLGEM YTE	GIS Specialist
2010-2013	PETRA Eng. And Cons.	Geological Eng.-GIS Spec.
2010 June	BM Holding	GIS Specialist

PUBLICATIONS

1. Topsakal, E. and Topal T., 2014, “Slope stability assessment of a re-activated landslide on the Artvin-Savsat junction of a provincial road in Meydancik, Turkey”, Arabian Journal of Geosciences, 10.1007/s12517-013-1210-0

HOBBIES

Pedagogy, Theater, Movies, Hiking